

THE PENNSYLVANIA STATE UNIVERSITY
THE GRADUATE SCHOOL
EBERLY COLLEGE OF SCIENCE

ASPECTS OF GAUSSIAN STATES
ENTANGLEMENT, SQUEEZING AND COMPLEXITY

A Dissertation in
Physics
by
Lucas Fabian Hackl

© Lucas Fabian Hackl

Submitted in Partial Fullfillment
of the Requirements
for the Degree of

Doctor of Philosophy

December 2018

The dissertation of Lucas Fabian Hackl was reviewed and approved* by the following:

Eugenio Bianchi
Assistant Professor of Physics
Dissertation Advisor
Chair of Committee

Abhay Ashtekar
Professor of Physics, Evan Pugh Professor, Eberly Chair

Marcos Rigol
Professor of Physics

Nigel Higson
Professor of Mathematics, Evan Pugh Professor

Richard Robinett
Professor of Physics
Associate Department Head, Director of Graduate Studies

*Signatures are on file in the Graduate School.

Abstract

We develop unifying mathematical methods to describe bosonic and fermionic states in systems with finitely and infinitely many degrees of freedom. Our approach is based on the triplet of Kähler structures, consisting of a positive definite metric, a symplectic form and a linear complex structure that are all defined on the classical phase space of the quantum system under consideration. We explain how the space of linear complex structures, either compatible with the symplectic form (bosons) or the metric (fermions), can be identified with the set of pure Gaussian states. Time evolution by quadratic Hamiltonians is described by the action of the Hamiltonian flow onto linear complex structures as phase space function. Reducing Gaussian states to subsystems corresponds to restricting their linear complex structure to sub phase spaces. These restricted complex structures are objects in their own right and can be identified with mixed Gaussian states. In particular, we can compute the von Neumann entanglement entropy and all Rényi entropies from their eigenvalues. Remarkably, we find identical expressions for these entropies in terms of their respective linear complex structures. Applying these methods we are able to study the properties of Gaussian states such as their time evolution, entanglement and complexity and we present a range of results related to understanding both bosonic and fermionic systems.

First, we prove a theorem on entanglement production in systems with instabilities. The rate of entropy production in a classical dynamical system is characterized by the Kolmogorov-Sinai entropy rate given by the sum of all positive Lyapunov exponents of the system. We prove a quantum version of this result valid for bosonic systems with unstable quadratic Hamiltonian. We show that the entanglement entropy of a Gaussian state grows linearly for large times in unstable systems, with a rate determined by the Lyapunov exponents and the choice of the subsystem. We conjecture that the same rate appears in the entanglement growth of chaotic quantum systems prepared in a semiclassical state.

Second, we show that the typical entanglement entropy of energy eigenstates can be vastly different from the typical entanglement entropy of general states in the Hilbert space. It is well known that typical pure states are maximally entangled with respect to any system decomposition in the thermodynamic limit. We develop tools to compute the entanglement entropy averaged over all eigenstates of quadratic fermionic Hamiltonians. In particular, we derive exact bounds for the most general translationally invariant models. We use this to prove that if the subsystem size is a finite fraction of the system size then the average over eigenstates of the Hamiltonian departs from the result for typical pure states. Furthermore, in the limit in which the subsystem size is a vanishing fraction of the system size, the average entanglement entropy is maximal. Based on numerical evidence, we conjecture that the average entanglement entropy of translationally invariant systems is universal and only depends on the subsystem fraction.

Third, we provide two alternative definitions of bosonic and fermionic Gaussian circuit complexity and show their equivalence. The circuit complexity associated to a quantum state quantifies the difficulty of reaching this target state by applying a sequence of unitary operations to a specified reference state. Defining circuit complexity in field theories is an important question of current

research as it is expected to be part of a new duality in holography. In approach A, we equip the Lie group of Gaussian transformations with a right-invariant positive definite metric and define circuit complexity as the minimal geodesic connecting the identity with a group element that prepares a given target state from the specified reference state. In approach B, we directly compute the geodesic distance between reference and target state on the Gaussian state manifold equipped with the canonical Fubini-Study metric. We prove that complexity computed in the two approaches are equivalent up to a relative normalization constant.

Contents

List of Figures	vii
List of Tables	viii
Conventions	ix
Preface	xi
Acknowledgement	xii
1 Introduction	1
1.1 Prelude: What are Gaussian states?	1
1.2 Kähler structures	5
1.3 Applications	14
I Mathematics of Gaussian states	16
2 Bosonic Gaussian states from Kähler structures	17
2.1 Pure bosonic Gaussian states	17
2.2 Mixed bosonic Gaussian states	20
2.3 Time evolution	24
3 Fermionic Gaussian states from Kähler structures	25
3.1 Pure fermionic Gaussian states	25
3.2 Mixed fermionic Gaussian states	28
3.3 Time evolution	30
4 Comparison: Bosons vs. fermions	32
II Applications	39
5 Entanglement production at instabilities	40
5.1 Linear growth of the entanglement entropy	42
5.2 Proof, part I: classical ingredients	46
5.3 Proof, part II: quantum ingredients	55
5.4 Examples: unstable potentials and periodic quenches	57

5.5 Examples: quantum field theory	64
5.6 Entanglement production of time-independent quadratic Hamiltonians	73
5.7 Beyond Gaussian states and quadratic Hamiltonians	80
5.8 Further exploration	85
6 Typical energy eigenstate entanglement	91
6.1 Translationally invariant spinless quadratic systems	92
6.2 XY model and transverse field Ising model	94
6.3 Conjecture about universality	102
6.4 XX model and free fermions	106
7 Circuit complexity of Gaussian states	121
7.1 Approaches to define circuit complexity	122
7.2 Minimal geodesics in approach A (Nielsen)	127
7.3 Minimal geodesics in approach B (Fubini-Study)	133
7.4 Relation between the two approaches	137
Summary and Outlook	139
8 Overview of results	140
8.1 Mathematics of Gaussian states	140
8.2 Applications	141
9 Beyond Gaussian states	146
Appendices	149
A Standard form of restricted linear complex structures	150
A.1 Compatible symplectic form (bosons)	151
A.2 Compatible positive definite metric (fermions)	153
B Dynamical systems and Lyapunov exponents	155
B.1 Linear Hamiltonian systems	155
B.2 Lyapunov exponents	158
B.3 Regular Hamiltonian systems	161
C Decomposition of symplectic generators	165
C.1 Jordan normal form of real matrices	165
C.2 Hamiltonian flow of time-independent quadratic systems	169
Publications	171
Bibliography	173

List of Figures

1.1	Triangle of Kähler structures	6
2.1	Entanglement structure of Gaussian states	22
5.1	Sketch of typical entanglement production	41
5.2	Subsystem exponents due to phase space stretching	52
5.3	Bounds on the entanglement entropy	56
5.4	Particle in a 2d inverted potential	59
5.5	Quadratic potential with instabilities	61
5.6	Instability bands in a periodic quantum quench	62
5.7	Periodic quantum quenches in a harmonic lattice	63
5.8	Symmetry breaking and the inverted quadratic potential	68
5.9	Preheating and parametric resonance	70
5.10	Quantum field in de Sitter space	72
5.11	Quadratic Hamiltonians with Gaussian and non-Gaussian initial states	82
5.12	Quadratic Hamiltonian with non-Gaussian initial states	83
5.13	Quadratic Hamiltonian with random non-Gaussian initial state	83
5.14	Non-quadratic Hamiltonians with Gaussian initial state	84
5.15	Entanglement entropy saturation for non-quadratic Hamiltonians	84
5.16	Non-quadratic Hamiltonians with non-Gaussian initial states	85
5.17	Non-quadratic Hamiltonians with random non-Gaussian initial state	85
6.1	Universal first order bound	95
6.2	Finite size correction to first order bound for XY model	99
6.3	Average entanglement entropy for XY model	102
6.4	Average entanglement entropy for translationally invariant models	104
6.5	Density plot for XX model	106
6.6	Upper and lower bounds from first to fourth order	109
6.7	Variance of the entanglement entropy	109
6.8	Integrand $I_3(y)$ and $I_4(y)$	119
7.1	Group foliation through stabilizer subgroup	125
7.2	Geometry of Gaussian circuits	130

List of Tables

4.1	Gaussian states from Kähler structures	37
6.1	Expansion of even traces t_n	107
6.2	List of all $(2, 2, 2)$ -contractions	115
6.3	List of all $(2, 2, 2, 2)$ -contractions	117
6.4	List of all $(2, 2, 4)$ - and $(4, 4)$ -contractions	118

Conventions

Symbol	Meaning
Part I: Mathematics of Gaussian states	
V	classical bosonic or fermionic phase space of dimension $2N$ describing N degrees of freedom
A, B	subsystem phase space, satisfies $V = A \oplus B$ with $N_A = \dim A$ and $N_B = \dim B$
V^*	dual phase space, space of linear observables
A^*, B^*	dual of subsystem phase spaces, canonically embedded in V^*
a, b, c, d	tangent/cotangent abstract indices on classical phase space V
r, s	tangent/cotangent abstract indices on subsystem phase space A, B
ξ^a	phase space vector
θ^r	phase space vector of subsystem A
Θ^r	phase space vector of subsystem A
G^{ab}	positive definite metric, defined on dual phase space
g_{ab}	inverse metric, defined on phase space, satisfies $G^{ac}g_{cb} = \delta^a{}_b$
Ω^{ab}	symplectic form, defined on dual phase space
ω^{ab}	dual symplectic form, defined on phase space, satisfies $\Omega^{ac}\omega_{cb} = \delta^a{}_b$
$J^a{}_b$	linear complex structure, satisfies $J^a{}_b = G^{ac}\omega_{cb} = -\Omega^{ac}g_{cb}$
$\mathcal{D}, \mathcal{D}_A, \mathcal{D}_B$	standard basis of V^* , A^* or B^* , symplectic basis (Darboux) or orthonormal basis (ONB)
$ \{n_i\}; \mathcal{D}\rangle$	Fock space basis vectors associated to \mathcal{D} with $0 \leq n_i \leq 1$ or $0 \leq n_i < \infty$
$\hat{a}_i^\dagger, \hat{a}_i$	creation and annihilation operators, usually with respect to a standard basis \mathcal{D}
Δ	relative covariance matrix $\Delta = -J\tilde{J}$
$ J\rangle$	homogeneous bosonic or fermionic Gaussian state vector, satisfying $\frac{1}{2}(\delta^a{}_b + iJ^a{}_b)\hat{\xi}^b J\rangle = 0$
$ J, \zeta\rangle$	inhomogeneous bosonic Gaussian state vector, satisfying $\frac{1}{2}(\delta^a{}_b + iJ^a{}_b)(\hat{\xi}^b - \zeta^b) J\rangle = 0$
$\rho(J)$	Gaussian density operator $\rho(J) = J\rangle\langle J $
$[.]_A$	restricted structure to subsystem A and A^*
r_i	squeezing parameters, related to eigenvalues $\pm i \cosh 2r_i$ or $\pm i \cos 2r_i$ of $[J]_A$
$\rho_A(J)$	reduced density operator $\rho_A(J) = \text{Tr}_{\mathcal{H}_B} J\rangle\langle J $ to subsystem A
q_{rs}	bilinear form defining $\rho_A(J) = \exp(-q_{rs}\hat{\theta}^r\hat{\theta}^s + E_0)$
\mathcal{G}	bosonic or fermionic Lie group, $\text{Sp}(2N, \mathbb{R})$ or $\text{SO}(2N)$
$M^a{}_b$	bosonic or fermionic group element, symplectic or orthogonal transformation
\mathfrak{g}	bosonic or fermionic Lie algebra, $\mathfrak{sp}(2N, \mathbb{R})$ or $\mathfrak{so}(2N)$
$K^a{}_b$	Lie algebra generator, satisfies $K^a{}_b = \Omega^{ac}h_{cb}$ or $K^a{}_b = G^{ac}h_{cb}$
H	quadratic Hamiltonian $H = \frac{1}{2}\xi^a h_{ab} \xi^b$ or $H = \frac{i}{2}\xi^a h_{ab} \xi^b$
$U(e^{-iH})$	unitary representation of e^K with $U = \exp\left(-\frac{i}{2}\omega_{ac}K^c{}_b \hat{\xi}^a \hat{\xi}^b\right)$ or $U = \exp\left(\frac{1}{2}g_{ac}K^c{}_b \hat{\xi}^a \hat{\xi}^b\right)$
S_A	entanglement entropy associated to subsystem A
$R_A^{(n)}$	Rényi entropy (of order n) associated to subsystem A

Part II: Applications — Entanglement production at instabilities

λ_ℓ	Lyapunov exponent associated to linear observable $\ell \in V^*$
Λ_A	Subsystem exponent associated to subsystem A
$\text{Vol}_G(\mathcal{V}_A)$	Volume of subspace region $\mathcal{V}_A \subset A^*$ measured by G restricted to A^*
L_a^b	Limiting matrix with Lyapunov exponents $(\lambda_1, \dots, \lambda_{2N})$ as its spectrum
\mathcal{D}_L	Lyapunov basis $\mathcal{D}_L = (\ell^1, \dots, \ell^{2N})$
\mathfrak{h}_{KS}	Kolmogorov-Sinai entropy rate
$\mathcal{E}_k^{l\sigma}$	generalized eigenvectors of symplectic generator K
$\mathbb{E}(\mathcal{E})$	exponential contribution of associated to generalized eigenvector \mathcal{E}
$\mathbb{P}(\mathcal{E})$	polynomial contribution of associated to generalized eigenvector \mathcal{E}
$\mathcal{J}(\kappa)$	Jordan block of symplectic generator K^\top for eigenvalue κ
$ n, n\rangle$	excited state $ n, n\rangle = (\hat{a}_1^\dagger \hat{a}_2^\dagger)^n 0, 0\rangle$
$ \text{ran}\rangle$	random non-Gaussian initial state
$\varrho_{ n,n\rangle}$	mixed Gaussian state matching the covariance matrix of $ n, n\rangle$

Part II: Applications — Typical energy eigenstate entanglement

$\hat{f}_x^\dagger, \hat{f}_y^\dagger$	creation and annihilation operators at site x and y
$\hat{\tilde{f}}_k^\dagger, \hat{\tilde{f}}_k$	Fourier transformed creation and annihilation operators
$\hat{S}_x^X, \hat{S}_x^Y, \hat{S}_x^Z$	spin operator at site x
$\hat{\eta}_\kappa^\dagger, \hat{\eta}_\kappa$	energy eigenstate creation and annihilation operators
α_{xk}, β_{xk}	fermionic Bogoliubov coefficients
$\mathfrak{D}, \mathfrak{D}_A$	Hilbert space dimension of system and subsystem, $\mathfrak{D} = \dim \mathcal{H}$ and $\mathfrak{D}_A = \dim \mathcal{H}_A$
$ J_\ell\rangle$	energy eigenstate labeled by integer ℓ with $1 \leq \ell \leq \mathfrak{D}$
$\mathfrak{H}, \mathfrak{J}, \gamma$	parameters of XY model
\hat{N}_κ	fermionic number operator $\hat{N}_\kappa = 2\hat{\eta}_\kappa^\dagger \hat{\eta}_\kappa - 1$ for energy eigenstates
r	sub system fraction, $r = V_A/V$ or $r = L_A/L$
$s(r)$	average entanglement entropy per degree of freedom in full system
$s_m^\pm(r)$	upper and lower bound of entanglement entropy per degree of freedom in full system
\mathfrak{c}_{2n}	coefficient for $2n$ -contraction in XX model

Part II: Applications — Circuit complexity of Gaussian states

$ J_R\rangle$	bosonic or fermionic Gaussian reference state
$ J_T\rangle$	bosonic or fermionic Gaussian target
\mathcal{M}	manifold of bosonic or fermionic Gaussian states
$\langle \cdot, \cdot \rangle_M^{(N)}$	Nielsen inner product on tangent space $T_M \mathcal{G}$ of group \mathcal{G}
$\langle \cdot, \cdot \rangle_M^{(\text{FS})}$	Fubini-Study inner product on tangent space $T_M \mathcal{G}$ of group \mathcal{G}
$U(N)$	sub Lie group associated to group elements preserving reference state
$\mathfrak{u}(N)$	sub Lie algebra associated to generators preserving reference state
$\mathfrak{u}_\perp(N)$	sub space of Lie algebra \mathfrak{g} orthogonal to $\mathfrak{u}(N)$
K_{\parallel}, K_{\perp}	decomposition of generator $K \in \mathfrak{g}$ into $K = K_{\parallel} + K_{\perp}$ with $K_{\parallel} \in \mathfrak{u}(N)$ and $K_{\perp} \in \mathfrak{u}_\perp(N)$
$\exp(\mathfrak{u}_\perp(N))$	sub manifold of \mathcal{G} generated by $\mathfrak{u}_\perp(N)$
γ	trajectory in group manifold $\gamma : [0, 1] \rightarrow \mathcal{G}$
$M(A, u)$	decomposition of $M(A, u) = e^A u \in \mathcal{G}$ with $A \in \exp(\mathfrak{u}_\perp(N))$ and $u \in U(N)$
$\mathcal{R}_{M(A, u)}$	normalized radially outgoing vector field $\mathcal{R}_{M(A, u)} = \frac{e^A A u}{\ A\ }$

Preface

This dissertation is based in part on published articles [[LH03](#), [LH07](#), [LH08](#), [LH09](#), [LH10](#)] and publications in preparation [[LH12](#), [LH11](#), [LH13](#), [LH15](#)]. Several chapters have significant overlap with the respective publications, which is noted accordingly in the introduction to each chapter. I wrote the first drafts for [[LH03](#), [LH07](#), [LH08](#), [LH10](#), [LH11](#), [LH13](#), [LH15](#)] which were then co-edited with my collaborators. I was responsible for the major parts of any analytical results and computations contained in [[LH03](#), [LH07](#), [LH08](#), [LH09](#), [LH10](#), [LH11](#), [LH13](#), [LH15](#), [LH14](#)]. The numerical data contained in [[LH09](#), [LH11](#), [LH14](#)] was kindly provided by Lev Vidmar and in [[LH10](#)] by Ranjan Modak. All plots, figures and sketches are my work.

The research laid out in this dissertation would not have been possible without the generous financial support from a number of sources. The German Studienstiftung des deutschen Volkes supported me during my first two years of my graduate studies. The Pennsylvania State University and its generous donors provided me with support through the Bert Elsbach Distinguished Graduate Fellowships in Physics, the David H. Rank Memorial Physics Award, the David C. Duncan Physics Award, the Edward M. Frymoyer Honors Scholarship, the Edward A. and Rosemary A. Mebus Graduate Fellowship in Physics and the Penn State Alumni Association Dissertation Award. I also would like to acknowledge several travel grants by the American Physical Society, in particular the APS US-Brazil Exchange travel grant, and from the Wilhelm und Else Heraeus-Stiftung which allowed me to attend the 66th Lindau Nobel Laureate Meeting in Physics. I thank the Perimeter Institute for Theoretical Physics and its Visiting Graduate Fellow program for hospitality during my stay in 2017. I was supported by the National Science Foundation under Grant No. PHY-1404204 awarded to Eugenio Bianchi. Finally, I would also like to acknowledge federal funds used by my collaborators: Ranjan Modak, Marcos Rigol and Lev Vidmar were supported by the National Science Foundation Grant No. PHY-1707482, Army Research Office Grant No. W911NF1410540 and Office of Naval Research Grant No. N00014-14-1-0540 all awarded to Marcos Rigol. Nelson Yokomizo was partially supported by the National Science Foundation Grant No. PHY-1505411 awarded to Abhay Ashtekar.

Acknowledgement

Advisor. I would like to thank my doctoral adviser, Eugenio Bianchi, who provided continuous support during my graduate studies at Penn State. He has been extremely encouraging of me to pursue ideas and opportunities whenever they arose. From him, I learned an approach to physics that combined rigorous study of the underlying mathematical structures with playful exploration of simple examples, while always reflecting on the overarching important questions.

Doctoral committee. Furthermore, I am indebted to the other members of my doctoral committee. Abhay Ashtekar's teaching and research style have been very inspiring. It was a pleasure to learn general relativity and advanced topics in fundamental theory from him. I had the chance to collaborate with Marcos Rigol in several research projects and I learned a number of very valuable lessons on how to get things done effectively. In particular, it was equally encouraging and useful to see him at work when dealing with referees. Finally, Nigel Higson taught me my first class on Lie groups and Lie algebras. It was not only delightful to see him teach this abstract subject with a lot of joy, but him giving his personal account of what and why the various topics are interesting proved to be invaluable when recalling them to apply to my own research.

Collaborators. During my graduate studies, I had many opportunities to collaborate with wonderful people from different fields. In my first summer, Yasha Neiman took me on as apprentice which resulted in my first publication at Penn State, where we studied horizon complimentarity in elliptic de Sitter space. After becoming Eugenio Bianchi's graduate student, Nelson Yokomizo quickly joined our effort to understand squeezed vacua and long range correlations in loop quantum gravity. This led to an ongoing and very productive collaboration which continues to the present days. In fact, part of this dissertation was written during a research visit of Nelson's group in Brazil. For the loop quantum gravity project, it was also a pleasure to work with Jonathan Guglielmon who laid the foundations for expanding squeezed spin network states in terms of normal ordered Wilson loop excitations. I also enjoyed a very productive collaboration with Marcos Rigol's research group, in particular with Ranjan Modak working on entanglement production and Lev Vidmar working on typical energy eigenstate entanglement. Finally, I am grateful to the Perimeter Institute for the opportunity to spend almost one year at the institute where I worked with Rob Myers on Gaussian circuit complexity and enjoyed numerous discussions with Shira Chapman, Ro Jefferson and Hugo Marrochio. For one of our projects, the five of us were joined by Jens Eisert, Michal Heller and Fernando Pastawski to form an unusually large collaboration of theorists.

Pennsylvania State University. The Institute for Gravitation and the Cosmos would not be complete without Randi Neshteruk who creates structure in chaos and fills the institute's corridors with a positive vibe. What made my time at the Institute for Gravitation and the Cosmos so enjoyable, was the diverse group of individuals. It was a pleasure to share an office with these wonderful people and I would regularly only come to the office to have lunch together and get distracted. Beatrice Bonga inspired us to be persistent and continue to ask the important questions, while diving into technical details of a problem. Moreover, it was always a pleasure to attend her scientific talks and to read her well-crafted writing. Anne-Sylvie Deutsch always filled the

office with joy, surprised us with Belgian chocolate and had something interesting to tell during lunch. The institute also had marvelous postdocs starting with Yasha Neiman with his wife Rada, then Marc Geiller, Wolfgang Wieland, Nelson Yokomizo, Brajesh Gupt, Javier Olmedo and Sina Bahrami. Brajesh taught us a lot about Indian cuisine and I had the pleasure to attend his extraordinary wedding in Mumbai. With my fellow graduate students Monica Rincon Ramirez and Miguel Fernandez, I spent almost four months at Perimeter Institute where we not only had lots of productive discussions, but also completed our pizzaiolo training under the supervision of our shared doctoral advisor, Eugenio Bianchi. After returning from Perimeter Institute, our office space was repopulated with more graduate students, including Ssohrab Borhanian and Sean Crowe. Finally, I want to mention my physicist house mate Pavlo Bulanchuk, whom I mostly saw after midnight in our kitchen, eager to discuss his newest ideas and research.

Perimeter Institute. Before coming to Penn State, I spent a wonderful ten month as student of the Perimeter Scholars International Master’s program at the Perimeter Institute for Theoretical Physics in Waterloo, which was probably one of the best time of my life. Rather than describing this experience, let me thank my 36 class mates: Tomiwa Ajagbonna, Katie Auchettl, Jonathan Blackman, Lance Boyer, Linqing Chen, Pavel Chvykov, Hjalmar Eriksson, Yvonne Geyer, Jiahua Gu, Henrik Gustafsson, Ali Hamed, Catherine Hughes, Lauri Lehtonen, Dalimir Mazac, Maryam Mirkamali, Ivan Panfilov, Brenda Penante, Raul Pereira, Brigitte Riley, Mark Penney, Andrzej Banburski, Lauren Hayward (now Sierens), Rosa Anajao, Aitor Lewkowycz, Peifeng Liu, Lenny Evans, Pedro Ponte, Ye Yuan, Robert Schuhmann, Grigory Sizov, Mohamad Shalaby, Eric Thewalt, Paulina Ugalde, Alexandre Vincart-Emard, Jacob Winding, Nosiphiwo Zwane. I also want to extend my gratitude to our six teaching fellows Tibra Ali, Sarah Croke, Denis Dalidovich, Anna Kostouki, David Kubiznak, Dan Wohns and the academic program manager Debbie Guenther. Finally, I am indebted to Tim Koslowski who supervised my essay project and from whom I learned a great deal about the Hamiltonian formulation of general relativity and constrained systems.

Humboldt-Universität zu Berlin. I took my first steps of learning physics at Humboldt-Universität zu Berlin. My time in Berlin was characterized by explorations, both of physics, mathematics and the cultural diversity of this wonderful city. My time there would not have been as enjoyable without Friederike Bartels, Michael Borinsky, David Jakobeit, Stephan Kirsten, Benjamin Maier, Gregor Richter, Christoph Rosenthal and Paul Schultz. After my second year, I had the chance to attend a summer school of the Studienstiftung des deutschen Volkes where I took a course on general relativity and quantum information, taught by Frederic Schuller and Achim Kempf. This course brought me, for the first time, in contact with research problems and it was my first introduction to general relativity and quantum field theory. At this school, I also met Robert Jonsson with whom I had the pleasure of co-instructing two summer courses on quantum information theory for gifted highschool students in Germany. After the school, I had the opportunity to complete an internship at the Max-Planck-Institut für Gravitationsphysik (Albert-Einstein-Institut) under Frederic Schuller’s supervision. His approach to research, academia and mathematical physics taught me a lot. Achim Kempf was the first to highlight to me the important connections between fundamental theory and quantum information to me. It was also him who told me about the Perimeter Scholars International master’s program. I also want to thank Jan Plefka and his doctoral student Theodor Schuster for supervision and support during my Bachelor thesis.

Technische Universität Kaiserslautern. Looking back where my path towards mathematical physics began, I would like to thank Klaus Wirthmüller whose mathematics lectures I remotely attended through the “Frühinstieg ins Mathematik-Studium (FiMS)” program at the Technische Universität Kaiserslautern. His inspiring lecture notes, his weekly letters to the remotely attending students and the excellent homework problems led me towards a more mathematical view of

physics. Taking my first steps of learning rigorous mathematics would not have been successful without the guidance of our online mentor, Lars Allermann, and regular online discussion with my fellow students, in particular, Michael Herbst and Jan Janßen, with whom I kept contact since then.

Parents. I would not be who I am without my parents, Marion Jurisch-Hackl and Gerd Hackl. During all my life, I have never experienced anything else than unconditional support for my dreams and decisions.

Katie. Finally, nothing would be as it is without Katie Auchettl. Since our time together at Perimeter Institute, I have rarely spent a day without her—either at the same place, via video chat when we apart or with her on my mind. Let us continue to inspire each other and explore the world.

Chapter 1

Introduction

Bosonic and Fermionic Gaussian states are widely used in all areas of quantum physics, ranging from condensed matter, optics and quantum information to quantum field theory and cosmology. This dissertation focuses on their mathematical structure, with applications to entanglement, squeezing and complexity.

In the first part of this dissertation, we focus on developing unifying mathematical framework based on Kähler structures to treat bosonic and fermionic Gaussian states. In the second part, we discuss three applications, namely the study of entanglement production in systems with instabilities, the analysis of typicality of the entanglement entropy when averaged over energy eigenstates of quadratic fermionic Hamiltonians and the definition of circuit complexity in free field theories.

In this introduction, we will start by giving some context on what Gaussian states are and in which areas of physics they play an important role. We then give a first glance on the mathematics of Kähler structures that we use to describe Gaussian states. We also foreshadow the main applications of these methods as discussed in this dissertation. Finally, we briefly outline the structure of this dissertation.

1.1 Prelude: What are Gaussian states?

The content of this dissertation focuses on *Gaussian quantum states* in bosonic and fermionic systems. Their name stems from the well-known Gauss function $f(x) = e^{-x^2}$ which plays a central role in probability theory and is also known as the *normal distribution*. This distribution appears in many areas of statistics and physics, as a natural consequence of the central limit theorem which states that the properly normalized sum of independent random variables follows a Gaussian normal distribution independently from the distributions of the individual variables. For bosonic Gaussian states, the connection to the Gauss function is literal, because such states are completely characterized by their Gaussian Wigner distribution

$$W(\xi) = \sqrt{\det \frac{g}{\pi}} \exp \left(-\frac{1}{2} g_{ab} \xi^a \xi^b \right), \quad (1.1)$$

where $\xi^a \in V$ represents a vector in the classical phase space V and g_{ab} a positive definite symmetric bilinear form on V .¹ For fermionic Gaussian states, the connection to the Gauss function is more

¹Note that the determinant depends on the basis, in which g_{ab} is represented, implying that $W(\xi)$ is technically not a function on phase space, but a scalar density of weight 1 or equivalently a volume form. We can integrate it over arbitrary regions of phase space to find the probability of quantum mechanical measurement outcomes. We should also mention that we can extend (1.1) to contain a linear term $f_a \xi^a$ shifting the center of the Gaussian.

indirect and based on the property of normal distributions that higher order correlation functions

$$\langle \xi^{a_1} \cdots \xi^{a_n} \rangle = \sum \prod \langle \xi^{a_i} \xi^{b_j} \rangle \quad (1.2)$$

can be computed from the two point function, also known as covariance matrix $\langle \xi^a \xi^b \rangle$. Here, $\sum \prod$ refers to summing over all distinct ways of partitioning $\xi^{a_1}, \dots, \xi^{a_n}$ into pairs and the product of their expectation values. This was first studied and proven by Leon Isserlis [1] in 1918 and later in 1950 rediscovered by Gian-Carlo Wick [2] in the context of computing higher order correlation functions in quantum field theory. In fermionic systems, linear phase space observables ξ^a anti-commute as Grassmann variables, but the underlying probability distribution continues to be Gaussian in the sense of Isserlis and Wick, *i.e.*, we can use the covariance matrix to compute any higher order correlation function, even though the underlying probability distribution is not a Gaussian function with real random variables anymore. This is the sense, in which bosonic and fermionic Gaussian states are related to Gauss' famous function.

Gaussian states are closely related to one of the most iconic systems studied in theoretical physics, the *harmonic oscillator*. In classical mechanics, it is one of the first non-trivial systems that can be solved analytically and it can be used to study perturbations and oscillations of any system around stable equilibrium positions. Its Hamiltonian is given by

$$H = \frac{p^2}{2m} + \frac{kq^2}{2}, \quad (1.3)$$

where m is the mass of a point particle, k is a positive constant and (q, p) are conjugate phase space variables, usually referred to as position and momentum. Quantizing the system will turn the Hamiltonian H into a quantum operator \hat{H} with a Gaussian state forming its ground state $|0\rangle$, *i.e.*, the state in the Hilbert space with lowest expectation value $\langle 0 | \hat{H} | 0 \rangle$. In fact, every Gaussian state can be interpreted as ground state of a Hamiltonian describing a collection of harmonic oscillators. More general, we can study the full class of quadratic Hamiltonians, *i.e.*, Hamiltonians characterized by a bilinear form $h_{ab}(t)$, such that

$$H(t) = \frac{1}{2} h_{ab}(t) \xi^a \xi^b. \quad (1.4)$$

For bosonic systems, such a Hamiltonian will describe a collection of harmonic oscillators if and only if h_{ab} is a positive definite symmetric bilinear form. For fermionic systems, such quadratic Hamiltonians can always be interpreted as a collection of fermionic oscillators, for which we can always choose a complete basis of eigenstates that are all Gaussian.

In physics, Gaussian states form the starting point of almost all explorations of more complicated systems and quantum states. Let us conclude with a non-exhaustive list of major scientific achievements and current research programs based on Gaussian states.

- **Quantum field theory**

Most of perturbative quantum field theory is based on an asymptotic expansion around a free field theory, *i.e.*, a quadratic Hamiltonian. Scattering amplitudes are computed based on the assumption that in the far future and distant past the field theory states are well-approximated by non-interacting (Gaussian) states [3]. One then expands the time evolution operator in terms of non-quadratic interacting operators that appear with powers of the coupling constant, for instance the fine structure constant α in the case of electromagnetic interaction. Computing inner products between initial and final states are then reduced to computing Gaussian expectation values of this operator power series, which leads to a

diagrammatic interpretation of Wick's theorem called Feynman diagrams [4]. Of course, many more subtleties due to the infinite number of degrees of freedom are involved, in particular one finds diverging integrals when applying Wick's theorem that need to be renormalized.

- **Quantum field theory in curved spacetime**

An important research field at the intersection of quantum theory and gravity is the study of quantum fields on curved spacetime [5, 6]. In general, we do not have enough symmetry to select a unique vacuum state, which means one needs to choose a specific unitary representation. Gaussian states do not only play an important role to describe quantum states and their time evolution, but the standard construction of a unitary representation is based on choosing a Gaussian state as vacuum and then construct a Fock space on top of it, carrying a representation of the algebra of observables.

- **Hawking radiation and Unruh effect**

A seminal contribution of Stephen Hawking was his discovery [7] that black holes radiate when studying a free scalar field in a Schwarzschild black hole spacetime. The original computation is fully based on Gaussian states and neglects backreaction, *i.e.*, the change of background geometry due to the loss of black hole mass that is radiated away. The global quantum state of the scalar field is different from the field theory vacuum of an observer far away from the black hole, so that this observer will see a continuous flow of outgoing particles emitted from the black hole horizon.

Hawking radiation is closely related to the finding of Stephen Fulling [8], Paul Davies [9] and William Unruh [10], which is nowadays referred to as the Unruh effect. They found that a constant accelerated observer will see the vacuum state of a free Klein-Gordon field in Minkowski space as a thermal bath of particle excitations. This is the so called Rindler horizon which becomes a source of thermal radiation. In simple terms, this implies that the concept of a particle itself is relative and the question of whether a quantum state describes an empty vacuum state or an excited state containing various particles is relative to the observers motion and acceleration.

- **Cosmic microwave background in cosmology**

An important research direction of cosmology is to better understand the cosmic microwave background observed today in terms of quantum perturbation of scalar field theory states in the past. Most of the computation of how the quantum state and its perturbations evolved is based on Gaussian states and their squeezing due to quadratic Hamiltonians (free field theory) with explicit time dependence. This assumption is supported by precision measurements that provide tight bounds on the non-Gaussian properties of the state [11]. It is also expected that the cosmic microwave background provides a window into the regime between unknown theories of quantum gravity and observations. For instance, loop quantum gravity and one of its branches, loop quantum cosmology [12], have made progress towards predicting properties of the field theory states that are Gaussian. In recent years, cosmologists have also started to explore the implications of non-Gaussian properties of the field theory state [13–15].

- **Quantum information theory**

The theory of quantum information [16] describes the information theoretic properties of quantum states, in particular, their information content, the effect of quantum channels on states to process or communicate information and their applications for computation and cryptography. Gaussian states have played an important role in the development of this research field [17].

- **Continuous variable systems**

While a large part of quantum information deals with finite dimension Hilbert spaces describing qubits (two-dimensional) or qudits (d -dimensional), the study of continuous variable quantum information refers to systems with the infinite dimensional Hilbert space of a collection of harmonic oscillators where one considers pure and mixed Gaussian states, known as continuous variable quantum systems [18]. Here, it is of great advantage that the entanglement entropy and other information theoretic quantities, such as the negativity and mutual information, are given by compact expressions in terms of the state's covariance matrix [19]. General quantum channels are known to be CPTP maps², *i.e.*, they are ensured to map quantum states into quantum states. There is natural restriction to those quantum channels that map Gaussian states onto Gaussian states, which are known as Gaussian quantum channels [20] that can be described in terms of linear maps between covariance matrices.

- **Relativistic quantum information**

In relativistic quantum information, one tries to understand the effects of general and special relativity on the processing and communication of quantum information [21, 22]. In this context, one often studies the coupling of local quantum systems with finite dimensional Hilbert spaces with certain modes of a relativistic quantum field, which is often a Klein-Gordon field in flat Minkowski space, but also in curved background spacetimes. The Unruh-DeWitt detector [10, 23, 24] is the simplest model of a particle detector that couples a two level quantum system linearly to a scalar field at a given position. Relativistic communication can then be studied by analyzing the effect of turning the coupling on and off at different points in spacetime. Most computations are based on Gaussian states, in particular the linear coupling ensures that the resulting states are a superposition of coherent states [25].

- **Condensed matter theory**

Gaussian states play an important role in the study of bosonic and fermionic condensed matter systems [26]. A lot of intuition in many-body physics stems from a Gaussian-like ground state with quasi-particle excitations on top of it, for instance in the description of Bose-Einstein condensates [27–29] and the Hubbard models [30].

- **Variational methods**

Given a complicated interacting condensed matter system, one is often mostly interested in understanding properties of the ground state and low excited states. Finding the ground state and its energy exactly is often impossible, but variational methods can help when numerical diagonalization is not feasible anymore. Instead of finding the ground state in the full Hilbert space, *i.e.*, the manifold of normalized states up to their phase (space of rays), one chooses a finite dimensional sub manifold that can be conveniently parametrized and such that the expectation value of the Hamiltonian can be efficiently computed. One then tries to minimize this expectation, for instance by computing Hamiltonian flow under imaginary time evolution restricted to this sub manifold [31]. This flow guarantees to always lower the energy expectation value, such that the evolution will approach fixed points that are at least local minima of the energy. To find the global minimum on the variational manifold, one often requires physical input on which initial state one should choose based on expected properties of the true ground state. The success of variational methods depends on the choice of variational manifold.

²CPTP maps are completely positive and trace preserving.

However, the manifolds of bosonic and fermionic Gaussian states plays a prominent role as versatile variational ansatz [32, 33], for fermions often referred to as the Hartree-Fock method [34]. Wick's theorem ensures that one can compute the expectation value and Hamiltonian flow of arbitrary Hamiltonians that are polynomial in linear observables (or equivalently, in terms of creation and annihilation operators). Moreover, Gaussian states can be efficiently parametrized by their covariance matrix and many ground states are well approximated by Gaussian states. Low excitations can then be studied by considering the tangent plane to the variational manifold at the approximate ground state [35]. A particularly important result from variational methods is the BCS theory of superconductivity [36].

– Integrable model

Quadratic Hamiltonians appear as the simplest example of integrable models, for which one can find the full spectrum analytically. For fermionic systems, all eigenstates are Gaussian states, while for bosons only the ground state is Gaussian. Examples of simple quadratic Hamiltonians include free spinless fermion models [37] and the transverse field Ising model [38]. Certain spin models, in particular the XY and the XX model [39], can be mapped to fermionic Hamiltonians that often consist of a quadratic part with higher order interactions. In general, one can already learn a lot about the system by just considering the quadratic, integrable part and then treat higher order terms as perturbations.

In summary, Gaussian states provide a versatile tool for the study of quantum systems in many areas physics. They are particularly powerful when one starts to explore new directions in a particular research field, especially for building intuition with simple examples and systems that can be treated analytically.

1.2 Kähler structures

In the first part of this dissertation, we will focus on a mathematical formalism that allows for a unified description of bosonic and fermionic Gaussian state, based on Kähler structures and in particular a linear complex structure. These structures are very well-studied in the context of Kähler manifolds, but for our purpose it suffices to study them on a single linear space, namely the classical phase space of the bosonic or fermionic theory. Using linear complex structures as convenient parametrization of Gaussian states was, to our knowledge, first done in quantum field theory in curved spacetime [5, 6], where it naturally arises in the context of distinguishing unitarily inequivalent representations of the observable algebra. However, the role of linear complex structures has also been recognized in the mathematical physics literature on quantization [40] and to some extent in field of quantum information [41].

Let us introduce the general setting of bosonic and fermionic Gaussian states, and the mathematical concept of Kähler structures. For both, fermions and bosons, a system of N degrees of freedom can be classically described by a $2N$ -dimensional phase space V with vectors $\xi^a \in V$ and linear observables $v_a \in V^*$ that commute in the bosonic and anti-commute in the fermionic case. Quantization is described by a linear map $\hat{\xi}^a : V^* \rightarrow \mathcal{O}$ that maps a linear classical observable v_a to its quantum operator $\hat{v} = v_a \hat{\xi}^a$. In a chosen basis of phase space, we have $\hat{\xi}^a \equiv (\hat{q}_1, \dots, \hat{q}_N, \hat{p}_1, \dots, \hat{p}_N)$.

Given a bosonic or fermionic Gaussian state $|\psi\rangle$, we can compute its 2-point function

$$\langle\psi|\hat{\xi}^a\hat{\xi}^b|\psi\rangle - \langle\psi|\hat{\xi}^a|\psi\rangle\langle\psi|\hat{\xi}^b|\psi\rangle = \frac{1}{2}\left(G^{ab} + i\Omega^{ab}\right), \quad (1.5)$$

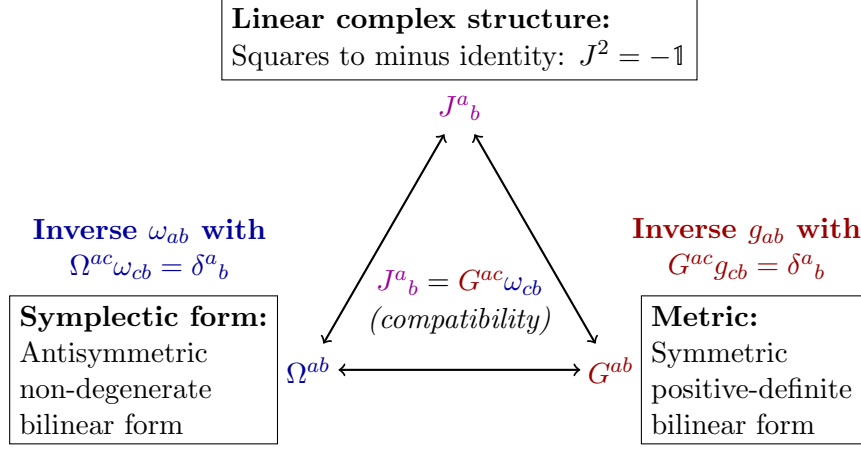


Figure 1.1: Triangle of Kähler structures. This sketch illustrates the triangle of Kähler structures, consisting of a symplectic form Ω , a positive definite metric G and a linear complex structure J . We also define the inverse symplectic form ω and the inverse metric g .

with symmetric part $G^{ab} = G^{ba}$ and antisymmetric part $\Omega^{ab} = -\Omega^{ba}$. We can define their inverses g_{ab} with $G^{ab}g_{bc} = \delta^a_c$ and ω_{ab} with $\Omega^{ab}\omega_{bc} = \delta^a_c$. We can construct the linear map $J : V \rightarrow V$ on phase space given by

$$J^a_c = \Omega^{ab}g_{bc}. \quad (1.6)$$

We refer to these structures as positive definite metric g and G , symplectic form ω and Ω , and linear complex structure J . They form a triangle, in which each two out of the three determines the third one via equation (1.6) solved for the structure in question.

For each structure, we can define a transformation $M^a_b : V \rightarrow V$ that leaves this structure invariant. We can choose a basis of V (and its dual basis of V^*) that brings the structure into a standard form.

- **Metric:** $g_{ab} = (M^\intercal)_a{}^c g_{cd} M^d{}_b \Leftrightarrow G^{ab} = M^a{}_c G^{cd} (M^\intercal)_d{}^b$

Transformations that preserve the metric are called orthogonal transformations, $M \in O(2N)$.

We can bring both g and G into the standard identity form:

$$g \equiv \begin{pmatrix} 1 & 0 \\ 0 & 1 \end{pmatrix}, \quad G \equiv \begin{pmatrix} 1 & 0 \\ 0 & 1 \end{pmatrix}. \quad (1.7)$$

- **Symplectic form:** $\omega_{ab} = (M^\intercal)_a{}^c \omega_{cd} M^d{}_b \Leftrightarrow \Omega^{ab} = M^a{}_c \Omega^{cd} (M^\intercal)_d{}^b$

Transformations that preserve the symplectic form are called symplectic transformations, $M \in Sp(2N, \mathbb{R})$. We can bring ω and Ω into the following standard form:

$$\omega \equiv \begin{pmatrix} 0 & -1 \\ 1 & 0 \end{pmatrix}, \quad \Omega \equiv \begin{pmatrix} 0 & 1 \\ -1 & 0 \end{pmatrix}. \quad (1.8)$$

- **Complex structure:** $J^a_b = M^a_c J^c_d (M^{-1})^d_b$

Transformations that preserve the complex structure are elements of the complex general linear group, $M \in GL(N, \mathbb{C})$. We can bring the complex structure into the following standard form:

$$J \equiv \begin{pmatrix} 0 & 1 \\ -1 & 0 \end{pmatrix}. \quad (1.9)$$

By choosing the right basis, we can bring all three structures simultaneously into their standard form. In fact, bringing two structures into the standard form is sufficient, because relation (1.6) ensures that also the third structure will be in its standard form. Moreover, all transformations that preserve two of the three structures will actually preserve all three structures. This remaining symmetry group is given by the intersection

$$U(N) = O(2N) \cup Sp(2N, \mathbb{R}) \cup GL(N, \mathbb{C}), \quad (1.10)$$

where the RHS satisfies the 2-out-of-3 property, meaning intersecting any two out of the three groups is sufficient.

For both, bosonic and fermionic systems, the complex structure J specifies a Gaussian state uniquely up to a choice of 1-point function $z^a = \langle \psi | \hat{\xi}^a | \psi \rangle$. On the other hand, the roles of metric and symplectic form are interchanged for the two:

- **Bosonic systems:**

The symplectic form is given and independent from a specific state, but is rather an underlying background structure that fixes the canonical commutation relations (CCR)

$$[\hat{\xi}^a, \hat{\xi}^b] = \hat{\xi}^a \hat{\xi}^b - \hat{\xi}^b \hat{\xi}^a = i \Omega^{ab}. \quad (1.11)$$

This implies that the metric provides an alternative to the complex structure in specifying a Gaussian state because given the symplectic form, complex structure and metric determine each other.

- **Fermionic system:**

Here, the metric is given and independent from a specific state, because the metric fixes the canonical anticommutation relations (CAR)

$$\{\hat{\xi}^a, \hat{\xi}^b\} = \hat{\xi}^a \hat{\xi}^b + \hat{\xi}^b \hat{\xi}^a = G^{ab}. \quad (1.12)$$

This means, that now the symplectic form provides an alternative to the complex structure in specifying a Gaussian state as the metric, complex structure and symplectic form determine each other.

We will now consider the smallest non-trivial spaces of Gaussian states, namely the space of bosonic Gaussian states associated to a single degree of freedom and the space of fermionic Gaussian states associated to two degrees of freedom.³ The following discussion is largely based on [LH10].

1.2.1 Single boson

We consider one bosonic degree of freedom, so the transformation group preserving the canonical commutation relations is simply $Sp(2, \mathbb{R})$ and we have $\xi^a \equiv (q, p)$. Now, another way to characterize the Gaussian states is in terms of annihilation and creation operators

$$a = \frac{1}{\sqrt{2}}(q + i p), \quad a^\dagger = \frac{1}{\sqrt{2}}(q - i p). \quad (1.13)$$

³We will see that the space of fermionic Gaussian states associated to a single degree of freedom is zero-dimensional, consisting of just two individual states.

That is, given these operators, there is a corresponding Gaussian state satisfying $a|\psi\rangle = 0$. However, there is some freedom in the precise definition the annihilation operator, namely the Bogoliubov transformations,⁴

$$\begin{aligned}\tilde{a} &= \alpha a + \beta a^\dagger, \\ \tilde{a}^\dagger &= \alpha^* a^\dagger + \beta^* a.\end{aligned}\tag{1.14}$$

In order to preserve the commutation relations $[\tilde{a}, \tilde{a}^\dagger] = [a, a^\dagger] = 1$, the coefficients α and β need to satisfy

$$|\alpha|^2 - |\beta|^2 = 1.\tag{1.15}$$

From this, we can conclude that the most general Bogoliubov transformation (for a single degree of freedom) is given by

$$\begin{aligned}\alpha &= e^{i\varphi} \cosh r, \\ \beta &= e^{i\vartheta} \sinh r.\end{aligned}\tag{1.16}$$

Now given two pairs of creation and annihilation operators, namely (a, a^\dagger) and $(\tilde{a}, \tilde{a}^\dagger)$, they define two distinct Gaussian states satisfying $a|\psi\rangle = 0$ and $\tilde{a}|\tilde{\psi}\rangle = 0$. Hence the Bogoliubov transformations (1.14) describe the desired group of transformations mapping the Gaussian states amongst themselves. We can invert (1.13) to $\xi^a \equiv (\tilde{q}, \tilde{p})$ for the pair $(\tilde{a}, \tilde{a}^\dagger)$. Then, the Bogoliubov transformation (1.14) from (a, a^\dagger) to $(\tilde{a}, \tilde{a}^\dagger)$ induces a linear transformation $M^a{}_b$ on the space V^* spanned by ξ^a and $\tilde{\xi}^a$, i.e., $\xi^a = M^a{}_b \tilde{\xi}^b$. Note that we define M to be the inverse transformation that maps $\tilde{\xi}$ into ξ . The condition of preserving the commutation relations then translates into

$$(M\Omega M^\top)^{ab} = M^a{}_c \Omega^{cd} (M^\top)_d{}^b = \Omega^{ab},\tag{1.17}$$

where Ω is a symplectic on V^* . This expression (1.17) extends trivially to the case of N degrees of freedom (by simply extending the range of the indices) and then reveals the $\text{Sp}(2N, \mathbb{R})$ group structure noted at the beginning of this section. Of course, we are also interested in the transformation of the symmetric two-point correlator

$$\tilde{G}^{ab} = (MGM^\top)^{ab} = M^a{}_c G^{cd} (M^\top)_d{}^b,\tag{1.18}$$

which encodes the transformation of the state, namely $\tilde{G}^{ab} = \langle \tilde{\psi} | \{\xi^a, \xi^b\} | \tilde{\psi} \rangle$, i.e., the expectation value of the original operators ξ^a in the transformed state. In particular, in a discussion of the circuit complexity of these states, we can represent the gates and unitary circuits with the appropriate symplectic transformations, and describe their action on the state in terms of the above transformation.

In our example with $N = 1$, the Bogoliubov transformation (1.14) gives the symplectic matrix

$$M \equiv \begin{pmatrix} \cos(\varphi) \cosh(r) + \cos(\vartheta) \sinh(r) & \sin(\vartheta) \sinh(r) - \sin(\varphi) \cosh(r) \\ \sin(\varphi) \cosh(r) + \sin(\vartheta) \sinh(r) & \cos(\varphi) \cosh(r) - \cos(\vartheta) \sinh(r) \end{pmatrix}.\tag{1.19}$$

⁴Note that we can change \hat{a} to $e^{i\varphi}\hat{a}$ without changing the vacuum, which corresponds to a $\text{U}(1)$ subgroup of Bogoliubov transformations that do not change the vacuum. For N bosonic degrees of freedom, there is the freedom of unitarily mixing all N annihilation operators (and creation operators respectively) among themselves, leading to a $\text{U}(N)$ subgroup of different choices of \hat{a}_i that all define the same vacuum.

If we start with an initial state $|\psi\rangle$, whose covariance matrix is $G \equiv 1$, then using (1.18), the transformed state $|\tilde{\psi}\rangle$ is described by

$$\tilde{G}^{ab} \equiv \begin{pmatrix} \cosh(2r) + \cos(\vartheta + \varphi) \sinh(2r) & \sin(\vartheta + \varphi) \sinh(2r) \\ \sin(\vartheta + \varphi) \sinh(2r) & \cosh(2r) - \cos(\vartheta + \varphi) \sinh(2r) \end{pmatrix}. \quad (1.20)$$

We notice that the final state $|\tilde{\psi}\rangle$ is independent of $(\vartheta - \varphi)$, which corresponds to the $U(1)$ subgroup where we just multiply creation and annihilation operators with opposite complex phases. As a manifold, we have $\text{Sp}(2, \mathbb{R}) = \mathbb{R}^2 \times U(1)$ where $(r, \vartheta + \varphi)$ provide polar coordinates of the plane and $(\vartheta - \varphi)$, the remaining coordinate on the circle $U(1)$. Since this overall phase is trivial, the space of states \mathcal{M} is properly described by the quotient $\mathcal{M} = \mathbb{R}^2 = \text{Sp}(2, \mathbb{R})/U(1)$. In the general case of N degrees of freedom, this expression for the space of states would become $\mathcal{M} = \text{Sp}(2N, \mathbb{R})/U(N)$, where the $U(N)$ group mixes the various annihilation operators amongst themselves leaving the corresponding Gaussian state unchanged. \mathcal{M} is also known as the symmetric space of type CI [42].

We add the following comments to conclude our review here: For every Gaussian state $|G\rangle$, we can choose a canonical basis $\xi^a \equiv (q_i, p_i)$, such that $G \equiv 1$. This means the bilinear form G does not contain information that is invariant under changing the canonical basis or put simply: “All Gaussian states look the same if we can choose the right basis for each individual state.” This changes of course, if we have two Gaussian states $|G\rangle$ and $|\tilde{G}\rangle$ in the same system and force ourselves to represent the two-point functions G and \tilde{G} with respect to the same canonical basis. Again, we can choose a basis, such that $G \equiv 1$, but we will not be able to accomplish the same for \tilde{G} . The remaining freedom of choosing a canonical basis is described by the group $U(N) = \text{Sp}(2N, \mathbb{R}) \cap \text{SO}(2N)$ consisting of canonical transformation (*i.e.*, $M\Omega M^\top = \Omega$) that simultaneously orthogonal with respect to G (*i.e.*, $MGM^\top = G$). The invariant information about the relation between the original state $|\psi\rangle$ and the transformed state $|\tilde{\psi}\rangle$ is completely captured by the eigenvalues of the relative covariance matrix⁵

$$\Delta^a{}_b = \tilde{G}^{ac} g_{cb} \quad \text{with} \quad g = G^{-1}, \quad (1.21)$$

i.e., $G^{ac}g_{cb} = \delta^a{}_b$. In particular, any quantities that depend on the two states in a $\text{Sp}(2N, \mathbb{R})$ -invariant way, for example their inner product, can be computed purely from Δ . This will apply to the complexity *provided* that we choose a geometry that is $\text{Sp}(2N, \mathbb{R})$ -invariant, for instance we do not introduce penalty factors which conflict with the group structure. For our Bogoliubov transformation (1.14), we have $\text{spec}(\Delta) = (e^{2r}, e^{-2r})$. We say that $|\tilde{\psi}\rangle$ arises from a one-mode squeezing of $|\psi\rangle$ with squeezing parameter r . For bosonic Gaussian states, understanding one-mode squeezing is the key to relate any two states. That is, for any two bosonic Gaussian states $|\psi\rangle$ and $|\tilde{\psi}\rangle$ with N degrees of freedom, there exists a normal mode basis $(q_1, \dots, q_N, p_1, \dots, p_N)$, such that $|\tilde{\psi}\rangle$ is the result of N independent one-mode squeezing operations in the N different normal modes. This is related to the Iwasawa (or KAN) decomposition of $\text{Sp}(2N, \mathbb{R})$, as discussed in [43, 44].

1.2.2 Two fermions

We now turn to the case of fermionic Gaussian states. In this case, the space of Gaussian states for N fermionic degrees of freedom is given by the quotient $\mathcal{M} = O(2N)/U(N)$, which has dimension $N(N-1)$. Of course, this space is a small submanifold within the full 2^N -dimensional Hilbert space \mathcal{H} of the fermionic system. Further, it is not preserved by general unitary transformations $U(2^N)$

⁵Note that one could have just as easily defined $\hat{\Delta} = G\tilde{g}$ with $\tilde{g} = \tilde{G}^{-1}$. However, one then has $\hat{\Delta} = \Delta^{-1}$ and due to the fact that Δ is symplectic, the two have the same spectrum.

acting on \mathcal{H} , but only the subgroup $O(2N)$ corresponding to Bogoliubov transformations. That is, the most straightforward way to think of characterizing the fermionic Gaussian states is in terms of the annihilation and creation operators. With N fermionic pairs (a_i, a_i^\dagger) satisfying $\{a_i, a_j^\dagger\} = \delta_{ij}$, the corresponding Gaussian state is again defined by $a_i|\psi\rangle = 0$ and the Bogoliubov transformations mixing these fermionic operators map Gaussian states to Gaussian states.

In analogy to (1.13) for the bosons, we begin by defining a set of Hermitian fermionic operators given by

$$q_i = \frac{1}{\sqrt{2}}(a_i^\dagger + a_i) \quad \text{and} \quad p_i = \frac{i}{\sqrt{2}}(a_i^\dagger - a_i), \quad (1.22)$$

which are commonly referred to as Majorana modes. In contrast to the analogous bosonic operators, they do not consist of conjugate pairs (q_i, p_i) , but rather they are governed by the anti-commutation relations: $\{q_i, q_j\} = \delta_{ij} = \{p_i, p_j\}$ and $\{q_i, p_j\} = 0$. Turning to the covariance matrix, if we choose the Majorana basis $\xi^a \equiv (q_1, \dots, q_N, p_1, \dots, p_N)$, the symmetric component becomes simply

$$G \equiv \mathbb{1}, \quad (1.23)$$

which means that G^{ab} expressed in this basis is just the identity. This result holds for any Gaussian state since G simply encodes the canonical anti-commutation relations which are preserved by the Bogoliubov transformations. Hence, in the fermionic case, the nontrivial component of is the antisymmetric two-point correlator

$$\Omega^{ab} = -i \langle \psi | [\xi^a, \xi^b] | \psi \rangle, \quad (1.24)$$

which characterizes the corresponding Gaussian state $|\psi\rangle$. Given (1.22) above, we may evaluate this matrix for the state $|\psi\rangle$ annihilated by a_i as

$$\Omega \equiv \begin{pmatrix} 0 & \mathbb{1} \\ -\mathbb{1} & 0 \end{pmatrix}. \quad (1.25)$$

We note that this Ω coincides with the form of the symplectic form Ω for bosons.

Now in analogy with our discussion of bosons, a pair (a_i, a_i^\dagger) and $(\tilde{a}_i, \tilde{a}_i^\dagger)$ defines two distinct Gaussian states satisfying $a_i|\psi\rangle = 0$ and $\tilde{a}_i|\tilde{\psi}\rangle = 0$. Hence understanding the group of transformations mapping fermionic Gaussian states amongst themselves is again understanding the Bogoliubov transformations acting on the fermionic annihilation and creation operators. It is simplest to work with the Majorana basis, *i.e.*, $\tilde{\xi}^a \equiv (\tilde{q}_i, \tilde{p}_i)$ and $\xi^a \equiv (q_i, p_i)$, where the Bogoliubov transformations act as a linear transformation. Again, we define the inverse transformation M , such that $\xi^a = M^a{}_b \tilde{\xi}^b$. The condition of preserving the anti-commutation relations translates into

$$(M G M^\dagger)^{ab} = M^a{}_c G^{cd} (M^\dagger)_d{}^b = G^{ab}. \quad (1.26)$$

Recalling that $G \equiv \mathbb{1}$ in the Majorana basis, (1.26) makes evident the $O(2N)$ group structure, which we referred to above. Of course, the transformation of the states is now encoded in the transformation of the antisymmetric two-point correlator

$$\tilde{\Omega}^{ab} = (M \Omega M^\dagger)^{ab} = M^a{}_c \Omega^{cd} (M^\dagger)_d{}^b. \quad (1.27)$$

Hence in a discussion of the circuit complexity of fermionic Gaussian states, we can represent the unitary circuits and gates with the appropriate orthogonal transformations and their generators, and describe their action on the states in terms of the above transformation.

To make this discussion more concrete, let us consider a simple example. However (as we now show), the simplest case of a single pair, *i.e.*, $N = 1$, turns out to be trivial. In this case, the most general Bogoliubov transformation is

$$\begin{aligned}\tilde{a} &= \alpha a + \beta a^\dagger, \\ \tilde{a}^\dagger &= \alpha^* a^\dagger + \beta^* a.\end{aligned}\tag{1.28}$$

Demanding that the anti-commutation relation is preserved, *i.e.*, $\{\tilde{a}, \tilde{a}^\dagger\} = 1$, yields

$$|\alpha|^2 + |\beta|^2 = 1.\tag{1.29}$$

However, fermionic creation and annihilation operators also need to satisfy $\tilde{a}^2 = (\tilde{a}^\dagger)^2 = 0$. Computing this explicitly for above transformation leads to a second requirement

$$\tilde{a}^2 = \alpha\beta\{a, a^\dagger\} = 2\alpha\beta = 0.\tag{1.30}$$

This means up to an overall phase, the only possible transformations are $\alpha = 1, \beta = 0$ or $\alpha = 0, \beta = 1$. That is, $\tilde{a} = a$ or we swap the role of creation and annihilation operators with $\tilde{a} = a^\dagger$. With $N = 1$, the space of Gaussian states is $\mathcal{M} = \mathrm{O}(2)/\mathrm{U}(1)$, where the $\mathrm{U}(1)$ corresponds to the overall complex phase, but this space simply consists of two points.⁶

This means that — in contrast to a single bosonic degree of freedom — the squeezing of a single fermionic degree of freedom is trivial. The first non-trivial system consists of two fermionic degrees of freedom, often interpreted as two qubits. With $N = 2$, the state manifold will be

$$\mathcal{M} = \mathrm{O}(4)/\mathrm{U}(2) = S^2 \cup S^2,\tag{1.31}$$

which is two-dimensional. In this case, we consider two pairs fermionic creation and annihilation operators, (a_1, a_1^\dagger) and (a_2, a_2^\dagger) . For this example, let us consider the fermionic Bogoliubov transformation

$$\begin{aligned}\tilde{a}_1 &= \alpha a_1 - \beta a_2^\dagger, \\ \tilde{a}_2^\dagger &= \beta^* a_1 + \alpha^* a_2^\dagger.\end{aligned}\tag{1.32}$$

This is not the most general transformation, but the natural choice if we want to mix a_1 with a_2^\dagger . In fact, one can show that one can bring any Bogoliubov transformation into this form by mixing a_1 with a_2 , and \tilde{a}_1 with \tilde{a}_2 via $\mathrm{U}(2)$, which does not change the corresponding Gaussian states, $|\psi\rangle$ and $|\tilde{\psi}\rangle$.

Further, for (1.32), we may choose α to be real so that the following parametrization works well:

$$\alpha = \cos \vartheta, \quad \beta = e^{i\varphi} \sin \vartheta.\tag{1.33}$$

⁶It is a general feature (for any N) that the full set of fermionic Gaussian states always consists of two disconnected components corresponding to the \mathbb{Z}_2 grading of states with even and odd fermion number. Note that neither of the two components is preferred and which corresponds to an even and odd fermion number depends on one's choice of the vacuum, or alternatively on one's notion of particle.

The induced transformation M that maps $\tilde{\xi}^a$ into ξ^a can then be written as

$$M \equiv \begin{pmatrix} 1 & 0 & 0 & 0 \\ 0 & \cos(\varphi) & 0 & -\sin(\varphi) \\ 0 & 0 & 1 & 0 \\ 0 & \sin(\varphi) & 0 & \cos(\varphi) \end{pmatrix} \begin{pmatrix} \cos(\vartheta) & \sin(\vartheta) & 0 & 0 \\ -\sin(\vartheta) & \cos(\vartheta) & 0 & 0 \\ 0 & 0 & \cos(\vartheta) & -\sin(\vartheta) \\ 0 & 0 & \sin(\vartheta) & \cos(\vartheta) \end{pmatrix} \begin{pmatrix} 1 & 0 & 0 & 0 \\ 0 & \cos(\varphi) & 0 & \sin(\varphi) \\ 0 & 0 & 1 & 0 \\ 0 & -\sin(\varphi) & 0 & \cos(\varphi) \end{pmatrix}$$

$$= \begin{pmatrix} \cos(\vartheta) & \sin(\vartheta)\cos(\varphi) & 0 & \sin(\vartheta)\sin(\varphi) \\ -\sin(\vartheta)\cos(\varphi) & \cos(\vartheta) & -\sin(\vartheta)\sin(\varphi) & 0 \\ 0 & \sin(\vartheta)\sin(\varphi) & \cos(\vartheta) & -\sin(\vartheta)\cos(\varphi) \\ -\sin(\vartheta)\sin(\varphi) & 0 & \sin(\vartheta)\cos(\varphi) & \cos(\vartheta) \end{pmatrix} \quad (1.34)$$

Here, we have decomposed M as a series of rotations and so it is clear that $M \in O(4)$ or rather $M \in SO(4)$, because we can continuously reach $\mathbb{1}$, and satisfies $MGM^\top = G$. The antisymmetric covariance matrix $\tilde{\Omega} = M\Omega M^\top$ of the transformed state $|\tilde{\psi}\rangle$ can then be evaluated to be

$$\tilde{\Omega} \equiv \begin{pmatrix} 0 & -\sin(2\vartheta)\sin(\varphi) & \cos(2\vartheta) & \sin(2\vartheta)\cos(\varphi) \\ \sin(2\vartheta)\sin(\varphi) & 0 & -\sin(2\vartheta)\cos(\varphi) & \cos(2\vartheta) \\ -\cos(2\vartheta) & \sin(2\vartheta)\cos(\varphi) & 0 & \sin(2\vartheta)\sin(\varphi) \\ -\sin(2\vartheta)\cos(\varphi) & -\cos(2\vartheta) & -\sin(2\vartheta)\sin(\varphi) & 0 \end{pmatrix}. \quad (1.35)$$

Note that we get the same state for $\vartheta = 0$ and $\vartheta = \pi$, which is perhaps half the expected range. This is due to the fact that the transformation with $\vartheta = \pi$ leads to $\tilde{a}_1 = -a_1$ and $\tilde{a}_2 = -a_2$, which leaves the vacuum invariant. Therefore the state which is most distant⁷ from the original Gaussian state $|\psi\rangle$ corresponds $\vartheta = \pi/2$, which we see trades the annihilation and creation operators, for instance (1.32) reduces to $(\tilde{a}_1, \tilde{a}_2) = (-\tilde{a}_2^\dagger, \tilde{a}_1^\dagger)$ with $\vartheta = \pi/2$ (and $\varphi = 0$).

As mentioned in (1.31), the space of states is given by the quotient $\mathcal{M} = O(4)/U(2) = S^2 \cup S^2$ because we need to divide by the subgroup $U(2)$ associated to mixing creation and annihilations operators among themselves, respectively. In particular, we see that the manifold of fermionic Gaussian states again consists of two disconnected components — see footnote 6. We can only continuously deform one state to the other, if they lie in the same component — unless we are willing to leave the space of Gaussian states. Our choice of Bogoliubov transformations parametrized by ϑ and φ corresponds to the S^2 connected to the identity.

Similar to the bosonic example, we can ask how to encode the invariant relative information between two fermionic Gaussian states $|\Omega\rangle$ and $|\tilde{\Omega}\rangle$. As a preliminary step towards answering this question, let us note that with an appropriate choice of an orthonormal basis $\xi^a \equiv (q_1, q_2, p_1, p_2)$ of Majorana modes, $G \equiv \mathbb{1}$ and the covariance matrix Ω takes the standard form

$$\Omega \equiv \begin{pmatrix} 0 & 1 \\ -1 & 0 \end{pmatrix}. \quad (1.36)$$

While preserving these forms, we would also like to bring $\tilde{\Omega}$ into a standard form. The allowed transformations are given by the subgroup $U(2) = O(4) \cap \text{Sp}(4, \mathbb{R})$, just like for the bosonic case.

⁷Of course, we mean ‘most distant’ on the S^2 component connected to the identity. We cannot reach the states on the other component along a continuous trajectory without leaving the space of Gaussian states.

One can show that the covariance matrix $\tilde{\Omega}$ can be brought into the standard form⁸

$$\tilde{\Omega} = \begin{pmatrix} 0 & 0 & \cos(2\vartheta) & -\sin(2\vartheta) \\ 0 & 0 & \sin(2\vartheta) & \cos(2\vartheta) \\ -\cos(2\vartheta) & -\sin(2\vartheta) & 0 & 0 \\ \sin(2\vartheta) & -\cos(2\vartheta) & 0 & 0 \end{pmatrix}, \quad (1.37)$$

provided that $|\Omega\rangle$ and $|\tilde{\Omega}\rangle$ belong to the same connected component. This indicates that the invariant relative information is encoded in ϑ alone, *i.e.*, the second angle φ in (1.33) is irrelevant.

Following the discussion of the bosonic theories, we can describe this invariant information about the relation between the two states in terms of the relative (fermionic) covariance matrix

$$\Delta^a{}_b = \tilde{\Omega}^{ac} \omega_{cb} \quad \text{with } \omega = \Omega^{-1}, \quad (1.38)$$

i.e., $\Omega^{ac} \omega_{cb} = \delta^a{}_b$. The invariant information is then captured in the eigenvalues of this matrix. For our choice of Bogoliubov transformation in (1.32) and (1.33), we have $\text{spec}(\Delta) = (e^{2i\vartheta}, e^{2i\vartheta}, e^{-2i\vartheta}, e^{-2i\vartheta})$ and as expected, φ does not appear here. We will later show that for a natural choice of invariant metric on the group, our Bogoliubov transformation that changes ϑ continuously from zero to its final value along a path of fixed φ is the minimal geodesic connecting a reference state $|\psi\rangle$ to a target state $|\tilde{\psi}\rangle$. In particular, the geodesic length will be given by $|2\vartheta| \in [0, \pi]$. These paths are just the great circles passing through the pole (at $\vartheta = 0$) on the corresponding two-sphere. This means in each linearly independent direction, the maximal path length is $\pi/2$.⁹ However, if with a large number of degrees of freedom, geodesic will be moving along several such paths in orthogonal directions at the same time. In particular, the overall path can become arbitrarily large in the field theory limit where we consider an infinite number of degrees of freedom.

For bosons, we reviewed that any two Gaussian states define a set of normal modes, such that there is a natural transformation built from linearly independent one-mode squeezing operations in these modes. In the case of fermions, we observed that: (a) there are two disconnected components on the manifold of states (separating states with even and odd fermion number); and (b) one-mode-squeezing is trivial and we need to perform two-mode squeezing operations. Therefore, we can only find normal modes if two Gaussian states lie in the same connected component and these normal modes always come in pairs, so that the two states are related by a collection of independent two-mode squeezing operations. In particular, if we have an odd number of fermionic degrees of freedom, there will always be a single normal mode left that is not squeezed when moving from one state to the other.

⁸Examining the transformation in (1.34), one finds the final rotation can be eliminated with the phase rotation $(\tilde{a}_1, \tilde{a}_2) \rightarrow (\tilde{a}_1, e^{-i\varphi} \tilde{a}_2)$, which of course leaves the $|\tilde{\psi}\rangle$ unchanged. Further, applying the latter transformation takes $\tilde{\Omega}$ from (1.35) to the canonical form (1.37).

⁹One may be surprised to find $\pi/2$ rather than π here. The reason is that at π , we would reach the group element $M = -1$, as shown by (1.34), which is as far away from 1 as possible. However, the transformed two-point function becomes $\tilde{\Omega} = M\Omega M^\dagger = \Omega$, for example (1.35) reduces to the initial covariance matrix in (1.36) with $\vartheta = \pi$, and so the final state is identical to the initial one at $\vartheta = \pi$. This means the group elements, which take our state as far away as possible from the initial one, are those sitting on the circle at $\vartheta = \pi/2$, *i.e.*, the equator of the connected S^2 component. Recall that at $\vartheta = 2\pi$, M returns to the identity, but when we measure the length of the circle covered by ϑ running from 0 to 2π (with fixed φ) using our metric $\langle \cdot, \cdot \rangle_1$, its length is actually 4π . Therefore the resulting distance to the maximally distant states is π .

1.3 Applications

In the second part of this dissertation, we will focus on applications of the previously introduced structures. The goal is to study aspects of fundamental theory through the perspective of quantum information, namely with an emphasis on entanglement and circuit complexity.

The first application concerns the production of correlations in systems with instabilities. Instabilities in classical dynamical systems are well-understood and can be quantified using Lyapunov exponents and the Kolmogorov-Sinai entropy rate, which describes how information about the initial state is erased through time evolution. Pesin's theorem states that the Kolmogorov-Sinai entropy rate can be computed as a sum over Lyapunov exponents. For unstable bosonic systems, we prove a quantum version of this result, namely that the entanglement entropy of Gaussian states grows linearly in time with a rate given by the sum over largest Lyapunov exponents when evolved with an unstable quadratic Hamiltonian. The number of summands is determined by the size of the subsystem under consideration. Linear growth of the entanglement entropy is observed in a large class of bosonic and fermionic systems and our result provides a new mechanism within the bosonic class. Our proof is based on three steps: First, we show that the von Neumann entropy has the same asymptotic behavior as the Renyi entropy (of order 2). Second, we identify the Renyi entropy of Gaussian state with the logarithm of the volume of certain regions in the classical phase space. Third, we show that unstable time evolution of the state leads to exponential stretching of this volume in phase space which implies a linear growth of the entropy, once the logarithm is taken into account. We discuss various examples ranging from periodically driven systems and different field theory models. Using numerical methods, we explore the regime beyond Gaussian states and quadratic Hamiltonians and identify regimes where our results continue to hold. Based on this, we formulate a conjecture on entanglement production in general quantum chaotic systems.

The second application analyzes the entanglement entropy for the ensemble of all energy eigenstates of quadratic fermionic Hamiltonians. This is a finite set of Gaussian states that grows exponentially with the number of fermionic degrees of freedom in the system. It is well known that the typical entanglement entropy of a Haar-randomly¹⁰ selected pure state is maximally entangled. We use a combination of numerical and analytical methods to study the statistical properties of the entanglement entropy within the ensemble of Gaussian energy eigenstates. We find a sequence of upper and lower bounds that converge to the average entanglement entropy and which can be efficiently computed from traces of powers in the restricted linear complex structure. This allows us to prove for translationally invariant systems that the average eigenstate entanglement entropy is not maximally entangled and thus differs from the typical entropy of Haar-randomly selected states. Using the Jordan-Wigner transformation, we investigate bipartite entanglement in the XY spin model and find that the average entanglement entropy converges to a universal function that only depends on the subsystem size, but is independent of the model parameters and the shape of the subsystem. Moreover, we find that the finite size correction to this universal limit provides a signature of criticality, *i.e.*, for parameter choices that are known to make the model critical, we find a distinct scaling of the finite size correction. Based on the universal limit for the XY model, we numerically explore the average entanglement entropy of various translationally invariant models and find the same universal limit. We therefore conjecture that the entanglement entropy is universal within the class of translationally invariant quadratic fermionic models. Based on this assumption, we use the simplest model in this class, free fermions, to compute the average entanglement entropy up to fourth order in our perturbative approach.

The third application deals with a recent effort to define circuit complexity in quantum field

¹⁰The state manifold is naturally equipped with a unique measure, called the Haar measure, that is invariant under the action of the unitary group.

theory. This is based on the idea that one can assign each quantum state a complexity based on how many elementary unitaries are required to evolve a fixed reference state into this state. Turning this rough idea into a precise definition is an open problem, but there have been two approaches to accomplish this free field theories and Gaussian states. Approach A defines circuit complexity as the minimal geodesic in the transformation group of Gaussian states¹¹ that maps a given reference state to the target state we are interested in. The group geometry is induced by a choice of a positive definite metric on the Lie algebra that is extended to the full Lie group by the requirement of right-invariance. Approach B defines circuit complexity as the minimal geodesic distance on the manifold of Gaussian states between reference and target state. In this case, the geometry is fixed by using the natural Fubini-Study metric¹² that is induced from the Hilbert space inner product. We explain how the reference state in approach A induces a natural Hilbert-Schmidt inner product on the Lie algebra, for which we can compute the minimal geodesics analytically. Furthermore, we prove that the projection of these geodesics onto the Gaussian state manifold coincides with the minimal geodesics in approach B. Finally, we show that the computed geodesic distance only differ by an overall normalization constant and thereby explain, why the two approaches led to the same complexity functions when applied to concrete models in praxis.

Outline of dissertation

The structure of this dissertation is as follows.

Part I introduces the mathematical formalism to describe and parametrize Gaussian states using Kähler structures. In chapter 2, we develop the formalism for bosons, and in chapter 3 for fermions. In chapter 4, we summarize and compare the different results with a focus on entanglement and time evolution through quadratic Hamiltonians.

Part II focuses on three applications of this formalism. In chapter 5, we give a geometric definition of entanglement entropy that allows us to prove several theorems about linear growth of the entanglement entropy in the presence of instabilities. In chapter 6, we construct upper and lower bounds for the entanglement entropy averaged over all energy eigenstates in quadratic systems and in particular, prove that the typical entanglement of such energy eigenstates is different from typical entanglement of Haar-random distributed states in the Hilbert space. In chapter 7, we compare two different approaches of defining circuit complexity in bosonic and fermionic free field theories and prove that the two definition coincide up to an overall normalization constant.

The last part provides summary and outlook. We conclude with a comprehensive overview of our results in chapter 8 and discuss possible future direction in chapter 9, in particular current approaches to extend some of our methods and results beyond the class of Gaussian states.

Additional material is provided in three appendices. In appendix A, we prove some basic results on symplectic and metric invariants of restricted complex structures which explains mathematically the admissible correlation structure of Gaussian states. In appendix B, we review some technical definitions relevant for the study of classical dynamical systems, in particular Lyapunov exponents and regular Hamiltonian systems. In appendix C, we review some standard material about the Jordan normal form of symplectic generators, which is relevant for the entanglement production of time-independent quadratic Hamiltonians.

¹¹This group is the symplectic or orthogonal group for bosonic and fermionic systems, respectively.

¹²The manifold of pure states comes with a natural Riemannian metric, called the Fubini-Study metric, which is inherited from the Hilbert space inner product.

Part I

Mathematics of Gaussian states

Chapter 2

Bosonic Gaussian states from Kähler structures

In this chapter, we develop and review methods to describe bosonic Gaussian states in terms of Kähler structures. The chapter is based on [LH08, LH15] with some parts already discussed in [LH03]. The underlying mathematics is discussed in great detail and clarity in [40]. A key idea is to use covariance matrix (encoded in metric G and symplectic form Ω) and linear complex structure to parametrize Gaussian states. Important properties, such as entanglement, can then be computed from invariants of these objects.

2.1 Pure bosonic Gaussian states

We review how symplectic methods and complex structures provide a tool for describing pure bosonic Gaussian states.

2.1.1 Bosonic quantum systems

We consider a quantum system with N bosonic degrees of freedom [45]. The Hilbert space \mathcal{H} of the system carries a regular representation of the commutation relations

$$[\hat{\xi}^a, \hat{\xi}^b] = i\Omega^{ab}. \quad (2.1)$$

Here Ω^{ab} is the symplectic form and the operators $\hat{\xi}^a$ can be understood as the quantization of the classical linear observables ξ^a with Poisson brackets $\{\xi^a, \xi^b\} = \Omega^{ab}$. A Fock representation of the commutation relations (2.1) is obtained by introducing creation and annihilation operators with canonical commutation relations $[\hat{a}_i, \hat{a}_j^\dagger] = \delta_{ij}$, $[\hat{a}_i, \hat{a}_j] = 0$, $[\hat{a}_i^\dagger, \hat{a}_j^\dagger] = 0$. These operators define a set of orthonormal vectors $|n_1, \dots, n_N; \mathcal{D}\rangle$ with $n_i \in \mathbb{N}$, a Fock basis. The Fock vacuum $|0, \dots, 0; \mathcal{D}\rangle$ is defined by

$$\hat{a}_i |0, \dots, 0; \mathcal{D}\rangle = 0, \quad i = 1, \dots, N \quad (2.2)$$

and the n -excitations state $|n_1, \dots, n_N; \mathcal{D}\rangle$ by

$$|n_1, \dots, n_N; \mathcal{D}\rangle = \left(\prod_{i=1}^N \frac{(\hat{a}_i^\dagger)^{n_i}}{\sqrt{n_i!}} \right) |0, \dots, 0; \mathcal{D}\rangle. \quad (2.3)$$

The Hilbert space \mathcal{H} is obtained by completing the span of these vectors in the norm induced by the scalar product $\langle 0, \dots, 0; \mathcal{D} | 0, \dots, 0; \mathcal{D} \rangle = 1$. The label \mathcal{D} refers to a Darboux basis $\mathcal{D} = (q_i, p_i)$ of the classical phase space V . It enters in the definition of the representation of the commutation relations (2.1) in the following way. We define position and momentum operators $\hat{q}_i = q_{ia} \hat{\xi}^a$, $\hat{p}_i = p_{ia} \hat{\xi}^a$ with $\Omega^{ab} q_{ia} p_b^j = \delta^{ij}$ and relate them to the creation and annihilation operators via¹

$$\hat{a}_i = \frac{\hat{q}_i + i \hat{p}_i}{\sqrt{2}}, \quad \hat{a}_i^\dagger = \frac{\hat{q}_i - i \hat{p}_i}{\sqrt{2}}. \quad (2.4)$$

These relations can be inverted to represent the operator $\hat{\xi}^a$ in terms of \hat{a}_i and \hat{a}_i^\dagger ,

$$\hat{\xi}^b = \sum_{i=1}^N (u_i^b \hat{a}_i + u_i^{*b} \hat{a}_i^\dagger), \quad (2.5)$$

with coefficients u_i^a determined by the choice of Darboux basis \mathcal{D} . With these definitions, $[\hat{\xi}^a, \hat{\xi}^b] = i \Omega^{ab}$ on the Hilbert space \mathcal{H} .

2.1.2 Gaussian states and the complex structure J

In (2.2) we defined the Fock vacuum $|0, \dots, 0; \mathcal{D}\rangle$ as the state annihilated by all operators a_i associated to an arbitrary choice of Darboux basis \mathcal{D} in (V, Ω) . Gaussian states provide a generalization of this notion. The relevant structure needed to define a Gaussian state is a complex structure $J^a{}_b$ compatible with the symplectic structure Ω^{ab} defined on phase space. A compatible complex structure $J^a{}_b$ is a linear map on phase space that (i) squares to minus the identity, (ii) is symplectic and (iii) gives rise to a symmetric positive definite metric g_{ab} :

$$(i) \quad J^a{}_c J^c{}_b = -\delta^a{}_b, \quad (ii) \quad J^a{}_c J^b{}_d \Omega^{cd} = \Omega^{ab}, \quad (iii) \quad g_{ab} = \omega_{ac} J^c{}_b. \quad (2.6)$$

We define also the map G^{ab} obtained by raising the indices of the metric g_{ab} with the symplectic structure Ω^{ab} ,

$$G^{ab} = \Omega^{ac} g_{cd} \Omega^{db}, \quad (2.7)$$

Note that by construction G^{ab} is the inverse of the metric g_{ab} , i.e. $G^{ac} g_{cb} = \delta^a{}_b$.

We define the Gaussian state $|J, \zeta\rangle$ as the state annihilated by the operator $a_{J\zeta}^b$, i.e. the solution of the align

$$a_{J\zeta}^b |J, \zeta\rangle = 0 \quad \text{with} \quad a_{J\zeta}^b = \frac{(\hat{\xi}^b - \zeta^b) + i J^b{}_a (\hat{\xi}^a - \zeta^a)}{\sqrt{2}}, \quad (2.8)$$

where $J^a{}_b$ is a compatible complex structure and $\zeta^a \in \mathbb{R}^{2N}$ a vector in phase space. This expression provides a formalization and generalization of (2.2).

The Fock vacuum $|0, \dots, 0; \mathcal{D}\rangle$ defined in (2.2) is an example of Gaussian state. It corresponds to the complex structure $J^a{}_b = \sum_i (\Omega^{ac} q_{ic} q_{ib} + \Omega^{ac} p_{ic} p_{ib})$ and zero shift vector $\zeta^a = 0$,

¹Following our index convention, it would be more natural to write $\hat{a}_i = a_{ib} \hat{\xi}^b$ to emphasize their relation to vectors in the complexified phase space V_C , but we follow the standard convention of writing creation and annihilations operators as \hat{a}_i^\dagger and \hat{a}_i .

i.e. $|0, \dots, 0; \mathcal{D}\rangle = |J, 0\rangle$. Different choices J and \tilde{J} of complex structure are related by a symplectic transformation, $\tilde{J} = M^{-1}JM$. In the language of creation and annihilation operators this operation corresponds to a Bogoliubov transformation [45]. Given a choice of Fock vacuum $|J, 0\rangle$, the state $|\tilde{J}, 0\rangle$ obtained by acting with a Bogoliubov transformation is generally called a squeezed vacuum [46]. On the other hand, a displaced Fock vacuum corresponds to a translation ζ^a in phase space, $|J, \zeta\rangle$, also called a coherent state. For any choice of Darboux basis $\mathcal{D} = (q_i, p_i)$, the Schrödinger representation function $\psi(q_i) = \langle q_i | J, \zeta \rangle$ of a Gaussian state is given by a complex Gaussian function of q_i , which explains their name.

The one-point and the two-point correlation functions of a Gaussian state can be computed directly from the definition (2.8) and are given by

$$\langle J, \zeta | \hat{\xi}^a | J, \zeta \rangle = \zeta^a, \quad (2.9)$$

$$\langle J, \zeta | \hat{\xi}^a \hat{\xi}^b | J, \zeta \rangle = \frac{G^{ab} + i\Omega^{ab}}{2} + \zeta^a \zeta^b \quad \text{with} \quad G^{ab} = -J^a{}_c \Omega^{cb}. \quad (2.10)$$

Higher n -point functions are determined by Wick theorem applied to the operator $\hat{\xi}^a - \zeta^a$. This property corresponds to the absence of non-Gaussianities: Correlations are completely determined by J and ζ . Conversely, given the expectation value ζ^a and the connected symmetric part G^{ab} of the 2-point correlation function, the Gaussian state $|J, \zeta\rangle$ is determined by $J^a{}_b = -G^{ac} \omega_{cb}$.

2.1.3 Action of symplectic group

The Hilbert space \mathcal{H} carries a projective unitary representation of the inhomogeneous symplectic group $\mathrm{ISp}(2N, \mathbb{R}) = \mathbb{R}^{2N} \ltimes \mathrm{Sp}(2N, \mathbb{R})$, which is the semi-direct product of phase space translations and the symplectic group [40, 47, 48]. An element of $\mathbb{R}^{2N} \ltimes \mathrm{Sp}(2N, \mathbb{R})$ can be uniquely parametrized by a pair (η, M) ,

$$\hat{\xi}^a \mapsto M^a{}_b \hat{\xi}^b + \eta^a \quad \text{with} \quad M^a{}_b \in \mathrm{Sp}(2N, \mathbb{R}) \quad \text{and} \quad \eta^a \in \mathbb{R}^{2N}. \quad (2.11)$$

A unitary representation of the inhomogeneous symplectic group,

$$U(M, \eta) \hat{\xi}^a U(M, \eta)^{-1} = M^a{}_b \hat{\xi}^b + \eta^a, \quad (2.12)$$

is provided by the unitary operator $U(M, \eta)$ given by

$$U(M, \eta) = \exp(i\Omega_{ab} \eta^a \hat{\xi}^b) \exp(i\frac{1}{2} h_{ab} \hat{\xi}^a \hat{\xi}^b), \quad (2.13)$$

where the symmetric matrix h_{ab} is defined in terms of the generator of a symplectic transformation by $M^a{}_b = e^{\Omega^{ac} h_{cb}}$.

An immediate consequence of (2.12) is that, for systems with a finite number of degrees of freedom, two Fock space representations associated to different choices of Darboux basis \mathcal{D} and $\tilde{\mathcal{D}} = M\mathcal{D}$ are related by the unitary transformation $U(M)$. This is a special case of the Stone-von Neumann theorem [47, 49]. A second consequence is that classical quadratic observables $\mathcal{O} = \frac{1}{2} h_{ab} \xi^a \xi^b$ promoted to operators $\hat{\mathcal{O}}$ with symmetric (Weyl) ordering have commutation relations that reproduce the classical Poisson brackets, $[\hat{\mathcal{O}}_1, \hat{\mathcal{O}}_2] = i\{\mathcal{O}_1, \mathcal{O}_2\}$.² A third consequence of (2.12) is that the unitary evolution generated by a quadratic Hamiltonian can be fully described in terms of linear symplectic transformations in phase space. This fact plays a major role in the analysis of this paper.

²This property cannot be extended to higher order observables as shown by the Groenewold-Van Hove no-go theorem [50].

2.2 Mixed bosonic Gaussian states

Mixed Gaussian states naturally arise as the reduction of pure Gaussian states to symplectic induced subsystems. However, we can also study mixed Gaussian state in their own right, without thinking of them as reductions to subsystems. The key idea for mixed states is based on bringing G , Ω and J into standard forms, which are derived in appendix A.

2.2.1 Subsystems and the restricted complex structure

We consider a bosonic quantum system consisting of two subsystems A and B with N_A and N_B degrees of freedom. The Hilbert space of the system decomposes in the tensor product of the Hilbert spaces of the two subsystems,

$$\mathcal{H} = \mathcal{H}_A \otimes \mathcal{H}_B. \quad (2.14)$$

The density matrix ρ_A of a pure state $|\psi\rangle \in \mathcal{H}$ restricted to the subsystem A is defined by

$$\rho_A = \text{Tr}_{\mathcal{H}_B}(|\psi\rangle\langle\psi|). \quad (2.15)$$

With this definition, the expectation value of any observable in the subsystem A can be computed directly from the density matrix as a trace over the Hilbert space \mathcal{H}_A ,

$$\langle\psi|\mathcal{O}_A|\psi\rangle = \text{Tr}_{\mathcal{H}_A}(\mathcal{O}_A \rho_A). \quad (2.16)$$

From an operational point of view a subsystem is determined by a subalgebra of observables, i.e. by a restriction of the set of measurements performed on the system. We discuss how the choice of subalgebra of observables identifies the subsystem A , its complement B , and allows us to compute the density matrix of a Gaussian state.

The observables of a bosonic quantum system form a Weyl algebra $\mathcal{A}_V = \text{Weyl}(2N, \mathbb{C})$ generated by linear observables $\hat{\xi}^a$ with commutation relations $[\hat{\xi}^a, \hat{\xi}^b] = i\Omega^{ab}$. We define a subsystem with N_A degrees of freedom by choosing a subalgebra $\mathcal{A}_A \subset \mathcal{A}_V$ generated by a set of N_A linear observables $\hat{\theta}^r$,

$$\hat{\theta}^r = \theta_a^r \hat{\xi}^a \quad \text{with} \quad r = 1, \dots, 2N_A \quad (2.17)$$

and canonical commutation relations

$$[\hat{\theta}^r, \hat{\theta}^s] = i\Omega_A^{rs} \quad (2.18)$$

where $\Omega_A^{rs} = \Omega^{ab}\theta_a^r\theta_b^s$ is required to be a symplectic structure on the vector space $A = \mathbb{R}^{2N_A}$, so that the couple (A, Ω_A) is a symplectic vector space. The Hilbert space \mathcal{H}_A is obtained as a Fock representation of the Weyl algebra $\mathcal{A}_A = \text{Weyl}(2N_A, \mathbb{C})$ as discussed in section 2.1.1. We call ϕ_i, π_i a set of canonical observables in A associated to the Darboux basis $\mathcal{D}_A = (\phi_1, \dots, \phi_{N_A}, \pi_1, \dots, \pi_{N_A})$.

The algebra of observables describing the rest of the system is given by \mathcal{A}'_A , the commutant of \mathcal{A}_A in \mathcal{A}_V defined by

$$\mathcal{A}'_A = \{\mathcal{O} \in \mathcal{A}_V \mid [\mathcal{O}_A, \mathcal{O}] = 0 \text{ for all } \mathcal{O}_A \in \mathcal{A}_A\}, \quad (2.19)$$

i.e. the set of all operators which commute with all operators in \mathcal{A}_A . Here, the commutant \mathcal{A}'_A is generated by linear operators with coefficients in B , the symplectic complement of A . Let us consider the subalgebra $\mathcal{A}_B \subset \mathcal{A}_V$ generated by a set of N_B linear observables $\hat{\Theta}^k$,

$$\hat{\Theta}^k = \Theta_a^k \hat{\xi}^a \quad \text{with} \quad k = 1, \dots, 2N_B \quad (2.20)$$

and canonical commutation relations

$$[\hat{\Theta}^k, \hat{\Theta}^h] = i\Omega_B^{kh} \quad \text{and} \quad [\hat{\theta}^r, \hat{\Theta}^k] = 0 \quad (2.21)$$

where $\Omega_B^{kh} = \Omega^{ab}\Theta_a^k\Theta_b^h$ is required to be a symplectic structure on the vector space $B^* = \mathbb{R}^{2N_B}$, so that (B^*, Ω_B) is a symplectic space. The requirement that B^* is the symplectic complement of A^* results in the commutation relation $[\hat{\theta}^r, \hat{\Theta}^k] = 0$. The Hilbert space \mathcal{H}_B is obtained as a Fock representation of the Weyl algebra $\mathcal{A}'_A = \mathcal{A}_B = \text{Weyl}(2N_B, \mathbb{C})$. We call Φ_i, Π_i a set of canonical observables in B^* dual to the Darboux basis $\mathcal{D}_B = (\Phi_1, \dots, \Phi_{N_B}, \Pi_1, \dots, \Pi_{N_B})$.

The subalgebra \mathcal{A}_A has a trivial center,³ i.e. $\mathcal{A}_A \cap \mathcal{A}'_A = \mathbb{1}$. As a result the algebra of observables of the systems decomposes in a tensor product over the subsystem A and its complement, $\mathcal{A}_V = \mathcal{A}_A \otimes \mathcal{A}_B$, and the Hilbert space of the system decomposes in the tensor product $\mathcal{H} = \mathcal{H}_A \otimes \mathcal{H}_B$. This decomposition reproduces at the quantum level the decomposition of phase space V in two symplectic complements A and B with Darboux basis $\mathcal{D}_V = (\mathcal{D}_A, \mathcal{D}_B)$.

Given a subsystem A , the Gaussian state $|J, \zeta\rangle \in \mathcal{H}$ admits a Schmidt decomposition that selects the Darboux basis \mathcal{D}_A and \mathcal{D}_B in the two complementary subsystems so that the state can be written in the form [51]

$$|J, \zeta\rangle = \sum_{n_i=0}^{\infty} \left(\prod_{i=1}^{N_e} \sqrt{\frac{2(\nu_i - 1)^{n_i}}{(\nu_i + 1)^{n_i+1}}} \right) U(\zeta_A) |n_1, \dots, n_{N_e}, 0, \dots; \mathcal{D}_A\rangle \otimes U(\zeta_B) |n_1, \dots, n_{N_e}, 0, \dots; \mathcal{D}_B\rangle. \quad (2.22)$$

The unitary operator $U(\zeta_A)$ generates a shift in A with parameter $\zeta_A^r = \theta_a^r \zeta^a$. Note that $U(\zeta) = U(\zeta_A) \otimes U(\zeta_B)$. The parameters ν_i are the positive eigenvalues of the matrix $[iJ]_A = (i\theta_a^r J^a{}_b \vartheta_s^b)$ obtained as the restriction to A of iJ ,

$$\text{Eig}([iJ]_A) = \{\pm \nu_i\} \quad \text{with} \quad \nu_i \geq 1. \quad (2.23)$$

The condition $\nu_i \geq 1$ follows from the fact that the matrix $[J]_A$ is the restriction of a complex structure in V . We define the number of *entangled pairs* in the decomposition $\mathcal{H}_A \otimes \mathcal{H}_B$ as the number of non-trivial terms in the sum in (2.22). This is also the number of positive eigenvalues of $[iJ]_A$ that differ from $+1$, or equivalently the rank of the matrix $\mathbb{1} - ([iJ]_A)^2$,

$$N_e = \text{rank}(\mathbb{1} - ([iJ]_A)^2) \leq \min(N_A, N_B). \quad (2.24)$$

Note that the positive eigenvalues $\nu_i \neq 1$ of $[iJ]_A$ and of $[iJ]_B$ coincide, see figure 2.1. If all $\nu_i = 1$, then $N_e = 0$ and the Gaussian state $|J, \zeta\rangle$ factorizes in a tensor product of Gaussian states.

The reduced density matrix ρ_A of a Gaussian state is immediate to obtain once the Schmidt decomposition is known,

$$\rho_A(J, \zeta) = \text{Tr}_{\mathcal{H}_A}(|J, \zeta\rangle \langle J, \zeta|) = U(\zeta_A) \rho_A(J) U(\zeta_A)^{-1} \quad (2.25)$$

³We give an example of subsystem defined by a subalgebra with non-trivial center. Consider a bosonic system with $N = 3$ degrees of freedom. The algebra \mathcal{A}_V of observables of the system is generated by elements of the Darboux basis $\mathcal{D}_V = (q_1, q_2, q_3, p_1, p_2, p_3)$. Let us consider the subalgebra \mathcal{A}_C generated by (q_1, p_1, q_2) . Its commutant is $\mathcal{A}'_C = (q_3, p_3, q_2)$. As a result this subalgebra has a non-trivial center $\mathcal{Z}_C = \mathcal{A}_C \cap \mathcal{A}'_C = (\mathbb{1}, q_2)''$. In this case the algebra of observables of the system decomposes in $\mathcal{A}_V = \bigoplus_{\lambda} (\mathcal{A}_C^{(\lambda)} \otimes \mathcal{A}'_C^{(\lambda)})$ and the Hilbert space decomposes in a direct sum of tensor products $\mathcal{H} = \bigoplus_{\lambda} (\mathcal{H}_C^{(\lambda)} \otimes \mathcal{H}'_C^{(\lambda)})$ where λ is a basis of simultaneous eigenstates of the operators in the center (eigenstates of q_2 in this example). Choosing a symplectic subspace as done in (2.18) guarantees that the center of the subalgebra is trivial and the Hilbert space decomposes into a tensor product.

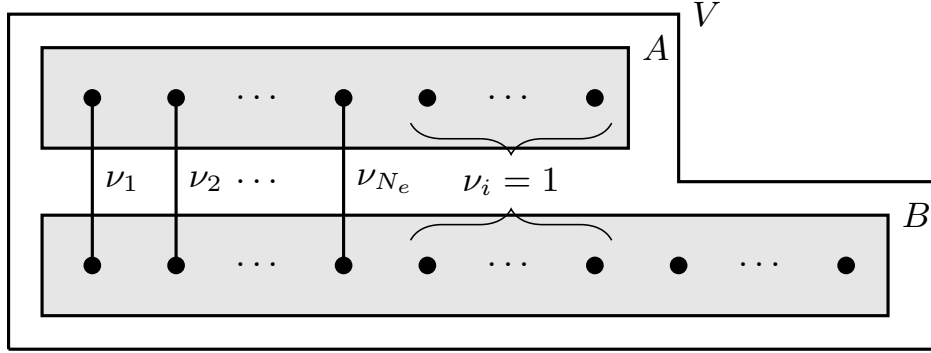


Figure 2.1: *Entanglement structure of Gaussian states.* We illustrate the entanglement structure of an arbitrary squeezed vacuum $|J\rangle$ with subsystems A and B : We can always find a Darboux frame $\mathcal{D}_V = (\mathcal{D}_A, \mathcal{D}_B)$, such that only pairs of degrees of freedom are entangled across A and B with squeezing parameters ν_i . Every black dot represents a degree of freedom, or equivalently a conjugate variable pair (φ_i, π_i) appearing as basis vectors in \mathcal{D}_A or \mathcal{D}_B , every link represents the entanglement between the two connected degrees of freedom. Note that we take $N_A \leq N_B$ and find that only up to N_A pairs can be entangled. The remaining $N_B - N_A$ degrees of freedom in subsystem B do not have a partner in subsystem A leading to squeezing parameters $\nu_i = 0$ for $i > N_A$. This is the reason why the maximal number of entangled degrees of freedom is dictated by the smaller of the two subsystems.

where

$$\rho_A(J) = \sum_{n_i=0}^{\infty} \left(\prod_{i=1}^{N_e} \frac{2}{\nu_i + 1} \left(\frac{\nu_i - 1}{\nu_i + 1} \right)^{n_i} \right) |n_1, \dots, n_{N_e}, 0, \dots; \mathcal{D}_A\rangle \langle n_1, \dots, n_{N_e}, 0, \dots; \mathcal{D}_A|. \quad (2.26)$$

We note that the density matrix can be written in the compact operatorial form

$$\rho_A(J) = e^{-H_A} = \sum_{n_1, \dots, n_{N_A}=0}^{\infty} \left(\prod_{i=1}^{N_A} \frac{(\tanh r_i)^{n_i}}{\cosh r_i} \right)^2 |n_1, \dots, n_{N_A}\rangle \langle n_1, \dots, n_{N_A}| \quad (2.27)$$

with the modular Hamiltonian H_A given by

$$\hat{H}_A = q_{rs} \hat{\theta}^r \hat{\theta}^s + E_0 \quad \text{with} \quad q = i\omega \operatorname{arcoth}(i[J]_A) \quad \text{and} \quad E_0 = \frac{\log \det([J]_A^2 (\mathbb{1}_A - [J]_A^2))}{4}, \quad (2.28)$$

where $(J^r_s) = (\theta_a^r J^a_b \vartheta_s^b) = [J]_A$, $(\omega_{rs}) = (\vartheta_r^a \omega_{ab} \vartheta_s^b) = [\omega]_A = [\Omega^{-1}]_A$, and E_0 is a constant that fixes the normalization $\operatorname{Tr}_{\mathcal{H}_A} \rho_A = 1$.

2.2.2 Entanglement entropy and Rényi entropy

Complete knowledge of the state of a system does not imply knowledge of the state of its subsystems. This genuinely quantum-mechanical property is captured by the notion of entanglement entropy. The entanglement entropy $S_A(|\psi\rangle)$ of a pure state $|\psi\rangle$ restricted to the subsystem A is given by the von Neumann entropy of the reduced state,

$$S_A(|\psi\rangle) = -\operatorname{Tr}_{\mathcal{H}_A} (\rho_A \log \rho_A). \quad (2.29)$$

To compute the entanglement entropy it is useful to introduce the function $Z(\beta)$ defined as the trace of the density matrix raised to the power β ,

$$Z(\beta) = \text{Tr}_{\mathcal{H}_A} (\rho_A^\beta). \quad (2.30)$$

By construction $Z(0) = N_A$ and $Z(1) = 1$. The function $Z(\beta)$ provides an efficient method for computing the entanglement entropy,

$$S_A(|\psi\rangle) = \left(1 - \beta \frac{\partial}{\partial \beta}\right) \log Z(\beta) \Big|_{\beta=1}. \quad (2.31)$$

In the case of a Gaussian state $|J, \zeta\rangle$, the function $Z(\beta)$ can be expressed in term of the eigenvalues of $[\text{i}J]_A$ using formulae (2.25) and (2.26),

$$\log Z(\beta) = - \sum_{i=1}^{N_e} \log \left(\left(\frac{\nu_i + 1}{2} \right)^\beta - \left(\frac{\nu_i - 1}{2} \right)^\beta \right). \quad (2.32)$$

It can also be expressed as a trace over the vector space A of a function of the matrix $[\text{i}J]_A$,

$$\log Z(\beta) = -\frac{1}{2} \text{tr} \log \left| \left| \frac{1 + [\text{i}J]_A}{2} \right|^\beta - \left| \frac{1 - [\text{i}J]_A}{2} \right|^\beta \right|. \quad (2.33)$$

The entanglement entropy of a Gaussian state can be computed from $Z(\beta)$ and expressed in terms of the eigenvalues ν_i , [17, 52–54]

$$S_A(|J, \zeta\rangle) = \sum_{i=1}^{N_e} S(\nu_i) \quad \text{where} \quad S(\nu) = \frac{\nu + 1}{2} \log \frac{\nu + 1}{2} - \frac{\nu - 1}{2} \log \frac{\nu - 1}{2}, \quad (2.34)$$

or equivalently in terms of the matrix $[\text{i}J]_A$, [51]

$$S_A(|J, \zeta\rangle) = \text{tr} \left(\frac{1 + [\text{i}J]_A}{2} \log \left| \frac{1 + [\text{i}J]_A}{2} \right| \right). \quad (2.35)$$

We can also compute the Rényi entropy of order two,⁴

$$R_A(|\psi\rangle) = -\log \text{Tr}_{\mathcal{H}_A} (\rho_A^2) = -\log Z(2). \quad (2.36)$$

The Rényi entropy of a Gaussian state is

$$R_A(|J, \zeta\rangle) = \sum_{i=1}^{N_e} \log \nu_i, \quad (2.37)$$

which can be expressed in terms of the determinant of the matrix $[\text{i}J]_A$,

$$R_A(|J, \zeta\rangle) = \frac{1}{2} \log |\det([\text{i}J]_A)|. \quad (2.38)$$

This expression plays a central role in the analysis presented in this paper in section 5.1.

⁴The Rényi entropy of order n is defined as $R_A^{(n)}(|\psi\rangle) = -\frac{1}{n-1} \log \text{Tr}_{\mathcal{H}_A} (\rho_A^n) = -\frac{1}{n-1} \log Z(n)$.

2.3 Time evolution

We consider a quadratic time-dependent Hamiltonian $H(t)$,

$$H(t) = \frac{1}{2} h_{ab}(t) \hat{\xi}^a \hat{\xi}^b + f_a(t) \hat{\xi}^a. \quad (2.39)$$

The unitary evolution operator solves the Schrödinger align $i \frac{\partial}{\partial t} U(t) = H(t) U(t)$ and is given by the time-ordered exponential

$$U(t) = \mathcal{T} \exp \left(-i \int_0^t H(t') dt' \right). \quad (2.40)$$

The evolution of the observable $\hat{\xi}^a$ is then given by

$$U(t) \hat{\xi}^a U(t)^{-1} = M^a{}_b(t) \hat{\xi}^b + \eta^a(t), \quad (2.41)$$

where $M^a{}_b(t)$ and $\eta^a(t)$ are defined by the classical Hamiltonian evolution.

An important property of Gaussian states is that they provide exact solutions of the Schrödinger align for a time-dependent quadratic Hamiltonian (2.39),

$$i \frac{\partial}{\partial t} |J_t, \zeta_t\rangle = H(t) |J_t, \zeta_t\rangle. \quad (2.42)$$

Given a Gaussian state $|J_0, \zeta_0\rangle$ at the time $t = 0$, the state at the time t is

$$|J_t, \zeta_t\rangle = U(t) |J_0, \zeta_0\rangle, \quad (2.43)$$

with J_t and ζ_t determined as follows. The align (2.42) defined on the Hilbert space \mathcal{H} results in linear aligns for the matrix J_t and the vector ζ_t on phase space,

$$\frac{\partial}{\partial t} J_t = K(t) J_t - J_t K(t), \quad (2.44)$$

$$\frac{\partial}{\partial t} \zeta_t = K(t) \zeta_t + k(t), \quad (2.45)$$

with the matrix $K^a{}_b(t) = (\Omega^{ac} h_{cb}(t))$ and the vector $k^a(t) = (\Omega^{ab} f_b(t))$ are defined in terms of the parameters of the quadratic time-dependent Hamiltonian $H(t)$, (2.39). The linear aligns for the complex structure J_t and the shift η_t can be solved as time-ordered series,

$$J_t = M(t) J_0 M^{-1}(t) \quad (2.46)$$

$$\zeta_t = M(t) \zeta_0 + M(t) \int_0^t M^{-1}(t') k(t') dt' \quad (2.47)$$

where J_0 and ζ_0 are initial conditions and

$$M(t) = \mathcal{T} \exp \left(\int_0^t K(t') dt' \right) \quad (2.48)$$

is the symplectic matrix discussed.

Given an initial state $|J_0, \zeta_0\rangle$ and a quadratic time-dependent Hamiltonian $H(t)$, the evolution of the one-point and two-point correlation functions are given by (2.9) and (2.10) with $\zeta = \zeta_t$ and $G_t^{ab} = -J_t{}^a{}_c \Omega^{cb}$.

Chapter 3

Fermionic Gaussian states from Kähler structures

In this chapter, we develop and review methods to describe fermionic Gaussian states in terms of Kähler structures. The chapter is based on [LH15] with some parts already discussed in [LH07]. The underlying mathematics is discussed in great detail and clarity in [40], similar to the bosonic structures. We should emphasize that this chapter follows closely the structure of chapter 2 to emphasize the similarities to the bosonic construction.

3.1 Pure fermionic Gaussian states

We begin by reviewing how fermionic Gaussian states can be described by linear complex structures, equipped with a natural action of the orthogonal group.

3.1.1 Fermionic quantum systems

We consider a quantum system with N fermionic degrees of freedom. The classical phase space V is isomorphic to \mathbb{R}^{2N} and the Hilbert space carries a regular representation of the anticommutation relations

$$\{\hat{\xi}^a, \hat{\xi}^b\} = G^{ab}. \quad (3.1)$$

Here, G^{ab} is a positive definite metric on the dual of phase space and $\hat{\xi}^a$ represents the quantization of linear observables and is often referred to as Majorana modes. A Fock representation of the anticommutation relations (3.1) is obtained by introducing creation and annihilation operators with anticommutation relations $\{\hat{a}_i, \hat{a}_j^\dagger\} = \delta_{ij}$ and $\{\hat{a}_i, \hat{a}_j\} = \{\hat{a}_i^\dagger, \hat{a}_j^\dagger\} = 0$. For this, we choose an orthonormal basis $\mathcal{D} = (q_1, p_1, \dots, q_N, p_N)$ of V^* with respect to G^{ab} . The associated quantum operators are given by $\hat{q}_i = q_i \hat{\xi}^a$, from which we can construct the creation annihilation operators

$$\hat{a}_i = \frac{\hat{q}_i + i\hat{p}_i}{\sqrt{2}} \quad \text{and} \quad \hat{a}_i^\dagger = \frac{\hat{q}_i - i\hat{p}_i}{\sqrt{2}}. \quad (3.2)$$

The Fock representation is then built on the Fock vacuum $|0, \dots, 0; \mathcal{D}\rangle$ satisfying

$$\hat{a}_i |0, \dots, 0; \mathcal{D}\rangle = 0. \quad (3.3)$$

The fermionic Fock space $\mathcal{H} = (\mathbb{C}^2)^N$ is then given by the completion of the vector span with respect to the orthonormal excited states

$$|n_1, \dots, n_N; \mathcal{D}\rangle = \left(\prod_{i=1}^N (\hat{a}_i^\dagger)^{n_i} \right) |0, \dots, 0; \mathcal{D}\rangle. \quad (3.4)$$

Similar to the bosonic case, we can invert these relations to express general linear observables $\hat{\xi}^a$ in terms of \hat{a}_i and \hat{a}_i^\dagger , namely

$$\hat{\xi}^b = \sum_{i=1}^N (u_i^b \hat{a}_i + u_i^{*b} \hat{a}_i^\dagger). \quad (3.5)$$

This choice gives rise to a representation of the abstract algebra generated by $\hat{\xi}^a$ as operators acting on \mathcal{H} .

3.1.2 Gaussian states and the complex structure J

In (3.3), we defined the fermionic Fock vacuum $|0, \dots, 0; \mathcal{D}\rangle$ as the state annihilated by all \hat{a}_i associated to the orthonormal basis \mathcal{D} . The set of all fermionic Fock vacua forms the space of Gaussian states, but given two bases \mathcal{D} and $\tilde{\mathcal{D}}$, they may define the same vacuum.¹ Similar to bosonic case, we can use a linear complex structure to parametrize the space of fermionic Gaussian states. In this case, we require compatibility with the metric G^{ab} that governs the anti-commutation relations. A compatible complex structure $J^a{}_b$ is a linear map on phase space that (i) squares to minus the identity and (ii) is orthogonal:

$$(i) \quad J^a{}_c J^c{}_b = -\delta^a{}_b, \quad (ii) \quad J^a{}_c J^b{}_d G^{cd} = G^{ab}. \quad (3.6)$$

The bilinear form $\Omega^{ab} = J^a{}_c G^{cb}$ is non-degenerate and antisymmetric, which implies that it is valid symplectic form on the dual of phase space. Its inverse is given by

$$\omega_{ab} = g_{ac} \Omega^{cd} g_{db}, \quad (3.7)$$

satisfying $\Omega^{ac} \omega_{cb} = \delta^a{}_b$.

We define the fermionic Gaussian state $|J\rangle$ as the state annihilated by the operator \hat{a}_J^b , *i.e.*, the solution of the equation

$$\hat{a}_J^b |J\rangle = 0 \quad \text{with} \quad \hat{a}_J^b = \frac{1}{\sqrt{2}} (\hat{\xi}^b + i J^b{}_a \hat{\xi}^a). \quad (3.8)$$

In contrast to fermions, we do not include a shift ζ^a , because such a shift vector would necessarily need to be a Grassmann number which means that the Hilbert space itself would need to be extended to allow Grassmann coefficients. Such “coherent fermionic states” can still be used as an

¹If \mathcal{D} and $\tilde{\mathcal{D}}$ define the same Fock vacuum, the relevant annihilation operators are mixed among themselves corresponding to a $U(N)$ transformation. Even though, the different bases define the same vacuum, the Fock representations will be different because for the full representation, we need to keep track of the individual excitations which will be different for \mathcal{D} and $\tilde{\mathcal{D}}$.

overcomplete basis of the Hilbert space, but not as physical states of the system. For our class of physical fermionic Gaussian states, we therefore have

$$\langle J | \hat{\xi}^a | J \rangle = 0 , \quad (3.9)$$

$$\langle J | \hat{\xi}^a \hat{\xi}^b | J \rangle = \frac{1}{2} \left(G^{ab} + i\Omega^{ab} \right) \quad \text{with} \quad \Omega^{ab} = J^a{}_c G^{cb} . \quad (3.10)$$

$$(3.11)$$

Higher n -point functions are determined by Wick's theorem applied to $\hat{\xi}^a$. The symmetric part of any n -point function is completely fixed by the anticommutation relations, while the antisymmetric part can be deduced from Ω^{ab} . This implies that we can use Ω^{ab} as equivalent way to parametrize the state. Comparing to the fermionic case, G and Ω have swapped their roles, while J provides in both cases a unifying structure to label Gaussian states.

3.1.3 Action of orthogonal group

The Hilbert space \mathcal{H} carries a projective representation of the orthogonal group $O(2N)$. We identify group elements with linear maps on V that preserve G^{ab} , namely

$$O(2N) = \left\{ M^a{}_b \in GL(V) \mid M^a{}_c G^{cd} (M^\intercal)_d{}^b = G^{ab} \right\} . \quad (3.12)$$

This representation is generated by quadratic generators of the form

$$\hat{H} = \frac{i}{2} h_{ab} \hat{\xi}^a \hat{\xi}^b , \quad (3.13)$$

where h_{ab} is an antrisymmetric bilinear form. Here, we identify the quantum generator \hat{H} with the orthogonal generator $K^a{}_b = G^{ac} h_{cb}$. The group component connected to the identity is given by the subgroup $SO(2N)$ whose projective representation formed by unitary operators

$$\hat{U}(M = e^K) = e^{-i\hat{H}} \quad (3.14)$$

and their products, can be identified with the spin group $Spin(2N)$. This can be extended to the full group $O(2N)$ and its projective representation that can be identified with a representation of the Pin group Pin . We can illustrate the construction based on the explicit representation with respect to an orthonormal basis \mathcal{D}_V , such that G , Ω and J take their standard forms

$$\Omega \equiv \bigoplus_{i=1}^N \begin{pmatrix} 0 & 1 \\ -1 & 0 \end{pmatrix} , \quad G \equiv \bigoplus_{i=1}^N \begin{pmatrix} 1 & 0 \\ 0 & 1 \end{pmatrix} , \quad J \equiv \bigoplus_{i=1}^N \begin{pmatrix} 0 & 1 \\ -1 & 0 \end{pmatrix} . \quad (3.15)$$

A natural example of an element $M \in O(2N) \setminus SO(2N)$ expressed in this basis is

$$M = \text{diag}(1, -1, 1, \dots, 1) . \quad (3.16)$$

In physical terms, just swappes $\hat{a}_1 \leftrightarrow \hat{a}_1^\dagger$, while leaving all other annihilation operators unchanged. Its unitary representation as quantum operator $\hat{U}(M) \in Pin(2N) \setminus Spin(2N)$ acting on the Fock basis is therefore given by

$$\hat{U}(M) |n_1, \dots, n_N; \mathcal{D}\rangle = |n_1 + 1, \dots, n_N; \mathcal{D}\rangle , \quad (3.17)$$

where we have $1 + 1 \equiv 0$ due to the \mathbb{Z}_2 structure occupation numbers. The full group of $O(2N)$ or $\text{Pin}(2N)$ is then generated by applying arbitrary group elements of $\text{SO}(2N)$ or $\text{Spin}(2N)$ to 1 and M or $\hat{U}(M)$, respectively. This is closely related to a \mathbb{Z}_2 grading of the space of Gaussian states. Representing a Gaussian state $|J\rangle$ with respect to a Fock basis $|n_1, \dots, n_N; \mathcal{D}\rangle$, it will only consist of linear combinations of even or odd basis states, *i.e.*, those basis vectors $|n_1, \dots, n_N; \mathcal{D}\rangle$ with $\sum_{i=1}^N n_i$ either even or odd. If it is even or odd will depend on the specific choice of \mathcal{D} , in particular, we can always choose \mathcal{D} , such that J takes the standard form and we have $|J\rangle = |0, \dots, 0; \mathcal{D}\rangle$.

In summary, the manifold of Gaussian states consists of two disconnected components and the group elements that are not connected to the identity are the ones that move us between these components when applied to states.

3.2 Mixed fermionic Gaussian states

The key idea of describing mixed fermionic Gaussian states with restricted complex structures is that all invariant properties, such as spectrum of the mixed density operator, can be read off from bringing the restricted complex structure into a standard form, as discussed in appendix A. For mixed Gaussian states, all features are fully encoded in the invariants of the restricted complex structure.

3.2.1 Subsections and restricted complex structure

We consider a fermionic system consisting of two subsystems A and B with N_A and N_B degrees of freedom. The Hilbert space of the system decomposes into a tensor product of the Hilbert spaces of the subsystems,

$$\mathcal{H} = \mathcal{H}_A \otimes \mathcal{H}_B. \quad (3.18)$$

The density matrix ρ_A of a pure state $|\psi\rangle$ reduced to A is defined as

$$\rho_A = \text{Tr}_{\mathcal{H}_B} (|\psi\rangle\langle\psi|). \quad (3.19)$$

From an operational point of view, the quantum state restricted to the subsystem A is fully characterized by all expectation values of observables \mathcal{O}_A in the subsystem, computed as

$$\langle \mathcal{O}_A \rangle = \langle \psi | \mathcal{O}_A | \psi \rangle = \text{Tr}(\mathcal{O}_A \rho_A). \quad (3.20)$$

This is related to the abstract algebraic perspective where a state is fully determined as positive linear functional on the algebra of observables determining the any expectation values.

The observables of a fermionic quantum system form a Clifford algebra $\mathcal{A}_V = \text{Cliff}(2N, \mathbb{C})$ generated by the linear observables $\hat{\xi}^a$ with anticommutation relations $\{\hat{\xi}^a, \hat{\xi}^b\} = G^{ab}$. Similar to the bosonic case, a subsystem with N_A degrees of freedom is a subalgebra $\mathcal{A}_A \subset \mathcal{A}_V$ generated by a set of $2N_A$ linear observables

$$\hat{\theta}^r = \theta_a^r \hat{\xi}^a \quad (3.21)$$

and canonical anticommutation relations $\{\hat{\theta}^r, \hat{\theta}^s\} = [G]_A^{rs}$. Therefore, the subsystem algebra is completely determined by an even dimensional subspace $A \subset V$.² The subsystem Hilbert space

²We should mention that there exist other sub algebras that are not generated in this way. For instance, by applying a general unitary transformation U to the representation of \mathcal{A}_A which will be generated by (in general) non-linear observables $U\hat{\theta}^a U^\dagger$. However, these subalgebras are usually not as interesting for physical applications, because they cannot be directly associated to a partial collection of degrees of freedom in V .

\mathcal{H}_A is constructed from $\hat{\theta}^a$ in the same way as \mathcal{H} from $\hat{\xi}^a$. The requirement for the complementary subalgebra \mathcal{A}_B is that its generators $\hat{\Theta}^r$ anticommute with the generators $\hat{\theta}^r$ of \mathcal{A}_A :

$$\{\hat{\theta}^r, \hat{\Theta}^s\} = 0. \quad (3.22)$$

This requirement is equivalent to A^* and B^* being orthogonal subspaces with respect to G^{ab} or, equivalently, A and B being orthogonal with respect to g_{ab} . Relating this to bosonic subsystems, we replace the decomposition into symplectic complements by a decomposition into orthogonal complements $V = A \oplus B$.

Given a subsystem decomposition $V = A \oplus B$, the Gaussian state admits a Schmidt decomposition related to the orthonormal bases $\mathcal{D}_A = (\phi_1, \pi_1, \dots, \phi_{N_A}, \pi_{N_A})$ and $\mathcal{D}_B = (\Phi_1, \Pi_1, \dots, \Phi_{N_B}, \Pi_{N_B})$ that bring J into the standard block diagonal form outlined in appendix A. Assuming $N_A \leq N_B$ without loss of generality, J can always be brought into the form

$$J \equiv \bigoplus_{i=1}^{N_A} \begin{pmatrix} 0 & \cos 2r_i & 0 & \sin 2r_i \\ -\cos 2r_i & 0 & -\sin 2r_i & 0 \\ 0 & -\sin 2r_i & 0 & \cos 2r_i \\ \sin 2r_i & 0 & -\cos 2r_i & 0 \end{pmatrix} \oplus \bigoplus_{i=1}^{N_B - N_A} \begin{pmatrix} 0 & 1 \\ -1 & 0 \end{pmatrix}, \quad (3.23)$$

where the first summands are with respect to $(\phi_i, \pi_i, \Phi_i, \Pi_i)$ for $1 \leq i \leq N_A$ and the second with respect to (Φ_i, Π_i) for $N_A + 1 \leq i \leq N_B$. This implies that the restricted complex structure takes on the standard form

$$[J]_A \equiv \bigoplus_{i=1}^{N_A} \begin{pmatrix} 0 & \cos 2r_i \\ -\cos 2r_i & 0 \end{pmatrix} \quad (3.24)$$

with eigenvalues $\pm \nu_i = \pm i \cos 2r_i$. This choice of basis identifies how each degree of freedom (ϕ_i, π_i) in A is entangled with a corresponding degree of freedom (Φ_i, Π_i) in B , except for $r_i = 0$. This reproduces the entanglement structure of bosonic Gaussian states illustrated in figure 2.1. We will be able to describe all entanglement properties of the reduced state ρ_A in terms of ν_i or, equivalently, the squeezing parameters r_i .

We can use this representation to find the Schmidt decomposition of the state $|J\rangle$ explicitly that is spanned by Fock basis elements $|n_1, \dots, n_N; \mathcal{D}\rangle$. The resulting expression is similar to the bosonic one and given by

$$|J\rangle = \sum_{n_i=0}^1 \left(\prod_{i=1}^{N_A} \frac{(\tan r_i)^{n_i}}{\sec r_i} \right) |n_1, \dots, n_{N_A}\rangle \otimes |n_1, \dots, n_{N_A}, 0, \dots, 0\rangle. \quad (3.25)$$

We can express the associated the density operator in compact operational form

$$\rho_A(J) = e^{-\hat{H}_A} = \sum_{n_1, \dots, n_{N_A}=0}^1 \left(\prod_{i=1}^{N_A} \frac{(\tan r_i)^{n_i}}{\sec r_i} \right)^2 |n_1, \dots, n_{N_A}\rangle \langle n_1, \dots, n_{N_A}| \quad (3.26)$$

with the modular Hamiltonian H_A given by

$$H_A = iq_{rs}\hat{\theta}^r\hat{\theta}^s + E_0 \quad \text{with} \quad q = i[g]_A \operatorname{arcoth}(i[J]_A) \quad \text{and} \quad E_0 = \frac{\log \det([J]_A^2(\mathbb{1}_A + [J]_A^2))}{4}, \quad (3.27)$$

where we find q and E_0 directly from $[J]_A$.

3.2.2 Entanglement entropy and Rényi entropy

The definitions of entanglement and Rényi entropy are identical for bosonic systems and given by

$$S_A(|\psi\rangle) = -\text{Tr}\rho_A \log \rho_A \quad \text{and} \quad R_A^{(n)}(|\psi\rangle) = -\frac{1}{n-1} \log \text{Tr}\rho_A^n. \quad (3.28)$$

Using the characteristic function $Z(\beta) = \text{Tr}(\rho_A^\beta)$, we can compute them efficiently as

$$S_A(|\psi\rangle) = \left(1 - \beta \frac{\partial}{\partial \beta}\right) \log Z(\beta) \Big|_{\beta=0} \quad \text{and} \quad R_A^{(n)} = -\frac{1}{n-1} \log Z(n). \quad (3.29)$$

For Gaussian states $|J\rangle$, we can use the explicit form of ρ_A given in (3.26) to find the characteristic function in terms of $[iJ]_A$ or its eigenvalues, namely

$$\log Z(\beta) = -\frac{1}{2} \text{Tr} \log \left| \left| \frac{\mathbb{1}_A + [iJ]_A}{2} \right|^{\beta} + \left| \frac{\mathbb{1}_A - [iJ]_A}{2} \right|^{\beta} \right| \quad (3.30)$$

$$= -\sum_{i=1}^{N_A} \left(\left(\frac{1+\nu_i}{2} \right)^{\beta} + \left(\frac{1-\nu_i}{2} \right)^{\beta} \right). \quad (3.31)$$

This leads to the entanglement entropy given by

$$S_A(|J\rangle) = \sum_{i=1}^{N_A} S(\nu_i) \quad \text{where} \quad S(\nu) = -\frac{1+\nu}{2} \log \frac{1+\nu}{2} - \frac{1-\nu}{2} \log \frac{1-\nu}{2}. \quad (3.32)$$

This can be rephrased for the linear complex structure in a compact formula that coincides for bosons and fermions and is given by

$$S_A(|J\rangle) = \left| \text{Tr} \left(\frac{\mathbb{1}_A + i[J]_A}{2} \right) \log \left| \frac{\mathbb{1}_A + i[J]_A}{2} \right| \right|, \quad (3.33)$$

where the outer absolute value is needed for fermions and the inner one for bosons. Even though, we found a single unifying expression of the entanglement entropy of bosonic and fermionic Gaussian states, the possible value for the entropy differs. For bosons, the entanglement entropy per degree of freedom can be arbitrarily large, while it is bounded from above by $\log 2$ for fermions as consequence of the finite dimensional Hilbert space \mathcal{H}_A .

The Rényi entropy of order n can be computed from $Z(\beta)$ and elegantly expressed in terms of the squeezing parameters r_i as

$$R_A^{(n)} = -\frac{1}{\alpha-1} \sum_{i=1}^{N_A} \log (\cos^{2n} r_i + \sin^{2n} r_i). \quad (3.34)$$

3.3 Time evolution

The most general quadratic fermionic Hamiltonian $H(t)$ is given by

$$\hat{H}(t) = \frac{i}{2} h_{ab}(t) \hat{\xi}^a \hat{\xi}^b. \quad (3.35)$$

In contrast to the bosonic case, the bilinear form h_{ab} is antisymmetric which leads to the requirement of i in front to make the operator hermitian. The solution of Schrödinger's equation $i\frac{\partial}{\partial t}U(t) = H(t)U(t)$ is given by the time ordered exponential

$$U(t) = \mathcal{T} \exp \left(-i \int_0^t H(t') dt' \right). \quad (3.36)$$

The evolution of the observable $\hat{\xi}^a$ satisfies

$$U(t)\xi^a(t)U^\dagger(t) = M^a{}_b(t)\xi^b, \quad (3.37)$$

where $M^a{}_b(t)$ is the classical Hamiltonian flow solving the classical equations of motion. It is generated by the orthogonal generator $K(t)^a{}_b = G^{ac}h_{cb} \in \mathfrak{so}(2N)$ and the solution can be written as time-ordered exponential

$$M(t) = \mathcal{T} \exp \left(\int_0^t K(t') dt' \right) \in \mathrm{SO}(2N). \quad (3.38)$$

We can use the representation of the orthogonal group which ensures that the time evolution of an initial Gaussian state stays Gaussian. We can therefore write the Schrödinger equation

$$i\frac{\partial}{\partial t}|J_t\rangle = \hat{H}(t)|J_t\rangle, \quad (3.39)$$

which is solved by $|J_t\rangle = U(t)|J_0\rangle$, directly as equation in terms of J_t :

$$\frac{\partial}{\partial t}J_t = K(t)J_t - J_tK(t), \quad (3.40)$$

which is solved by $J_t = M(t)J_0M^{-1}(t)$.

Chapter 4

Comparison: Bosons vs. fermions

In this chapter, we summarize and compare the methods developed in the previous chapters. This chapter is based on [LH15], but a similar discussion with slightly different conventions can also be found in [40].

We can go through the individual steps of constructing the unitary representation of the algebra of observables in both cases, on which we then define Gaussian states using linear complex structures.

1. Classical phase space

For both, bosonic and fermionic systems, we begin our construction with a classical phase space V given by a linear real vector space that is $2N$ dimensional for systems with N degrees of freedom. We denote a phase space vector by ξ^a .

2. Linear observables

We have a canonical notion of linear observables given by linear forms w_a in the dual phase space V^* . If we want to emphasize the phase space function character of w_a , we might also write $w(\xi) = w_a \xi^a$. Any basis of linear observables $w^b(\xi) = w^b{}_a \xi^a$ gives rise to a phase space isomorphism $w^b{}_b : V \rightarrow V$.¹

3. Background structure

The key difference in the definition of bosonic and fermionic systems lies in the different background structure that we equip the space of linear observables with. For bosons, we equip V^* with the symplectic form Ω^{ab} and V with the dual structure ω_{ab} satisfying $\Omega^{ac}\omega_{cb} = \delta^a{}_b$. For fermions, we choose a positive metric G^{ab} on V instead, which comes with the dual metric g_{ab} satisfying $G^{ac}g_{cb} = \delta^a{}_b$. In both cases, our choice provides a natural isomorphism between V and V^* , but the resulting symmetry group preserving these structures are vastly different. For bosons, we have the connected, but non-compact symplectic group

$$\mathrm{Sp}(2N, \mathbb{R}) = \left\{ M^a{}_b \in \mathrm{GL}(V) \mid M^a{}_c \Omega^{cd} (M^\top)_d{}^b = \Omega^{ab} \right\}, \quad (4.1)$$

while for fermions, we find the compact group

$$\mathrm{O}(2N) = \left\{ M^a{}_b \in \mathrm{GL}(V) \mid M^a{}_c G^{cd} (M^\top)_d{}^b = G^{ab} \right\}, \quad (4.2)$$

consisting of two copies of $\mathrm{SO}(2N)$.

¹When quantizing the system, we find a basis of observables given by the operator valued vector \hat{w}^b . A special role is played by the identity $\delta^b{}_a$ whose quantization is given by the unique operator valued vector $\hat{\xi}^a$ that encodes the quantization. In particular, we have $\hat{w} = w_a \hat{\xi}^a$ and $\hat{w}^b = w^b{}_a \hat{\xi}^a$.

4. General observables

General observables form an associative algebra with identity that is generated by V^* . For bosons, we require that this algebra is symmetric (commutative) leading to the unique symmetric algebra $\text{Sym}(V^*)$.² For fermions, we require that the algebra is antisymmetric (anti-commutative) leading to the unique Grassmann algebra $\text{Grassmann}(V^*)$.

5. Poisson bracket

Still classically, we use the background structure Ω and G to equip the space of general observables with an additional structure, called the Poisson bracket. This is an additional product on the algebra defined by

$$\{f, g\}_- = (\partial_a f)(\partial_b g)\Omega^{ab} \quad \text{for bosons}, \quad \{f, g\}_+ = (\partial_a f)(\partial_b g)G^{ab} \quad \text{for fermions}. \quad (4.3)$$

6. Abstract algebra

Using the previous two ingredients, namely the algebra of general observables and the Poisson bracket, we can construct the abstract algebra of quantum observables. This is the first step of the quantization, but at this point we have not yet chosen a representation of algebra elements as operators acting on some Hilbert space. Instead we use the Poisson bracket of linear observables to modify the symmetric algebra for bosons and the Grassmann algebra for fermions. For bosons, we impose the canonical commutation relations (CCR)

$$[\hat{\xi}^a, \hat{\xi}^b] = \hat{\xi}^a \hat{\xi}^b - \hat{\xi}^b \hat{\xi}^a = i\Omega^{ab} \mathbb{1} \quad (4.4)$$

where the RHS is proportional to the identity element in the algebra. This turns the symmetric algebra of observables into the Weyl algebra $\text{Weyl}(V^*, \Omega)$. For fermions, we impose canonical anti-commutation relations (CAR)

$$\{\hat{\xi}^a, \hat{\xi}^b\} = \hat{\xi}^a \hat{\xi}^b + \hat{\xi}^b \hat{\xi}^a = iG^{ab} \mathbb{1}, \quad (4.5)$$

which turns the Grassmann algebra of fermionic observables into the Clifford algebra $\text{Cliff}(V^*, G)$.

7. Quantization

For finitely many degrees of freedom, the Stone-von Neumann theorem [49, 55] ensures under some mild assumptions that there is a unique representation for bosonic systems. For fermionic systems, uniqueness follows from the uniqueness of the spinor representation [40] of $\text{Cliff}(V^*, G)$ for finite dimensional V^* . In both cases, we can construct the representation by complexifying phase space and choosing a set of creation and annihilation operators. This selects a unique vacuum state, from which we can construct a topological basis of the full Hilbert space by successive action of creation operators. This is the well-known Fock space construction. Only for field theories where we have an infinite number of degrees of freedom, different choices of vacuum states may give rise to unitarily inequivalent representations. The quantization is fully encoded in the operator-valued vector $\hat{\xi}^a$, such that a classical linear observable w_a becomes $\hat{w} = w_a \hat{\xi}^a$ and a quadratic observable $H = \frac{1}{2}h_{ab}\xi^a\xi^b$ becomes $\hat{H} = \frac{1}{2}h_{ab}\hat{\xi}^a\hat{\xi}^b$.

²Technically, we then complete this algebra to allow for infinite power series leading to the space of smooth phase space functions that physicists usually use to describe observables. Such considerations are not necessary for fermions, where the Grassmann algebra stays finite dimensional for finitely many degrees of freedom.

8. Pure Gaussian state

Bosonic and fermionic Gaussian states $|J\rangle$ are fully described by their linear complex structure J using the defining equation

$$\frac{1}{2}(\delta^a{}_b + iJ^a{}_b)\hat{\xi}^b|J\rangle, \quad (4.6)$$

where we require $\langle J|\hat{\xi}^a|J\rangle$, sometimes referred to as *homogeneous Gaussian states*. For bosons, we could lift the condition of homogeneity and define a general inhomogeneous state $|J, \zeta\rangle$ satisfying

$$\frac{1}{2}(\delta^a{}_b + iJ^a{}_b)(\hat{\xi}^b - \zeta^b)|J, \zeta\rangle, \quad (4.7)$$

where $\zeta^a = \langle J, \zeta|\hat{\xi}^a|J, \zeta\rangle$ refers to the point in phase space where the state is peaked. If we want to do something similar for fermions, we are led to choose a Grassmann variable ζ^a as shift vector which means that the resulting inhomogeneous fermionic state does not live in the regular Hilbert space, but in its extension where we allow state vectors to be multiplied by Grassmann variables. This approach is used in the context of fermionic path integrals and to define fermionic coherent states, but is less useful when one is interested in a larger class of physical states.

The linear complex structure J together with background structure, Ω^{ab} for bosons and G^{ab} for fermions, defines the remaining structure via

$$G^{ab} = J^a{}_c \Omega^{cb} \quad (\text{bosons}) \quad \text{and} \quad \Omega^{ab} = -J^a{}_c \Omega^{cb} \quad (\text{fermions}). \quad (4.8)$$

This leads to the triangle of Kähler structure. The covariance matrix is completely determined by these structures as

$$\langle J|\hat{\xi}^a\hat{\xi}^b|J\rangle = \frac{1}{2}\left(G^{ab} + i\Omega^{ab}\right) \quad (4.9)$$

and all higher n -point functions follow from Wick's theorem. Every linear complex structure induces a phase space decomposition and dual phase space decomposition

$$V_{\mathbb{C}} = V^+ \oplus V^- \quad \text{and} \quad V_{\mathbb{C}}^* = (V^*)^+ \oplus (V^*)^-, \quad (4.10)$$

where V^\pm and $(V^*)^\pm$ refers to the right and left eigenspaces of J with eigenvalue $\pm i$, respectively. The term $\frac{1}{2}(\delta^a{}_b + iJ^a{}_b)$ is a projector $V_{\mathbb{C}} \rightarrow V^+$, which projects the operator-valued vector $\hat{\xi}^a$ onto the space of annihilation operators.

The choice of a Fock space vacuum is equivalent to selecting a homogeneous Gaussian state. In the case of a quantum field theory, we check if two vacua $|J\rangle$ and $|\tilde{J}\rangle$ give rise to unitarily equivalent Fock space representations by confirming that the Hilbert-Schmidt norm of $J - \tilde{J}$ is finite.³

We can also use the linear complex structures to compute the inner product $|\langle J|\tilde{J}\rangle|^2$ between two Gaussian states. Using the relative covariance matrix $\Delta = -J\tilde{J}$, we find

$$|\langle J|\tilde{J}\rangle|^2 = \begin{cases} \det \frac{\sqrt{2}\Delta^{1/4}}{\sqrt{1+\Delta}} & (\text{bosons}) \\ \det \frac{\sqrt{1+\Delta}}{\sqrt{2}\Delta^{1/4}} & (\text{fermions}) \end{cases}. \quad (4.11)$$

³Note that the definition of Hilbert-Schmidt norm requires an inner product on the classical phase space. For fermions, we can use the one induced by the background structure G , while for bosons we can equivalently use $G^{ab} = J^a{}_c \Omega^{cb}$ induced by J or $\tilde{G}^{ab} = \tilde{J}^a{}_c \Omega^{cb}$ induced by \tilde{J} .

9. Mixed Gaussian state

Any phase space decomposition $V = A \oplus B$, such that A and B are either symplectic complements for bosonic systems or orthogonal complements for fermionic systems, induces a tensor product decomposition $\mathcal{H} = \mathcal{H}_A \otimes \mathcal{H}_B$. Not all such decompositions are induced in this way, but those which are, give rise to reduced Gaussian states. Given a pure Gaussian state $\rho(J) = |J\rangle\langle J|$, the reduced state $\rho_A(J) = \text{Tr}_{\mathcal{H}_B}\rho(J)$ is again Gaussian provided that the tensor product was induced in the way described. In general, the mixed Gaussian state is described as

$$\rho_A(J) = e^{-H_A} \quad \text{with} \quad H_A = q_{rs}\hat{\theta}^r\hat{\theta}^s + E_0, \quad (4.12)$$

where $\hat{\theta}^r$ corresponds to the linear quantum observables in subsystem A , *i.e.*, the equivalent of $\hat{\xi}^a$ in the subsystem. The mixed Gaussian state $\rho_A(J)$ is fully described by the restricted Kähler structures given by $[\Omega]_A^{rs}$, $[G]_A^{rs}$ and $[J]_A^{rs}$. The restricted covariance matrix satisfies

$$\text{Tr}(\rho_A(J)\hat{\theta}^r\hat{\theta}^s) = \frac{1}{2}([G]_A^{rs} + i[\Omega]_A^{rs}). \quad (4.13)$$

The bilinear form q_{rs} is symmetric and real for bosons, but anti-symmetric and purely imaginary for fermions. It can be elegantly written in terms of the restricted linear complex structure as

$$q = \begin{cases} i[\omega]_A \operatorname{arcoth}(i[J]_A) & (\text{bosons}) \\ [g]_A \operatorname{arcoth}(i[J]_A) & (\text{fermions}) \end{cases} \quad (4.14)$$

where $[\omega]_A = [\Omega]_A^{-1}$ and $[g]_A = [G]_A^{-1}$. We can always choose a basis $\theta^r = (\varphi_1, \pi_1, \dots, \varphi_{N_A}, \pi_{N_A})$ of A , such that the restricted Kähler structures and q for bosons and fermions take the following standard forms:

bosons	fermions
$[J]_A \equiv \bigoplus_{i=1}^{N_A} \begin{pmatrix} 0 & \cosh 2r_i \\ -\cosh 2r_i & 0 \end{pmatrix}$	$[J]_A \equiv \bigoplus_{i=1}^{N_A} \begin{pmatrix} 0 & \cos 2r_i \\ -\cos 2r_i & 0 \end{pmatrix}$
$[\Omega]_A \equiv \bigoplus_{i=1}^{N_A} \begin{pmatrix} 0 & 1 \\ -1 & 0 \end{pmatrix}$	$[\Omega]_A \equiv \bigoplus_{i=1}^{N_A} \begin{pmatrix} 0 & \cos 2r_i \\ -\cos 2r_i & 0 \end{pmatrix}$
$[G]_A \equiv \bigoplus_{i=1}^{N_A} \begin{pmatrix} \cosh 2r_i & 0 \\ 0 & \cosh 2r_i \end{pmatrix}$	$[G]_A \equiv \bigoplus_{i=1}^{N_A} \begin{pmatrix} 1 & 0 \\ 0 & 1 \end{pmatrix}$
$q \equiv \bigoplus_{i=1}^{N_A} \begin{pmatrix} \log \tanh r_i & 0 \\ 0 & \log \tanh r_i \end{pmatrix}$	$q \equiv \bigoplus_{i=1}^{N_A} \begin{pmatrix} 0 & \log \tan r_i \\ -\log \tan r_i & 0 \end{pmatrix}$

We can use this basis to find an explicit representation of the states with respect to the number operators given by $\hat{n}_i = \frac{1}{2}(\varphi_i^2 + \pi_i^2 - 1)$ for bosons and $\hat{n}_i = \frac{1}{2}(i\varphi_i\pi_i - i\pi_i\varphi_i + 1)$,

namely

$$\rho_A = \begin{cases} \sum_{n_1, \dots, n_{N_A}=0}^{\infty} \left(\prod_{i=1}^{N_A} \frac{(\tanh r_i)^{n_i}}{\cosh r_i} \right)^2 |n_1, \dots, n_{N_A}\rangle \langle n_1, \dots, n_{N_A}| & (\text{bosons}) \\ \sum_{n_1, \dots, n_{N_A}=0}^1 \left(\prod_{i=1}^{N_A} \frac{(\tan r_i)^{n_i}}{\sec r_i} \right)^2 |n_1, \dots, n_{N_A}\rangle \langle n_1, \dots, n_{N_A}| & (\text{fermions}) \end{cases} . \quad (4.15)$$

We can read off the entanglement spectrum as eigenvalues of ρ_A which allows the computation of entanglement entropy S_A as

$$S_A = \begin{cases} \sum_{i=1}^{N_A} (\cosh^2 r_i \log \cosh^2 r_i - \sinh^2 r_i \log \sinh^2 r_i) & (\text{bosons}) \\ -\sum_{i=1}^{N_A} (\cos^2 r_i \log \cos^2 r_i + \sin^2 r_i \log \sin^2 r_i) & (\text{fermions}) \end{cases} . \quad (4.16)$$

Similarly, we find that the Rényi entropy $S_A^{(\alpha)}$ of order α is given by

$$S_A^{(\alpha)} = \begin{cases} \frac{1}{\alpha-1} \sum_{i=1}^{N_A} \log (\cosh^{2\alpha} r_i - \sinh^{2\alpha} r_i) & (\text{bosons}) \\ -\frac{1}{\alpha-1} \sum_{i=1}^{N_A} \log (\cos^{2\alpha} r_i + \sin^{2\alpha} r_i) & (\text{fermions}) \end{cases} . \quad (4.17)$$

We can use the restricted complex structure $[J]_A$ to find a particularly compact trace formula for the entanglement entropy valid for both bosons and fermions, namely

$$S_A = \left| \text{Tr} \left(\frac{\mathbb{1}_A + [iJ]_A}{2} \log \left| \frac{\mathbb{1}_A + i[J]_A}{2} \right| \right) \right| . \quad (4.18)$$

For bosonic systems, we can also consider inhomogeneous Gaussian states $|J, \zeta\rangle$, for which the same formulas for entanglement entropy and Rényi entropy are valid.

10. Time evolution

The time evolution of Gaussian states under the evolution of quadratic Hamiltonians is fully encoded in the Gaussian group, either the symplectic group for bosons or the orthogonal group for fermions. The most general quadratic Hamiltonian is given by

$$\hat{H} = \begin{cases} \frac{1}{2} h_{ab} \hat{\xi}^a \hat{\xi}^b & \text{with } h_{ab} = h_{ba} \quad (\text{bosons}) \\ \frac{1}{2} h_{ab} \hat{\xi}^a \hat{\xi}^b & \text{with } h_{ab} = -h_{ba} \quad (\text{fermions}) \end{cases} \quad (4.19)$$

where we allow for explicit time-dependence. The classical equations of motion can be written as Hamilton equations given by

$$\frac{d}{dt} \xi^a(t) = K(t)^a{}_b \xi^b(t) \quad \text{with} \quad K(t)^a{}_b = \begin{cases} \Omega^{ac} h_{cb}(t) \in \mathfrak{sp}(2N, \mathbb{R}) & (\text{bosons}) \\ G^{ac} h_{cb}(t) \in \mathfrak{so}(2N) & (\text{fermions}) \end{cases} . \quad (4.20)$$

The solution is encoded in the Hamiltonian flow written as time ordered exponential

$$M(t) = \mathcal{T} \exp \int_0^t dt' K(t') , \quad (4.21)$$

such that $\xi^a(t) = M(t)^a{}_b \xi^b(0)$. The time evolution of homogeneous Gaussian states is governed by the differential equation

$$J(t) = [K(t), J(t)] = K(t)J(t) - J(t)K(t) \quad (4.22)$$

Table 4.1: *Gaussian states from Kähler structures.* This table summarizes and compares our methods to describe bosonic and fermionic Gaussian states using Kähler structures.

structure	bosons	fermions
classical phase space	$\xi^a \equiv (q_1, \dots, q_N, p_1, \dots, p_N) \in V \simeq \mathbb{R}^{2N}$	
dual phase space	$v_a \in V^* \simeq \mathbb{R}^{2N}$	
defining structure	symplectic form Ω^{ab} ω_{ab} with $\Omega^{ac}\omega_{cb} = \delta^a{}_b$	positive definite metric G^{ab} g_{ab} with $G^{ac}g_{cb} = \delta^a{}_b$
Poisson bracket	$\{f_a, g_b\}_- = f_a g_b \Omega^{ab}$	$\{f_a, g_b\}_+ = f_a g_b G^{ab}$
general observables	Symmetric algebra generated by V^*	Grassmann algebra generated by V^*
abstract algebra structure relations	Weyl algebra Weyl($2N, \mathbb{C}$) canonical commutation relations (CCR): $[\hat{\xi}^a, \hat{\xi}^b] = i\Omega^{ab}$	Clifford algebra Cliff($2N, \mathbb{C}$) canonical anticommutation relations (CAR): $\{\hat{\xi}^a, \hat{\xi}^b\} = G^{ab}$
complex structure	$J^a{}_b$ compatible with Ω and ω	$J^a{}_b$ compatible with G and g
equivalent structure	metric $G^{ab} = -J^a{}_c \Omega^{cb}$	symplectic form $\Omega^{ab} = J^a{}_c G^{cb}$
Gaussian state $ J\rangle$	$\langle J \hat{\xi}^a J \rangle = 0$	$\langle J \hat{\xi}^a \hat{\xi}^b J \rangle = \frac{1}{2} (G^{ab} + i\Omega^{ab})$
system decomposition $V = A \oplus B$	even dimensional symplectic complements	even dimensional orthogonal complements
Restricted complex structure $[J]_A$	$[J]_A = \bigoplus_{i=1}^{N_A} \begin{pmatrix} 0 & \cosh 2r_i \\ -\cosh 2r_i & 0 \end{pmatrix}$	$[J]_A = \bigoplus_{i=1}^{N_A} \begin{pmatrix} 0 & \cos 2r_i \\ -\cos 2r_i & 0 \end{pmatrix}$
restricted Gaussian state $\rho_A = \text{Tr}_B J\rangle \langle J $	$\sum_{n_1, \dots, n_{N_A}=0}^{\infty} \left(\prod_{i=1}^{N_A} \frac{(\tanh r_i)^{n_i}}{\cosh r_i} \right)^2 n_1, \dots, n_{N_A}\rangle \langle n_1, \dots, n_{N_A} $	$\sum_{n_1, \dots, n_{N_A}=0}^1 \left(\prod_{i=1}^{N_A} \frac{(\tan r_i)^{n_i}}{\sec r_i} \right)^2 n_1, \dots, n_{N_A}\rangle \langle n_1, \dots, n_{N_A} $
entanglement entropy	$S_A = \sum_{i=1}^{N_A} (\cosh^2 r_i \log \cosh^2 r_i - \sinh^2 r_i \log \sinh^2 r_i)$	$S_A = - \sum_{i=1}^{N_A} (\cos^2 r_i \log \cos^2 r_i + \sin^2 r_i \log \sin^2 r_i)$
entanglement entropy trace formula	$S_A = \text{Tr} \left(\frac{\mathbb{1}_A + i[J]_A}{2} \log \left \frac{\mathbb{1}_A + i[J]_A}{2} \right \right)$	$S_A = -\text{Tr} \left(\frac{\mathbb{1}_A + i[J]_A}{2} \log \frac{\mathbb{1}_A + i[J]_A}{2} \right)$
Rényi entropy of order n	$R_A^{(n)} = \frac{1}{n-1} \sum_{i=1}^{N_A} \log (\cosh^{2n} r_i - \sinh^{2n} r_i)$	$R_A^{(n)} = -\frac{1}{n-1} \sum_{i=1}^{N_A} \log (\cos^{2n} r_i + \sin^{2n} r_i)$
quadratic Hamiltonian	$\hat{H} = \frac{1}{2} h(t)_{ab} \hat{\xi}^a \hat{\xi}^b$ with symmetric $h(t)_{ab}$	$\hat{H} = \frac{i}{2} h(t)_{ab} \hat{\xi}^a \hat{\xi}^b$ with antisymmetric $h(t)_{ab}$
Generator	$K(t)_b^a = \Omega^{ac} h_{cb} \in \mathfrak{sp}(2N, \mathbb{R})$	$K(t)_b^a = G^{ac} h_{cb} \in \mathfrak{so}(2N)$
Unitary operator	$\hat{U}(e^K) = \exp \left(\frac{i}{2} \hat{\xi}^a \omega_{ac} K^c{}_b \hat{\xi}^b \right)$ with $K \in \mathfrak{sp}(2N, \mathbb{R})$	$\hat{U}(e^K) = \exp \left(-\frac{1}{2} \hat{\xi}^a g_{ac} K^c{}_b \hat{\xi}^b \right)$ with $K \in \mathfrak{so}(2N)$
Evolution group	Metaplectic group $\text{Mp}(2N, \mathbb{R})$	Spin group $\text{Spin}(2N)$
Structure preserving subgroup	$\text{U}(N) = \text{Sp}(2N) \cap \text{GL}(N, \mathbb{C})$	$\text{U}(N) = \text{SO}(2N) \cap \text{GL}(N, \mathbb{C})$

which is solved by $J(t) = M(t)J(0)M(t)^{-1}$.

Time evolution is an example of the natural group action of an element $M \in \mathcal{G}$ onto any Gaussian state $|J\rangle$ leading to $|MJM^{-1}\rangle$. This forms a natural representation of the group \mathcal{G} , but every Gaussian state $|J\rangle$ selects an invariant subgroup

$$\text{Sta}_{|J\rangle} = \{M \in \mathcal{G} \mid MJM^{-1} = J\} \quad (4.23)$$

isomorphic to $\text{U}(N)$. This group arises naturally as the intersection

$$\text{U}(N) = \text{Sp}_\Omega(2N, \mathbb{R}) \cap \text{O}_G(2N) \cap \text{GL}_J(N, \mathbb{C}) \quad (4.24)$$

for any triple (Ω, G, J) of Kähler structures. Technically, this is only a proper representation on the space of Gaussian quantum states $\rho(J) = |J\rangle\langle J|$, while for Gaussian state vectors $|J\rangle$ we need to take complex phases into account. The unitary sub group generated by hermitian operators \hat{H} from (4.20) is in fact not given by \mathcal{G} , but by its double cover $\overline{\mathcal{G}}$ which is given by metaplectic group $\text{Mp}(2N, \mathbb{R})$ for bosonic systems and the spin group $\text{Spin}(N)$ for fermionic systems.

In this summary, we reviewed the description of Gaussian states in terms of Kähler structures. This formulation provides a unified framework for both, bosonic and fermionic systems that clearly distinguishes basis independent objects, such as the Kähler structures and the underlying group, and basis dependent objects, such as specific choices of creation and annihilation operators or expressions thereof. We believe that this framework is broadly applicable and can be extended to incorporate any invariant quantities that might be of relevance in the study of Gaussian states. This includes information theoretic quantities, such as the mutual information and fidelity between Gaussian states.

Part II

Applications

Chapter 5

Entanglement production at instabilities

In this chapter, we apply our mathematical framework to study the time evolution of the entanglement entropy of Gaussian states for quadratic Hamiltonians with instabilities. This chapter is largely based on [LH08, LH09] with some results already discussed in [LH03].

Entanglement plays a central role in the thermalization of isolated quantum systems [56–58]. The paradigmatic setting consists in a Hamiltonian system prepared in a pure state and evolving unitarily, $|\psi_t\rangle = e^{-iHt}|\psi_0\rangle$. The objective is to study the thermalization of observables \mathcal{O}_A belonging to a subalgebra of observables \mathcal{A}_A which define a bipartition $\mathcal{H} = \mathcal{H}_A \otimes \mathcal{H}_B$ of the system in a subsystem A and its complement B . While the von Neumann entropy of the system vanishes at all times, the entropy of the subsystem A ,

$$S_A(t) = -\text{Tr}_A(\rho_A(t) \log \rho_A(t)) \quad \text{with} \quad \rho_A(t) = \text{Tr}_B(|\psi_t\rangle\langle\psi_t|), \quad (5.1)$$

in general does not vanish and has a non-trivial evolution. The origin of this entropy is the entanglement between the degrees of freedom in the subsystem A and its complement. Equilibration in the subsystem A occurs when the entanglement entropy $S_A(t)$ approaches an equilibrium value S_{eq} , with thermalization corresponding to S_{eq} given by the thermal entropy.

A generic behavior has been observed for various systems prepared in a state with initially low entanglement entropy, $S_A(t_0) \ll S_{\text{eq}}$: After a transient which depends on the details of the initial state of the system, the entropy of the subsystem goes through a phase of *linear growth*,

$$S_A(t) \sim \Lambda_A t, \quad (5.2)$$

until it saturates to an equilibrium value as described in figure 5.1. This behavior is observed in the evolution of various isolated quantum systems, in particular in systems that show the signatures of quantum chaos [59–63], in many-body quantum systems [64] and quantum fields [65–67] after a quench, and in the thermalization of strongly-interacting quantum field theories studied using holographic methods [68–72]. Understanding the mechanism of this process is of direct relevance for the puzzle of fast thermalization of the quark gluon plasma produced in heavy-ion collisions [73–75], in models of black holes as fast scramblers of quantum information [76], and in the study of the quantum nature of space-time [77–81]. In particular, being able to predict from first principles the rate of growth Λ_A of the entanglement entropy in the phase of linear growth can provide us with crucial information on the time-scale of thermalization.

On the other hand, at the classical level—in Hamiltonian chaotic systems—the coarse-grained entropy $S_{\text{cl}}(t)$ shows a behavior similar to the one described in figure 5.1, with a linear phase which

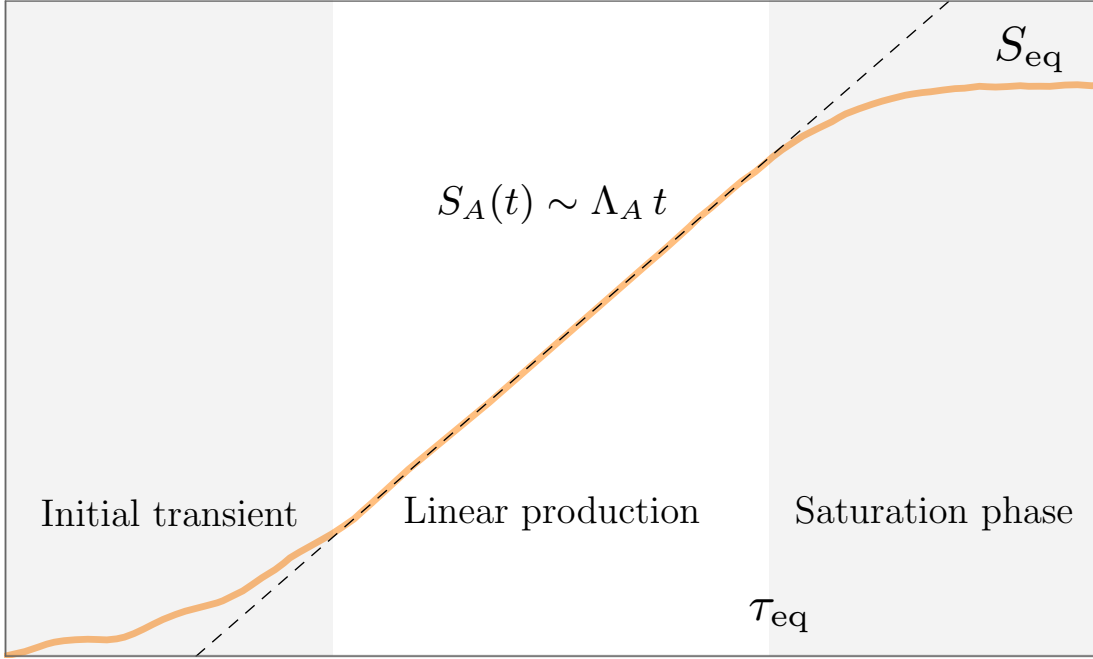


Figure 5.1: Sketch of typical entanglement production. Typical time dependence of the entanglement entropy $S_A(t)$ under unitary time evolution: After an initial transient (a), linear production occurs with characteristic rate Λ_A (b), and finally the system equilibrates in the saturation phase (c). The typical time scale for the equilibration of a state with initially vanishing entanglement entropy is $\tau_{\text{eq}} \sim S_{\text{eq}}/\Lambda_A$.

has a known rate of growth \mathfrak{h}_{KS} [82, 83],

$$S_{\text{cl}}(t) \sim \mathfrak{h}_{\text{KS}} t, \quad (5.3)$$

where \mathfrak{h}_{KS} is the Kolmogorov-Sinai rate of the system, an information-theoretic quantity that measures the uncertainty remaining on the future state of a system, once an infinitely long past is known. The Kolmogorov-Sinai rate has dimension of time^{-1} and for regular Hamiltonian systems is given by the sum of the positive Lyapunov exponents λ_i of the system [84–87].

In quantum systems that have a classical chaotic counterpart, a relation between the rate of growth of the entanglement entropy Λ_A and the classical Lyapunov exponents λ_i is expected [59–63, 88, 89], despite the fact that Lyapunov exponents are global quantities which probe the phase space of the full system, not just of the subsystem A .

We investigate the relation between Λ_A and the Lyapunov exponents λ_i by studying the evolution of Gaussian states in many-body systems and quantum field theories with quadratic time-dependent Hamiltonians. Non-trivial Lyapunov exponents arise in the presence of instabilities and of parametric resonances. In this context we prove that the linear growth of the entanglement entropy $S_A(t)$ has a classical counterpart: The entanglement rate Λ_A equals the exponential rate of growth of the volume of a cell in the sub phase space of the subsystem A . We then provide an algorithm for computing Λ_A in terms of the Lyapunov exponents λ_i of the classical system and the choice of subsystem A . The methods developed apply both to quantum systems with finitely many degrees of freedom and to quantum fields in external time-dependent backgrounds when the subsystem is given by a finitely-generated Weyl subalgebra \mathcal{A}_A .

5.1 Linear growth of the entanglement entropy

We state the main result which relates the asymptotic rate of growth of the entanglement entropy of a quantum system to classical instabilities encoded in the Lyapunov exponents of the classical system. Our proof is based on a set of technical results presented in sections 5.2 and 5.3.

5.1.1 Entanglement entropy growth, instabilities and the volume exponent

We consider a quadratic bosonic system with N degrees of freedom. We denote linear observables by $\xi^a = (q_1, \dots, q_N, p_1, \dots, p_N)$ and assume canonical commutation relations $[q_i, q_j] = [p_i, p_j] = 0$ and $[q_i, p_j] = i\delta_{ij}$. These relations can be more compactly phrased by stating $[\xi^a, \xi^b] = i\Omega^{ab}$ where Ω^{ab} is a symplectic form. The most general quadratic Hamiltonian is given by

$$H(t) = \frac{1}{2} h_{ab}(t) \xi^a \xi^b + f_a(t) \xi^a, \quad (5.4)$$

where we explicitly allow for dependence on time t . The time-evolution of an initial state $|\psi_0\rangle$ under the unitary dynamics $U(t)$ generated by $H(t)$ results in the evolution of the entanglement entropy of a subsystem

$$S_A(t) = S_A(U(t)|\psi_0\rangle). \quad (5.5)$$

Before we state the main result, let us introduce two important notions:

- **Subsystem exponents in classical dynamical systems**

In classical dynamical systems, a quadratic Hamiltonian $H(t)$ generates a linear symplectic flow $M(t) : V \rightarrow V$ on the classical phase space V of the theory. The transpose $M(t)^\top$ of this flow acts on the dual phase space V^* . Given a linear observable $\ell \in V^*$, we can define the Lyapunov exponent of ℓ as the limit

$$\lambda_\ell = \lim_{t \rightarrow \infty} \log \frac{1}{t} \frac{\|M(t)^\top \ell\|}{\|\ell\|}, \quad (5.6)$$

which is independent from the metric we choose to measure the length. A system decomposition $V = A \oplus B$ of the classical phase space into subsystem phase spaces A and B induces an equivalent decomposition $V^* = A^* \oplus B^*$ of the dual phase space. Here, we can generalize the notion of Lyapunov exponents to define the subsystem exponent Λ_A defined by

$$\Lambda_A = \lim_{t \rightarrow \infty} \frac{1}{t} \log \frac{\text{vol}(M(t)^\top \mathcal{V}_A)}{\text{vol}(\mathcal{V}_A)}, \quad (5.7)$$

where $\mathcal{V}_A \subset A^*$ is an arbitrary parallelepiped in the subspace A^* . The subsystem exponent captures the exponential volume growth of subsystem regions. The volume vol is measured on the subspace where $M(t)^\top \mathcal{V}_A$ lives, but the subsystem exponent is independent of the global metric on V^* one chooses to define the volume form on arbitrary subspaces. We explain the relation between Λ_A and λ_ℓ in section 5.2, while more technical details are summarized in appendix B.

- **Entanglement of Gaussian states**

It is well-known that a Gaussian bosonic state $|\psi\rangle$ can be completely characterized by its expectation value $\zeta^a = \langle \psi | \xi^a | \psi \rangle$ and its covariance matrix $G^{ab} = \langle \psi | \xi^a \xi^b + \xi^b \xi^a | \psi \rangle - 2\zeta^a \zeta^b$. Recent progress on unifying methods for bosonic and fermionic Gaussian states suggests an equivalent description where G^{ab} is replaced by a linear complex structure $J^a_b = -G^{ac}\omega_{cb}$

with ω being the inverse of Ω . Choosing a system decomposition $A \oplus B$ with complementary subsystems A and B allows us to compute the entanglement entropy $S_A(|\psi\rangle)$ between them. For a Gaussian state $|\psi\rangle$, this entanglement entropy can be directly computed from J , which we use in section 5.3.

With these preliminaries in hand, we can state the following theorem that applies to the evolution of the entanglement entropy of any Gaussian initial state.

Theorem 1 (Entanglement growth)

Given a quadratic time-dependent Hamiltonian $H(t)$ and a subsystem A with subsystem exponent Λ_A , the long-time behavior of the entanglement entropy of the subsystem is

$$S_A(t) \sim \Lambda_A t \quad (5.8)$$

for all initial Gaussian states $|J_0, \zeta_0\rangle$.

Proof: The proof of this theorem involves three steps that rely on ingredients reviewed in section 5.3.

(i) **The entanglement entropy is bounded by the Rényi entropy:**

We define the asymptotic rate of growth of the entanglement entropy as its long-time linear scaling $\lim_{t \rightarrow \infty} \frac{1}{t} S_A(U(t)|J_0, \zeta_0\rangle)$. We note that quadratic time-dependent Hamiltonians evolve the initial Gaussian state into a Gaussian state, (2.43). In section 5.3.1 we prove that the entanglement entropy of a Gaussian state is bounded from below by the Rényi entropy $R_A(U(t)|J_0, \zeta_0\rangle)$ and from above by the Rényi entropy plus a state-independent constant, inequality (5.74). Therefore, we have the equality

$$\lim_{t \rightarrow \infty} \frac{S_A(U(t)|J_0, \zeta_0\rangle)}{t} = \lim_{t \rightarrow \infty} \frac{R_A(U(t)|J_0, \zeta_0\rangle)}{t}, \quad (5.9)$$

i.e., the asymptotic rate of growth of the entanglement entropy and of the Rényi entropy coincide.

(ii) **The Rényi entropy is given by a phase space volume:**

In section 5.3.2 we prove that the Rényi entropy of a Gaussian state equals the logarithm of the phase space volume of a symplectic cube \mathcal{V}_A spanning the subsystem A , (5.78). The volume is measured with respect to the metric induced by the state, (5.75). In the case of the time-dependent Gaussian state $U(t)|J_0, \zeta_0\rangle$, we can measure the volume with respect to the time-dependent induced metric $G_t = M(t)G_0M^\top(t)$. Equivalently, we can consider the time-dependent symplectic cube $M^\top(t)\mathcal{V}_A$ and measure its volume with respect to the initial metric G_0 induced by the initial state,

$$R_A(U(t)|J_0, \zeta_0\rangle) = \log \text{Vol}_{G_0}(M^\top(t)\mathcal{V}_A). \quad (5.10)$$

(iii) **The Rényi entropy grows as regions in phase space are stretched:**

The subsystem exponent Λ_A introduced in (5.7) and discussed in section 5.2.3 provides a generalization of the notion of Lyapunov exponents of a classical Hamiltonian system. It involves the choice of a subsystem A , a symplectic dynamics $M(t)$ and a reference metric G_0 ,

$$\Lambda_A = \lim_{t \rightarrow \infty} \frac{1}{t} \log \frac{\text{Vol}_{G_0}(M^\top(t)\mathcal{V}_A)}{\text{Vol}_{G_0}(\mathcal{V}_A)}. \quad (5.11)$$

Despite the metric G_0 is needed for the definition, the value of the subsystem exponent Λ_A is independent of G_0 for regular Hamiltonian systems. The subsystem exponent can be expressed in terms of the Lyapunov exponents of the system using the algorithm described in theorem 3, (5.54).

Using (i), (ii) and (iii), we find that the asymptotic rate of growth of the entanglement entropy is given by the subsystem exponent Λ_A ,

$$\lim_{t \rightarrow \infty} \frac{S_A(U(t)|J_0, \zeta_0)}{t} = \Lambda_A \quad (5.12)$$

for all initial Gaussian states, therefore proving the statement of the theorem. \square

We note that, as the entanglement entropies of complementary subsystems A and B coincide, $S_A(|\psi\rangle) = S_B(|\psi\rangle)$, also their asymptotic rates of growth have to coincide. Consistency with the statement of the theorem implies that, at the classical level, the subsystem exponents defined in section 5.2.3 for a symplectic decomposition $V = A \oplus B$ coincide

$$\Lambda_A = \Lambda_B. \quad (5.13)$$

This statement can be proven using the expression (5.54) of the subsystem exponents or more directly using the property $\det[J]_A = \det[J]_B$ for the restriction of a complex structure J to complementary symplectic subspaces.

5.1.2 Entanglement and the Kolmogorov-Sinai entropy rate

Theorem 2 (Entanglement growth – generic subsystem)

Given a quadratic time-dependent Hamiltonian $H(t)$ with Lyapunov exponents λ_i , the long-time behavior of the entanglement entropy of a generic subsystem A is

$$S_A(t) \sim \left(\sum_{i=1}^{2N_A} \lambda_i \right) t \quad (5.14)$$

for all initial Gaussian states $|J_0, \zeta_0\rangle$ and all generic subsystems with N_A degrees of freedom.

In particular, the rate of growth of the entanglement entropy is bounded from above by the Kolmogorov-Sinai rate h_{KS} ,

$$\lim_{t \rightarrow \infty} \frac{1}{t} S_A(t) \leq h_{\text{KS}}. \quad (5.15)$$

The decomposition in two complementary subsystems both with dimension larger than the number of instabilities results in an entanglement growth proportional to the Kolmogorov-Sinai rate,

$$S_A(t) \sim h_{\text{KS}} t \quad \text{for} \quad 2N_A \geq N_I \quad \text{and} \quad 2N_B \geq N_I, \quad (5.16)$$

and therefore saturates the bound (5.15).

Proof: The asymptotic rate of growth of the entanglement entropy of a Gaussian state is given by the subsystem exponent Λ_A as stated in theorem 1, (5.12). For a generic subsystem, theorem 4 states that the subsystem exponent equals the sum of the $2N_A$ largest Lyapunov exponents, (5.67). Together with Pesin's theorem (5.65), this result implies that the asymptotic rate of growth is bounded from above by the Kolmogorov-Sinai rate of the system,

$$\lim_{t \rightarrow \infty} \frac{1}{t} S_A(t) = \sum_{i=1}^{2N_A} \lambda_i \leq h_{\text{KS}}. \quad (5.17)$$

Moreover, the subsystem exponent Λ_A equals the Kolmogorov-Sinai rate h_{KS} when its dimension is in the range $N_I \leq 2N_A \leq 2N - N_I$, (5.69). Recalling that $N_A + N_B = N$, this range coincides with the requirement that the dimension of each of the two complementary subsystems is larger than the number of instabilities, $2N_A \geq N_I$ and $2N_B \geq N_I$. In this case the bound (5.15) is saturated. \square

We note that quantum many-body systems often have only a small finite number of unstable directions N_I compared to the number of degrees of freedom of the system, $N_I \ll N$. A generic decomposition in two complementary subsystems that encompass the fractions $f_A = N_A/N$ and $f_B = 1 - f_A$ of the full system satisfies (5.16) if the fractions are in the range

$$\frac{N_I}{2N} \leq f_A \leq 1 - \frac{N_I}{2N}. \quad (5.18)$$

As a result, in the limit $N \rightarrow \infty$ with N_I finite, we have that the entanglement growth is proportional to the Kolmogorov-Sinai rate $S_A(t) \sim h_{\text{KS}} t$ for all partitions of the system into two complementary subsystems each spanning a finite fraction of the system, except for a set of partitions of measure zero.

5.1.3 Bounds on non-Gaussian initial states

Computing the entanglement entropy growth of non-Gaussian states is a non-trivial problem as efficient tools similar to the ones discussed in (2.35) are not available. Nevertheless upper bounds that generalize theorems 1 and 2 can be established in the case of evolution driven by a quadratic time-dependent Hamiltonian.

Let us consider an initial non-Gaussian state $|\psi_0\rangle$ and the unitary evolution $U(t)$ generated by a quadratic time-dependent Hamiltonian of the most general form described in (2.39). The symmetric part of the connected 2-point function at the time t is given by

$$G_t^{ab} = \langle \psi_t | \hat{\xi}^a \hat{\xi}^b + \hat{\xi}^b \hat{\xi}^a | \psi_t \rangle - 2 \langle \psi_t | \hat{\xi}^a | \psi_t \rangle \langle \psi_t | \hat{\xi}^b | \psi_t \rangle = M^a{}_c(t) M^b{}_d(t) G_0^{cd} \quad (5.19)$$

where $|\psi_t\rangle = U(t)|\psi_0\rangle$ and $M^a{}_b(t)$ is the symplectic matrix defined in (5.34). There always exists a mixed Gaussian state ρ_0 which has the same correlation function G_0^{ab} at the time $t = 0$ [90]. By construction, the 2-point function of the unitarily evolved Gaussian state $U(t)\rho_0 U^{-1}(t)$ is the function G_t^{ab} of (5.19). Moreover one can show that the entanglement entropy of the non-Gaussian state $|\psi_t\rangle$ is bounded from above by the entanglement entropy of the mixed Gaussian state having the same 2-point function G_t^{ab} , i.e. $S_A(\rho_{NG}) \leq S_A(\rho_G)$ where $\rho_{NG} = \text{Tr}_B(|\psi_t\rangle\langle\psi_t|)$ is the reduced density matrix of the non-Gaussian state, and $\rho_G = \text{Tr}_B(U(t)\rho_0 U^{-1}(t)) = \exp(-\frac{1}{2}k_{rs}(t)\hat{\xi}^r \hat{\xi}^s + E_0(t))$ is the reduced density matrix of the Gaussian state. The proof is immediate: Recalling that the relative entropy is a positive function [91, 92], we have

$$0 \leq S(\rho_{NG}\|\rho_G) = \text{Tr}_A(\rho_{NG} \log \rho_{NG} - \rho_{NG} \log \rho_G) \quad (5.20)$$

$$= -S_A(\rho_{NG}) + S_A(\rho_G) + \underbrace{\frac{1}{2}k_{rs}(t) \left(\text{Tr}_A(\hat{\xi}^r \hat{\xi}^s \rho_{NG}) - \text{Tr}_A(\hat{\xi}^r \hat{\xi}^s \rho_G) \right)}_{=0}, \quad (5.21)$$

where $S(\rho_{NG}\|\rho_G)$ is the relative entropy and the term in parenthesis vanishes as the two states have the same correlation function by construction. On the other hand, theorem 1 generalizes to mixed Gaussian states implying the asymptotic growth $S_A(\rho_G) \sim \Lambda_A t$ for the entanglement entropy of a subsystem A . As a result we find the inequality

$$\lim_{t \rightarrow \infty} \frac{1}{t} S_A(|\psi_t\rangle) \leq \Lambda_A \quad (5.22)$$

which states that the asymptotic rate of growth of the entanglement entropy of a non-Gaussian state $|\psi_t\rangle$ which evolves unitarily with a quadratic Hamiltonian is bounded from above by the subsystem exponent Λ_A . This result generalizes theorems 1 and 2 to non-Gaussian states and

establishes the Kolmogorov-Sinai rate \mathfrak{h}_{KS} as the upper bound for the asymptotic rate of growth of the entanglement entropy.

Preliminary numerical investigations presented in section 5.7 indicate that, under the unitary evolution given by a quadratic time-dependent Hamiltonian, the upper bound Λ_A in (5.22) might in fact be saturated by all initial states and not just by Gaussian states.

5.2 Proof, part I: classical ingredients

In this section and the subsequent section we collect and prove results used in the proof of the main theorem presented in section 5.1.

We consider a classical dynamical system with N degrees of freedom. We assume that the system has a Hamiltonian dynamics defined in a linear phase space [93]. We also restrict attention to quadratic time-dependent Hamiltonians. In this case we discuss the notions of stability, Lyapunov exponents and the growth of the volume of subsystems [86, 87].

5.2.1 Linear phase space and quadratic time-dependent Hamiltonians

We consider a system with N degrees of freedom described by a linear phase space $V = \mathbb{R}^{2N}$. Phase space observables \mathcal{O} are smooth functions of $2N$ real variables denoted ξ^a ,

$$\begin{aligned}\mathcal{O} : \mathbb{R}^{2N} &\rightarrow \mathbb{R} \\ \xi^a &\mapsto \mathcal{O}(\xi).\end{aligned}\tag{5.23}$$

The space of observables is equipped with a Lie algebra structure defined by the Poisson brackets

$$\{f(\xi), g(\xi)\} = \Omega^{ab} \partial_a f(\xi) \partial_b g(\xi)\tag{5.24}$$

where Ω^{ab} is a nondegenerate antisymmetric matrix. In this paper we mostly focus on linear observables $v = v_a \xi^a$ and quadratic observables $\mathcal{O} = \frac{1}{2} h_{ab} \xi^a \xi^b$. We call V^* the vector space formed by all linear observables, and denote by v_a the elements of V^* and by w^a the elements of V . The restriction of the Poisson brackets to the space of linear observables is

$$\{u, v\} = \Omega^{ab} u_a v_b.\tag{5.25}$$

A Darboux basis¹ (also called symplectic basis) of phase space functions consists of a set $\mathcal{D}_V = (q_1, \dots, q_N, p_1, \dots, p_N)$ of linear observables²

$$q_i = q_{ia} \xi^a \quad \text{and} \quad p_i = p_{ia} \xi^a \quad \text{with} \quad i = 1, \dots, N\tag{5.26}$$

satisfying canonical Poisson brackets $\{q_i, q_j\} = 0$, $\{p_i, p_j\} = 0$, $\{q_i, p_j\} = \delta_{ij}$.

The notions of symplectic vector space and symplectic transformations play a central role in the description of the system. A symplectic structure on V is an antisymmetric non-degenerate

¹Technically, \mathcal{D}_V is a basis of the dual phase space V^* , but we refrained from bloating our notation by writing \mathcal{D}_{V^*} . All Darboux bases \mathcal{D} in this paper will live in the dual phase space V^* .

²When using abstract indices, a Darboux basis $\mathcal{D}_V = (\xi_a^1, \dots, \xi_a^{2N})$ consisting of $2N$ linear observables ξ_b^a can be read as a concrete representation of the Kronecker delta $\delta^a{}_b = \xi_c^a \xi_b^c = \xi_b^a$ when we read both indices as abstract indices. However, when referring to an explicit basis $(q_1, \dots, q_N, p_1, \dots, p_N)$, we will use lower indices to match standard conventions.

bilinear map $\omega_{ab} : V \times V \rightarrow \mathbb{R}$. It provides a canonical map from V to V^* given by $v_a = \omega_{ab}v^b$. The couple (V, ω_{ab}) defines a symplectic vector space. The inverse of the symplectic structure, denoted Ω^{ab} , is the antisymmetric bilinear map defined by $\Omega^{ac}\omega_{cb} = \delta^a_b$ and is a symplectic structure on V^* . The space V^* of linear observables on a linear phase space, equipped with the bilinear map Ω^{ab} describing the restriction of the Poisson brackets to V^* as in (5.25), is a symplectic vector space. In a Darboux basis, the symplectic structure Ω^{ab} and its inverse ω_{ab} take the $2N \times 2N$ matrix form $\Omega = (\Omega^{ab})$ and $\omega = (\omega_{ab})$,

$$\Omega = \begin{pmatrix} 0 & +\mathbb{1} \\ -\mathbb{1} & 0 \end{pmatrix}, \quad \omega = \Omega^{-1} = \begin{pmatrix} 0 & -\mathbb{1} \\ +\mathbb{1} & 0 \end{pmatrix}. \quad (5.27)$$

The linear symplectic group $\text{Sp}(2N)$ is the group of $2N \times 2N$ matrices M^a_b satisfying the relation $M^a_c M^b_d \Omega^{cd} = \Omega^{ab}$. In matrix form we have $M\Omega M^\top = \Omega$. Note that the inverse of a symplectic matrix is given by $M^{-1} = \Omega M^\top \omega$. The matrices M^a_b can be interpreted as linear maps either on V or on V^* , and preserve the corresponding symplectic structures.

The dynamics of a Hamiltonian system is prescribed by a Hamilton function $H(t)$ that we allow to be time-dependent. The Hamilton equations of motion of an observable \mathcal{O} are

$$\dot{\mathcal{O}}(t) = \{\mathcal{O}(t), H(t)\} + \frac{\partial \mathcal{O}(t)}{\partial t}. \quad (5.28)$$

In particular, for the linear observables ξ^a we have

$$\dot{\xi}^a(t) = \Omega^{ab} \partial_b H(t). \quad (5.29)$$

In this paper we focus on time-dependent quadratic Hamiltonians, i.e. phase space functions of the form

$$H(t) = \frac{1}{2} h_{ab}(t) \xi^a \xi^b + f_a(t) \xi^a. \quad (5.30)$$

In this case the Hamilton equations simplify to the linear equation

$$\dot{\xi}^a(t) = K^a_b(t) \xi^b + \Omega^{ab} f_b(t) \quad (5.31)$$

where the matrix $K^a_b(t)$ is defined in terms of the quadratic term in the Hamiltonian by

$$K^a_b(t) = \Omega^{ac} h_{cb}(t). \quad (5.32)$$

The solution of this equation provides the time evolution of the linear observable ξ^a ,

$$\xi^a(t) = M^a_b(t) \xi^b(0) + \eta^a(t). \quad (5.33)$$

The matrix $M^a_b(t)$ solves the differential equation $\dot{M}^a_b(t) = K^a_c(t) M^c_b(t)$ with the identity as initial condition, and can be expressed as a time-ordered exponential,

$$M^a_b(t) = \mathcal{T} \exp \left(\int_0^t K^a_b(t') dt' \right). \quad (5.34)$$

As the time evolution preserves the Poisson brackets, the matrix $M^a_b(t)$ belongs to the linear symplectic group $\text{Sp}(2N)$, i.e. $M^a_c(t) M^b_d(t) \Omega^{cd} = \Omega^{ab}$. The time-dependent shift $\eta^a(t)$ in (5.33) satisfies $\dot{\eta}^a(t) = K^a_b(t) \eta^b(t) + \Omega^{ab} f_b(t)$. It is given by

$$\eta^a(t) = M^a_b(t) \int_0^t M^{-1}(t')^b_c \Omega^{cd} f_d(t') dt' \quad (5.35)$$

and it vanishes if the linear term $f_a(t)\xi^a$ is not present in the Hamiltonian.

A simple example of time-dependent quadratic Hamiltonian of the form (5.30) is given by a system of coupled harmonic oscillators with time-dependent couplings or driven by external forces. Another important example arises in the description of the lowest-order expansion of the evolution of a time-independent non-linear system around a classical solution chosen as background. In this case the time-dependence of the effective Hamiltonian arises from the background classical solution.

5.2.2 Linear stability and Lyapunov exponents

To characterize the linear stability of a dynamical system we consider a small perturbation $\delta\xi^a(t)$ of a classical solution $\xi_0^a(t)$ that satisfies the Hamilton equations. Substituting $\xi^a(t) = \xi_0^a(t) + \delta\xi^a(t)$ into (5.29) and expanding at linear order in the perturbation we find the linear equation

$$\delta\dot{\xi}^a(t) = \Omega^{ac}\partial_c\partial_b H(t)|_{\xi_0} \delta\xi^b(t), \quad (5.36)$$

with $K^a{}_b(t) = \Omega^{ac}\partial_c\partial_b H(t)|_{\xi_0}$ the stability matrix of the classical solution $\xi_0^a(t)$. For the quadratic Hamiltonian (5.30) the stability matrix is simply given by $K^a{}_b(t) = \Omega^{ac}h_{cb}(t)$. As a result, the time evolution of the perturbation is given by

$$\delta\xi^a(t) = M^a{}_b(t) \delta\xi^b(0) \quad (5.37)$$

where the symplectic matrix $M(t)$ is given by (5.34). In order to measure the separation of two configurations in phase space we introduce a metric g_{ab} , i.e. a positive definite symmetric bilinear, and define the norm $\|\delta\xi\| = \sqrt{g_{ab}\delta\xi^a\delta\xi^b}$. The exponential rate of separation of two sufficiently close classical solutions is given by the Lyapunov exponent $\lambda_{\delta\xi}$ defined as

$$\lambda_{\delta\xi} = \lim_{t \rightarrow \infty} \frac{1}{t} \log \frac{\|\delta\xi(t)\|}{\|\delta\xi(0)\|}. \quad (5.38)$$

We note that the Lyapunov exponent $\lambda_{\delta\xi}$ is independent from the choice of metric g_{ab} used to measure the distance between the classical trajectories $\xi_0^a(t)$ and $\xi_0^a(t) + \delta\xi^a(t)$. See appendix B.2 for a proof of this statement.

It is also useful to define Lyapunov exponents of linear observables $\ell(\delta\xi) = \ell_a\delta\xi^a$ that probe the perturbation $\delta\xi^a(t)$ and live in the dual phase space $\ell_a \in V^*$. From the time evolution equation (5.37), we can read off that $\ell(t)$ evolves as

$$\ell_a(t) = M^b{}_a(t) \ell_b(0) = (M^\dagger(t) \ell(0))_a. \quad (5.39)$$

In order to define a norm $\|\ell\| = \sqrt{G^{ab}\ell_a\ell_b}$, we use the inverse metric G^{ab} , such that $G^{ac}g_{cb} = \delta^a{}_b$. Again, the Lyapunov exponent

$$\lambda_\ell = \lim_{t \rightarrow \infty} \frac{1}{t} \log \frac{\|\ell(t)\|}{\|\ell(0)\|}. \quad (5.40)$$

will be independent of the metric that we choose.

The metric g_{ab} , used above to define Lyapunov exponents, is said to be compatible with the symplectic structure ω_{ab} with inverse Ω^{ab} if the matrix $J^a{}_b = \Omega^{ac}g_{cb}$ is symplectic, $J^a{}_c J^b{}_d \Omega^{cd} = \Omega^{ab}$, and squares to minus the identity $J^a{}_c J^c{}_b = -\delta^a{}_b$. In this case, $J^a{}_b$ defines a complex structure. The inverse metric G^{ab} is then compatible with the symplectic structure Ω^{ab} in the dual space. A compatible metric g_{ab} allows us to define the limiting matrix $L_a{}^b$,

$$L_a{}^b = \lim_{t \rightarrow \infty} \frac{1}{2t} \log \left(g_{ac} M^c{}_d G^{de} M^b{}_e \right), \quad (5.41)$$

that characterizes the long-time stability of the system.³ Provided that the Hamiltonian system is regular in the sense of appendix B.3, Lyapunov exponents exist for all linear observables ℓ_a and are given by the eigenvalues of the limiting matrix L_a^b . As the matrix L_a^b is symmetric and belongs to the symplectic algebra $\text{sp}(2N)$, its eigenvalues are real and come in pairs with opposite sign $(\lambda, -\lambda)$. The Lyapunov spectrum consists of the ordered Lyapunov exponents given by

$$\lambda_1 \geq \cdots \geq \lambda_N \geq 0 \geq \lambda_{N+1} \geq \cdots \geq \lambda_{2N}, \quad (5.42)$$

with $\lambda_{2N+1-i} = -\lambda_i$ for regular Hamiltonian systems, as explained in appendix B.1. The dimension of an eigenspace is how often the associated exponent appears in this list. The eigenvectors ℓ_b of L_a^b provide us with a Darboux basis of V^* adapted to the unstable directions of the system. This basis, called the Lyapunov basis \mathcal{D}_L ,

$$\mathcal{D}_L = (\ell^1, \dots, \ell^{2N}), \quad (5.43)$$

is defined so that the only non-trivial Poisson brackets are $\{\ell^i, \ell^{2N-i+1}\} = 1$ for $i = 1, \dots, N$ and $\lim_{t \rightarrow \infty} \frac{1}{t} \log \|\ell^i(t)\| / \|\ell^i(0)\| = \lambda_i$ with $\ell^i(0) = \ell^i$. Note that \mathcal{D}_L is not unique because it depends on our choice of metric G^{ab} , but subsequent results will be independent of this choice [94, 95].

We will discuss examples of unstable quadratic systems in section 5.1. The prototypical example is the inverted harmonic oscillator, with a potential V that is unbounded from below. The Lyapunov exponents of the system are related to the unstable directions of the potential. Another example is provided by periodically driven systems, i.e., systems with a quadratic time-dependent Hamiltonian of the form (5.30) with periodic coefficients $h_{ab}(t+T) = h_{ab}(t)$. In this case instabilities appear due to the phenomenon of parametric resonance [93]. The real part of the Floquet exponents of the system coincide with the notion of Lyapunov exponents described above.

5.2.3 Subsystems and the subsystem exponent Λ_A

The partition of a Hamiltonian system in two complementary subsystems corresponds to a decomposition of the phase space V and its dual V^* into direct sums

$$V = A \oplus B \quad \text{and} \quad V^* = A^* \oplus B^* \quad (5.44)$$

with dimension $\dim A = 2N_A$, $\dim B = 2N_B$ where N_A is the number of degrees of freedom in the subsystem A and $N_A + N_B = N$. This decomposition can be understood as induced by a choice of subspace of linear observables $\phi_i = \phi_{ia}\xi^a$ and $\pi_i = \pi_{ia}\xi^a$ with $i = 1, \dots, 2N_A$ and canonical Poisson brackets $\{\phi_i, \phi_j\} = 0$, $\{\pi_i, \pi_j\} = 0$, $\{\phi_i, \pi_j\} = \delta_{ij}$.

This set of observables provides us with a Darboux basis of linear observables A^* that only probe the degrees of freedom in A

$$\mathcal{D}_A = (\theta^1, \dots, \theta^{2N_A}) = (\phi_i, \pi_i), \quad (5.45)$$

and it can be completed to a Darboux basis of the full system by introducing a Darboux basis of B^* ,

$$\mathcal{D}_B = (\Theta^1, \dots, \Theta^{2N_B}) = (\Phi_i, \Pi_i). \quad (5.46)$$

so that

$$\mathcal{D}_V = (\mathcal{D}_A, \mathcal{D}_B). \quad (5.47)$$

³In matrix form, $L = \lim_{t \rightarrow \infty} \frac{1}{2t} \log (gM(t)GM^\top(t))$.

Given a Darboux basis θ^r of A^* and its dual basis ϑ_r of A satisfying $\theta_a^r \vartheta_s^a = \delta_s^r$, we can restrict tensors to the subsystem by appropriate contractions. Most importantly, we will consider the restriction $[J]_A$ of the complex structure $J^a{}_b$ and $[G]_A$ of a metric G^{ab} :

$$[J]_A = (\theta_a^r J^a{}_b \vartheta_s^b) \quad \text{and} \quad [G]_A = (\theta_a^r G^{ab} \theta_b^s). \quad (5.48)$$

Note that, as θ_a^r is a Darboux basis, the restriction of the symplectic structure Ω^{ab} is still a symplectic structure, $[\Omega]_A = \Omega_A$. On the other hand, the restriction $[J]_A$ of a complex structure J is not in general again a complex structure, because it does not necessarily satisfy $[J]_A^2 = -\mathbb{1}_A$.

We give some examples of subsystems. Consider for instance a linear chain of N oscillators, with the oscillator at site i having canonical coordinates (q_i, p_i) . A first example of subsystem A corresponds to the subset of observables (q_i, p_i) with $i = 1, \dots, N_A$ associated to a geometric decomposition of the chain in two complementary intervals. A second example of subsystem is given by a subset of normal-mode observables $(\tilde{\phi}_k, \tilde{\pi}_k)$ with $k = 1, \dots, N_A$ corresponding to the long-wavelength perturbations of the system. A third example is provided by a detector that makes measurement of the localized observables (Q, P) only, with $Q = \frac{1}{N_d} \sum_{i=1}^{N_d} q_i$ and $P = \sum_{i=1}^{N_d} p_i$ probing only average properties of a localized subset of oscillators. Each example shows that the choice of a subsystem A corresponds to a coarse graining of the system that preserves the symplectic structure of the accessible observables.

Given a subsystem A we introduce a new notion of characteristic exponent Λ_A that generalizes the notion of Lyapunov exponents of the system. A Darboux basis $\mathcal{D}_A = (\theta^1, \dots, \theta^{2N_A})$ of the subsystem defines a symplectic cube

$$\mathcal{V}_A = \left\{ \sum_{r=1}^{2N_A} c_r \theta^r \middle| 0 \leq c_i \leq 1 \right\} \subset A^*. \quad (5.49)$$

Given the metric G^{ab} , we can compute the volume $\text{Vol}_G(\mathcal{V}_A)$ of the symplectic cube \mathcal{V}_A as the square root of the determinant of the $2N_A \times 2N_A$ Gramian matrix $(\theta_a^r G^{ab} \theta_b^s)$,

$$\text{Vol}_G(\mathcal{V}_A) = \sqrt{\det(\theta_a^r G^{ab} \theta_b^s)} = \sqrt{\det[G]_A}. \quad (5.50)$$

We will be interested in how this volume changes under time evolution. Let us recall that the action on V^* is given by the transpose $M^\top(t)_a{}^b = M^b{}_a(t)$. If we evolve the symplectic cube \mathcal{V}_A with M^\top , we have

$$\text{Vol}_G(M^\top(t)\mathcal{V}_A) = \sqrt{\det([M(t) G M^\top(t)]_A)}. \quad (5.51)$$

We define the subsystem exponent Λ_A as the exponential rate of growth of the volume of the subsystem measured with respect to the metric G^{ab} ,

$$\Lambda_A = \lim_{t \rightarrow \infty} \frac{1}{t} \log \frac{\text{Vol}_G(M^\top(t)\mathcal{V}_A)}{\text{Vol}_G(\mathcal{V}_A)}. \quad (5.52)$$

For a regular Hamiltonian system this limit exists and is independent of the metric g_{ab} , see appendix B.3. Note that the exponent of the full system Λ_V vanishes because $[M^\top(t)]_V = M^\top(t)$ and the determinant of a symplectic matrix is equal to one. The vanishing of Λ_V is a special case of the Liouville theorem. We say that the subsystem A is unstable under time evolution if it has a positive exponent Λ_A .

5.2.4 Relation of the exponent Λ_A to Lyapunov exponents

We now show how to compute the subsystem exponent Λ_A once the Lyapunov spectrum of the system is known. The result is stated and proven below.

Theorem 3 (*Subsystem exponent*)

Given a regular Hamiltonian system with Lyapunov spectrum $(\lambda_1, \dots, \lambda_{2N})$ and Lyapunov basis $\mathcal{D}_L = (\ell^1, \dots, \ell^{2N})$, the subsystem exponent Λ_A associated to the symplectic decomposition $V = A^* \oplus B^*$ can be determined as follows:

1. Choose a Darboux basis $\mathcal{D}_A = (\theta^1, \dots, \theta^{2N_A})$ of the symplectic subspace $A^* \subset V^*$.
2. Compute the unique transformation matrix T that expresses \mathcal{D}_A in terms of the Lyapunov basis $\mathcal{D}_L = (\ell^1, \dots, \ell^{2N})$:

$$\begin{pmatrix} \theta^1 \\ \vdots \\ \theta^{2N_A} \end{pmatrix} = \begin{pmatrix} T_1^1 & \cdots & T_{2N}^1 \\ \vdots & \ddots & \vdots \\ T_1^{2N_A} & \cdots & T_{2N}^{2N_A} \end{pmatrix} \begin{pmatrix} \ell^1 \\ \vdots \\ \ell^{2N} \end{pmatrix} \quad (5.53)$$

$\underbrace{\hspace{1cm}}_{\vec{t}_1} \qquad \qquad \qquad \underbrace{\hspace{1cm}}_{\vec{t}_{2N}}$

We refer to the $2N$ columns of T as \vec{t}_i .

3. Find the first $2N_A$ linearly independent ⁴ columns \vec{t}_i of T which we can label by \vec{t}_{i_k} with k ranging from 1 to $2N_A$. The result is a map $k \mapsto i_k \in (1, \dots, 2N)$ with $i_{k+1} > i_k$.

The subsystem exponent Λ_A is then given by the sum over the $2N_A$ Lyapunov exponents λ_{i_k} ,

$$\Lambda_A = \sum_{k=1}^{2N_A} \lambda_{i_k}, \quad (5.54)$$

where the index i_k is defined above.

Proof: The rectangular matrix T in (5.53) allows us to express the elements of the Darboux basis \mathcal{D}_A of the subsystem in terms of the Lyapunov basis, $\theta^r = \sum^{2N} T_i^r \ell^i$. Denoting the columns of T by \vec{t}_i we can select the first $2N_A$ linearly independent columns in the ordered set $(\vec{t}_1, \dots, \vec{t}_{2N})$. We label them \vec{t}_{i_k} and organize them in the $2N_A \times 2N_A$ square matrix U ,

$$U = (\vec{t}_{i_1} \mid \dots \mid \vec{t}_{i_{2N_A}}). \quad (5.55)$$

Due to their linear independence, the inverse U^{-1} exists and turns T into an upper triangular matrix \tilde{T} of the form

$$\tilde{T} = U^{-1}T = \begin{pmatrix} 0 & \dots & 0 & 1 & * & * & \dots & \dots & * \\ 0 & \dots & & 0 & 1 & * & * & \dots & * \\ \vdots & & \vdots & & \vdots & & & \vdots & \\ 0 & \dots & & & 0 & 1 & * & * & \dots & * \end{pmatrix}, \quad (5.56)$$

where the $*$ represents an unspecified value. Acting with U^{-1} on the left and the right-hand side of (5.53) we find

$$\tilde{\theta}^k = \ell^{i_k} + \sum_{j>i_k}^{2N} \tilde{T}_j^k \ell^j, \quad (5.57)$$

$$S_A(t) \sim \log \text{Vol}(M^\tau(t)\mathcal{V}_A) \sim \sum_{k=1}^{2N_A} \lambda_{i_k} t$$

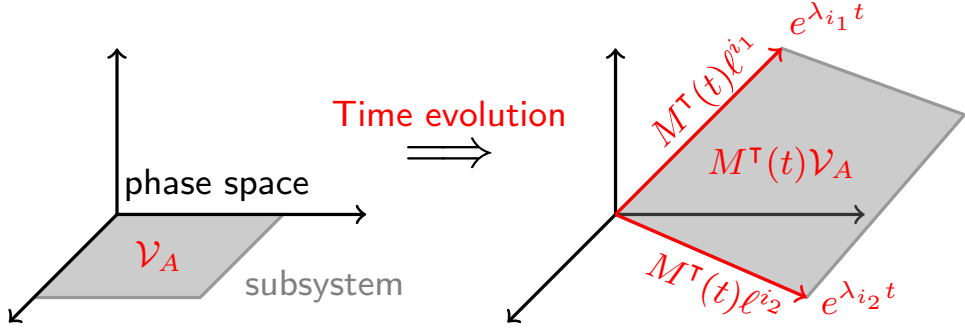


Figure 5.2: Subsystem exponents due to phase space stretching. We illustrate the statement of theorem 3. We start with a symplectic cube $\mathcal{V}_A \subset A^*$ in the subsystem and time-evolve it to the deformed cube $M^\tau(t)\mathcal{V}_A$ that is dominantly stretched into the $2N_A$ directions of $M^\tau(t)\ell^{i_k}$ with Lyapunov exponents λ_{i_k} . Consequently, the logarithm of its metric volume behaves as $\log \text{Vol}(M^\tau(t)\mathcal{V}_A) \sim \sum_{k=1}^{2N_A} \lambda_{i_k} t$. In generic situations, λ_{i_k} are just the $2N_A$ largest Lyapunov exponents, as explained in theorem 4. The quantity $\log \text{Vol}(M^\tau(t)\mathcal{V}_A)$ is related to the entanglement entropy S_A as explained in section 5.3.2.

where $\tilde{\theta}_k = (U^{-1}\theta)_k$. Note that the vectors $\tilde{\theta}^k$ satisfy $\lim_{t \rightarrow \infty} \frac{1}{t} \log \|M^\tau(t)\tilde{\theta}^k\| / \|\tilde{\theta}^k\| = \lambda_{i_k}$. Moreover the $2N_A$ vectors $\tilde{\theta}^k$ are linearly independent and form a (generally non-symplectic) basis of A^* . Therefore the cube $M^\tau(t)\mathcal{V}_A$ is given by a time-independent linear transformation of the one spanned by $M^\tau(t)\tilde{\theta}_k$. In the limit $t \rightarrow \infty$ the volume of the subsystem scales as $\text{Vol}_G(M^\tau(t)\mathcal{V}_A) \sim \exp(\sum_{k=1}^{2N_A} \lambda_{i_k} t)$ if there are no directions that become collinear in an exponentially fast way under time evolution. As the exponential collinearity is excluded by the assumption of regularity (see appendix B.3), the subsystem exponent is given by (5.54). \square

This theorem, together with the fact that both $\mathcal{D}_L = (\ell^1, \dots, \ell^{2N})$ and $\mathcal{D}_A = (\theta^1, \dots, \theta^{2N_A})$ are symplectic bases, implies the following important property of the subsystem exponent Λ_A .

Corollary 1

The subsystem exponent is non-negative,

$$\Lambda_A \geq 0. \quad (5.58)$$

Proof: Let us denote the elements of the Lyapunov basis by $\ell^i = Q_i$ for $i \leq N$ and $\ell^i = P_{2N+1-i}$ for $i > N$ so that $(\ell^1, \dots, \ell^{2N}) = (Q_1, \dots, Q_N, P_N, \dots, P_1)$. Each vector \tilde{v}_{i_k} with $i_k > N$ consists of a linear superposition of momenta P_i only, as follows from (5.57). As a result, to span a symplectic subspace, for each such \tilde{v}_{i_k} there has to be a $\tilde{v}_{i_{k'}}$ with $i_{k'} \leq 2N+1-i_k$ so to contain the conjugate position Q_i in the linear superposition. Therefore, negative Lyapunov exponents λ_{i_k} with $i_k > N$ are paired with positive Lyapunov exponents $\lambda_{i_{k'}}$, resulting in a sum of non-negative terms $\lambda_{i_k} + \lambda_{i_{k'}} \geq 0$ in (5.54). \square

We illustrate this result with some examples of subsystems and the associated exponents. Consider a system with $N = 2$ degrees of freedom, Lyapunov spectrum

$$(\lambda_1, \lambda_2, -\lambda_2, -\lambda_1) \quad (5.59)$$

and Lyapunov basis $\mathcal{D}_L = (\ell^1, \ell^2, \ell^3, \ell^4) = (Q_1, Q_2, P_2, P_1)$. A subsystem A with $N_A = 1$ degree of freedom can be identified by specifying a canonical couple (ϕ, π) . Here we give three examples:

$$(1) \quad \begin{cases} \phi = Q_1 \\ \pi = Q_2 + P_1 \end{cases} \quad \Rightarrow \quad T = \begin{pmatrix} 1 & 0 & 0 & 0 \\ 0 & 1 & 0 & 1 \end{pmatrix} \quad \Rightarrow \quad \Lambda_A = \lambda_1 + \lambda_2 \geq 0, \quad (5.60)$$

$$(2) \quad \begin{cases} \phi = Q_1 + Q_2 \\ \pi = P_2 \end{cases} \quad \Rightarrow \quad T = \begin{pmatrix} 1 & 1 & 0 & 0 \\ 0 & 0 & 1 & 0 \end{pmatrix} \quad \Rightarrow \quad \Lambda_A = \lambda_1 - \lambda_2 \geq 0, \quad (5.61)$$

$$(3) \quad \begin{cases} \phi = Q_1 + Q_2 \\ \pi = P_1 \end{cases} \quad \Rightarrow \quad T = \begin{pmatrix} 1 & 1 & 0 & 0 \\ 0 & 0 & 0 & 1 \end{pmatrix} \quad \Rightarrow \quad \Lambda_A = \lambda_2 - \lambda_1 = 0. \quad (5.62)$$

In particular the subsystem given by a single couples (Q_i, P_i) has vanishing subsystem exponent $\Lambda_A = 0$. Note also that the difference of positive Lyapunov exponents can appear as in example (5.61). We will reconsider these examples in section 5.4.1 and relate the subsystem exponents Λ_A to the production of entanglement entropy.

5.2.5 Relation of the exponent Λ_A to the Kolmogorov-Sinai entropy rate

From an information-theory perspective, the Hamiltonian evolution of a dynamical system with sensitive dependence on initial conditions produces entropy. This is because two initial conditions that are indistinguishable at a fixed resolution will evolve into distinguishable states after a finite time. The Kolmogorov-Sinai entropy rate provides a quantitative characterization of this behavior: It measures the uncertainty remaining on the next state of a system, if an infinitely long past is known [84–87]. It is defined as follows.

We decompose the phase space V into cells $(\mathcal{C}_1, \dots, \mathcal{C}_n)$ belonging to a partition \mathcal{P} . Given a sampling time Δt , we can compute the probability $\mu(\mathcal{C}_1, \dots, \mathcal{C}_n)$ that a trajectory starting in cell \mathcal{C}_1 will successively go through $\mathcal{C}_2, \mathcal{C}_3$ and so on. The entropy per unit time with respect to such a given partition is given by Shannon's formula,

$$\mathfrak{h}(\mathcal{P}) = - \lim_{\Delta t \rightarrow 0} \lim_{n \rightarrow \infty} \frac{1}{n \Delta t} \sum_{\mathcal{C}_1, \dots, \mathcal{C}_n} \mu(\mathcal{C}_1, \dots, \mathcal{C}_n) \log \mu(\mathcal{C}_1, \dots, \mathcal{C}_n). \quad (5.63)$$

The Kolmogorov-Sinai entropy rate is then defined as the supremum over all possible partitions:

$$h_{\text{KS}} = \sup_{\mathcal{P}} \mathfrak{h}(\mathcal{P}). \quad (5.64)$$

The quantity h_{KS} is a global invariant of the system and it provides a quantitative characterization of the notion of deterministic chaos in a Hamiltonian system.

A positive Lyapunov exponent corresponds to the exponential divergence in time of some initially nearby trajectories. This phenomenon results in the unpredictability of the evolution at finite resolution, and therefore contributes to h_{KS} . Pesin's theorem [94, 96] states that, for Hamiltonian dynamical systems, the Kolmogorov-Sinai entropy rate is equal to the sum over all the positive Lyapunov exponents of the system. Let us call $N_I \leq N$ the number of non-vanishing positive Lyapunov exponents. Using the ordering (5.42) of the Lyapunov spectrum, we have

$$h_{\text{KS}} = \sum_{i=1}^{N_I} \lambda_i. \quad (5.65)$$

This formula, together with (5.54), clearly shows that the Kolmogorov-Sinai entropy rate provides an upper bound to the characteristic exponent Λ_A of a subsystem,

$$\Lambda_A \leq h_{\text{KS}}. \quad (5.66)$$

In the following we discuss when this inequality is saturated and show that, for a large class of system decompositions, the characteristic exponent Λ_A equals the rate h_{KS} . The following theorem is instrumental.

Theorem 4 (Subsystem exponent – generic subsystem)

The subsystem exponent of a generic subsystem A of dimension N_A is given by the sum of the first $2N_A$ Lyapunov exponents, a special case of (5.54),

$$\Lambda_{A \text{ generic}} = \sum_{i=1}^{2N_A} \lambda_i. \quad (5.67)$$

This behavior holds for all subsystems $A \in V$, except for a set of measure zero.

Proof: The space of $2N_A$ -dimensional symplectic subspaces of V has the structure of a differentiable manifold and is called the symplectic Grassmannian $\text{SpGr}(2N_A, V)$. Let us consider the set of points on this manifold where the generic asymptotics (5.67) does *not* apply. The statement of the theorem is that this set forms a lower dimensional submanifold. All standard measures on differentiable manifolds will therefore assign a measure zero to this subset.

By applying theorem 3, (5.54), we find $\Lambda_{A \text{ generic}} = \sum_{i=1}^{2N_A} \lambda_i$ whenever the first $2N_A$ columns of the transfer matrix T are linearly independent. Let us therefore analyze for how many system decompositions this does not hold. The space of $2N_A$ -dimensional symplectic subspaces $\text{SpGr}(2N_A, V)$ can be identified with the space of transformation matrices such that the restricted symplectic form $[\Omega]_A$ is non-degenerate, modulo $\text{GL}(2N_A)$:

$$\text{SpGr}(2N_A, V) = \{T \in \text{Mat}(2N \times 2N_A) \mid \det(T\Omega T^T) \neq 0\} / \text{GL}(2N_A). \quad (5.68)$$

This follows from the fact that, for a given choice of Lyapunov basis and of a Darboux basis of A , every subspace $A \in \text{SpGr}(2N_A, V)$ defines a unique transfer matrix T . The different basis choices are equivalent to acting with a $\text{GL}(2N_A)$ -matrix on T from the left. The space of full rank $(2N \times 2N_A)$ -matrices is $(2N)(2N_A)$ -dimensional and $\text{GL}(2N_A)$ is $(2N_A)^2$ -dimensional. The condition $\det(T\Omega T^T) \neq 0$ only cuts out a lower dimensional submanifold which does not change the dimension. This fact implies that the dimension of $\text{SpGr}(2N_A, V)$ is $4N_A(N - N_A)$.

Let us now compare this to the space of subspaces for which the subsystem exponent Λ_A is not given by the sum over the first $2N_A$ largest Lyapunov exponents. For this to happen, it is a necessary condition that the first $2N_A$ columns of the transfer matrix are linearly dependent. This space is $(4NN_A - 1)$ -dimensional which we still need to quotient by $\text{GL}(2N_A)$. Therefore, the subset of spaces of subsystems A , for which we find $\Lambda_A \neq \Lambda_{A \text{ generic}}$, has a dimension of at most $4N_A(N - N_A) - 1$. This is a set of measure zero with respect to any standard measure on $\text{SpGr}(2N_A, V)$ because it lies in a lower dimensional submanifold. \square

This behavior was conjectured by Zurek and Paz in [59] and later discussed by Asplund and Berenstein [89].

Of the three examples discussed at the end of section 5.2.3, only the one-dimensional subsystem (ϕ, π) with $\Lambda_A = \lambda_1 + \lambda_2$ is generic, (5.60). Note that most numerical algorithms for the computation of the Lyapunov exponents of a dynamical system start with the computation of the exponential rate of expansion of the volume of a subsystem [97]. Lyapunov exponents are computed by taking the difference between the exponential rate of expansion of subsystems of different dimension. The efficiency of these algorithms relies on the generic behavior discussed above.

Now we investigate when the subsystem exponent equals the rate \mathfrak{h}_{KS} assuming that the subsystem is generic, (5.67).

In a stable Hamiltonian system, all Lyapunov exponents vanish. The system becomes unstable as soon as a single Lyapunov exponent turns positive. We call N_I the number of non-vanishing positive Lyapunov exponents. Pesin's formula for the Kolmogorov-Sinai entropy rate then reads $h_{\text{KS}} = \sum_{i=1}^{N_I} \lambda_i$. On the other hand the characteristic exponent of a generic subsystem A of dimension N_A in the range $N_I \leq 2N_A \leq 2N - N_I$ is given by $\Lambda_{A \text{ generic}} = \sum_{i=1}^{N_I} \lambda_i$. Therefore, we have the equality

$$\Lambda_{A \text{ generic}} = h_{\text{KS}} \quad \text{for} \quad N_I \leq 2N_A \leq 2N - N_I, \quad (5.69)$$

that identifies subsystems that saturates the inequality (5.66).

Note that unstable many-body systems often have a number of unstable directions N_I that is much smaller than the number of degrees of freedom of the system, $N_I \ll N$. A generic subsystem that encompasses a fraction $f = N_A/N$ of the full system satisfies (5.69) if the fraction is in the range

$$\frac{N_I}{2N} \leq f \leq 1 - \frac{N_I}{2N}. \quad (5.70)$$

In particular, in the limit $N \rightarrow \infty$ with N_I finite, we have $\Lambda_A = h_{\text{KS}}$ for all partitions of the system into two complementary subsystems each spanning a finite fraction f of the system, except for a set of partitions of measure zero.

5.3 Proof, part II: quantum ingredients

The main result, theorem 1, is proven in three steps which heavily rely on the three ingredient presented in the following subsections. We show how the Rényi entropy provides bounds for the entanglement entropy, we explain how the Rényi entropy can be understood as the logarithm of the volume of a region in the dual phase space and finally, we derive the time evolution of the Rényi entropy as the volume deformation of this region under the classical symplectic flow.

5.3.1 Upper and lower bounds on the entanglement entropy

We recall that there are different entanglement measures that quantify the amount of correlations in a state $|\psi\rangle$ with respect to some system decomposition into subsystems A and B . Beside the entanglement entropy $S_A(|\psi\rangle)$, we have the class of Rényi entropies defined by

$$R_A^{(n)}(|\psi\rangle) = -\frac{1}{n-1} \log \text{Tr}_{\mathcal{H}_A}(\rho_A^n), \quad (5.71)$$

where $S_A(|\psi\rangle) = \lim_{n \rightarrow 1} R_A^{(n)}(|\psi\rangle)$. For a Gaussian state $|J, \eta\rangle$ labeled by a complex structure J , all these entropies can be computed directly from the eigenvalues $\pm i\nu_i$ of $[J]_A$, the complex structure restricted to the subsystem A . If we take the positive value ν_i of each eigenvalue pair, the Rényi entropy⁵ $R_A = R_A^{(2)}$ and the entanglement entropy S_A are given by

$$R_A = \sum_{i=1}^{N_A} \log(\nu_i) \quad \text{and} \quad S_A = \sum_{i=1}^{N_A} S(\nu_i) \quad \text{with} \quad S(\nu) = \frac{\nu+1}{2} \log \frac{\nu+1}{2} - \frac{\nu-1}{2} \log \frac{\nu-1}{2}, \quad (5.72)$$

⁵From now on, we will refer to the Rényi entropy of order 2 as *the* Rényi entropy.

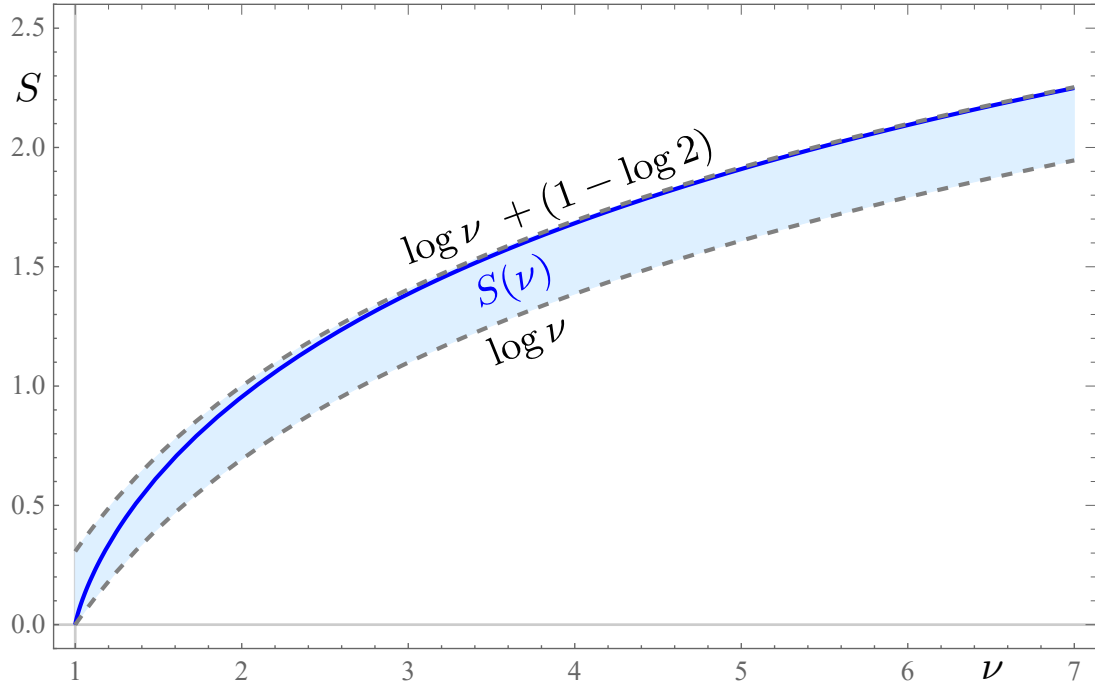


Figure 5.3: *Bounds on the entanglement entropy.* The plot shows how the contribution $S(\nu)$ to the entanglement entropy coming from a single entangled pair is bounded from below by $\log \nu$ and from above by $\log \nu + (1 - \log 2)$. For large ν , the asymptotic behavior is $S(\nu) \sim \log \nu + (1 - \log 2) - O(\nu^{-2})$.

which is derived in appendix 2.2.2. Here, we derive upper and lower bounds on the entanglement entropy of Gaussian states. Consider the function $S(\nu)$ defined in (5.71) and the inequality

$$0 \leq S(\nu) - \log \nu < (1 - \log 2) \approx 0.31 \quad (5.73)$$

holding for $\nu \geq 1$ as shown in figure 5.3. An immediate consequence of this inequality is that the entanglement entropy of a Gaussian state is bounded from below by the Rényi entropy and from above by the Rényi entropy plus a state-independent constant,

$$R_A(|J, \zeta\rangle) \leq S_A(|J, \zeta\rangle) < R_A(|J, \zeta\rangle) + (1 - \log 2) \min(N_A, N_B). \quad (5.74)$$

This means that the Rényi entropy R_A determines a corridor for the entanglement entropy S_A . This implies immediately that both of them will grow asymptotically with the same rate which we use for the main result of this paper.

5.3.2 Rényi entropy as phase space volume

A Gaussian state $|J, \eta\rangle$ equips the dual phase space V^* with a metric G^{ab} defined by (2.6), which is really just the covariance matrix of the state. The complex structure J can be expressed in terms of the metric

$$J^a{}_b = -G^{ac}\omega_{cb}. \quad (5.75)$$

Furthermore, the restriction of the complex structure to the subsystem A can be written in matrix form as a product of the symplectic Ω_A and the restriction of the metric,

$$[J]_A = -[G]_A \omega_A. \quad (5.76)$$

In a Darboux basis, where we have $\det \omega_A = 1$ and $\det[G]_A > 0$, we find that the determinant of the restriction of the complex structure can be expressed in terms of the phase space volume $\text{Vol}_G(\mathcal{V}_A)$ of a symplectic cube \mathcal{V}_A (spanned by a Darboux basis and with symplectic volume 1) measured with respect to the induced metric.

$$|\det[iJ]_A| = \det[G]_A \det \omega_A = \left(\text{Vol}_G(\mathcal{V}_A) \right)^2. \quad (5.77)$$

As a result, the Rényi entropy of a Gaussian state is given by the logarithm of the phase space volume of a symplectic cube \mathcal{D}_A defining the subsystem, measured with respect to the metric G^{ab} defined by the state,

$$R_A(|J, \zeta\rangle) = \log \text{Vol}_G(\mathcal{V}_A). \quad (5.78)$$

Note that the symplectic cube \mathcal{V}_V associated to a Darboux basis of the full system satisfies $\text{Vol}_G(\mathcal{V}_V) = 1$ and therefore the Rényi entropy vanishes $R_V(|J, \zeta\rangle)$. On the other hand, the restriction to a subsystem A can result in a larger volume $\text{Vol}_G(\mathcal{V}_A) \geq 1$ and a non-vanishing Rényi entropy.

5.3.3 Entanglement entropy growth as phase space stretching

Let us consider a one-parameter family of Gaussian states $|J_t, \eta_t\rangle = U(t)|J_0, \eta_0\rangle$ generated under time evolution of some quadratic Hamiltonian. In particular, we have $J_t = M(t)J_0M^{-1}(t)$ where $M(t) : V \rightarrow V$ is the classical Hamiltonian flow on phase space. We call G_t the time-dependent metric associated with J_t , and G_0 the initial metric associated with J_0 . The evolution of the Rényi entropy is given by (5.78), where the volume is now measured with respect to the time-varying metric:

$$R_A(U(t)|J_0, \eta_0\rangle) = \log \text{Vol}_{G_t}(\mathcal{V}_A). \quad (5.79)$$

In this formula, the symplectic cube \mathcal{V}_A is kept fixed while the metric evolves. However, the same volume is obtained if we let the symplectic cube evolve according to $M^\top(t)\mathcal{V}_A$ for a fixed metric G_0 . Hence, we can compute

$$R_A(U(t)|J_0, \eta_0\rangle) = \log \text{Vol}_{G_0}(M^\top(t)\mathcal{V}_A). \quad (5.80)$$

The symplectic basis of the subsystem A is stretched by the Hamiltonian flow $M^\top(t) : V^* \rightarrow V^*$ on the dual phase space, and the variation in its volume determines the evolution of the Rényi entropy.

Since the absolute difference between the entanglement entropy and the Rényi entropy of a Gaussian states is bounded by a state independent constant, we have that:

$$\lim_{t \rightarrow \infty} \frac{1}{t} [S_A(U(t)|J_0, \eta_0\rangle) - R_A(U(t)|J_0, \eta_0\rangle)] = 0, \quad (5.81)$$

i.e., the asymptotic rate of growth of the entanglement entropy and of the Rényi entropy coincide. This allows us to compute the asymptotic rate of growth of the entanglement entropy from (5.80) as:

$$\lim_{t \rightarrow \infty} \frac{S_A(U(t)|J_0, \eta_0\rangle)}{t} = \lim_{t \rightarrow \infty} \frac{1}{t} \log \text{Vol}_{G_0}(M^\top(t)\mathcal{V}_A), \quad (5.82)$$

in terms of the stretching of the symplectic cube under time-evolution.

5.4 Examples: unstable potentials and periodic quenches

We briefly discuss three examples of simple systems that show a linearly growing entanglement entropy and allow us to test our results.

5.4.1 Particle in a 2d inverted potential

In our first example, we study a simple system consisting of just two degrees of freedom. Despite its simplicity, the example captures the main features of the theorems presented above. It also resembles the system studied in [89] and thereby illustrates how our theorems simplify the involved steps to understand the asymptotic behavior of the entanglement entropy.

We consider a system which can be described as a quantum particle with mass $m = 1$ moving in a plane with coordinates (q_1, q_2) and corresponding momenta (p_1, p_2) . The instabilities arise from an inverted harmonic potential $V(q_1, q_2) = -\frac{\lambda_1^2}{2}q_1^2 - \frac{\lambda_2^2}{2}q_2^2$ with $\lambda_1 \geq \lambda_2 > 0$. The Hamiltonian of this system is explicitly given by

$$H = \frac{1}{2} (p_1^2 + p_2^2 - \lambda_1^2 q_1^2 - \lambda_2^2 q_2^2). \quad (5.83)$$

If we choose the Darboux basis $\mathcal{D}_V = (p_1, p_2, q_1, q_2)$, the matrices h and $K = \Omega h$ become

$$h = \begin{pmatrix} 1 & & & \\ & 1 & & \\ & & -\lambda_1 & \\ & & & -\lambda_2 \end{pmatrix} \Rightarrow K = \begin{pmatrix} & -\lambda_1^2 & & \\ & & -\lambda_2^2 & \\ -1 & & & \\ & -1 & & \end{pmatrix}. \quad (5.84)$$

The Lyapunov exponents $(\lambda_1, \lambda_2, -\lambda_2, -\lambda_1)$ are given by the eigenvalues of K and the Lyapunov basis $\mathcal{D}_L = (\ell^1, \ell^2, \ell^3, \ell^4) = (Q_1, Q_2, P_2, P_1)$ are the corresponding eigenvectors

$$\begin{cases} Q_1 = q_1 - \lambda_1 p_1 \\ Q_2 = q_2 - \lambda_2 p_2 \\ P_2 = p_2 + \frac{1}{\lambda_2} q_2 \\ P_1 = p_1 + \frac{1}{\lambda_1} q_1 \end{cases} \quad (5.85)$$

With these definitions, let us consider the three different choices of subsystem A discussed also in section 5.2.4:

$$(1) \begin{cases} \phi = Q_1 \\ \pi = Q_2 + P_1 \end{cases} \Rightarrow T = \begin{pmatrix} 1 & 0 & 0 & 0 \\ 0 & 1 & 0 & 1 \end{pmatrix} \Rightarrow \Lambda_A = \lambda_1 + \lambda_2 \geq 0, \quad (5.86)$$

$$(2) \begin{cases} \phi = Q_1 + Q_2 \\ \pi = P_2 \end{cases} \Rightarrow T = \begin{pmatrix} 1 & 1 & 0 & 0 \\ 0 & 0 & 1 & 0 \end{pmatrix} \Rightarrow \Lambda_A = \lambda_1 - \lambda_2 \geq 0, \quad (5.87)$$

$$(3) \begin{cases} \phi = Q_1 + Q_2 \\ \pi = P_1 \end{cases} \Rightarrow T = \begin{pmatrix} 1 & 1 & 0 & 0 \\ 0 & 0 & 0 & 1 \end{pmatrix} \Rightarrow \Lambda_A = \lambda_2 - \lambda_1 = 0. \quad (5.88)$$

We can study the entanglement entropy for these subsystems numerically where we start with the (entangled) initial state given by $G_0(\ell^i, \ell^j) = \delta^{ij}$. Figure 5.4 shows excellent agreement with our predictions. In particular, we also see that the entanglement entropy $S_A(t)$ and the Rényi entropy $R_A(t)$ only differ by the constant $1 - \log(2)$ if the system is strongly entangled.

5.4.2 Quadratic potential with instabilities

The second example consists in the evolution in a time-independent potential with instabilities. Let us consider a classical system with N degrees of freedom which we parametrize by N conjugate

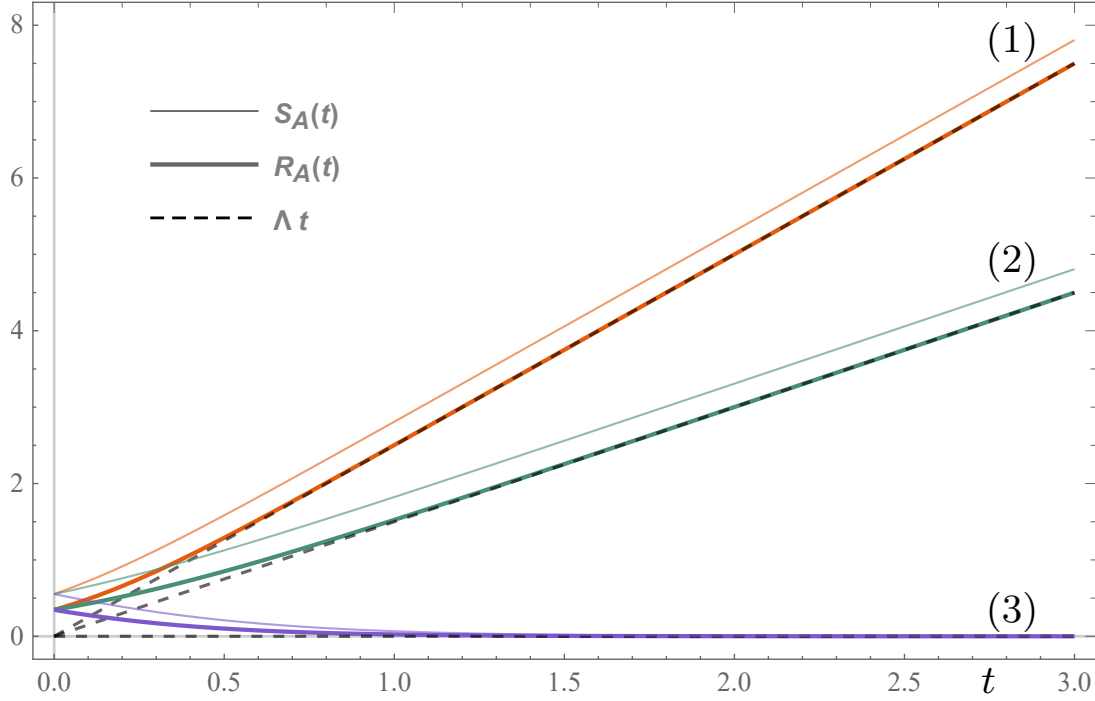


Figure 5.4: Particle in a 2d inverted potential. The plot shows the exact behavior of the Rényi entropy $R_A(t)$ (thick) and entanglement entropy $S_A(t)$ (thin) in comparison to the predicted asymptotics Λt (dashed). The system is defined in (5.83) with subsystems specified in (5.86–5.88). For the computation, we choose $\lambda_1 = -\lambda_4 = 2$ and $\lambda_2 = -\lambda_3 = 1/2$. The initial state is chosen to be $|J_0\rangle$ with associated metric $G_0(\ell^i, \ell^j) = \delta^{ij}$. In the case of examples (1) and (2), we have $S_A(t) - R_A(t) \rightarrow c = 0.31$, while for example (3), we have $S_A(t) \rightarrow R_A(t) \rightarrow 0$ for large t .

pairs (q_i, p_i) of coordinates in phase space. The Hamiltonian H of the system consists of a standard kinetic term and a quadratic potential,

$$H = \sum_{i=1}^N \frac{1}{2} p_i^2 + \sum_{i,j=1}^N \frac{1}{2} V_{ij} q_i q_j. \quad (5.89)$$

The potential is determined by the symmetric matrix V_{ij} with eigenvalues v_i . This classical system has $2N$ Lyapunov exponents λ_i determined by the eigenvalues of V_{ij} and given by $\lambda_i = \pm \text{Im}(\sqrt{v_i})$. Positive eigenvalues correspond to stable directions of the potential, lead to oscillatory motion and vanishing Lyapunov exponent. In the presence of negative eigenvalues $v_i < 0$, the system is unstable, the classical motion is unbounded and nearby trajectories in phase space diverge at an exponential rate given by the $\lambda_i = +\text{Im}(\sqrt{v_i})$. Now we consider the associated quantum system prepared in a Gaussian state and study the behavior of a generic subsystem. If the potential V_{ij} couples the subsystem A with the rest of the system, we expect that the entanglement entropy of the subsystem changes in time. Our theorem states that the entanglement entropy of a generic subsystem A with N_A degrees of freedom asymptotically grows at a rate given by the sum of the $2N_A$ largest Lyapunov exponents, (5.14). We give a concrete example: We consider a system with $N = 20$ degrees of freedom and quadratic potential specified by a $N \times N$ real symmetric random matrix V_{ij} . Negative eigenvalues of V_{ij} correspond to unstable directions of the potential and

non-vanishing Lyapunov exponents with the following values:

$$\begin{array}{ccccccccccccccccc} \lambda_1 & \lambda_2 & \lambda_3 & \lambda_4 & \lambda_5 & \lambda_6 & \cdots & \lambda_{15} & \lambda_{16} & \lambda_{17} & \lambda_{18} & \lambda_{19} & \lambda_{20} \\ +.55 & +.45 & +.34 & +.31 & +.29 & 0 & \cdots & 0 & -.29 & -.31 & -.34 & -.45 & -.55 \end{array} \quad (5.90)$$

figure 5.5 shows the growth of the entanglement entropy of an initially un-entangled Gaussian state for generic subsystems of different dimensions. For a one-dimensional subsystem $N_A = 1$, theorem 2 predicts the asymptotic growth $S_A(t) \sim (\lambda_1 + \lambda_2)t$. Note that, as the Lyapunov exponents appear in couples $(\lambda, -\lambda)$, the asymptotic growth of the rest of the system has the same rate, $S_B(t) \sim (\lambda_1 + \dots + \lambda_{18})t = (\lambda_1 + \lambda_2)t$, as expected for the entanglement entropy of a pure state.

Clearly, the statement that the entanglement growth is linear in time applies only to generic subsystems and not to subsystems that are aligned to the shape of the potential. As an example, let us call $(Q_1, \dots, Q_N, P_N, \dots, P_1)$ the Lyapunov basis of the system and consider the subsystem spanned by the canonical couple (Q_1, P_1) . Theorem 1 predicts a sublinear rate $S_A(t) \sim (\lambda_1 + \lambda_{20})t = (\lambda_1 - \lambda_1)t \sim o(t)$, which is consistent with the statement that the entropy will stay constant as the subsystem is isolated. Moreover, note that the difference of Lyapunov exponents can also appear in the asymptotic rate of the entanglement growth, for instance the subsystem spanned by $(Q_2, P_2 + P_3)$ has asymptotic rate $S_A(t) \sim (\lambda_2 - \lambda_3)t$. This is the quantum version of the example discussed in (5.61). It is important to remark however that these subsystems are non-generic and form a subset of measure zero as discussed in the proof of theorem 4.

The random quadratic potential V_{ij} with Lyapunov exponents specified in (5.90) has $N_I = 5$ unstable directions and classical Kolmogorov-Sinai rate $h_{KS} = \lambda_1 + \dots + \lambda_5 \simeq 1.94$. Theorem 2 states that at the quantum level the long-time behavior of the entanglement entropy is linear with rate h_{KS} for all generic subsystem decompositions such that $2N_A \geq N_I$ and $2N_B \geq N_I$, i.e., $S_A(t) \sim h_{KS}t$ for generic subsystems of dimension $3 \leq N_A \leq 18$. Figure 5.5 shows the numerical evolution of the entanglement entropy and the cases $N_A = 3, N_A = 4, N_A = 5$ exhibit a linear growth with rate given by the Kolmogorov-Sinai rate as predicted.

A remarkable feature of the predictions stated in theorems 1 and 2 is that the asymptotic growth of the entanglement entropy is determined by the subsystem and completely independent from the choice of initial Gaussian state. This feature is a consequence at the quantum level of the fact that the Lyapunov exponents of a classical system are independent of the choice of metric used to measure the distance between trajectories. In the language of complex structures J_0 that specify the initial Gaussian state $|J_0, \zeta_0\rangle$, the Lyapunov exponents are given by the eigenvalues of the matrix $L = \lim_{t \rightarrow \infty} \frac{1}{2t} \log(M^{-1}(t) J_0 M(t))$ defined in (5.41) and are independent of J_0 . Figure 5.5 shows only initial states with vanishing entanglement entropy, but the two theorems 1 and 2 apply to all Gaussian states, even to ones that have large initial entanglement entropy. Clearly the theorem applies only to the asymptotic behavior of the entanglement entropy. In fact we could take as initial state the time-reversal of the Gaussian state used in figure 5.5 at late times. In this case the entanglement entropy would initially decrease, reach a minimum and eventually start growing linearly as predicted by the theorems on the asymptotic growth.

5.4.3 Periodic quantum quenches in a harmonic lattice

As a third example of a system that displays a linear growth of the entanglement entropy, we discuss the case of a harmonic lattice subject to periodic quantum quenches. The Hamiltonian of the system is

$$H(t) = \sum_{i=1}^N \frac{1}{2} \left(p_i^2 + \Omega^2(t) q_i^2 + \kappa (q_{i+1} - q_i)^2 \right), \quad (5.91)$$

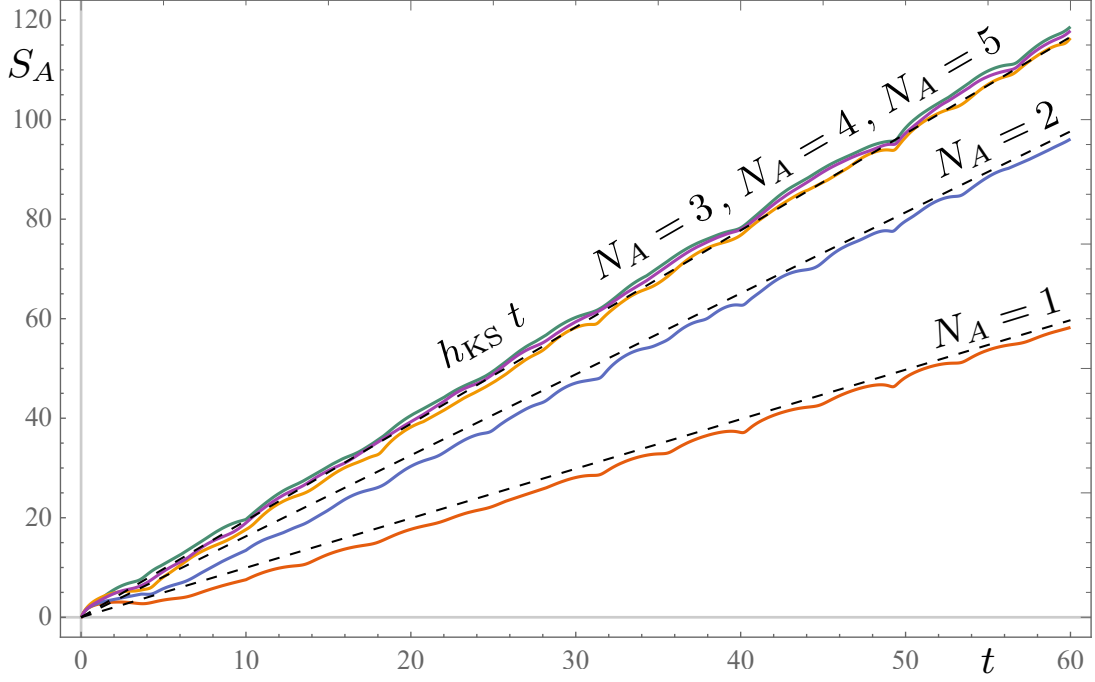


Figure 5.5: *Quadratic potential with instabilities.* This plot compares the behavior of the entanglement entropy with the asymptotic prediction of our theorem. The system consists of $N = 10$ degrees of freedom. The time evolution is determined by a Hamiltonian with random quadratic potential V . The $2N = 20$ Lyapunov exponents are given by $(.55, .45, .34, .31, .29, 0, \dots, 0, -.29, -.31, -.34, -.45, -.55)$. We plot five subsystems with $1 \leq N_A \leq 5$. The entanglement entropy (colored lines) agrees with the predicted asymptotics (dashed lines). Note that for $N_A \geq 3$, the asymptotic behavior is the same due to the stable Lyapunov exponents $\lambda_i = 0$ for $6 \leq i \leq 15$. These are exactly the cases for which we have $\Lambda_A = \hbar_{\text{KS}}$, which means that entropy production rate coincides with the classical Kolmogorov-Sinai entropy rate.

which describes the dynamics of a one-dimensional chain of N bosons with nearest-neighbor coupling κ and boundary conditions $q_{N+1} = q_1$, $p_{N+1} = p_1$. The one-particle oscillation frequency $\Omega(t)$ is periodically switched between the values $\Omega_0 \pm \varepsilon$ with period $2T_0$,

$$\Omega(t) = \begin{cases} \Omega_0 - \varepsilon & \text{for } 0 \leq t < T_0 \\ \Omega_0 + \varepsilon & \text{for } T_0 \leq t < 2T_0 \end{cases} \quad (5.92)$$

$$\Omega(t + 2T_0) = \Omega(t) \quad \text{and} \quad \varepsilon \ll \Omega_0. \quad (5.93)$$

The system is prepared in the ground state of the instantaneous Hamiltonian $H(0)$ at the time $t = 0$ and then let evolve unitarily. The state of the system at stroboscopic times $t_n = 2nT_0$ which are multiples of the period $2T_0$ can be obtained by computing the Floquet Hamiltonian of the system, H_F :

$$U(2nT_0) = \left(U(2T_0) \right)^n = e^{-i2nT_0 H_F} \quad \text{with} \quad H_F = \frac{i}{2T_0} \log \left(e^{-iH_2 T_0} e^{-iH_1 T_0} \right), \quad (5.94)$$

where $H_1 = H(T_0)$ and $H_2 = H(2T_0)$. We note that the Floquet Hamiltonian H_F is quadratic and time-independent, but is not of the standard form consisting of the sum of a kinetic and a potential term as in the case of (5.89). This general form is taken into account in theorems 1 and 2 which apply to all quadratic Hamiltonians.

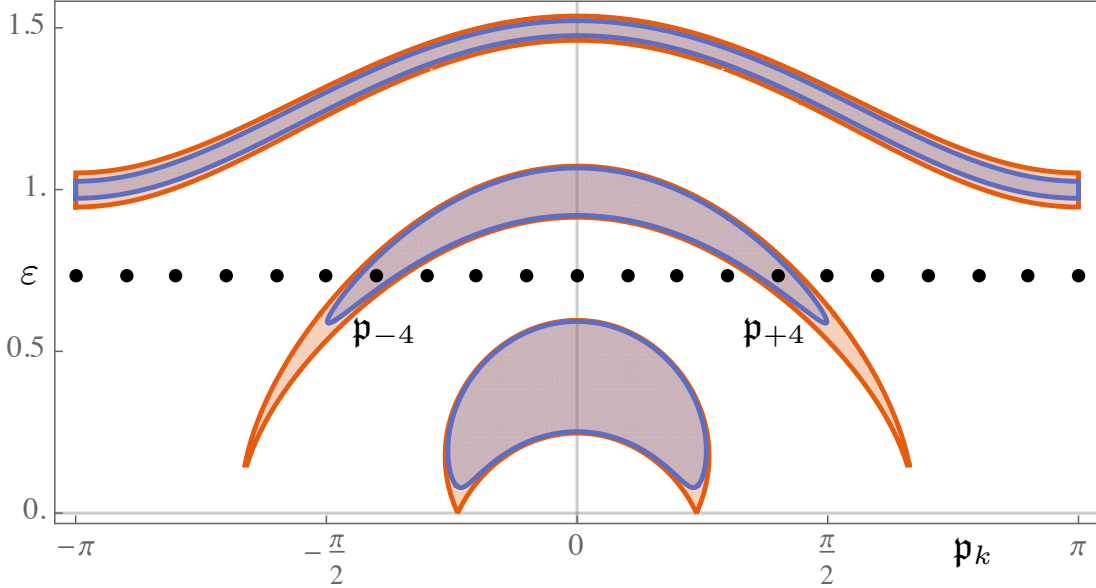


Figure 5.6: *Instability bands in a periodic quantum quench.* We sketch the instability region of Floquet exponents μ with positive real part (red: $\text{Re}(\mu) > 0.03$, blue: $\text{Re}(\mu) > 0.05$) for the system described in (5.95) as a function of ε and p_k . We chose the values $T_0 \simeq \pi$, $\Omega_0 \simeq 0.3$ and $\kappa \simeq 0.3$. Furthermore, we indicate the discrete momenta p_k for a periodic chain with $N \simeq 20$ and $\varepsilon \simeq 0.735$, such that there are two modes with unstable Floquet exponents, namely $p_{\pm 4} = \pm \frac{2\pi}{5}$.

The classical system described by (5.91) shows instabilities when small perturbations from the equilibrium configuration are amplified via the mechanism of parametric resonance. Floquet theory [98, 99] provides the tools for the description of the dynamics driven by an Hamiltonian which is periodic in time, as is the case for (5.91). The eigenvalues of the symplectic evolution matrix (5.34) evaluated at a period $M(2T_0)$ come in quadruplets $(e^{+2T_0\mu}, e^{-2T_0\mu}, e^{+2T_0\mu^*}, e^{-2T_0\mu^*})$ where the complex numbers μ are the Floquet exponents of the system. The stability of the system is measured by the real part of the Floquet exponents which coincide with the Lyapunov exponents, $\lambda = \text{Re}(\mu)$.

The Lyapunov exponents of the system (5.91) can be easily determined. In Fourier transformed variables⁶ Q_k , P_k with $k = 0, \pm 1, \pm 2, \dots, \pm(N-1)/2$, the Hamiltonian takes the form

$$H(t) = \sum_k \frac{1}{2} \left(|P_k|^2 + \omega_k^2(t) |Q_k|^2 \right), \quad (5.95)$$

with

$$\omega_k(t) = \sqrt{\Omega^2(t) + 4\kappa \sin^2(p_k/2)} \quad \text{and} \quad p_k = \frac{2\pi k}{N}. \quad (5.96)$$

In particular, the speed of sound of the mode of momentum p_k switches periodically between the values $v_k(T_0)$ and $v_k(2T_0)$, with $v_k(t) = \partial \omega_k(t) / \partial p_k$. As Fourier modes with different $|k|$ are decoupled, we can analyze the stability of the system mode by mode. The classical evolution of

⁶The Fourier transformed canonical variables are defined as $Q_k = \frac{1}{\sqrt{N}} \sum_l q_l e^{i \frac{2\pi k l}{N}}$, $P_k = \frac{1}{\sqrt{N}} \sum_l p_l e^{i \frac{2\pi k l}{N}}$, so that $[Q_k, P_{-k'}] = i \delta_{k,k'}$

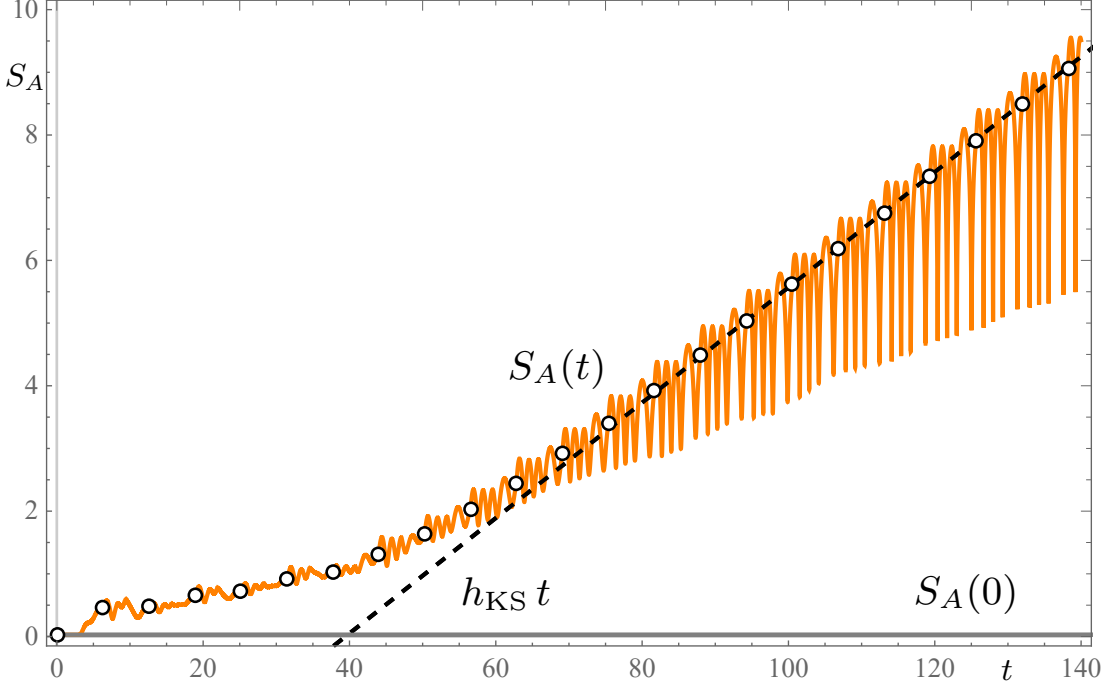


Figure 5.7: Periodic quantum quenches in a harmonic lattice. We show the entanglement entropy $S_A(t)$ as a function of time for the subsystem spanned by (q_1, p_1) . The stroboscopic entanglement entropy $S_A(n2T_0)$ is indicated by white dots. The asymptotic prediction of the Kolmogorov-Sinai production rate $S_A(t) \sim \hbar_{\text{KS}} t$ with $\hbar_{\text{KS}} = 0.092$ is shown as a dashed line where we adjusted the offset for easy comparison of the slope. Note that the entanglement entropy stays constant in the interval $[0, T_0]$ as expected from the fact that the system is prepared in the ground state of the initial Hamiltonian $H(0)$.

the coupled modes $(Q_k, Q_{-k}, P_{-k}, P_k)$ is given by

$$\begin{pmatrix} Q_k(t) \\ P_k(t) \end{pmatrix} = M_k(t) \begin{pmatrix} Q_k(0) \\ P_k(0) \end{pmatrix} \quad (5.97)$$

with

$$M_k(2T_0) = \begin{pmatrix} \cos(\omega_2 T_0) & -\omega_2 \sin(\omega_2 T_0) \\ \frac{1}{\omega_2} \sin(\omega_2 T_0) & \cos(\omega_2 T_0) \end{pmatrix} \begin{pmatrix} \cos(\omega_1 T_0) & -\omega_1 \sin(\omega_1 T_0) \\ \frac{1}{\omega_1} \sin(\omega_1 T_0) & \cos(\omega_1 T_0) \end{pmatrix} \quad (5.98)$$

given by a symplectic block of the symplectic matrix $M(2T_0)$ defined in (5.34), and $\omega_1 = \omega(T_0)$ and $\omega_2 = \omega(2T_0)$. The Lyapunov exponents of the system are the real parts of the Floquet exponents, i.e.

$$\pm \lambda_k = \text{Re} \left(\frac{1}{2T_0} \log \text{Eig}[M_k(2T_0)] \right). \quad (5.99)$$

Analytic expressions of λ_k can be found assuming that the periodic perturbation is small $\varepsilon \ll \Omega_0$ and the mode is at or near a parametric resonance. Defining $\delta\omega = \omega_2 - \omega_1$, $\omega_0 = \frac{\omega_1 + \omega_2}{2}$, with $\delta\omega \ll \omega_0$, we find that the system is in parametric resonance when the average frequency ω_0 of the mode is an half-integer multiple of the frequency of the perturbation, i.e.,

$$\omega_0 = \frac{n\pi}{2T_0}. \quad (5.100)$$

At the parametric resonance, the positive Lyapunov exponents of the system are given by

$$\lambda_k = \begin{cases} +\frac{\delta\omega}{n\pi} & \text{if } n \text{ odd,} \\ +\frac{T_0(\delta\omega)^2}{4n\pi} & \text{if } n \text{ even.} \end{cases} \quad (5.101)$$

For a finite perturbation, the stability of the system can be determined numerically. Figure 5.6 shows which modes p_k are unstable for a given finite value of the perturbation parameter ε . In the example we have $N = 20$, $\Omega_0 \simeq 0.3$, $\kappa \simeq 0.3$ and $T_0 \simeq \pi$. For $\varepsilon \simeq 0.735$ we have two unstable modes with $k = \pm 4$ and Lyapunov exponents $\lambda_{+4} \simeq \pm 0.046$, $\lambda_{-4} \simeq \pm 0.046$. The Kolmogorov-Sinai rate of the system is $\mathfrak{h}_{KS} = 0.092$. Figure 5.7 shows the growth of the entanglement entropy of a subsystem and the relation to \mathfrak{h}_{KS} .

5.5 Examples: quantum field theory

In section 5.1 we presented our main results for a bosonic quantum system with N degrees of freedom. These results can be extended with minor modifications to the case of a bosonic quantum field. In particular, the formulation of theorems 1 and 2 in terms of complex structures J is motivated by and tailored to applications to quantum field theory in curved spacetimes [5, 6, 100].

5.5.1 Definition of a subsystem and the algebraic approach

The presence of infinitely many degrees of freedom in quantum field theory has two immediate consequences which are relevant for our analysis [101]:

- i) the existence of unitarily inequivalent representations of the algebra of observables,
- ii) the lack of a factorization of the Hilbert space into a tensor product over local factors.

The algebraic approach to quantum field theory—together with the language of complex structures—provides a natural setting for discussing both aspects and formulating the analysis of the growth of the entanglement entropy of a subsystem in quantum field theory.

At the classical level, the phase space V of a free scalar field has coordinates $\xi^a = (\varphi(\vec{x}), \pi(\vec{x}))$ with \vec{x} a point on a Cauchy slice Σ . We adopt abstract indices and use the symbol ω_{ab} for the symplectic form on the infinite-dimensional vector space V . Carrying out the rigorous construction of the infinite-dimensional phase space requires the choice of a positive definite metric g_{ab} compatible with the symplectic form ω_{ab} , such that V arises as the completion with respect to this metric. Contracting ω_{ab} with the inverse metric G^{ab} gives rise to the complex structure $J^a{}_b = -G^{ac}\omega_{cb} : V \rightarrow V$. Given a reference complex structure J_0 and a symplectic transformation M , we can define a transformed complex structure $J_M = M^{-1}J_0M$. The transformation M is said to belong to the *restricted* symplectic group if the commutator $A = [J_0, J_M]$ is a Hilbert-Schmidt operator, i.e. $\text{tr}(A^\dagger A) < +\infty$ [102–104].

At the quantum level, the choice of a complex structure J_0 defines a Gaussian state $|J_0\rangle$ which can be used as vacuum for building a Fock representation of the algebra of observables [5, 6, 100]. Representations built over Fock vacua $|J_0\rangle$ and $|J_M\rangle$ are unitarily equivalent if and only if the symplectic transformation M belongs to the restricted symplectic group described above. When interpreted in terms of particle excitations, the state $|J_M\rangle$ describes a superposition of particle pairs over the vacuum $|J_0\rangle$. A symplectic transformation M which does not belong to the restricted group corresponds to a Bogoliubov transformation that produces an infinite number of particles [45].

Gaussian states and quadratic time-dependent Hamiltonians appear in the description of particle production in the early universe [105, 106], Hawking radiation in black hole evaporation [7], in the Schwinger effect [107, 108], in the dynamical Casimir effect [109, 110] and more generally in all cases where the free quantum field evolves in a time-dependent background. It is known that, for some time-dependent backgrounds, the time-evolution—which, at the classical level, is encoded in a symplectic transformation M —cannot be implemented as a unitary operator in a Fock space at the quantum level [111]. Nevertheless the correlation functions in the quantum theory are still well-defined in terms of a complex structure J_0 and a symplectic transformation M as described in (2.10) [112]. The algebraic approach focuses on correlation functions and does not involve the construction of a Fock space. It provides sufficient structure for defining the (abstract) state of the system and computing the evolution of the entanglement entropy of a subsystem, despite the potential lack of a standard unitary implementation of the time evolution in a Fock space, (i).

The second aspect which needs some clarification regards the definition of a subsystem in quantum field theory, (ii). It is a well-known fact about the ground state of a quantum field that the entanglement entropy of a region of space is divergent and—when an ultraviolet cutoff is introduced—it scales as the area of the boundary of the region [113–115]. The divergence of the geometric entanglement entropy has an algebraic origin: The local subalgebra of observables associated to a region in space is of type III, i.e. it does not identify a factorization of the Fock space in a tensor product of Hilbert spaces [101, 116]. Three standard strategies to address this issue are: (a) a modification the ultraviolet behavior of the theory, for instance introducing a lattice cut-off [113, 114, 117], or (b) computing the mutual information between a region and a carved version of its complement so to introduce a “safety corridor” [116, 118, 119], or (c) focusing on the excess entropy of a state with respect to the one of the ground state [119, 120]. Here we illustrate a different strategy: We focus on the entanglement entropy of a subsystem with a finite number N_A of degrees of freedom. The geometric entanglement entropy which captures infinitely many degrees of freedom can be recovered in the limit of increasingly large subsystems [121].

A simple example of a subsystem with a single degree of freedom, $N_A = 1$, is provided by a linear smearing of the fields against given test functions $f(\vec{x})$ and $g(\vec{x})$:

$$\hat{\varphi}_f = \int f(\vec{x}) \hat{\varphi}(\vec{x}) d^3\vec{x}, \quad \hat{\pi}_g = \int g(\vec{x}) \hat{\pi}(\vec{x}) d^3\vec{x}. \quad (5.102)$$

The observables $\hat{\varphi}_f$ and $\hat{\pi}_f$ generate a Weyl algebra \mathcal{A}_A of type I which, as in section 5.3, induces a factorization of the Hilbert space into $\mathcal{H} = \mathcal{H}_A \otimes \mathcal{H}_B$. The symplectic structure Ω_A of the subsystem can be computed from the commutator,

$$[\hat{\varphi}_f, \hat{\pi}_g] = i \int f(\vec{x}) g(\vec{x}) d^3\vec{x}. \quad (5.103)$$

Given a Gaussian state $|J\rangle$ of the quantum field, the symmetrized correlation function restricted to the subsystem A is

$$[G]_A = \begin{pmatrix} 2 \langle J | \hat{\varphi}_f \hat{\varphi}_f | J \rangle & \langle J | \hat{\varphi}_f \hat{\pi}_g + \hat{\pi}_g \hat{\varphi}_f | J \rangle \\ \langle J | \hat{\varphi}_f \hat{\pi}_g + \hat{\pi}_g \hat{\varphi}_f | J \rangle & 2 \langle J | \hat{\pi}_g \hat{\pi}_g | J \rangle \end{pmatrix}. \quad (5.104)$$

The restricted complex structure $[J]_A$ is given by $[J]_A{}^a{}_b = -[G]_A^{ac} (\Omega_A^{-1})_{cb}$ and its eigenvalues $\pm\nu$ determine the entanglement entropy of the subsystem A through (2.34).

We illustrate our result on three paradigmatic cases in quantum field theory where the time-dependence of the entanglement entropy of a subsystem can be computed and our results on the linear growth can be tested.

5.5.2 Dynamics of symmetry breaking and the inverted quadratic potential

We consider a scalar field $\varphi(x)$ which goes through a symmetry breaking transition in real time [122, 123]. A simple model is described by the action⁷

$$S[\varphi] = \int \left(-\frac{1}{2} \partial_\mu \varphi \partial^\mu \varphi - V(\varphi) \right) d^4x \quad (5.105)$$

with a quartic potential,

$$V(\varphi) = \frac{1}{2} \alpha(t) \varphi^2 + \frac{1}{4!} \varepsilon \varphi^4. \quad (5.106)$$

The quadratic coupling $\alpha(t)$ is chosen so that, for $t > 0$, a minimum of the potential breaks the symmetry $\varphi \rightarrow -\varphi$. We set

$$\alpha(t) = \begin{cases} +m^2, & t \leq 0 \\ -\mu^2, & t > 0 \end{cases} \quad \text{and} \quad 0 < \varepsilon \ll 1. \quad (5.107)$$

The system is initially prepared in the ground state at $t < 0$ and then let evolve. For small quartic coupling ε and short time, the evolution is described perturbatively by a tachyonic instability: At the onset of the symmetry-breaking transition, the scalar field evolves as if it was free and had a negative mass-squared, $-\mu^2$. We focus on this initial phase.

We set $\varepsilon = 0$ and study the free evolution governed by a quadratic Hamiltonian which transitions from a stable phase to an unstable phase. It is useful to adopt Fourier transformed canonical variables

$$\varphi(\vec{k}) = \int d^3\vec{x} \varphi(\vec{x}) e^{i\vec{k}\cdot\vec{x}} , \quad \pi(\vec{k}) = \int d^3\vec{x} \pi(\vec{x}) e^{i\vec{k}\cdot\vec{x}} \quad (5.108)$$

so that the canonical commutation relations read $[\varphi(\vec{k}), \pi(\vec{k}')] = i(2\pi)^3 \delta^3(\vec{k} + \vec{k}')$ and the symplectic structure in these coordinates is

$$\Omega(\vec{k}, \vec{k}') = \begin{pmatrix} 0 & +1 \\ -1 & 0 \end{pmatrix} (2\pi)^3 \delta^3(\vec{k} + \vec{k}'). \quad (5.109)$$

For $t < 0$, the Hamiltonian is

$$H = \int \frac{d^3\vec{k}}{(2\pi)^3} \frac{1}{2} \left(|\pi(\vec{k})|^2 + (\vec{k}^2 + m^2) |\varphi(\vec{k})|^2 \right) \quad (5.110)$$

and the system is stable. The ground state is the Gaussian state $|J_0\rangle$ with correlation functions

$$G_0(\vec{k}, \vec{k}') = \begin{pmatrix} 2 \langle J_0 | \varphi(\vec{k}) \varphi(\vec{k}') | J_0 \rangle & \langle J_0 | \varphi(\vec{k}) \pi(\vec{k}') + \pi(\vec{k}') \varphi(\vec{k}) | J_0 \rangle \\ \langle J_0 | \varphi(\vec{k}) \pi(\vec{k}') + \pi(\vec{k}') \varphi(\vec{k}) | J_0 \rangle & 2 \langle J_0 | \pi(\vec{k}) \pi(\vec{k}') | J_0 \rangle \end{pmatrix} \quad (5.111)$$

$$= \begin{pmatrix} \frac{1}{\sqrt{\vec{k}^2 + m^2}} & 0 \\ 0 & \sqrt{\vec{k}^2 + m^2} \end{pmatrix} (2\pi)^3 \delta^3(\vec{k} + \vec{k}'). \quad (5.112)$$

⁷We adopt the notation $x = (t, \vec{x})$ for a spacetime point and use the signature $(- +++)$.

The complex structure of the ground state is therefore $J_0 = -G_0 \Omega^{-1}$, i.e.,

$$J_0(\vec{k}, \vec{k}') = \begin{pmatrix} 0 & \frac{1}{\sqrt{\vec{k}^2 + m^2}} \\ -\sqrt{\vec{k}^2 + m^2} & 0 \end{pmatrix} (2\pi)^3 \delta^3(\vec{k} - \vec{k}'). \quad (5.113)$$

For $t > 0$, that is, after the transition from the stable to the unstable phase, the Hamiltonian governing the free evolution is given by

$$H = \int \frac{d^3 \vec{k}}{(2\pi)^3} \frac{1}{2} \left(|\pi(\vec{k})|^2 + (\vec{k}^2 - \mu^2) |\varphi(\vec{k})|^2 \right). \quad (5.114)$$

Modes with \vec{k}^2 smaller than μ^2 are unstable and have Lyapunov exponents which come in pairs $\pm \lambda(\vec{k})$, with

$$\lambda(\vec{k}) = \sqrt{\mu^2 - \vec{k}^2} \quad \text{for} \quad 0 \leq \vec{k}^2 < \mu^2. \quad (5.115)$$

As a result, infrared modes are unstable and the largest Lyapunov exponent $\lambda(0) = \mu$ is associated to the homogeneous mode.

The classical evolution generated by the unstable Hamiltonian (5.114) is given by the symplectic transformation $M_t(\vec{k}, \vec{k}') = M_t(\vec{k}) (2\pi)^3 \delta^3(\vec{k} + \vec{k}')$, with

$$M_t(\vec{k}) = \begin{pmatrix} \cosh(\sqrt{\mu^2 - \vec{k}^2} t) & \sqrt{\mu^2 - \vec{k}^2} \sinh(\sqrt{\mu^2 - \vec{k}^2} t) \\ \frac{1}{\sqrt{\mu^2 - \vec{k}^2}} \sinh(\sqrt{\mu^2 - \vec{k}^2} t) & \cosh(\sqrt{\mu^2 - \vec{k}^2} t) \end{pmatrix}. \quad (5.116)$$

As a result, in the quantum theory, the correlation functions at the time t for the system initially prepared in the Gaussian state $|J_0\rangle$ are given by the evolved complex structure $J_t(\vec{k}, \vec{k}')$,

$$J_t(\vec{k}, \vec{k}') = M_t(\vec{k})^{-1} \begin{pmatrix} 0 & \frac{1}{\sqrt{\vec{k}^2 + m^2}} \\ -\sqrt{\vec{k}^2 + m^2} & 0 \end{pmatrix} M_t(\vec{k}) (2\pi)^3 \delta^3(\vec{k} - \vec{k}'), \quad (5.117)$$

which defines a Gaussian state $|J_t\rangle$ at the time t .

Let us consider a measuring device which probes the field and its momentum only in a neighborhood of the point $\vec{x} = 0$ with a linear size R . This device can be modeled by a Gaussian smearing function $f(\vec{x})$. The subsystem A defined by such measurements is encoded in the subalgebra of observables \mathcal{A}_A generated by

$$\hat{\varphi}_A = \int \hat{\varphi}(\vec{x}) f(\vec{x}) d^3 \vec{x}, \quad \hat{\pi}_A = \int \hat{\pi}(\vec{x}) f(\vec{x}) d^3 \vec{x} \quad \text{with} \quad f(\vec{x}) = \frac{1}{(\sqrt{2\pi} R)^3} e^{-\frac{|\vec{x}|^2}{2R^2}}. \quad (5.118)$$

This subsystem has $N_A = 1$ bosonic degrees of freedom. Fluctuations of the observables $\hat{\varphi}_A$ and $\hat{\pi}_A$ at the time t are encoded in the correlation functions of the subsystem

$$[G_t]_A = \begin{pmatrix} 2 \langle J_t | \hat{\varphi}_A \hat{\varphi}_A | J_t \rangle & \langle J_t | \hat{\varphi}_A \hat{\pi}_A + \hat{\pi}_A \hat{\varphi}_A | J_t \rangle \\ \langle J_t | \hat{\varphi}_A \hat{\pi}_A + \hat{\pi}_A \hat{\varphi}_A | J_t \rangle & 2 \langle J_t | \hat{\pi}_A \hat{\pi}_A | J_t \rangle \end{pmatrix} = \int G_t(\vec{k}, \vec{k}') f(\vec{k}) f(\vec{k}') \frac{d^3 \vec{k}}{(2\pi)^3} \frac{d^3 \vec{k}'}{(2\pi)^3}, \quad (5.119)$$

where $f(\vec{k}) = e^{-\frac{1}{2} R^2 |\vec{k}|^2}$ is the Fourier transform of $f(\vec{x})$. Similarly, the restricted complex structure is the 2×2 matrix

$$[J_t]_A = \int J_t(\vec{k}, \vec{k}') f(\vec{k}) f(\vec{k}') \frac{d^3 \vec{k}}{(2\pi)^3} \frac{d^3 \vec{k}'}{(2\pi)^3}. \quad (5.120)$$

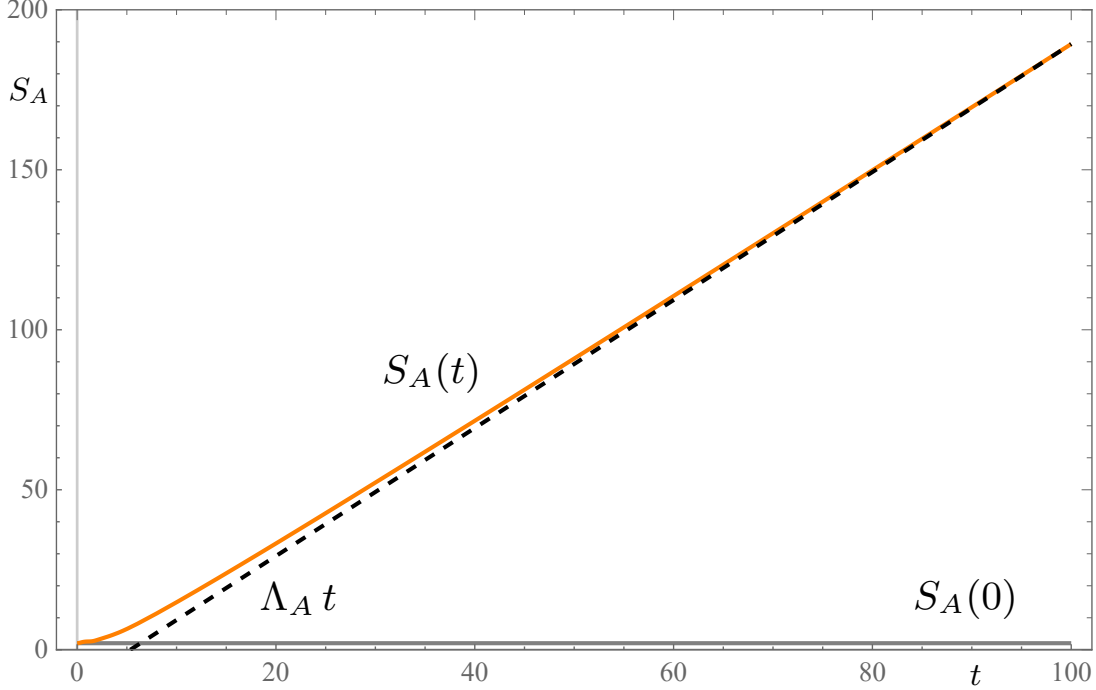


Figure 5.8: Symmetry breaking and the inverted quadratic potential. We compute the entanglement entropy $S_A(t)$ numerically for the time evolution with the unstable Hamiltonian (5.114). We set $\mu = 1$. The subsystem A is defined in (5.118) with $R = 1$.

The eigenvalues of $i[J_t]_A$ come in pairs $\pm\nu(t)$ and the entanglement entropy of the subsystem A is given by

$$S_A(t) = S(\nu(t)) \quad (5.121)$$

where $S(\nu)$ is the function (2.34). The predicted asymptotic rate of growth of the entanglement entropy of a subsystem with $N_A = 1$ is given by the subsystem exponent $\Lambda_A = 2\mu$, which is the sum of the two largest Lyapunov exponents, i.e.,

$$S_A(t) \sim 2\mu t. \quad (5.122)$$

A numerical plot of the entanglement entropy as a function of time, together with the predicted rate of growth, is shown in figure 5.8.

We note that, as the positive Lyapunov exponents of the system appear in a continuous band $\lambda(\vec{k}) = \sqrt{\mu^2 - \vec{k}^2}$, the prediction for the asymptotic growth of the entanglement entropy of a subsystem with N_A degrees of freedom is simply $S_A(t) \sim 2N_A \mu t$. In the case of a subsystem with infinitely many degrees of freedom, it is useful to induce an infrared cutoff, for instance a cubic volume $V = L^3$. The boundary conditions induce a quantization of the momentum $\vec{k} = (\frac{2\pi}{L}n_x, \frac{2\pi}{L}n_y, \frac{2\pi}{L}n_z)$ which splits the degeneracy of the Lyapunov exponents and results in a discrete sequence $\lambda(\vec{k})$. We can now define the number N_I of unstable degrees of freedom of the system. In the limit $L \gg \frac{2\pi}{\mu}$ we find

$$N_I \sim L^3 \int \Theta(\lambda(\vec{k})) \frac{d^3 \vec{k}}{(2\pi)^3} = \frac{(\mu L)^3}{6\pi^2}. \quad (5.123)$$

A generic subsystem which probes infinitely many degrees of freedom, as in the case of the geometric entanglement entropy of a region of space, would probe all the unstable degrees of freedom of the system. As a result the asymptotic growth of the entanglement entropy is expected to be given by

$$S_A(t) \sim \mathfrak{h}_{\text{KS}} L^3 t, \quad (5.124)$$

where \mathfrak{h}_{KS} is the Kolmogorov-Sinai rate per unit volume,

$$\mathfrak{h}_{\text{KS}} = \int \Theta(\lambda(\vec{k})) \lambda(\vec{k}) \frac{d^3 \vec{k}}{(2\pi)^3} = \frac{\mu^4}{32\pi}. \quad (5.125)$$

As a result, for a generic subsystem with infinitely many degrees of freedom, the quantity \mathfrak{h}_{KS} describes the asymptotic behavior of the entanglement entropy per unit space-time volume.

In this analysis we assumed that the quartic term $\frac{1}{4!} \varepsilon \varphi^4$ is not present in the potential and the evolution is simply described by a quadratic Hamiltonian with instabilities. In section 5.8.1 we discuss when this approximation is expected to be valid.

5.5.3 Preheating and parametric resonance

The simplest model of parametric resonance in quantum field theory is described by the Hamiltonian

$$H(t) = \int \frac{d^3 \vec{k}}{(2\pi)^3} \frac{1}{2} \left(|\pi(\vec{k})|^2 + (\vec{k}^2 + v_0^2 \sin^2(M_0 t)) |\varphi(\vec{k})|^2 \right) \quad (5.126)$$

which has a quadratic potential that oscillates in time with period $2\pi/M_0$. For small values of the amplitude of oscillation,

$$v_0^2 \ll M_0^2, \quad (5.127)$$

we have a narrow resonance band around the frequency of the perturbation,

$$|\vec{k}| \in \left[M_0 - \frac{v_0^2}{4M_0}, M_0 + \frac{v_0^2}{4M_0} \right]. \quad (5.128)$$

Modes with momentum $|\vec{k}| \approx M_0$ are parametrically amplified. The Lyapunov exponents of the system can be determined via Floquet analysis as we already did in section 5.4.3. The canonical subsystem spanned by $(\varphi(\vec{k}), \pi(-\vec{k}))$ with \vec{k} in the band (5.128) has Lyapunov exponents $\pm \lambda(\vec{k})$ with

$$\lambda(\vec{k}) \approx \sqrt{\left(\frac{v_0^2}{4M_0} \right)^2 - (M_0 - |\vec{k}|)^2}. \quad (5.129)$$

Given an initial Gaussian state—for instance the Minkowski vacuum—the evolution of the correlation functions of the system can be computed analytically in terms of Mathieu functions. In figure 5.9 we show the time-evolution of the entanglement entropy of a subsystem A defined by a subalgebra of observables \mathcal{A}_A generated by the linear observables (5.118). At the classical level, the subsystem exponent Λ_A can be easily computed: It is given by the sum of the two largest Lyapunov exponents of the systems, which are degenerate in value and correspond to modes exactly at the resonance $|\vec{k}| = M_0$. Therefore we have

$$\Lambda_A = 2 \lambda(M_0) = \frac{v_0^2}{2M_0}. \quad (5.130)$$

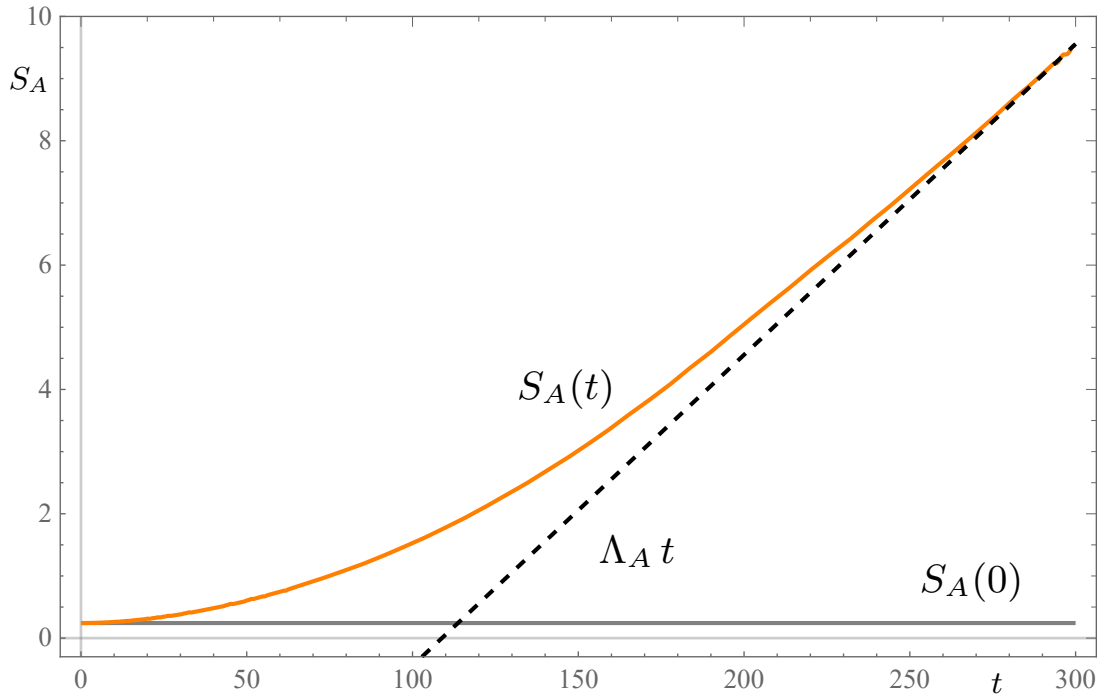


Figure 5.9: *Preheating and parametric resonance.* We compute the entanglement entropy $S_A(t)$ numerically. The subsystem is defined in (5.118), the time evolution is governed by the Hamiltonian presented in (5.126) and we start in the Minkowski vacuum state. We set $R = 1$, $M_0 = 1$ and $v_0^2 = 0.1$ leading to the entanglement production rate $\Lambda_A = 0.05$. The quantity $S_A(0)$ is the entanglement entropy of the Minkowski vacuum and the linear production phase is reached after an initial transient.

As predicted by theorem 1, the entanglement entropy of the subsystem initially prepared in a Gaussian state $|J_0\rangle$ is observed to grow as $S_A(t) \sim \Lambda_A t$.

The phenomenon of parametric resonance plays a central role in a variety of far-from-equilibrium processes in quantum field theory [124–126]. We briefly discuss three examples: preheating in cosmology [127–130], the formation of the chiral condensate in relativistic heavy-ion collisions [131], and the dynamical Casimir effect in trapped Bose-Einstein condensates [132].

At the end of cosmological inflation, the inflaton oscillates coherently around the minimum of its potential. Such oscillations excite the vacuum of matter fields via the phenomenon of parametric resonance. This phase of explosive non-thermal particle production is called preheating and is followed by a thermalization phase which provides the initial conditions for Big Bang Nucleosynthesis. A simple model of preheating consists in a coupling $V = \frac{1}{2}g^2\Phi^2\varphi^2$ between the inflaton Φ and a field φ which serves as proxy for Standard Model fields. Coherent oscillations of the inflaton, $\langle\Phi(\vec{x},t)\rangle = \Phi_0 \sin(M_0 t)$, result in an effective dynamics for the matter field described by an Hamiltonian of the form (5.126) with a coupling constant $v_0^2 = g^2\Phi_0^2$. At the beginning of the oscillatory phase, the state of matter can be assumed to be the vacuum $|J_0\rangle$ because of the dilution effect of the inflationary phase. Its evolution in the preheating phase results in a Gaussian state $|J_t\rangle$ which is far from equilibrium: The Floquet instability of the Hamiltonian results in an explosive production of particles with momenta in the resonance band. For a given subalgebra of observables \mathcal{A}_A , such as the one discussed in (5.118), theorem 1 predicts a linear growth of the entropy with a rate given by

the subsystem exponents Λ_A . Phenomenologically, the relevant choice of subalgebra of observables or coarse graining of the system is dictated by the interaction with its environment. The interaction of the produced particles and the expansion of the universe have the effect of reducing the efficiency of the resonance and eventually lead to a thermal-equilibrium radiation-dominated phase, with an expected entropy profile qualitatively similar to the one illustrated in figure 5.5.

A similar preheating phenomenon is discussed in the context of relativistic heavy-ion collisions where, in the late stages of the evolution of a quark-gluon plasma, a chirally symmetric state rolls down and oscillates around to the minimum of the effective chiral potential [131]. Coherent pion excitations are described by a quark condensate $\Phi = \langle \bar{q}q \rangle$ and $\vec{\phi} = \langle \bar{q}\vec{\sigma}q \rangle$ and a $O(4)$ linear sigma model with $\phi_a = (\Phi, \vec{\phi})$ with explicit symmetry breaking. The action of the system is

$$S[\Phi, \vec{\phi}] = \int d^4x \left(-\frac{1}{2} \partial_\mu \phi_a \partial_\mu \phi^a - \frac{1}{4} g (\phi_a \phi^a - f_\pi^2)^2 - m_\pi^2 f_\pi \Phi_0 \right) \quad (5.131)$$

with parameters $g \approx 20$, $f_\pi \approx 90$ MeV and $m_\pi \approx 140$ MeV. The coherent field ϕ_a is initially in a chirally symmetric state. As it rolls down the potential and oscillates around the minimum $\phi_a \approx (f_\pi, \vec{0})$, a squeezed state of coherent pion pair excitations is produced via parametric resonance. In this phase, the entanglement entropy of a generic subsystem A is predicted to grow with a rate given by the subsystem exponent Λ_A . As discussed in [73], the linear entropy growth is expected to be bounded by the Kolmogorov-Sinai rate of the system.

Time-dependent Hamiltonians of the form (5.126) appear also in the description of stimulated quasi-particle production in cold atomic Bose gases [133, 134]. A periodic modulation of the external potential that traps the gas induces a response in the condensed portion of the gas which acts as a time-dependent background for quasi-particles. The study of entanglement entropy growth in cold atomic Bose gases is of particular relevance because of current experiments which can probe the non-separability of phonon pair creation [135, 136].

5.5.4 Cosmological perturbations and slow-roll inflation

During slow-roll inflation, quantum perturbations of the metric and the inflaton field are stretched and squeezed. We illustrate this phenomenon—together with the associated growth of the entanglement entropy—using a simple model consisting of a minimally-coupled massless scalar field in a cosmological spacetime. The action of the system is

$$S[\varphi] = - \int d^4x \frac{1}{2} \sqrt{-g} g^{\mu\nu} \partial_\mu \varphi \partial_\nu \varphi \quad (5.132)$$

where with a metric $g_{\mu\nu}$ that defines the line element of a Friedmann-Lemaître-Robertson-Walker spacetime, $ds^2 = g_{\mu\nu} dx^\mu dx^\nu = -dt^2 + a(t)^2 d\vec{x}^2$. The evolution of the field in the cosmic time t is generated by the time-dependent Hamiltonian

$$H(t) = \int \frac{d^3\vec{k}}{(2\pi)^3} \frac{1}{2} \left(\frac{|\pi(\vec{k})|^2}{a(t)^3} + a(t) \vec{k}^2 |\varphi(\vec{k})|^2 \right), \quad (5.133)$$

where \vec{k} is the comoving momentum and $\pi(\vec{k}) = a(t)^3 d\varphi(\vec{k})/dt$. During slow-roll inflation, the Hubble rate changes slowly in time. To illustrate the analysis of the stability of the system, here we model this quasi-de Sitter phase with a de Sitter scale factor,

$$a(t) = e^{H_0 t}. \quad (5.134)$$

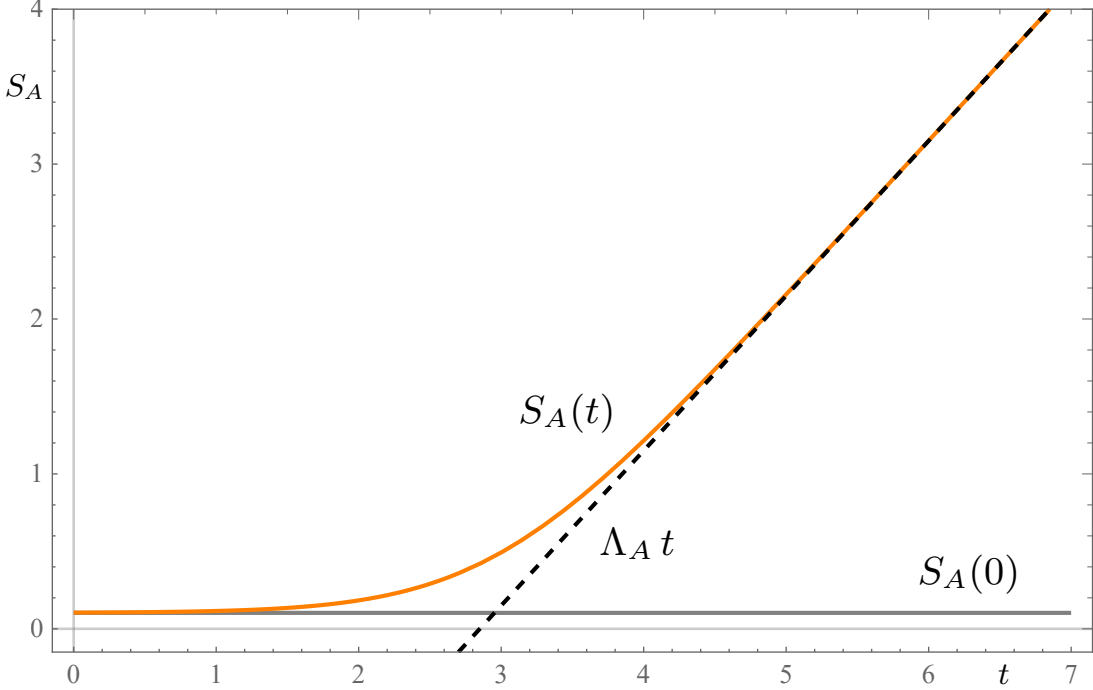


Figure 5.10: *Quantum field in de Sitter space.* We plot the entanglement entropy $S_A(t) = S(\nu(t))$ from (5.138) associated to the subsystem described in (5.137). In the phase of linear growth, the entropy is observed to grow with rate given by the Hubble rate H_0 as predicted by theorem 1. We set $H_0 = 1$ and $R = 1$ in this plot.

The canonical subsystem spanned by $(\varphi(\vec{k}), \pi(-\vec{k}))$ with comoving momentum \vec{k} is not a regular Hamiltonian system because of exponential collinearity (see appendix B.3). In fact the angle between the two Lyapunov vectors $\ell_1(\vec{k})$ and $\ell_2(\vec{k})$ approaches 0 as $e^{-H_0 t}$. As a result, the Lyapunov exponents of the mode \vec{k} do not have to be opposite in sign. In fact they are found to be given by

$$\lambda_1(\vec{k}) = H_0 \quad \text{and} \quad \lambda_2(\vec{k}) = 0, \quad (5.135)$$

where H_0 is the Hubble rate. In the quantum theory we consider an initial state at the time $t_0 \rightarrow -\infty$ given by the Bunch-Davies vacuum. The correlation functions of this state at the time t can be determined in closed form and are given by

$$G_t(\vec{k}, \vec{k}') = 2 \begin{pmatrix} \frac{1}{2|\vec{k}|} e^{-2H_0 t} + \frac{H_0^2}{2|\vec{k}|^3} & -\frac{H_0}{2|\vec{k}|} e^{+H_0 t} \\ -\frac{H_0}{2|\vec{k}|} e^{+H_0 t} & \frac{|\vec{k}|}{2} e^{+2H_0 t} \end{pmatrix} (2\pi)^3 \delta^3(\vec{k} + \vec{k}'), \quad (5.136)$$

from which we can read the complex structure $J_t(\vec{k}, \vec{k}')$.

We analyze the entanglement growth of a subsystem spanned by a linear smearing of the field and the momentum. In order to guarantee that the dispersion of the linear observables are finite, we consider a smearing of the form

$$\hat{\varphi}_A = \int \Delta \hat{\varphi}(\vec{x}) f(\vec{x}) d^3 \vec{x}, \quad \hat{\pi}_A = \int \Delta \hat{\pi}(\vec{x}) f(\vec{x}) d^3 \vec{x} \quad \text{with} \quad f(\vec{x}) = \frac{1}{(\sqrt{2\pi} R)^3} e^{-\frac{|\vec{x}|^2}{2R^2}}, \quad (5.137)$$

where $\Delta\hat{\varphi}(\vec{x}) = \delta^{ij}\partial_i\partial_j\hat{\varphi}(\vec{x})$ is the comoving Laplacian and the Gaussian smearing is over a region of comoving size R . The eigenvalues of the restricted complex structure $[iJ_t]_A$ come in pairs $\pm\nu(t)$ and are given by

$$\nu(t) = \frac{16}{5\sqrt{3\pi}}\sqrt{1 + \frac{1}{6}H_0^2R^2 e^{+2H_0 t}}. \quad (5.138)$$

The entanglement entropy $S_A(t) = S(\nu(t))$ of the subsystem is plotted in figure 5.10 and for long time, i.e. for large number of efoldings, grows linearly as $S_A(t) \sim H_0 t$. This is exactly the asymptotic growth predicted by theorem 1 written in terms of the subsystem exponent $\Lambda_A = H_0$.⁸

We note that previous studies of the growth of the entanglement entropy of cosmological perturbations focus on the $(\vec{k}, -\vec{k})$ subsystem [137–140]. On the other hand the results presented here apply to all subsystems defined by smeared fields.

5.6 Entanglement production of time-independent quadratic Hamiltonians

In this section, we study the evolution of the entanglement entropy for Gaussian states under quadratic time-independent Hamiltonians.

5.6.1 Decomposition of quadratic Hamiltonians

Every quadratic Hamiltonian $\hat{H} = \frac{1}{2}h_{ab}\hat{\xi}^a\hat{\xi}^b$ can be uniquely decomposed into the three parts

$$\hat{H} = \hat{H}_{\text{unstable}} + \hat{H}_{\text{stable}} + \hat{H}_{\text{metastable}}. \quad (5.139)$$

We show that these three parts contribute to the time-evolution of the entanglement entropy $S_A(t)$ in a characteristic way, namely:

- (a) Unstable Hamiltonian
 $\Rightarrow S_A(t)$ entropy grows linearly: $S_A(t) \sim \Lambda_A t$
- (b) Stable Hamiltonian
 $\Rightarrow S_A(t)$ oscillates: $S_A(t) \sim X_A(t)$
- (c) Metastable Hamiltonian
 $\Rightarrow S_A(t)$ grows logarithmically: $S_A(t) \sim C_A \ln(t)$

The decomposition is best understood by looking at the matrix $K^a_b = \Omega^{ac}h_{cb}$. This is a real square matrix and, as such, can always be decomposed into the following three commuting parts

$$K = K_{\text{real}} + K_{\text{imaginary}} + K_{\text{nilpotent}}, \quad (5.140)$$

such that K_{real} is a diagonalizable matrix with real eigenvalues, $K_{\text{imaginary}}$ is a diagonalizable matrix with imaginary eigenvalues, and $K_{\text{nilpotent}}$ is a nilpotent matrix. This decomposition is the well-known Jordan decomposition of real matrices, which we review in Appendix C.1. In order to find

⁸At the classical level, the momentum π_A grows exponentially fast as $e^{H_0 t}$ while the smeared field φ_A has a norm which does not change exponentially and does not approach π_A exponentially fast. As a result the two vectors span a parallelogram whose area grows as $e^{H_0 t}$ leading to a subsystem exponent $\Lambda_A = H_0$.

the decomposition of \hat{H} , we contract the different parts of K with ω_{ab} :

$$\hat{H}_{\text{unstable}} = \frac{1}{2}(h_{\text{unstable}})_{ab}\hat{\xi}^a\hat{\xi}^b, \quad (5.141)$$

$$\hat{H}_{\text{stable}} = \frac{1}{2}(h_{\text{stable}})_{ab}\hat{\xi}^a\hat{\xi}^b, \quad (5.142)$$

$$\hat{H}_{\text{metastable}} = \frac{1}{2}(h_{\text{metastable}})_{ab}\hat{\xi}^a\hat{\xi}^b, \quad (5.143)$$

where $(h_{\text{unstable}})_{ab} = \omega_{ac}(K_{\text{real}})^c{}_b$, $(h_{\text{stable}})_{ab} = \omega_{ac}(K_{\text{imaginary}})^c{}_b$, and $(h_{\text{metastable}})_{ab} = \omega_{ac}(K_{\text{nilpotent}})^c{}_b$. The condition for two quadratic Hamiltonians to commute is given by

$$[\hat{H}_1, \hat{H}_2] = \frac{1}{2} \underbrace{\left[(h_1)_{ab}\Omega^{bc}(h_2)_{cd} - (h_2)_{ab}\Omega^{bc}(h_1)_{cd} \right]}_{=\omega_{ab}[K_1, K_2]^b{}_d} \hat{\xi}^a\hat{\xi}^d = 0. \quad (5.144)$$

This condition is equivalent to $[K_1, K_2] = K_1K_2 - K_2K_1 = 0$, namely, requiring that the corresponding matrices $(K_i)^a{}_b = \Omega^{ac}(h_i)_{cb}$ commute. We can conclude that the decomposition of a Hamiltonian into the three aforementioned parts induces an equivalent decomposition of the time evolution operator into the three commuting parts

$$\hat{U}(t) = e^{-i\hat{H}_{\text{unstable}}t}e^{-i\hat{H}_{\text{stable}}t}e^{-i\hat{H}_{\text{metastable}}t}, \quad (5.145)$$

where each part contributes to the time dependence of the entanglement entropy.

The asymptotics of the entanglement entropy is closely related to how the classical Hamiltonian flow $M(t) = e^{Kt}$ deforms regions of the classical phase space [see Appendix C.2 for a derivation of how $M(t)$ corresponds to the classical flow solving the classical Hamiltonian equations of motion].

We are mostly interested in the dual flow $M^\intercal(t) = e^{tK^\intercal}$ on the dual phase space that describes the time evolution of classical observables. This flow can be best understood by studying its action on a linear observable $\theta \in V^*$ in the dual phase space. To do this, we first bring K^\intercal into its Jordan normal form

$$K^\intercal \equiv \begin{pmatrix} \boxed{\mathcal{J}(\kappa_1)} & & & \\ & \boxed{\mathcal{J}(\kappa_2)} & & \\ & & \ddots & \\ & & & \boxed{\mathcal{J}(\kappa_n)} \end{pmatrix}, \quad (5.146)$$

$$\text{with } \mathcal{J}(\kappa) \equiv \begin{pmatrix} \boxed{\mathcal{J}_1(\kappa)} & & & \\ & \ddots & & \\ & & \boxed{\mathcal{J}_{j_\kappa}(\kappa)} & \end{pmatrix},$$

by finding a basis consisting of a complete set of generalized eigenvectors for every Jordan block $\mathcal{J}_k(\kappa)$ associated with the eigenvalue κ :

- **Real eigenvalue $\kappa = \lambda$:**

For every Jordan block $\mathcal{J}_k(\kappa)$ of the real eigenvalue κ , we have $\dim \mathcal{J}_k(\kappa)$ distinct generalized eigenvectors $\mathcal{E}_k^l(\kappa)$. Here, κ runs over all real eigenvalues of K , k runs over the number of Jordan blocks associated with κ , and l runs up to the dimension $\dim \mathcal{J}_k(\kappa)$. The action of $M^\intercal(t)$ on $\mathcal{E}_k^l(\kappa)$ is given by

$$M^\intercal(t) \mathcal{E}_k^l(\kappa) = e^{\lambda t} \sum_{l'=1}^l \frac{t^{l-l'}}{(l-l')!} \mathcal{E}_k^{l'}(\kappa). \quad (5.147)$$

Its length behaves asymptotically as $\ln \|M^\tau(t)\mathcal{E}_k^{l'\pm}(\kappa)\| \sim \lambda t + (l-1)\ln(t)$ as $t \rightarrow \infty$.

- **Complex eigenvalue** $\kappa = \lambda + i\omega$

For every Jordan block $\mathcal{J}_k(\kappa)$ of the complex eigenvalue κ with $\omega > 0$, all generalized eigenvectors $\mathcal{E}_k^{l\pm}(\kappa)$ come in pairs. Therefore, we have the additional label \pm to distinguish the two vectors per pair, besides the labels κ , k , and l . The action of $M^\tau(t)$ on $\mathcal{E}_k^l(\kappa)$ is given by

$$M^\tau(t) \mathcal{E}_k^{l+}(\kappa) = e^{\lambda t} \sum_{l'=1}^l \frac{t^{l-l'}}{(l-l')!} [\cos(\omega t) \mathcal{E}_k^{l'+}(\kappa) + \sin(\omega t) \mathcal{E}_k^{l'-}(\kappa)], \quad (5.148)$$

$$M^\tau(t) \mathcal{E}_k^{l-}(\kappa) = e^{\lambda t} \sum_{l'=1}^l \frac{t^{l-l'}}{(l-l')!} [\cos(\omega t) \mathcal{E}_k^{l'-}(\kappa) - \sin(\omega t) \mathcal{E}_k^{l'+}(\kappa)], \quad (5.149)$$

Its length behaves asymptotically as $\ln \|M^\tau(t)\mathcal{E}_k^{l'\pm}(\kappa)\| \sim \lambda t + (l-1)\ln(t)$ as $t \rightarrow \infty$, which is the same as in the real case.

The decomposition discussed here is closely related to the normal forms of quadratic Hamiltonians discussed in [141].

5.6.2 Floquet Hamiltonian

The quadratic Hamiltonians in the previous section are all time-independent, but the same methods also apply to time-periodic Hamiltonians. A quadratic Hamiltonian with time dependence given by

$$\hat{H}(t) = \frac{1}{2} h(t)_{ab} \hat{\xi}^a \hat{\xi}^b \quad (5.150)$$

is time periodic if $h(t)_{ab} = h(t+T)_{ab}$ for some period T . Such Hamiltonians describe periodically driven systems. Interestingly, this does not imply that the time-evolution is periodic nor that the entanglement entropy just oscillates. We can write the time evolution operator as the time-ordered exponential

$$\hat{U}(t) = \mathcal{T} \exp \left[-i \int_0^t dt' \hat{H}(t') \right]. \quad (5.151)$$

At stroboscopic times, $t = nT$ with $n \in \mathbb{N}$, we can write $\hat{U}(t) = U(T)^n$. We can therefore compute the stroboscopic time evolution of such systems using the time-independent Floquet Hamiltonian

$$\hat{H}_F = \frac{1}{T} \ln \hat{U}(T). \quad (5.152)$$

Provided that $\hat{H}(t)$ is quadratic, the Floquet Hamiltonian or *stroboscobic* Hamiltonians is quadratic as well. This means that our methods for time-independent Hamiltonians can still be used to study periodically driven systems.

The associated generator K_F can be directly computed from the symplectic flow

$$M(t) = \mathcal{T} e^{\int_0^t K(t') dt'}, \quad (5.153)$$

which can be computed as time-ordered exponential from the time-periodic symplectic generator $K^a_b(t) = \Omega^{ac} h_{cb}(t)$. Due to the periodicity of $h(t)_{ab}$, it is easy to see that the symplectic flow satisfies

$$M(nT + t) = M(t)M(T)^n \quad (5.154)$$

for $t \in [0, T]$. This means that the time behavior over long times is completely encoded in $M(T)$, while $M(t)$ with $t \in [0, T)$ only contributes bounded variations of the state. Clearly, we have

$$M(T) = e^{nT K_F} \quad \text{for} \quad K_F = \frac{1}{T} \log M(T), \quad (5.155)$$

which is completely equivalent to the previous definition of \hat{H}_F .

5.6.3 Asymptotic volume growth

In order to study the asymptotic behavior of the entanglement entropy, we need to understand how the volume of the parallelepipeds \mathcal{V} grows asymptotically under the action of the Hamiltonian flow $M^\top(t)$. In order to answer this question, it is helpful to first consider L vectors Φ^j selected out of the generalized eigenvectors, namely

$$\Phi^j = \mathcal{E}_{k_j}^{l_j \sigma_j}(\kappa_{i_j}), \quad (5.156)$$

where σ_j vanishes for real κ_j , but can take values $\sigma_j \in \{+, -\}$ for complex κ_j . Given such a set, we can define the L -dimensional parallelepiped spanned by them as the set

$$\mathcal{V} = \left\{ \sum_{j=1}^L c_j \Phi^j \mid 0 \leq c_j \leq 1 \right\}, \quad (5.157)$$

which is a subset of the hyperplane $\text{span}(\Phi^1, \dots, \Phi^L) \subset V^*$. We define the time evolved parallelepiped as

$$M^\top(t)\mathcal{V} = \left\{ \sum_{j=1}^L c_j M^\top(t) \theta^j \mid 0 \leq c_j \leq 1 \right\}, \quad (5.158)$$

where each spanning vector Φ^j evolves to $M^\top(t)\Phi^j$. The following theorem provides a precise answer for how the volume grows asymptotically.

Theorem 5 (Volume asymptotics)

The asymptotic behavior of the volume $M^\top(t)\mathcal{V}$ is

$$\ln \text{Vol}[M^\top(t)\mathcal{V}] \sim \Lambda t + C \ln(t), \quad \text{with} \quad (5.159)$$

$$\Lambda = \sum_{j=1}^L \lambda_{i_j} \quad \text{and} \quad C = \sum_{j=1}^L l_j - \sum_{n_k^\sigma(\kappa)} \frac{n_k^\sigma(\kappa)[n_k^\sigma(\kappa) + 1]}{2},$$

where $n_k^\sigma(\kappa)$ is the number of vectors θ^j that were selected out of the $m_k(\kappa)$ vectors

$$\mathcal{E}_k^{1\sigma}(\kappa), \quad \mathcal{E}_k^{2\sigma}(\kappa), \quad \dots \quad \mathcal{E}_k^{j_k(\kappa)\sigma}(\kappa). \quad (5.160)$$

For real κ , σ vanishes, and for complex κ , we have $\sigma \in \{+, -\}$. Note that this asymptotic behavior is universal, that is, it is independent of the specific (time-independent) metric or volume form used to compute it.

Proof: We know that the length $\|M^\top(t)\mathcal{E}_{k_j}^{l_j\sigma_j}(\kappa_{i_j})\|$ of each vector grows asymptotically as

$$\ln\|M^\top(t)\mathcal{E}_{k_j}^{l_j\sigma_j}(\kappa_{i_j})\| \sim \lambda_{i_j}t + (l_j - 1)\ln(t). \quad (5.161)$$

From this, we can make a first guess that the asymptotic volume growth should be given by

$$\sum_{j=1}^L [\lambda_{i_j}t + (l_j - 1)\ln(t)]. \quad (5.162)$$

However, one can convince oneself that the second term cannot be correct if two or more vectors come from the same sequence consisting of the $m_k(\kappa)$ vectors

$$\mathcal{E}_k^{1\sigma}(\kappa), \quad \mathcal{E}_k^{2\sigma}(\kappa), \quad \dots, \quad \mathcal{E}_k^{j_k(\kappa)\sigma}(\kappa). \quad (5.163)$$

Let $n_k^\sigma(\kappa)$ be the number of vectors in this sequence that we selected as part of the L vectors Φ^j . Let us refer to these vectors as

$$\mathcal{E}_k^{r_j\sigma}(\kappa) \quad (5.164)$$

with $1 \leq r_j \leq n_k^\sigma(\kappa)$ and $r_j < r_{j+1}$. When we evolve each of these vectors, their dominating growth points into the same direction, namely

$$\mathcal{E}_k^{r_j\sigma}(\kappa) \sim t^{r_j-1} M^\top(t)\mathcal{E}_k^{1\sigma}(\kappa). \quad (5.165)$$

Even though each vector grows with the asymptotic $e^{\lambda t}t^{r_j-1}$, the volume spanned by these vectors cannot be the product of the length growth because all $n_k^\sigma(\kappa)$ grow dominantly in the same direction, the direction that $M^\top(t)\mathcal{E}_k^{1\sigma}(\kappa)$ is evolving. In order to find the volume growth, we need to consider the first $n_k^\sigma(\kappa)$ linearly independent directions that these vectors are dominantly growing into. The dominant directions will therefore be the first $n_k^\sigma(\kappa)$ vectors of the above sequence, namely

$$\mathcal{E}_k^{1\sigma}(\kappa), \quad \mathcal{E}_k^{2\sigma}(\kappa), \quad \dots, \quad \mathcal{E}_k^{n_k^\sigma(\kappa)\sigma}(\kappa). \quad (5.166)$$

This means the j -th vector of our sequence only contributes $(r_j - j)$ rather than $r_j - 1$ as power of t to the overall volume growth. If we sum the exponents for all j , we find

$$\sum_{j=1}^{n_k^\sigma(\kappa)} (r_j - j) = \sum_{j=1}^{n_k^\sigma(\kappa)} r_j - \frac{n_k^\sigma(\kappa)[n_k^\sigma(\kappa) + 1]}{2}. \quad (5.167)$$

This is the contribution for the vectors θ^j belonging to a specific sequence. If we sum over all contributions from vectors θ^j belonging to all possible sequences, we find

$$\ln \text{Vol}[M^\top(t)\mathcal{V}] \sim \Lambda t + C \ln(t), \quad \text{with} \quad (5.168)$$

$$\Lambda = \sum_{j=1}^L \lambda_{i_j} \quad \text{and} \quad C = \sum_{j=1}^L l_j - \sum_{n_k^\sigma(\kappa)} \frac{n_k^\sigma(\kappa)[n_k^\sigma(\kappa) + 1]}{2},$$

as expected. Let us point out two subtleties that are crucial for the argument:

- For complex eigenvalues, the time evolution does not just stretch vectors $\mathcal{E}_k^{l\sigma}(\kappa)$, but also rotates them. However, this does not change their asymptotic growth, just an overall prefactor that may depend on time as the vector rotates in the subspace spanned by $\mathcal{E}_k^{l\sigma}(\kappa)$ for $1 \leq l \leq \dim \mathcal{J}_k(\kappa)/2$ and $\sigma \in \{+, -\}$. This prefactor is always bounded because the rotation occurs in a closed orbit with frequency $\omega = \text{Im}(\kappa)$. Finally, we do not need to worry about the fact that vectors in the $\sigma = +$ sequence become linearly dependent on vectors in the $\sigma = -$ sequence. Even though they rotate in the same subspace, they always stay linearly independent and do not approach the same direction due to a phase difference of $\pi/2$.

- A similar argument can be used to explain why we can consider sequences associated with different Jordan blocks $\mathcal{J}_k(\kappa)$ independently and do not need to worry about different vectors approaching the same direction. The time evolution of vectors $\mathcal{E}_k^{l\sigma}(\kappa)$ with fixed k and κ always stay in the subspace spanned by them and never approach directions of vectors with different k' or κ' .

This concludes the proof. \square

We found the precise volume asymptotics for a given choice of L vectors Φ^j . The next question is for which choice of L vectors Φ^j the volume grows most rapidly. This is answered by the next theorem.

Theorem 6 (Maximal volume growth)

The following algorithm allows us to find L vectors $\Phi^j \in V^*$, such that the corresponding parallelepiped $\mathcal{V} \subset V^*$ grows most rapidly among all L -dimensional parallelepipeds, and its asymptotics is given by

$$\ln M^\top(t)\mathcal{V} \sim \Lambda_{\max}^L t + C_{\max}^L \ln(t), \quad (5.169)$$

where Λ_{\max} and C_{\max} are computed below.

1. We define the exponential and polynomial contribution of a vector $\mathcal{E}_k^{l\sigma}(\kappa)$ as

$$\begin{aligned} \mathbb{E}\left(\mathcal{E}_k^{l\sigma}(\kappa)\right) &= \text{Re}(\kappa) \quad \text{and} \\ \mathbb{P}\left(\mathcal{E}_k^{l\sigma}(\kappa)\right) &= \begin{cases} 2l - 1 - \dim \mathcal{J}_k(\kappa), & \text{Im}(\kappa) = 0 \\ 2l - 1 - \dim \mathcal{J}_k(\kappa)/2, & \text{Im}(\kappa) \neq 0 \end{cases}. \end{aligned} \quad (5.170)$$

2. We sort all $2N$ generalized eigenvectors $\mathcal{E}_k^{l\sigma}(\kappa)$ into a long list

$$(\Phi^1, \Phi^2, \dots, \Phi^{2N}), \quad (5.171)$$

such that $\mathbb{E}(\Phi^j) \geq \mathbb{E}(\Phi^{j+1})$ is always satisfied and such that $\mathbb{P}(\Phi^j) \geq \mathbb{P}(\Phi^{j+1})$ is satisfied whenever $\mathbb{E}(\Phi^j) = \mathbb{E}(\Phi^{j+1})$. This sorting may not be unique, but it is sufficient for finding the maximal volume growth.

3. A maximally growing parallelepiped is spanned by the first L vectors Φ^j and its asymptotics is given by

$$\Lambda_{\max}^L = \sum_{j=1}^L \mathbb{E}(\Phi^j) \quad \text{and} \quad C_{\max}^L = \sum_{j=1}^L \mathbb{P}(\Phi^j). \quad (5.172)$$

Note that we maximize the asymptotics and not Λ and C individually.

Proof: The proof goes in two steps. First, we ask what specific vector $\mathcal{E}_k^l(\kappa)$ contributes to the asymptotics of the volume, and second, how do we need to sort them in order to get maximal contributions.

Step 1: Every vector $\mathcal{E}_k^{l\omega}(\kappa)$ may contribute to both the exponential asymptotics Λ and the polynomial asymptotics C . From Theorem 5, we recall that a specific vector $\mathcal{E}_k^{l\sigma}(\kappa)$ contributes

$$\mathbb{E}(\mathcal{E}_k^{l\sigma}(\kappa)) = \lambda = \text{Re}(\kappa) \quad (5.173)$$

to the exponential asymptotics. For the contribution to the polynomial asymptotics, we need to know how many vectors of the same sequence are already contributing. If there are already s vectors

in the sequence, the vector $\mathcal{E}_k^{l\sigma}(\kappa)$ contribute exactly

$$\mathbb{P}(\mathcal{E}_k^{l\sigma}(\kappa)) = (l - 1) - s \quad (5.174)$$

to the polynomial exponent. However, if there are $m_k(\kappa)$ vectors in the sequence, we would only choose the vector $\mathcal{E}_k^l(\kappa)$ for our parallelepiped if we have already chosen the $s = m_k(\kappa) - l$ vectors $\mathcal{E}_k^{l+1}(\kappa), \dots, \mathcal{E}_k^{m_k(\kappa)}(\kappa)$. Here, we have $m_k(\kappa) = \dim \mathcal{J}_k(\kappa)$ for real eigenvalue κ and $m_k(\kappa) = \dim \mathcal{J}_k(\kappa)/2$ for complex eigenvalue κ . In total, this leads to a contribution of

$$\mathbb{P}(\mathcal{E}_k^{l\sigma}(\kappa)) = \begin{cases} 2l - 1 - \dim \mathcal{J}_k(\kappa), & \text{Im}(\kappa) = 0 \\ 2l - 1 - \dim \mathcal{J}_k(\kappa)/2, & \text{Im}(\kappa) \neq 0 \end{cases}. \quad (5.175)$$

Step 2: It is clear that when we choose vectors of a parallelepiped in order, we maximize the asymptotics of its volume if we choose vectors first based on their exponential contribution and only second based on their polynomial contribution. Moreover, if two vectors have identical exponential and polynomial contribution, it does not matter which one we choose. \square

5.6.4 Asymptotic entanglement production

When studying the time evolution of the entanglement entropy, we found the volume expression

$$S_A(t) \sim \ln \text{Vol}[M^\top(t)\mathcal{V}_A], \quad (5.176)$$

where $\mathcal{V}_A \subset A$ is an arbitrary $2N_A$ -dimensional parallelepiped in subsystem A . The most important feature is that this formula is independent of the initial state and is also independent from the metric that we use to measure the $2N_A$ dimensional volume of $M^\top(t)\mathcal{V}_A \subset A^*$.

When we select a subsystem, we choose a subset of N_A out of N pairs $(\hat{a}_i^\dagger, \hat{a}_i)$ of creation and annihilation operators. Mathematically, this corresponds to choosing a $2N_A$ dimensional subspace $A \subset V$ of the classical phase space V that induces a tensor product decomposition $\mathcal{H}_N = \mathcal{H}_A \otimes \mathcal{H}_B$. For the volume formula, we only need to select a parallelepiped $\mathcal{V}_A \subset A$ by choosing $2N_A$ basis vectors θ^i with $\text{span}(\theta^1, \dots, \theta^{2N_A}) = A$. Note that these $2N_A$ vectors do not, in general, coincide with the generalized eigenvectors Φ^j . However, the following theorem shows that, essentially, all generic subsystems exhibit the same asymptotics of the entanglement entropy, which coincides with the maximal volume growth of a $2N_A$ -dimensional parallelepiped.

Theorem 7 (Generic entanglement production)

Given a quadratic time-independent Hamiltonian $\hat{H} = \frac{1}{2}h_{ab}\hat{\xi}^a\hat{\xi}^b$ and a Gaussian initial state, the entanglement entropy for a generic subsystem $A \subset V$ with N_A degrees of freedom grows asymptotically as

$$S_A(t) \sim \Lambda_{\max}^{2N_A} t + C_{\max}^{2N_A} \ln(t), \quad (5.177)$$

where $\Lambda_{\max}^{2N_A}$ and $C_{\max}^{2N_A}$ are the same as in Theorem 6 on the maximal volume growth.

Proof: Using the volume formula, we reduce the problem to studying the time evolution of a $2N_A$ dimensional parallelepiped. However, in contrast to Theorem 5 and 6, the parallelepiped is not necessarily spanned by the generalized eigenvectors $\mathcal{E}_k^{l\sigma}(\kappa)$. Still, we can always decompose the $2N_A$ vectors in terms of the $2N$ generalized eigenvectors Φ^j sorted as explained in Theorem 6. This leads to the transformation matrix T with column vectors \vec{t}_i :

$$\left(\begin{array}{c} \theta^1 \\ \vdots \\ \theta^{2N_A} \end{array} \right) = \left(\begin{array}{ccc} \underbrace{\left[\begin{array}{c} T_1^1 \\ \vdots \\ T_{2N_A}^1 \end{array} \right]}_{\vec{t}_1} & \cdots & \underbrace{\left[\begin{array}{c} T_1^{2N} \\ \vdots \\ T_{2N_A}^{2N} \end{array} \right]}_{\vec{t}_{2N}} \end{array} \right) \left(\begin{array}{c} \Phi^1 \\ \vdots \\ \Phi^{2N} \end{array} \right). \quad (5.178)$$

Provided that the first $2N_A$ columns \vec{t}_i are linearly independent, we can build the invertible $2N_A$ -by- $2N_A$ matrix $U = (\vec{t}_1, \dots, \vec{t}_{2N_A})$ and move to the new basis vectors $\tilde{\theta}^j$:

$$\begin{pmatrix} \tilde{\theta}^1 \\ \vdots \\ \tilde{\theta}^{2N_A} \end{pmatrix} = \begin{pmatrix} \mathbb{1}_{2N_A} & U^{-1}\vec{t}_{2N_A+1} & \cdots & U^{-1}\vec{t}_{2N} \end{pmatrix} \begin{pmatrix} \Phi^1 \\ \vdots \\ \Phi^{2N} \end{pmatrix}. \quad (5.179)$$

The vectors $\tilde{\theta}^j$ span another parallelepiped in the same subspace $A \subset V$, which grows asymptotically as \mathcal{V}_A . Moreover, each vector $\tilde{\theta}^j$ is of the form

$$\tilde{\theta}^j = \Phi^j + \sum_{i=2N_A+1}^{2N} c_i \Phi^i, \quad (5.180)$$

with some coefficients c_i . This ensures that the volume growth is dominated by the first $2N_A$ vectors Φ^j , which therefore leads to the same asymptotic behavior as the one of the parallelepiped spanned by just $(\Phi^1, \dots, \Phi^{2N_A})$. This asymptotics was already derived in Theorem 6. Only if the subsystem A is such that the first $2N_A$ columns of T are not linearly independent the asymptotics will change and its analysis is more complicated. However, such subsystems correspond to a subset of measure zero in the space of all subsystems. This legitimizes our statement that the entanglement production found here is generic for almost all subsystems. \square

5.7 Beyond Gaussian states and quadratic Hamiltonians

In section 5.6, we restricted our study to quadratic time-independent Hamiltonians and Gaussian initial states. We were able to derive the exact asymptotics of the entanglement entropy thanks to powerful analytical tools to compute the following:

- **Entanglement entropy of Gaussian states:**

Calculating the entanglement entropy of an arbitrary state in the Hilbert space is a challenging computational problem. (Its computational cost scales with the dimension of the Hilbert space.) Here we are interested in bosonic Hilbert spaces that are infinite dimensional. In order to use standard numerical methods, we need to truncate the Hilbert space to a finite-dimensional subsector, and compute the entanglement entropy of states projected onto that subsector. This is only a good approximation if the states of interest have little overlap with the orthogonal complement of the truncated space. Analytical methods only exist for specific subclasses of states and specific systems decompositions. However, an important subclass consists of Gaussian states. For those, we presented a wide range of analytical techniques to compute and bound the entanglement entropy for arbitrary system decompositions (up to a measure zero set). In particular, writing the entanglement entropy of a state as the volume of a region \mathcal{V}_A was crucial:

$$S_A \approx \ln \text{Vol}(\mathcal{D}_A). \quad (5.181)$$

- **Time evolution of quadratic Hamiltonians:**

For generic Hamiltonians, the quantum time evolution is more complicated than the classical one. While the Hamiltonian equations of motion are ordinary differential equations, quantum evolution is based on the Schrödinger equation, which is a partial differential equation. Knowing the classical solution of the equation of motion does not help to find the quantum mechanical time evolution, unless the Hamiltonian is quadratic. In this special case, the time

evolution of arbitrary connected n -point functions $C_{|\psi(t)\rangle}^{a_1 \dots a_n}$, for arbitrary initial states $|\psi_0\rangle$, can be computed from the classical time evolution $M(t)^a_b$:

$$C_{|\psi(t)\rangle}^{a_1 \dots a_n} = M(t)^{a_1}_{b_1} \cdots M(t)^{a_n}_{b_n} C_{|\psi_0\rangle}^{b_1 \dots b_n}. \quad (5.182)$$

Another important property of quadratic Hamiltonians is their interplay with Gaussian states. If the Hamiltonian is quadratic, an initial Gaussian state remains Gaussian at all times. Since our analytical techniques only allow us to compute the entanglement entropy of Gaussian states, we can evolve them only with quadratic Hamiltonians to be able to study the time evolution of the entanglement entropy. Moreover, the change of the entanglement entropy is the result of the change of the volume of \mathcal{V}_A under the classical Hamiltonian flow $M(t)$:

$$S_A(t) \sim \ln \text{Vol}[M^\top(t)\mathcal{V}_A]. \quad (5.183)$$

It is natural to ask in which way our conclusions change in systems that violate one or both these simplifying conditions. We can distinguish the following three scenarios:

1. Quadratic Hamiltonian, non-Gaussian initial states
2. Non-quadratic Hamiltonian, Gaussian initial states
3. Non-quadratic Hamiltonian, non-Gaussian initial states

For the first scenario, there is already an analytic upper bound for the entanglement entropy production explained in section 5.1.3, which we test numerically and find to be saturated at long times. For scenarios two and three, we discuss in which regimes the analytically obtained behaviors for Gaussian initial states evolving under quadratic Hamiltonians still apply.

In order to study the entanglement entropy, we use a class of toy models that show different asymptotic features and which are simple enough to allow us to evaluate the entanglement entropy numerically with high accuracy. We consider two degrees of freedom with creation (annihilation) operators \hat{a}_i^\dagger (\hat{a}_i) for $i \in \{1, 2\}$. We truncate the corresponding Fock space \mathcal{H}_V of two degrees of freedom to the following $(T + 1)$ -dimensional subsector

$$\mathcal{H}_{\text{trunc}} = \text{span}\{|n, n\rangle \text{ with } 0 \leq n \leq T\} \subset \mathcal{H}_V \quad (5.184)$$

where we choose different truncation sizes with up to $T = 100,000$. This truncation can be used only if the time evolution results in a state that mostly remains in the truncated subspace. We therefore require that the Hamiltonian \hat{H} commutes with the difference number operator $\hat{n}_1 - \hat{n}_2 = \hat{a}_1^\dagger \hat{a}_1 - \hat{a}_2^\dagger \hat{a}_2$. This ensures that the time evolution preserves the subspace whose states $|\psi\rangle$ satisfy $(\hat{n}_1 - \hat{n}_2)|\psi\rangle = 0$. Specifically, we choose

$$\hat{H}(\Delta, U) = (\hat{n}_1 + \hat{n}_2) + \Delta \left(\hat{a}_1^\dagger \hat{a}_2^\dagger + \hat{a}_1 \hat{a}_2 \right) + \frac{U}{2} (\hat{n}_1^2 + \hat{n}_2^2) \quad (5.185)$$

as our Hamiltonian, with free parameters Δ and U .

The noninteracting part of this Hamiltonian in the basis of $(\hat{q}_1, \hat{q}_2, \hat{p}_1, \hat{p}_2)$ is

$$\hat{H}(\Delta, 0) = \frac{1}{2}(\hat{p}_1^2 + \hat{p}_2^2 - 2\Delta \hat{p}_1 \hat{p}_2) + \frac{1}{2}(\hat{q}_1^2 + \hat{q}_2^2 + 2\Delta \hat{q}_1 \hat{q}_2),$$

with

$$h \equiv \begin{pmatrix} 1 & -\Delta & 0 & 0 \\ -\Delta & 1 & 0 & 0 \\ 0 & 0 & 1 & \Delta \\ 0 & 0 & \Delta & 1 \end{pmatrix} \Rightarrow K \equiv \begin{pmatrix} 0 & 0 & \Delta & -1 \\ 0 & 0 & -1 & \Delta \\ \Delta & 1 & 0 & 0 \\ 1 & \Delta & 0 & 0 \end{pmatrix}. \quad (5.186)$$

Different choices of those parameters correspond to different classes of Hamiltonians.

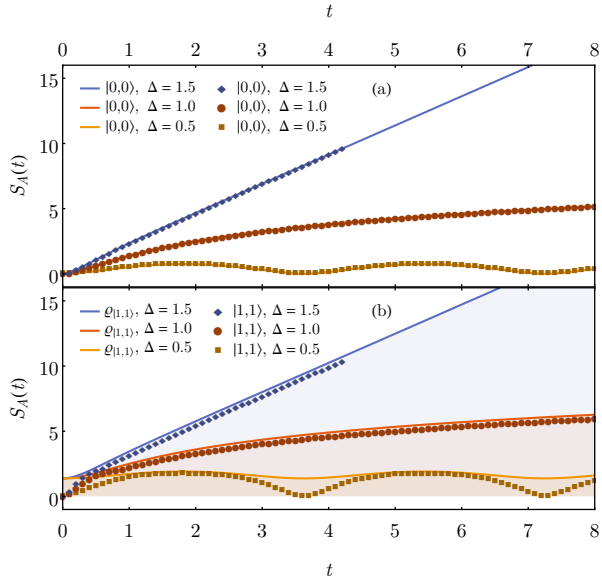


Figure 5.11: Quadratic Hamiltonians with Gaussian and non-Gaussian initial states. We compare numerical (symbols) and analytical (lines) results for the unstable ($\Delta = 1.5$), stable ($\Delta = 0.5$), and metastable ($\Delta = 1.0$) Hamiltonians. (a) Gaussian initial state $|0,0\rangle$. (b) Non-Gaussian state initial state $|1,1\rangle$ compared to analytical results for the Gaussian state $\varrho_{|1,1\rangle}$. The Hilbert space truncation is $T = 50,000$.

(1) **Quadratic Hamiltonian $\hat{H}(\Delta, 0)$:**

The eigenvalues of the matrix K are: $K = \{\sqrt{\Delta^2 - 1}, \sqrt{\Delta^2 - 1}, -\sqrt{\Delta^2 - 1}, -\sqrt{\Delta^2 - 1}\}$. Hence, the Hamiltonian is : (a) unstable for $|\Delta| > 1$ (all eigenvalues of K are real), (b) stable for $|\Delta| < 1$ (all eigenvalues of K are imaginary), and (c) metastable for $|\Delta| = 1$ (all eigenvalues of K are zero). We then consider: (a) $\Delta = 1.5$, (b) $\Delta = 0.5$, and (c) $\Delta = 1$. The entanglement entropy is computed from $J(t) = M(t)J_0M^{-1}(t)$ and $M(t) = e^{tK}$. The initial complex structure J_0 can be computed from the initial 2-point function $(G_0)^{ab}$ via $(J_0)^a_b = -(G_0)^{ac}\omega_{cb}$.

(2) **Non-quadratic Hamiltonian $\hat{H}(\Delta, U)$:**

We investigate the effect of non-quadratic perturbations by adding the quartic term $(\hat{n}_1^2 + \hat{n}_2^2)$ with a small prefactor $U > 0$. This Hamiltonian is always bounded from below. $\hat{H}(\Delta, 0)$ is the expansion of $\hat{H}(\Delta, U)$ to quadratic order in creation and annihilation operators.

We compute the time evolution of the entanglement entropy for various initial states:

(A) **Fock states:** $|n, n\rangle$.

(B) **Gaussian states:** $\varrho_{|n,n\rangle}$.

We construct the Gaussian part of $|n, n\rangle$, namely, $\varrho_{|n,n\rangle}$, numerically. The state $\varrho_{|n,n\rangle}$ has the same 1- and 2-point functions as $|n, n\rangle$, but all higher n -point functions are constructed via Wick's theorem. Note that this may mean that $\varrho_{|n,n\rangle}$ is not a pure state. The entanglement entropy $S_A(\varrho_{|n,n\rangle})$ is computed using $\varrho_{|n,n\rangle}$ to evaluate our analytic expressions, and is compared to the entanglement entropy $S_A(|n, n\rangle)$. They satisfy the inequality $S_A(|n, n\rangle) \leq S_A(\varrho_{|n,n\rangle})$ at all times

(C) **Random state:** $|\text{ran}\rangle$.

In order to study the behavior of the entanglement entropy for random states in the truncated

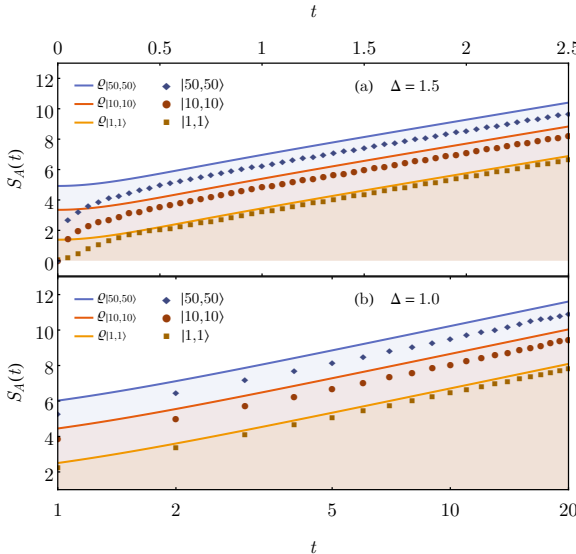


Figure 5.12: Quadratic Hamiltonian with non-Gaussian initial states. We compare analytical (lines) with numerical (symbols) results for: (a) an unstable Hamiltonian ($\Delta = 1.5$) for a truncation $T = 50,000$, and (b) a metastable Hamiltonian ($\Delta = 1.0$) for a truncation $T = 100,000$.

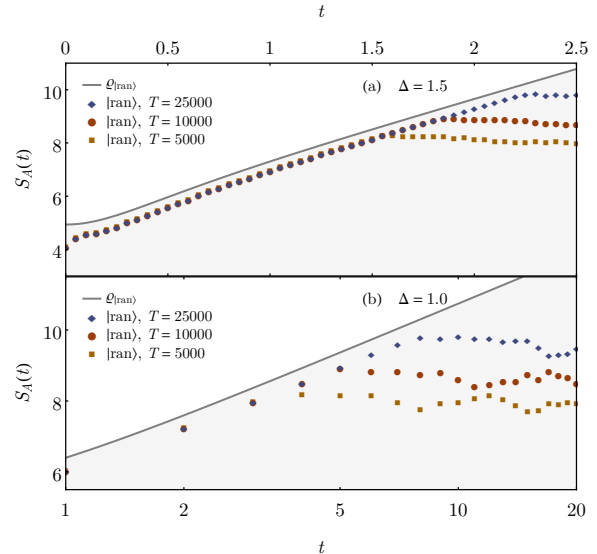


Figure 5.13: Quadratic Hamiltonian with random non-Gaussian initial state. We compare analytical (lines) with numerical (symbols) results for: (a) an unstable ($\Delta = 1.5$), and (b) a metastable ($\Delta = 1.0$) Hamiltonian when the Hilbert space truncation T is varied.

Hilbert space, we generate a random state

$$|\text{ran}\rangle = \frac{1}{\sqrt{\sum_{n=0}^{100} c_n^2}} \sum_{n=0}^{100} c_n |n, n\rangle, \quad (5.187)$$

where c_n are selected randomly between 0 and 1 with uniform probability.

We compare our analytical results for Gaussian states and quadratic Hamiltonians (lines) with numerical computations of various Gaussian and non-Gaussian states evolving under quadratic and non-quadratic Hamiltonians (symbols). Figure 5.11(a) illustrates that our numerical results agree perfectly with the analytical ones for the Gaussian initial state $|0,0\rangle$ evolving under a quadratic Hamiltonian. For the non-Gaussian initial state $|1,1\rangle$, see figure 5.11(b), we compare the numerical results to the analytical ones for $\varrho_{|1,1\rangle}$. The latter serve as an upper bound to the former ones.

5.7.1 Non-Gaussian initial states evolving under quadratic Hamiltonians

In figure 5.12, we present a more comprehensive study of the entropy production during the dynamics of non-Gaussian initial states under quadratic Hamiltonians. We compare the entanglement entropy $S_A(t)$ for the non-Gaussian initial states $|1,1\rangle$, $|10,10\rangle$, and $|50,50\rangle$ with the one of the corresponding Gaussian initial states $\varrho_{|n,n\rangle}$, for an unstable [figure 5.12(a)] and a metastable [figure 5.12(b)] Hamiltonian. The numerical results show that the corresponding Gaussian initial states provide an upper bound for the non-Gaussian ones. More importantly, we find that $S_A(t)$ for non-Gaussian states shows the characteristic asymptotic behavior of the entropy derived analytically for Gaussian states. Namely, a linear increase for unstable Hamiltonians and a logarithmic one for metastable ones. This leads us to conjecture that for both, unstable and metastable Hamiltonians, the asymptotic predictions for Gaussian initial states apply to any initial state.

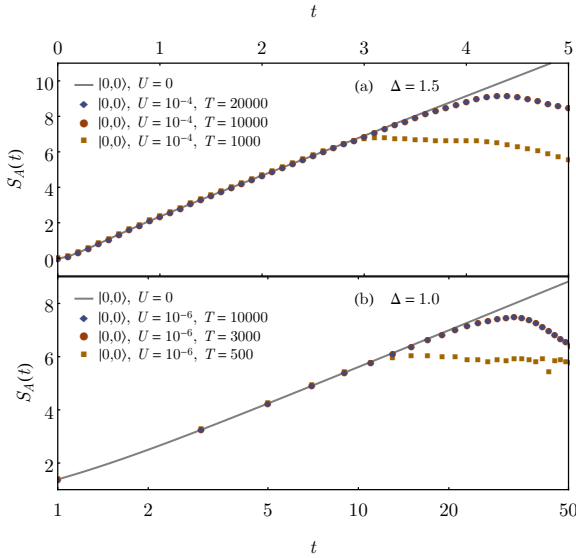


Figure 5.14: Non-quadratic Hamiltonians with Gaussian initial state. The entanglement production under non-quadratic Hamiltonians (symbols) is compared to the one under their quadratic parts (lines). We also vary the Hilbert space truncation T . The results for the two largest values of T overlap in each panel.

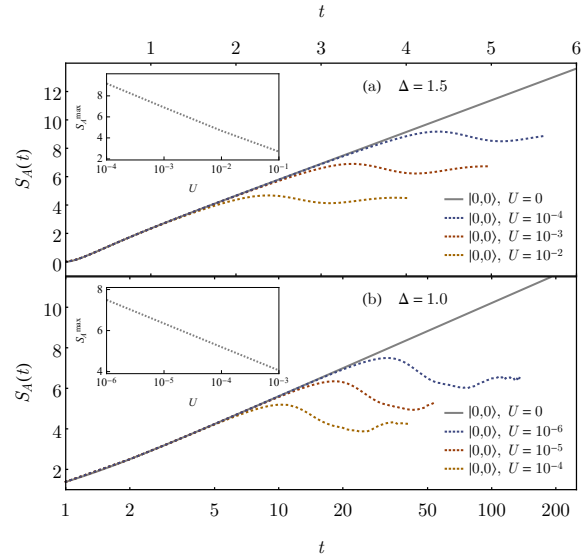


Figure 5.15: Entanglement entropy saturation for non-quadratic Hamiltonians. In each panel, we compare results obtained for different values of U . In the insets, we plot the entanglement entropy at the first maximum during the time evolution, S_A^{\max} , as a function of U . The Hilbert space truncation is $T = 50,000$.

Results for the entropy production during the dynamics of an initial random state, for different truncations of the Hilbert space, are presented in figure 5.13. The asymptotic behavior (with increasing T) of the entanglement entropy in figure 5.13 is identical to the one in figure 5.12. Finite values of T lead to a saturation of the entanglement entropy at times that grow with increasing T .

5.7.2 Gaussian initial states evolving under non-quadratic Hamiltonians

Next, we consider Gaussian initial states evolving under non-quadratic Hamiltonians. Because of the non-quadratic part, the overall Hamiltonian is bounded from below, which implies that the entanglement entropy is bounded from above by the thermal entropy at the energy of the time-evolving state. We are interested in the regime in time in which the entanglement production exhibits the same behavior as for the nearby quadratic Hamiltonian. It is expected that, as long as the non-quadratic part can be neglected compared to the quadratic one for a given initial state, the entanglement production will be dominated by the quadratic part. However, there will always be a time at which the entanglement entropy will depart from the result for the quadratic part. As mentioned before, an initial Gaussian state does not remain Gaussian under the time evolution with a non-quadratic Hamiltonian.

In figure 5.14, we show the entanglement production for an initial Gaussian state ($|0,0\rangle$) evolving under unstable, see figure 5.14(a)], and metastable Hamiltonians, see figure 5.14(b). We compare the numerical results with the analytical prediction for the entanglement production of the corresponding quadratic Hamiltonian. We find a perfect agreement at short and intermediate times, but eventually the entanglement entropy in the non-quadratic systems saturates. In figure 5.14, we report results for various Hilbert space truncations to demonstrate that, for sufficiently large truncations, the saturation value is independent of the truncation chosen. Figure 5.15 shows how

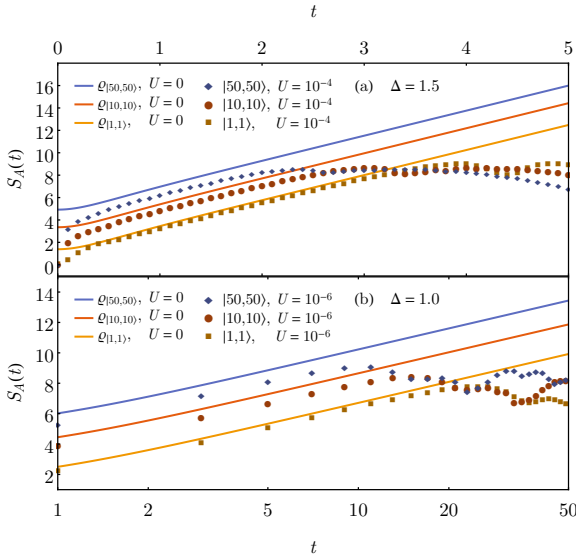


Figure 5.16: Non-quadratic Hamiltonians with non-Gaussian initial states. We compare analytical results for dynamics under quadratic Hamiltonians (lines) with numerical results (symbols) for: (a) an unstable ($\Delta = 1.5$), and (b) a metastable ($\Delta = 1.0$) Hamiltonian. The Hilbert space truncation is $T = 50,000$.

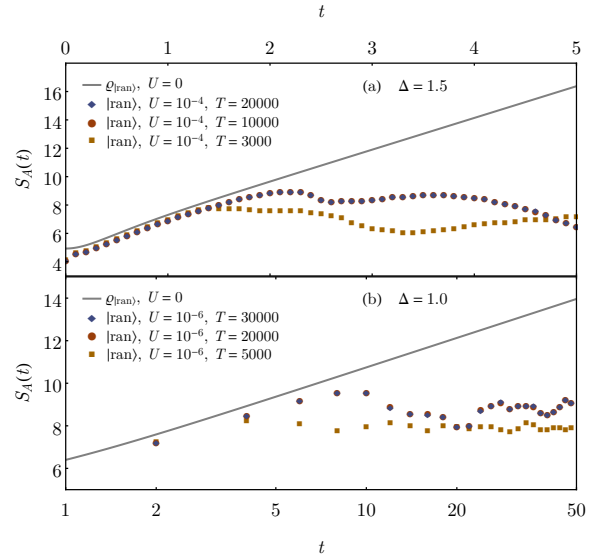


Figure 5.17: Non-quadratic Hamiltonians with random non-Gaussian initial state. We compare the analytical results for dynamics under quadratic Hamiltonians (lines) with the numerical results (symbols) for: (a) an unstable ($\Delta = 1.5$), and (b) a metastable ($\Delta = 1.0$) Hamiltonian when the Hilbert space truncation T is varied. The results for the two largest values of T overlap in each panel.

the saturation value depends on U for sufficiently large Hilbert space truncations. In particular, in the insets we plot the entanglement entropy at the first maximum during the time evolution, S_A^{\max} , as a function of U . In the regime studied, S_A^{\max} decreases near logarithmically with U .

5.7.3 Non-Gaussian initial states evolving under non-quadratic Hamiltonians

To close the numerical part of our study, we explore the evolution of non-Gaussian initial states under non-quadratic Hamiltonians. Clearly, if the initial state has an entanglement entropy that is close to that of the thermal state with the same energy, there is no intermediate regime in the entanglement entropy dynamics exhibiting a linear or logarithmic growth (the entanglement entropy cannot change much). Hence, we focus on non-Gaussian initial states whose entanglement entropy is much smaller than the thermal one.

The results for the entanglement production at short and intermediate times in such states are very similar for the dynamics under non-quadratic Hamiltonians (see figures. 5.16 and 5.17) and quadratic ones (see figures. 5.12 and 5.13). The main difference between them is the U dependent saturation that occurs in the former. At intermediate times they are all very similar, and are bounded from above by the analytical predictions for Gaussian initial states.

5.8 Further exploration

We discuss the role of interactions in the saturation phase of the entanglement growth, explain the relation to results on quantum quenches and present a conjecture on entanglement and chaos.

5.8.1 Interactions and the production of non-Gaussianities

Quadratic Hamiltonians appear naturally in the analysis of small perturbations around equilibrium configurations, both stable and unstable. Let us consider for instance a dynamical system with a “Mexican hat” potential and an initial Gaussian state which is sufficiently peaked at the top of the potential. For short times the evolution of this initial state is well described by a perturbative quadratic Hamiltonian with unstable directions as in (5.89). As a result, if the scales of the problem are sufficiently separated, the entanglement entropy of a subsystem will show an intermediate linear growth with rate Λ_A , followed by a non-Gaussian phase. In particular the linear growth driven by the perturbative instability stops when the spread of the state starts to probe the bottom of the potential and interactions become non-negligible. As the full Hamiltonian of the system is stable at the non-perturbative level, the entanglement entropy of the subsystem is bounded from above by the entanglement entropy S_{eq} of the thermal state with the same energy as the initial Gaussian state. In the presence of an equilibration and a thermalization mechanism, the entropy S_{eq} provides also the saturation value as shown in figure 5.1.

Quadratic Hamiltonians appear also in the analysis of small perturbations of classical solutions. In this case the perturbative Hamiltonian inherits the time-dependence of the classical solution. For instance if the classical solution is periodic in time, then it provides a time-dependent background for the perturbations which leads to a perturbative Hamiltonian that is periodic in time. The stroboscopic dynamics of the system can be analyzed with the same methods discussed for the Hamiltonian (5.91). In particular, in the presence of parametric resonances, the Floquet exponents of the system determine the subsystem exponent Λ_A and the growth of the entanglement entropy as described in theorems 1 and 2. When the conditions (5.16) for the subsystem are satisfied, the rate of growth is given by the classical Kolmogorov-Sinai entropy rate as discussed also in [89]. After the initial phase of linear growth, two distinct phenomena render the parametric resonance inefficient and lead to a saturation phase. The first phenomenon is dephasing: large perturbations are not harmonic; their period depends on the amplitude of the oscillation and, when the period is driven far from resonance, the periodic background cannot pump energy efficiently into the perturbation. The second phenomenon is backreaction: clearly the linear entropy growth is accompanied by the production of a large number of excitations that at some point start to interact and backreact, thus leading to a saturation phase in which non-Gaussianities cannot be neglected. The phase of linear growth manifests itself only if the typical scales of the problem are sufficiently separated.

5.8.2 Relation to linear growth in quantum quenches

Quantum quenches lead also to a phase of linear growth of the entanglement entropy, followed by a saturation phase. This phenomenon has been studied extensively in free field theories [65–67] and in many-body quantum systems [64, 142–147]. Despite the similarities in the behavior of the entanglement entropy, the mechanism behind this phenomenon is distinct from the one discussed in this article.

A standard example of global quantum quench is provided by an harmonic lattice similar to the one discussed in section 5.4.3. The Hamiltonian of the system consists of two terms,

$$H_\kappa = \frac{1}{2} \sum_{i=1}^N (p_i^2 + \Omega_0^2 q_i^2) + \frac{1}{2} \kappa \sum_{i=1}^N (q_{i+1} - q_i)^2, \quad (5.188)$$

the first term is ultralocal, while the second encodes the coupling of first neighboring oscillators. A quantum quench consists in preparing the system in the ground state $|\psi_0\rangle$ of the Hamiltonian H_0 with vanishing coupling $\kappa = 0$. At the time $t = 0$ the coupling is instantaneously switched on,

and the state is let to evolve unitarily, $|\psi(t)\rangle = e^{iH_\kappa t}|\psi_0\rangle$. The entanglement entropy of a local subset of the lattice evolves in a way similar to the one depicted in figure 5.1. Instabilities play no role in this phenomenon. In fact the Hamiltonian (5.188) is stable for $\kappa > -\Omega_0^2/4$, as it can be seen from (5.96). The relevant mechanism for the linear growth of the entanglement entropy in this quantum quench is not instabilities, but transport instead. The quench results in the local production of quasi-particles which travel at a finite speed. The phase of linear growth can be understood to be the result of the entanglement produced by the free propagation of entangled couples of quasi-particles, with the entanglement production rate determined by their propagation speed [65–67, 147].

Interactions or coupling between many degrees of freedom, together with propagation of quasi-particles, play a key role in the phenomenon of entanglement growth in quantum quenches. On the other hand, the phenomenon studied in this paper relies on the existence of instabilities of some modes of a quantum system, as discussed in section 5.4 and 5.5. The difference between the two phenomena is easily illustrated by the case of bosonic systems and Gaussian states for which formula (2.34) holds, [17, 52–54]

$$S_A = \sum_{i=1}^{N_e} \left(\frac{\nu_i + 1}{2} \log \frac{\nu_i + 1}{2} - \frac{\nu_i - 1}{2} \log \frac{\nu_i - 1}{2} \right). \quad (5.189)$$

In the case of quantum quenches, the number of entangled pairs N_e with fixed weight ν_i grows linearly in time until saturation. On the other hand, in the presence of instabilities, unstable modes have weight ν_i which grows exponentially in time until saturation, therefore leading to an entanglement growth of the form depicted in figure 5.1. While the linear regime for quantum quenches can only be seen for a sufficiently large number of degrees of freedom in the system, linear growth due to instabilities can already occur for a system with two degrees of freedom and a single instability. As a result, despite the intriguing similarity, the two phenomena are distinct.

5.8.3 A conjecture on entanglement, chaos and thermalization times

There is an intimate relationship between chaos, thermalization and entanglement [56–58, 148–150]. Here we discuss how semiclassical methods allow us to estimate the rate of growth of the entanglement entropy in the early phase of the thermalization process.

Let us consider a classical Hamiltonian system with linear phase space $(\mathbb{R}^{2N}, \Omega)$ and a Hamiltonian H which does not depend on time so that, as a result, the energy of the system is conserved. We assume also that the Hamiltonian is bounded from below and, at fixed energy, trajectories in phase space are bounded. This classical system displays a chaotic behavior if its Kolmogorov-Sinai entropy rate is non-vanishing, i.e. $\hbar_{KS} > 0$ with \hbar_{KS} defined by (5.64), [151–153]. We are interested in the process of thermalization in the associated quantum system with Hamiltonian H . We argue that the Kolmogorov-Sinai entropy rate \hbar_{KS} studied in this paper plays a central role in determining the relevant time scale in the process of quantum thermalization.

An isolated quantum system thermalizes when observables that probe only part of the system cannot distinguish a pure state from a thermal state. More precisely, let us consider a pure state and a thermal state with the same energy,

$$|\psi_t\rangle = e^{-iHt}|\psi_0\rangle \quad \text{and} \quad \sigma = \frac{e^{-\beta H}}{Z}. \quad (5.190)$$

The requirement that they have the same energy fixes the temperature β^{-1} of the thermal state, i.e., $E = \langle\psi_t|H|\psi_t\rangle = \text{Tr}(H\sigma)$. Now we consider a subsystem A and the subalgebra of bounded

observables⁹ \mathcal{O}_A in A . We say that the subsystem A thermalizes if all bounded observables \mathcal{O}_A attain a thermal expectation value, i.e.,

$$\langle \psi_t | \mathcal{O}_A | \psi_t \rangle \longrightarrow \text{Tr}(\mathcal{O}_A \sigma). \quad (5.191)$$

This condition can be formulated in terms of entanglement between the subsystem A and its complement B . Let us define the restricted states¹⁰

$$\rho_A(t) = \text{Tr}_B(|\psi_t\rangle\langle\psi_t|) \quad \text{and} \quad \sigma_A = \text{Tr}_B(\sigma) \equiv \frac{e^{-\beta\tilde{H}_A}}{Z_A}. \quad (5.192)$$

Thermalization in A is a measure of how distinguishable is the restricted states $\rho_A(t)$ from the restricted thermal state σ_A . The relative entropy [91, 92],

$$S(\rho_A(t)\|\sigma_A) \equiv \text{Tr}_A(\rho_A \log \rho_A - \rho_A \log \sigma_A), \quad (5.193)$$

provides a measure of such distinguishability. In fact, using the inequalities $S(\rho\|\sigma) \geq \frac{1}{2}\|\rho - \sigma\|^2$ together with the Schwarz inequality $\|\sigma\| \geq \text{Tr}(\mathcal{O}\sigma)/\|\mathcal{O}\|$, one can prove the inequality

$$\frac{\left(\langle \psi_t | \mathcal{O}_A | \psi_t \rangle - \text{Tr}(\mathcal{O}_A \sigma) \right)^2}{2 \|\mathcal{O}_A\|^2} \leq S(\rho_A(t)\|\sigma_A), \quad (5.194)$$

which holds for all bounded observables in A . Therefore, proving $S(\rho_A(t)\|\sigma_A) \rightarrow 0$ as $t \rightarrow \infty$ provides a proof of thermalization in A . Now, the relative entropy can be expressed in turn as the sum of two terms,

$$S(\rho_A(t)\|\sigma_A) = \left(S_A^{\text{eq}}(E) - S_A(t) \right) + \beta \left(\langle \psi_t | \tilde{H}_A | \psi_t \rangle - \text{Tr}(\tilde{H}_A \sigma) \right). \quad (5.195)$$

The first term is the difference between the equilibrium entropy $S_A^{\text{eq}}(E) = -\text{Tr}_A(\sigma_A \log \sigma_A)$ and the entanglement entropy $S_A(t)$ of the subsystem. The second term measures energy flow between the subsystem A and its complement, as measured by the effective Hamiltonian \tilde{H}_A of the subsystem defined in (5.192). At equilibrium, both terms vanish independently. This paper and the following conjecture focus on the evolution of the first term, i.e., the growth and saturation of the entanglement entropy $S_A(t)$.

When a subsystem thermalizes, the entanglement entropy $S_A(t)$ approaches the equilibrium value $S_A^{\text{eq}}(E)$. The eigenstate thermalization hypothesis (ETH) [148–150] provides a sufficient condition for such subsystem thermalization to occur. In a chaotic quantum system with local interactions one observes that energy eigenstate, $H|E_n\rangle = E_n|E_n\rangle$, in the bulk of the energy spectrum have a non-trivial entanglement structure: their restriction to a local subsystem results in a thermal state of the form of (5.192), i.e., $\text{Tr}_B(|E_n\rangle\langle E_n|) \approx \sigma_A(E_n)$. As a result, the restriction $\rho_A(t)$ of a pure state $|\psi_t\rangle = \sum_n e^{-iE_n t} c_n |E_n\rangle$ with support in a narrow band of energy E is also well approximated by a thermal state when averaged over time, i.e. $\frac{1}{T} \int_0^T \rho_A(t) dt \approx \sigma_A(E)$ for large T . This condition is sufficient to prove thermalization in average, but it does not provide a time-scale for the thermalization process.

We propose a conjecture which complements previous arguments to the quantum thermalization of subsystems [56–58, 148–150]. The conjecture applies to semiclassical states and provides a time-scale for subsystem thermalization:

⁹Bounded observables have finite norm defined as $\|\mathcal{O}\|^2 = \text{Tr}(\mathcal{O}^\dagger \mathcal{O}) < \infty$.

¹⁰Note that the operator \tilde{H}_A is defined in terms of the restricted thermal state and in general it does not coincide with the restriction of the Hamiltonian H to the subsystem A .

Given an initial state $|\psi_0\rangle = \sum_n c_n |E_n\rangle$ peaked on a classical configuration of energy $E = \langle\psi_0|H|\psi_0\rangle$ with E large compared to the energy gap of the system, and a local subsystem A such that its initial entanglement entropy is small compared to the thermal entropy at the same energy, $S_A(|\psi_0\rangle) \ll S_A^{\text{eq}}(E)$, the time-evolution of the entropy $S_A(t) \equiv S_A(e^{-iHt}|\psi_0\rangle)$ displays a linear phase $S_A(t) \sim \Lambda_A(E)t$ before saturating to the plateau at $S_A^{\text{eq}}(E)$ as described in figure 5.1. The rate $\Lambda_A(E)$ can be computed from the classical chaotic dynamics of the Hamiltonian H on the energy-shell E . The rate is given by the subsystem exponent discussed in section 5.2.3 and, apart from its energy, it is largely independent of the initial state $|\psi_0\rangle$. In particular, the subsystem exponent sets the time-scale of subsystem thermalization, $\tau_{\text{eq}} \sim S_A^{\text{eq}}(E)/\Lambda_A(E)$.

The conjecture is based on theorem 1 presented in section 5.1, together with semiclassical arguments. Let us consider a classical solution $(q_i^{\text{cl}}(t), p_i^{\text{cl}}(t))$ with energy $H(q_i^{\text{cl}}(t), p_i^{\text{cl}}(t)) = E$. At the leading order in a semiclassical expansion, the evolution of a perturbation $\xi^a = (q_i^{\text{cl}}(t) + \delta q_i, p_i^{\text{cl}}(t) + \delta p_i)$ of the classical solution is governed by the perturbative Hamiltonian

$$H_{\text{pert}}(t) = \frac{1}{2} h_{ab}(t) \delta\xi^a \delta\xi^b \quad (5.196)$$

where $\delta\xi^a = (\delta q_i, \delta p_i)$ and

$$h_{ab}(t) = \left. \frac{\partial^2 H}{\partial \xi^a \partial \xi^b} \right|_{\xi_{\text{cl}}^a(t)} . \quad (5.197)$$

The Lyapunov exponents of a non-perturbative chaotic system with Hamiltonian H can be computed directly from the perturbative Hamiltonian $H_{\text{pert}}(t)$, which is quadratic time-dependent and for which our theorem 2 applies. In fact, because of ergodicity of a chaotic system, all trajectories on the same energy-shell E (except a set of measure zero) have the same Lyapunov exponents.¹¹ Moreover, under standard assumptions of regularity [94], the Kolmogorov-Sinai rate $h_{\text{KS}}(E)$ on the shell of energy E is given by Pesin's formula (5.65) in terms of the positive Lyapunov exponents $\lambda_i(E)$. We consider now a symplectic subsystem (A, Ω_A) and define its subsystem exponent $\Lambda_A(E)$ as in section 5.2.3. This is also the rate of growth of the entanglement entropy derived assuming a Gaussian state and a quadratic Hamiltonian in theorem 3. The conjecture extends this result to a full non-quadratic system with bounded and chaotic motion, within the regime of validity of the semiclassical expansion. The inequality $\Lambda_A(E) \leq h_{\text{KS}}(E)$ provides an upper bound on the rate of entanglement growth during the linear phase. Clearly, the linear phase ends when the semiclassical approximation breaks down, i.e. when the spread of the wavefunction is so large that higher-order terms in the expansion $H = E + H_{\text{pert}}(t) + \dots$ cannot be neglected. An estimate of this time is provided by $\tau_{\text{eq}} \sim S_A^{\text{eq}}(E)/h_{\text{KS}}(E)$ which measures the ratio between the accessible volume in phase space and the rate of growth of the phase space volume occupied by the perturbation.

The conjectured behavior of the entanglement entropy $S_A(t)$ depicted in figure 5.1 is expected to manifest itself only in the regime where the semiclassical approximation holds. This conjecture can be tested on a model system such as the one described by the Hamiltonian

$$H = \frac{1}{2}(p_x^2 + p_y^2 + p_z^2) + \frac{1}{2}(x^2y^2 + x^2z^2 + y^2z^2) . \quad (5.198)$$

This is a well-studied model which appears in the analysis of the homogeneous sector of Yang-Mills gauge theory [154, 155]. Its Lyapunov exponents are known to scale with the energy as $\lambda_i(E) \sim E^{\frac{1}{4}}$

¹¹For ergodic dynamics, time averages along an endless trajectory equal ensemble averages over the energy shell. Short periodic orbits may still retain their individual Lyapunov exponents, but they form a set of measure zero.

and its equilibrium entropy, estimated as the log of the phase space volume at fixed energy, scales as $S^{\text{eq}}(E) \sim \log E$. As a result, for a semiclassical initial state of energy E we expect our conjecture to apply: the entanglement entropy of a subsystems such as (x, p_x) is expected to initially grow linearly with a rate $\sim E^{1/4}$ and then saturate in a time $\tau_{\text{eq}} \sim E^{-1/4} \log E$. This behavior can in principle be tested via numerical investigations. The numerical analysis involves the unitary evolution of a pure state under a chaotic quantum Hamiltonian.

We note that the conjecture is expected to apply only to initial states which are semiclassical, i.e. states with average energy much larger than the energy gap, small spread in energy and, in general, small spread around a point in phase space. On the other hand, when the energy E of the initial state is comparable to the energy gap of the Hamiltonian, classical orbits of that energy have an action comparable to \hbar and there is no reason to expect that they provide a useful tool for predicting the behavior of the entanglement entropy in the linear regime of figure 5.1. In fact, recent results from quantum field theories with a gravity duals [156] show that—at low energy—the rate of growth of the entanglement entropy is bounded from above by the energy of the subsystem divided by \hbar and therefore deviates from the semiclassical prediction [157].

Chapter 6

Typical energy eigenstate entanglement

In this chapter, we use Kähler methods for fermionic Gaussian states to study the behavior of the typical eigenstate entanglement entropy as a function of the subsystem size. This chapter is largely based on [LH07, LH11, LH14].

Different measures of entanglement have been extensively used to probe the structure of pure quantum states [158], and they have started to be measured in experiments with ultracold atoms in optical lattices [159, 160]. Here, we are interested in the bipartite entanglement entropy (referred to as the entanglement entropy) in fermionic lattice systems. In such systems, an upper bound for the entanglement entropy of a subsystem A (smaller than its complement) is $S_{\max} = \log \mathfrak{D}_A$, where \mathfrak{D} and \mathfrak{D}_A are the dimensions of the Hilbert space of the system and of the subsystem, with $\mathfrak{D}_A \leq \sqrt{\mathfrak{D}}$. Note that $\log \mathfrak{D}_A \propto V_A$, where V_A is the number of sites in A, i.e., this upper bound scales with the “volume” of A. (When A is larger than its complement, the Hilbert space of the complement is the one that determines S .) Almost twenty-four years ago, motivated by the puzzle of information in black hole radiation [161], Page proved [162] that typical (with respect to the Haar measure) pure states nearly saturate that bound (the correction is exponentially small) [163–167]. Their reduced density matrices are thermal at infinite temperature [168–170].

In stark contrast with typical pure states, ground states and low-lying excited states of local Hamiltonians are known to exhibit an *area-law* entanglement [158]. Namely, their entanglement entropy scales with the area of the boundary of the subsystem. On the other hand, most eigenstates of local Hamiltonians at nonzero energy densities above the ground state are expected to have a volume-law entanglement entropy (with the exception of many-body localized systems [171, 172]). Within the eigenstate thermalization hypothesis (ETH) [148–150], one expects volume-law entanglement in all eigenstates (excluding those at the edges of the spectrum) of quantum chaotic Hamiltonians [58, 173–176], with those in the center of the spectrum exhibiting maximal entanglement [58].

Thanks to the availability of powerful analytical and computational tools to study ground states, many remarkable results have been obtained for the entanglement entropy of such states [66, 114, 177–180]. On the other hand, for excited states there is a wide gap between what is expected and what has been shown. For interacting Hamiltonians, computational studies are severely limited by finite-size effects so it is difficult to know what happens to the entanglement entropy with increasing the subsystem size. This question was recently addressed for quadratic [181–183] and non-quadratic but integrable [184] Hamiltonians, for which one can study much larger lattices, revealing that randomly generated eigenstates are generally maximally entangled in the limit in

which the size of the subsystem is a vanishing fraction of the size of the system (in short, a vanishing subsystem fraction).

6.1 Translationally invariant spinless quadratic systems

We study the most general quadratic Hamiltonian of spinless fermions

$$\hat{H} = - \sum_{x,y=1}^V (\mathfrak{d}_{xy} \hat{f}_x^\dagger \hat{f}_y^\dagger + \mathfrak{d}_{xy}^* \hat{f}_y \hat{f}_x + \mathfrak{t}_{xy} \hat{f}_x^\dagger \hat{f}_y), \quad (6.1)$$

where $\mathfrak{d}_{xy} = -\mathfrak{d}_{yx}$ and $\mathfrak{t}_{xy} = \mathfrak{t}_{yx}^*$, and \hat{f}_x is the fermionic annihilation operator at site x . A Bogoliubov transformation

$$\hat{f}_x = \sum_{k=1}^V (\alpha_{xk} \hat{\eta}_k + \beta_{xk} \hat{\eta}_k^\dagger) \quad \text{and} \quad \hat{f}_x^\dagger = \sum_{k=1}^V (\alpha_{xk}^* \hat{\eta}_k^\dagger + \beta_{xk}^* \hat{\eta}_k) \quad (6.2)$$

rotates defines quasiparticle number operator $\hat{N}_k = 2\hat{\eta}_k^\dagger \hat{\eta}_k - 1$ that commutes with the Hamiltonian. Hence, the many-body energy eigenkets $|J_\ell\rangle$ satisfy $\hat{N}_k |J_\ell\rangle = N_k |J_\ell\rangle$ with $N_k = \pm 1$, and we adopt the binary representation $\ell = 1 + \sum_{k=1}^V \frac{1+N_k}{2} 2^{k-1}$ (ℓ runs from 1 to $\mathfrak{D} = 2^V$, V is the number of lattice sites).

Correlations of a state $|J\rangle$ are captured by the linear complex structure J , which can be written with respect to the basis $(\hat{f}_x, \hat{f}_x^\dagger)$ as

$$iJ \equiv \begin{pmatrix} \langle J | \hat{f}_x^\dagger \hat{f}_y - \hat{f}_y \hat{f}_x^\dagger | J \rangle & \langle J | \hat{f}_x^\dagger \hat{f}_y^\dagger - \hat{f}_y^\dagger \hat{f}_x^\dagger | J \rangle \\ \langle J | \hat{f}_x \hat{f}_y - \hat{f}_y \hat{f}_x | J \rangle & \langle J | \hat{f}_x \hat{f}_y^\dagger - \hat{f}_y^\dagger \hat{f}_x | J \rangle \end{pmatrix}. \quad (6.3)$$

Since the many-body eigenstates $\{|J_\ell\rangle | 1 \leq \ell \leq 2^V\}$ are Gaussian states, the matrix iJ fully characterizes them [185–187]. Correlations of a subsystem A containing V_A sites are encoded in the restricted complex structure $[iJ]_A$, the $2V_A \times 2V_A$ matrix obtained by restricting the matrix iJ to the entries with $x, y \in A$. The entanglement entropy of subsystem A in the eigenstate $|J\rangle$ can be computed as [185, 186]

$$S = -\text{Tr} \left(\frac{\mathbb{1}_A + [iJ]_A}{2} \right) \log \left(\frac{\mathbb{1}_A + [iJ]_A}{2} \right). \quad (6.4)$$

Expanding (6.4) in powers of $[iJ]_A$, about $[iJ]_A = 0$, allows one to compute the entanglement entropy without calculating the eigenvalues of $[iJ]_A$

$$S_A(|J\rangle) = V_A \log 2 - \sum_{n=1}^{\infty} \frac{\text{Tr}[iJ]_A^{2n}}{4n(2n-1)}. \quad (6.5)$$

Since the restricted complex structure satisfies $[iJ]_A^2 \leq \mathbb{1}$, one has

$$0 \leq \text{Tr}[iJ]_A^{2(m+1)} \leq \text{Tr}[iJ]_A^{2m} \leq 2V_A \quad (6.6)$$

and the series in (6.5) is convergent.

Equation (6.5) allows one to compute the average over the ensemble of all eigenstates $\{|J_\ell\rangle\}$ as

$$\langle S_A \rangle = V_A \log 2 - \sum_{n=1}^{\infty} \frac{\langle \text{Tr}[iJ]_A^{2n} \rangle}{4n(2n-1)}, \quad (6.7)$$

where we define $\langle \mathcal{O} \rangle = \mathfrak{D}^{-1} \sum_{\ell=1}^{\mathfrak{D}} \mathcal{O}(|J_\ell\rangle)$.

6.1.1 Entanglement bounds

A remarkable property of the series in (6.7) is that every higher-order term lowers the average entanglement entropy. After computing all traces $\text{Tr}[\text{i}J]_A^{2n}$ up to order m , we can truncate the sum to get the upper bound

$$S_m^+(V_A) = V_A \log 2 - \sum_{n=1}^m \frac{\langle \text{Tr}[\text{i}J]_A^{2n} \rangle}{4n(2n-1)} \quad (6.8)$$

at this order. Using the inequality in (6.6), namely

$$\text{Tr}[\text{i}J]_A^{2(m+1)} \leq \text{Tr}[\text{i}J]_A^{2m}, \quad (6.9)$$

we can also compute a lower bound by replacing all traces of higher powers by $\text{Tr}[\text{i}J]_A^{2m}$, such that we subtract “too much”, which gives

$$S_m^-(V_A) = V_A \log 2 - \sum_{n=1}^m \frac{\langle \text{Tr}[\text{i}J]_A^{2n} \rangle}{4n(2n-1)} - \langle \text{Tr}[\text{i}J]_A^{2m} \rangle \sum_{n=m+1}^{\infty} \frac{1}{4n(2n-1)}. \quad (6.10)$$

To obtain the first-order lower and upper bounds, $S_1^-(V_A) \leq \langle S_A \rangle \leq S_1^+(V_A)$, we only need to compute $\langle \text{Tr}[\text{i}J]_A^2 \rangle$ since: (i) truncating the series in (6.7) after the first term results in S_1^+ , and (ii) substituting all averages of higher-order traces by $\langle \text{Tr}[\text{i}J]_A^2 \rangle$ results in S_1^- . This gives

$$V_A \log 2 - \frac{\langle \text{Tr}[\text{i}J]_A^2 \rangle}{2} \log 2 \leq \langle S_A \rangle \leq V_A \log 2 - \frac{\langle \text{Tr}[\text{i}J]_A^2 \rangle}{4}. \quad (6.11)$$

For a given eigenstate $|J\rangle$ of our Hamiltonian, $[\text{i}J]_A$ is linear in the quantum numbers N_k and we can write the linear complex structure as

$$\text{i}J \equiv \sum_{k=1}^V N_k \begin{pmatrix} \alpha_{xk}^* \alpha_{yk} - \beta_{xk}^* \beta_{yk} & \left| \begin{array}{c} \alpha_{xk}^* \beta_{yk}^* - \beta_{xk}^* \alpha_{yk}^* \\ \beta_{xk} \beta_{yk}^* - \alpha_{xk} \alpha_{yk}^* \end{array} \right. \end{pmatrix}. \quad (6.12)$$

The average $\langle \text{Tr}[\text{i}J]_A^{2n} \rangle$ can therefore be computed from the binomial correlation function $\langle N_{k_1} \cdots N_{k_{2n}} \rangle$. In particular, to compute $\langle \text{Tr}[\text{i}J]_A^2 \rangle$, we use that $\langle N_{k_1} N_{k_2} \rangle = \delta_{k_1 k_2}$ to get

$$\langle \text{Tr}[\text{i}J]_A^2 \rangle = 2 \sum_{k=1}^V \sum_{x,y \in A} (|\alpha_{xk}^* \alpha_{yk} - \beta_{xk}^* \beta_{yk}|^2 + |\beta_{xk} \alpha_{yk} - \alpha_{xk} \beta_{yk}|^2). \quad (6.13)$$

Whenever $\langle \text{Tr}[\text{i}J]_A^2 \rangle / V_A$ does not vanish in the thermodynamic limit, $\langle S_A \rangle / V_A < \log 2$. This means that the typical entanglement of energy eigenstates differs from Page’s result about the typical entanglement of pure states with respect to the Haar measure. This may surprise at first, but it is a direct consequence that the set of all pure states and the discrete set of energy eigenstates are different statistical ensembles. Of course, the latter is a subset of the former, but there is a priori no reason to assume that it is representative subset.

6.1.2 Universal first order bound

The Bogoliubov coefficients for a translationally invariant system in D dimensions are given by

$$\alpha_{il} = \frac{1}{\sqrt{V}} e^{i\vec{k}_l \cdot \vec{x}_i} u_{\vec{k}_l} \quad \text{and} \quad \beta_{il} = \frac{1}{\sqrt{V}} e^{-i\vec{k}_l \cdot \vec{x}_i} v_{\vec{k}_l} \quad (6.14)$$

with $u_{\vec{k}} = u_{-\vec{k}}$, $v_{\vec{k}} = -v_{-\vec{k}}$, and $|u_{\vec{k}}|^2 + |v_{\vec{k}}|^2 = 1$. Substituting these in (6.13) leads to

$$\langle \text{Tr}[\text{i}J]_A^2 \rangle = \frac{2V_A^2}{V} - \sum_{l=1}^V \sum_{i,j \in A} \frac{8|v_{\vec{k}_l}|^2|u_{\vec{k}_l}|^2 \cos 2\vec{k}_l(\vec{x}_i - \vec{x}_j)}{V^2} \quad (6.15)$$

$$= \frac{2V_A^2}{V} - \sum_{l=1}^V \frac{8|v_{\vec{k}_l}|^2|u_{\vec{k}_l}|^2}{V^2} \prod_{d=1}^D \frac{\sin^2((L_A)_d(k_l)_d)}{\sin^2((k_l)_d)}, \quad (6.16)$$

where the space sum runs within an D -dimensional hypercube A with side lengths $(L_A)_d$ containing $V_A = \prod_{d=1}^D L_A^d$ sites. One can bound $\langle \text{Tr}[\text{i}J]_A^2 \rangle$ from below using $|u_{\vec{k}_l}|^2|v_{\vec{k}_l}|^2 \leq 1/4$ which follows from $|u_{\vec{k}_l}|^2 + |v_{\vec{k}_l}|^2 = 1$. As $V \rightarrow \infty$, one can substitute $\sum_l \rightarrow \frac{V}{(2\pi)^D} (\int_{-\pi}^{\pi} dk)^D$. Since $\int_{-\pi}^{\pi} dk \sin^2(L_d k) / \sin^2(k) = 2\pi L_d$, we find the inequality $\langle \text{Tr}[\text{i}J]_A^2 \rangle \geq 2V_A^2/V - 2V_A/V$. In the thermodynamic limit, we get that $\langle \text{Tr}[\text{i}J]_A^2 \rangle = 2V_A^2/V$. The resulting first order bounds are given by

$$\begin{aligned} S_1^+(V_A) &= V_A \log 2 - \frac{1}{2} \frac{V_A^2}{V} = \log \mathfrak{D}_A - \frac{1}{2 \log 2} \frac{(\log \mathfrak{D}_A)^2}{\log \mathfrak{D}}, \\ S_1^-(V_A) &= V_A \log 2 \left(1 - \frac{V_A}{V} \right) = \log \mathfrak{D}_A - \frac{(\log \mathfrak{D}_A)^2}{\log \mathfrak{D}}. \end{aligned} \quad (6.17)$$

and they are *universal* for all translational invariant spinless quadratic systems. Note that (i) S_1^+ and S_1^- fulfill a volume law as they are proportional to V_A , and (ii) for any nonvanishing subsystem fraction, $\lim_{V \rightarrow \infty} V_A/V \neq 0$, $S_1^+ < V_A \log 2$ in the thermodynamic limit, *i.e.*, the average departs from the result for typical states in the Hilbert space. If the subsystem fraction vanishes in the thermodynamic limit, $\lim_{V \rightarrow \infty} V_A/V = 0$, the lower and the upper bounds coincide and $\lim_{V_A/V \rightarrow 0} S_1^- = \lim_{V_A/V \rightarrow 0} S_1^+ = V_A \log 2$. In this limit, the average entanglement entropy is maximal, *i.e.*, typical eigenstates of the Hamiltonian have a typical (*à la* Page [162]) entanglement entropy.

6.2 XY model and transverse field Ising model

While the previous example considered the full class of translationally invariant models, let us now focus onto an important class of spin models that can be mapped to quadratic fermionic Hamiltonians, for which our methods can be used. We therefore consider the XY spin model [188] in one dimension with L sites arranged in circle, such that site $L+1$ is identified with site 1. For simplicity, we will assume that L is an even integer. The Hamiltonian is given by

$$\hat{H}_{\text{XY}} = -\mathfrak{J} \sum_{x=1}^L \left((1+\gamma) \hat{S}_x^X \hat{S}_{x+1}^X + (1-\gamma) \hat{S}_x^Y \hat{S}_{x+1}^Y \right) - \mathfrak{h} \sum_{x=1}^L \hat{S}_x^Z, \quad (6.18)$$

where \hat{S}_x^X , \hat{S}_x^Y and \hat{S}_x^Z are the well-known spin operators. This model can be solved by combining a Jordan-Wigner and Fourier transformation:

1. We can express the spin operators \hat{S}_x^X and \hat{S}_x^Y in terms of ladder operators $\hat{S}_x^\pm = \hat{S}_x^X \pm i\hat{S}_x^Y$.
2. We can then perform a Jordan-Wigner transformation by expressing all spin operators in

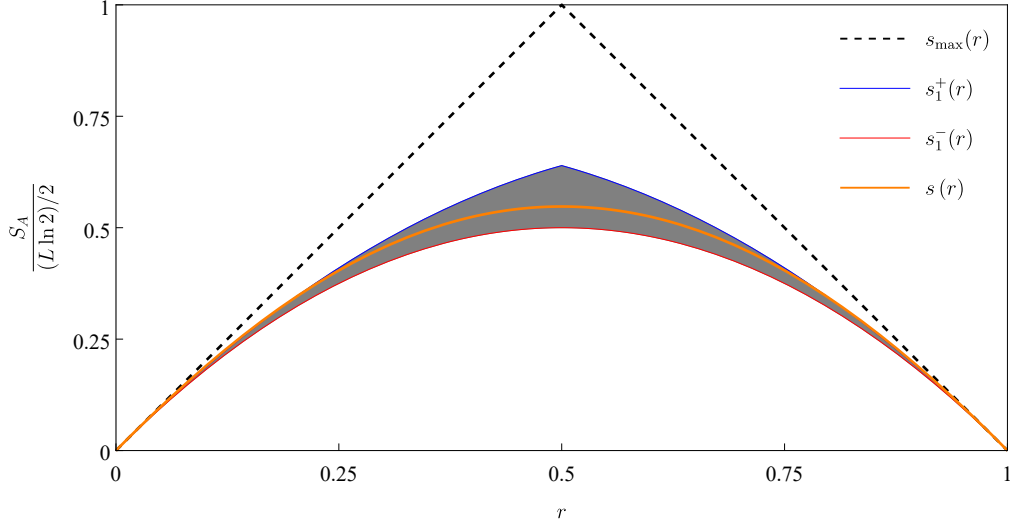


Figure 6.1: Universal first order bound. We show the universal first order bound (gray area) between $s_1^+(r)$ and $s_1^-(r)$ where $r = V_A/V$. We also show the expected universal thermodynamic limit $s(r)$ as conjectured in section 6.3 which we compute numerically for 36 sites for the XX model discussed in section 6.4.

terms of fermionic creation and annihilation operators \hat{f}_x^\dagger and \hat{f}_x , namely

$$\hat{S}_x^+ = \hat{f}_x^\dagger \exp \left(-i\pi \sum_{y=1}^{x-1} \hat{f}_y^\dagger \hat{f}_y \right), \quad \hat{S}_x^- = \exp \left(-i\pi \sum_{y=1}^{x-1} \hat{f}_y^\dagger \hat{f}_y \right) \hat{f}_x \quad \text{and} \quad \hat{S}_x^Z = \hat{f}_x^\dagger \hat{f}_x - \frac{1}{2}. \quad (6.19)$$

This transformation does not only provide an isomorphism between operators, but it also preserves bipartite entanglement, *i.e.*, the entanglement entropy associated to a region consisting of adjacent sites x is the same regardless if we use the tensor product structure induced by the spin operators or the fermionic creation and annihilation operators. This is quite remarkable because the Jordan-Wigner transformation is non-local, but it is well-understood how this is made possible by the fact that \hat{S}_x^\pm only depends on creation and annihilation operators \hat{f}_y^\dagger and \hat{f}_y in the range $1 \leq y \leq x$.

3. The Hamiltonian expressed in terms of the new variables is given by

$$\hat{H}_{\text{XY}} = \frac{\mathfrak{J}}{2} \sum_{x=1}^L \left[\hat{f}_x^\dagger (\hat{f}_{x+1} + \gamma \hat{f}_{x+1}^\dagger) + \text{h.c.} \right] - \mathfrak{H} \hat{f}_x^\dagger \hat{f}_x - \frac{\mathfrak{J}}{2} [\hat{f}_1^\dagger (\hat{f}_L + \gamma \hat{f}_L^\dagger) + \text{h.c.}] (\hat{P} + 1), \quad (6.20)$$

where $\hat{P} = e^{i\pi\hat{\mathcal{N}}}$ is the parity operator with $\hat{\mathcal{N}} = \sum_{x=1}^L \hat{f}_x^\dagger \hat{f}_x$. The last term is a boundary term. For $\gamma = 0$ we have $[\hat{H}_{\text{XY}}, \hat{\mathcal{N}}] = 0$ and we can diagonalize the system using Fourier transforms. In fact, this implies that for $\gamma = 0$ the eigenstates remain unchanged if we drop this boundary term, leading to the simpler Hamiltonian $\hat{H}_{\text{NI}} = \frac{1}{2} \sum_{x=1}^L (\hat{f}_x^\dagger \hat{f}_{x+1} + \text{h.c.})$ of non-interacting fermions studied in [LH12, LH14]. For $\gamma \neq 0$, an additional transformation allows us to write the Hamiltonian as the sum of two quadratic terms acting on different sectors of the Hilbert space.

4. Because of the operator \hat{P} in (6.20), the Hamiltonian is not quadratic in \hat{f}_x^\dagger and \hat{f}_x . The non-quadratic term containing \hat{P} distinguishes the sectors of even and odd eigenvalues of the number operator $\hat{\mathcal{N}}$. The Hilbert space can be decomposed as direct sum $\mathcal{H} = \mathcal{H}^+ \oplus \mathcal{H}^-$ where \mathcal{H}^+ and \mathcal{H}^- are the eigenspaces of the number parity operator $\hat{P} = e^{i\pi\hat{\mathcal{N}}}$ with eigenvalues ± 1 . The projectors onto these eigenspaces are given by

$$\hat{\mathcal{P}}^\pm = \frac{1}{2}(\mathbb{1} \pm \hat{P}). \quad (6.21)$$

We can diagonalize \hat{H}_{XY} over \mathcal{H}^\pm individually by applying the Fourier transformations

$$\hat{f}_\kappa = \frac{1}{\sqrt{L}} \sum_{x=1}^L e^{i\kappa x} \hat{f}_x \quad \text{and} \quad \hat{f}_\kappa^\dagger = \frac{1}{\sqrt{L}} \sum_{x=1}^L e^{-i\kappa x} \hat{f}_x^\dagger. \quad (6.22)$$

We can write the Hilbert space $\mathcal{H} = \mathcal{H}^+ \oplus \mathcal{H}^-$ as direct sum of \mathcal{H}^+ and \mathcal{H}^- , which are the eigenspaces of the number parity operator $\hat{P} = e^{i\pi\hat{\mathcal{N}}}$ with eigenvalues ± 1 . We can write down projectors onto these eigenspaces given by

$$\hat{\mathcal{P}}^\pm = \frac{1}{2}(\mathbb{1} \pm \hat{P}) \quad (6.23)$$

and diagonalize \hat{H}_{XY} over each eigenspace individually. Of course, this is only possible because we have $[\hat{H}_{XY}, \hat{P}] = 0$. The resulting Hamiltonian is given by

$$\hat{H}_{XY} = \hat{H}_{XY}^+ \hat{\mathcal{P}}^+ + \hat{H}_{XY}^- \hat{\mathcal{P}}^-. \quad (6.24)$$

Here, the Hamiltonians \hat{H}_{XY}^\pm are now quadratic and explicitly given by

$$\hat{H}_{XY}^+ = \sum_{\kappa \in \mathcal{K}^+ > 0} \left[a_\kappa \left(\hat{f}_\kappa^\dagger \hat{f}_\kappa + \hat{f}_{-\kappa}^\dagger \hat{f}_{-\kappa} - 1 \right) - b_\kappa \left(i\hat{f}_\kappa^\dagger \hat{f}_{-\kappa}^\dagger - i\hat{f}_{-\kappa} \hat{f}_\kappa \right) \right] \quad (6.25)$$

$$\hat{H}_{XY}^- = \sum_{\kappa \in \mathcal{K}^- > 0} \left[a_\kappa \left(\hat{f}_\kappa^\dagger \hat{f}_\kappa + \hat{f}_{-\kappa}^\dagger \hat{f}_{-\kappa} - 1 \right) - b_\kappa \left(i\hat{f}_\kappa^\dagger \hat{f}_{-\kappa}^\dagger - i\hat{f}_{-\kappa} \hat{f}_\kappa \right) \right] \quad (6.26)$$

$$- (\mathfrak{J} + \mathfrak{H}) \hat{f}_0^\dagger \hat{f}_0 + (\mathfrak{J} - \mathfrak{H}) \hat{f}_{-\pi}^\dagger \hat{f}_{-\pi} + \mathfrak{H}, \quad (6.27)$$

where we used different sets \mathcal{K}^\pm defined as

$$\mathcal{K}^+ = \left\{ \frac{\pi}{L} + \frac{2\pi k}{L} \middle| k = -\frac{L}{2}, -\frac{L}{2} + 1, \dots, \frac{L}{2} - 1 \right\}, \quad (6.28)$$

$$\mathcal{K}^- = \left\{ \frac{2\pi k}{L} \middle| k = -\frac{L}{2}, -\frac{L}{2} + 1, \dots, \frac{L}{2} - 1 \right\}. \quad (6.29)$$

The other variables are given by

$$\begin{aligned} \epsilon_\kappa &= \sqrt{\mathfrak{H}^2 + 2\mathfrak{H}\mathfrak{J} \cos(\kappa) + \mathfrak{J}^2 + (\gamma^2 - 1)\mathfrak{J}^2 \sin(\kappa)^2} \\ a_\kappa &= -\mathfrak{J} \cos(\kappa) - \mathfrak{H}, \quad b_\kappa = \gamma \mathfrak{J} \sin(\kappa), \\ u_\kappa &= \frac{\epsilon_\kappa + a_\kappa}{\sqrt{2\epsilon_\kappa(\epsilon_\kappa + a_\kappa)}}, \quad v_\kappa = \frac{ib_\kappa}{\sqrt{2\epsilon_\kappa(\epsilon_\kappa + a_\kappa)}}. \end{aligned} \quad (6.30)$$

5. At this point, we only need to perform a single fermionic two-mode squeezing transformation mixing the mode pair $(\kappa, -\kappa)$ given by

$$\hat{\eta}_\kappa = u_\kappa \hat{f}_\kappa - v_\kappa^* \hat{f}_{-\kappa}^\dagger. \quad (6.31)$$

We need to treat the cases $\kappa \in \{0, \pi\}$ individually, for which the Hamiltonian is already diagonal, so that we can take

$$\hat{\eta}_0 = \hat{f}_0^\dagger \quad \text{and} \quad \hat{\eta}_\pi = \hat{f}_{-\pi}^\dagger. \quad (6.32)$$

This case can be consistently treated with equation (6.31) by defining the special coefficients

$$u_0 = u_{-\pi} = 0 \quad \text{and} \quad v_0 = v_{-\pi} = 1. \quad (6.33)$$

After performing the last transformation, we finally managed to diagonalize the quadratic Hamiltonians that are now given by

$$\hat{H}_{XY}^+ = \sum_{\kappa \in \mathcal{K}^+ > 0} \epsilon_\kappa \left(\hat{\eta}_\kappa^\dagger \hat{\eta}_\kappa + \hat{\eta}_{-\kappa}^\dagger \hat{\eta}_{-\kappa} - 1 \right), \quad (6.34)$$

$$\hat{H}_{XY}^- = \sum_{\kappa \in \mathcal{K}^- > 0} \epsilon_\kappa \left(\hat{\eta}_\kappa^\dagger \hat{\eta}_\kappa + \hat{\eta}_{-\kappa}^\dagger \hat{\eta}_{-\kappa} - 1 \right) + (\mathfrak{H} + \mathfrak{J}) \hat{\eta}_0^\dagger \hat{\eta}_0 + (\mathfrak{H} - \mathfrak{J}) \hat{\eta}_\pi^\dagger \hat{\eta}_\pi - \mathfrak{H}. \quad (6.35)$$

With this in hand, we can analyze the entanglement structure of eigenstates. The relevant information is fully contained in the transformation from the (local) fermionic operators $(\hat{f}_x, \hat{f}_x^\dagger)$ to the (non-local) operators $(\hat{\eta}_\kappa, \hat{\eta}_\kappa^\dagger)$.

6.2.1 First order bound

We were able to rewrite the XY model, such that it consists of two quadratic fermionic Hamiltonians over direct summands of the fermionic Hilbert space. Therefore, the overall Hamiltonian is almost quadratic, but not quite. In essence, we have two distinct notions of particle excitations described by \hat{H}_{XY}^+ and \hat{H}_{XY}^- depending on the number of excitations we have, *i.e.*, for an even number of excitations we need to use \hat{H}_{XY}^+ and for an odd number of excitations we use \hat{H}_{XY}^- . In particular, the ground state characterized by zero quasiparticle excitations is given by the ground state of \hat{H}_{XY}^+ , while the ground state of \hat{H}_{XY}^- is not an energy eigenstate of the system.

The XY model was translationally invariant to start with, so we might be tempted to apply directly the universal first order bound derived in section 6.1.2. However, due to the fact that the system is just almost quadratic, we need to be more careful here.

Let us write down the linear complex structure of state $|J\rangle$ in the even or odd sector given by

$$iJ = \frac{1}{L} \sum_{\kappa \in \mathcal{K}^\pm} N_\kappa \begin{pmatrix} |u_\kappa|^2 e^{i\kappa(x-y)} - |v_\kappa|^2 e^{i\kappa(y-x)} \\ u_\kappa^* v_\kappa^* (e^{i\kappa(y-x)} - e^{i\kappa(x-y)}) \end{pmatrix}, \quad (6.36)$$

where we choose the set \mathcal{K}^\pm depending on if we have an even or odd number of excitations in the state. If we are interested in taking the average over all eigenstates, we need to treat the even and the odd case independently and then average the two results weighted by the total number of even and odd states. It is easy to verify that the number of states with odd excitations is equal to the

number of even excitation.¹ For the first order bound, we are interested in the averages $\langle \text{Tr}[\text{i}J]_A^2 \rangle_{\pm}$ in the individual sectors separately, where we either take an even number of excitations (+) or odd number of excitations (-). In order to compute the average in each sector, we can apply the same technique as section 6.1.1 based on the averages $\langle N_{\kappa_1} \cdots N_{\kappa_n} \rangle_{\pm}$. We can check explicitly that for $n < L$, the correlation functions are unchanged and still given by

$$\begin{aligned}\langle N_{\kappa} \rangle_{\pm} &= 0, \quad \langle N_{\kappa_1} N_{\kappa_2} \rangle_{\pm} = \delta_{\kappa_1 \kappa_2}, \\ \langle N_{\kappa_1} \cdots N_{\kappa_n} \rangle_{\pm} &= \begin{cases} 1 & \text{each } \kappa_i \text{ appears with even multiplicity} \\ 0 & \text{else} \end{cases},\end{aligned}\tag{6.37}$$

while the correlation functions at highest order becomes modified.² With this in hand, we can compute

$$\begin{aligned}\langle \text{Tr}[\text{i}J]_A^2 \rangle_{\pm} &= \frac{1}{L^2} \sum_{\kappa \in \mathcal{K}^{\pm}} \sum_{x,y=1}^{L_A} \\ \text{Tr} \left(\frac{(|u_{\kappa}|^2 + |v_{\kappa}|^2)^2 - 4|u_{\kappa}|^2|v_{\kappa}|^2 \cos 2\kappa(x-y)}{2u_{\kappa}v_{\kappa}(e^{-2i\kappa x} - e^{-2i\kappa y})(|u_{\kappa}|^2e^{2i\kappa y} - |v_{\kappa}|^2e^{2i\kappa x})} \middle| \frac{2u_{\kappa}^*v_{\kappa}^*(e^{-2i\kappa y} - e^{-2i\kappa x})(|u_{\kappa}|^2e^{2i\kappa x} - |v_{\kappa}|^2e^{2i\kappa y})}{(|u_{\kappa}|^2 + |v_{\kappa}|^2)^2 - 4|u_{\kappa}|^2|v_{\kappa}|^2 \cos 2\kappa(x-y)} \right) .\end{aligned}\tag{6.38}$$

$$= 2 \frac{L_A^2}{L^2} - \frac{2}{L^2} \sum_{x,y=1}^{L_A} \sum_{\kappa \in \mathcal{K}^{\pm}} 4|u_{\kappa}|^2|v_{\kappa}|^2 \cos 2\kappa(x-y).\tag{6.39}$$

Therefore, taking the average of the contributions of each sector is equivalent to just summing over all $\kappa \in \mathcal{K}^+ \cup \mathcal{K}^-$, but dividing by 2. Thus, we find

$$\langle \text{Tr}[\text{i}J]_A^2 \rangle = \frac{1}{2} (\langle \text{Tr}[\text{i}J]_A^2 \rangle_+ + \langle \text{Tr}[\text{i}J]_A^2 \rangle_-)\tag{6.40}$$

$$= 2 \frac{L_A^2}{L^2} - \frac{1}{L^2} \sum_{x,y=1}^{L_A} \sum_{k=1-L}^{L-1} 4|u_{\pi k/L}|^2|v_{\pi k/L}|^2 \cos \left(\frac{2\pi k(x-y)}{L} \right),\tag{6.41}$$

where we started the sum at $k = 1 - L$ because $u_{-\pi} = 0$ for $k = -L$. Using (6.11), we can compute the first order bound numerically. Next, we will be interested in the thermodynamic limit of this quantity.

In order to understand the thermodynamic limit of $\langle \text{Tr}[\text{i}J]_A^2 \rangle$, we will focus on the non-trivial quantity given by

$$Z(L_A, L) = 2 \frac{L_A^2}{L} - \langle \text{Tr}[\text{i}J]_A^2 \rangle = \frac{1}{L^2} \sum_{k=1-L}^{L-1} z(\pi k/L),\tag{6.42}$$

¹Consider $0 = (1 - 1)^L = \sum_{l=0}^L \binom{L}{l} (-1)^l (1)^{L-l}$. Here, l represents the number of excitations correctly weighted by the binomial coefficient. The positive terms represent the even sectors (even l) and the negative ones the odd sector (odd l). Clearly, both terms cancel each other, *i.e.*, the even and odd sector both have Hilbert space dimension 2^{L-1} .

²For instance, the binomial expectation value $\langle N_{\kappa_1} N_{\kappa_2} \cdots N_{\kappa_L} \rangle = 0$, while the expectation value over even states is given by $\langle N_{\kappa_1} N_{\kappa_2} \cdots N_{\kappa_L} \rangle_+ = (-1)^L$.

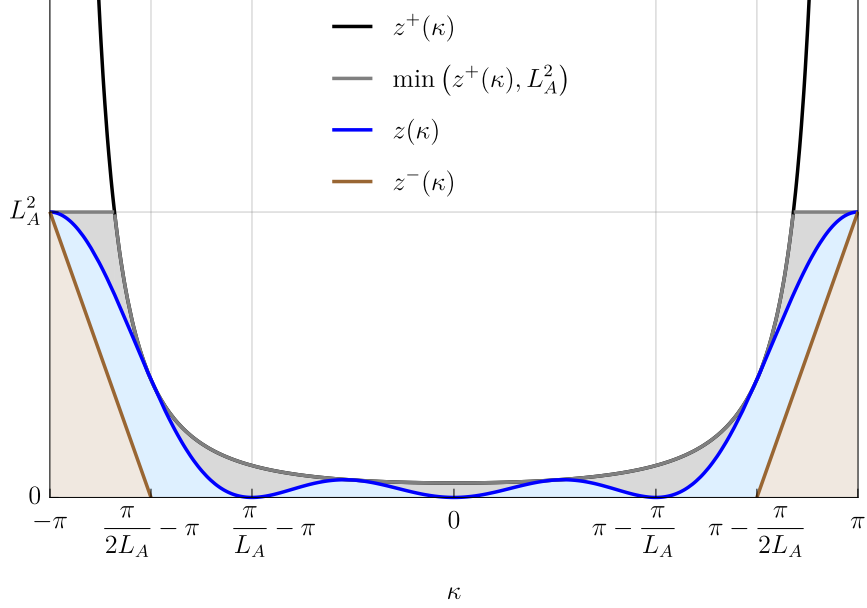


Figure 6.2: Finite size correction to first order bound for XY model. We sketch the function $z(\kappa)$ and its bounds $z^\pm(\kappa)$ for $\gamma = .9$, $\mathfrak{H} = \mathfrak{J}$, $L_A = 2$ and $L = 4$. We have the inequality $z^-(\kappa) \leq z(\kappa) \leq \min(L_A^2, z^+(\kappa)) \leq z^+(\kappa)$. The integrals over $z^-(\kappa)$ and $\min(L_A^2, z^+(\kappa))$ corresponding to the shaded surfaces in brown and gray, respectively, both scale as L_A , which implies that the same scaling applies to $Z(L_A, L) \sim \frac{1}{\pi L} \int_{-\pi}^{\pi} d\kappa z(\kappa) \sim \mathcal{O}(L_A)$.

where we defined a function z , in which we can perform the sum over x and y ,

$$z(\kappa) = \sum_{x,y=1}^{L_A} 4 |u_\kappa|^2 |v_\kappa|^2 \cos(2(x-y)\kappa) \quad (6.43)$$

$$= \sum_{x,y=1}^{L_A} \frac{\gamma^2 \mathfrak{J}^2 \sin^2(\kappa) \cos(2(x-y)\kappa)}{\mathfrak{H}^2 + 2\mathfrak{H}\mathfrak{J} \cos(\kappa) + (\gamma^2 - 1) \mathfrak{J}^2 \sin^2(\kappa) + \mathfrak{J}^2} \quad (6.44)$$

$$= \frac{\gamma^2 \mathfrak{J}^2 \sin^2(L_A \kappa)}{\mathfrak{H}^2 + 2\mathfrak{H}\mathfrak{J} \cos(\kappa) + (\gamma^2 - 1) \mathfrak{J}^2 \sin^2(\kappa) + \mathfrak{J}^2}. \quad (6.45)$$

We note immediately that for $\gamma = 0$, we have $Z = z = 0$ reproducing the result for the XX model. For general parameter choices, the correction Z is given by

$$Z(L_A, L) = \frac{1}{L^2} \sum_{k=1-L}^{L-1} \frac{\gamma^2 \mathfrak{J}^2 \sin^2(\pi k L_A / L)}{\mathfrak{H}^2 + 2\mathfrak{H}\mathfrak{J} \cos(\pi k / L) + (\gamma^2 - 1) \mathfrak{J}^2 \sin^2(\pi k / L) + \mathfrak{J}^2}, \quad (6.46)$$

In order to bound the scaling of Z as $L \rightarrow \infty$ for fixed $r = L_A/L$, we need to distinguish two cases:

- **Critical at $\mathfrak{H} = \mathfrak{J}$ and $\gamma > 0$**

We first consider the simplest case with $\gamma = 1$, for which we can perform the sum analytically

$$Z(L_A, L) = \frac{1}{L^2} \sum_{k=1-L}^{L-1} \frac{\sin^2(\pi k L_A / L)}{2 + 2 \cos(\pi k / L)} \quad (6.47)$$

$$= \frac{L_A}{L} - \left(\frac{L_A}{L} \right)^2, \quad (6.48)$$

where we used the fact that L_A is an integer to simplify the summation. Clearly, this is a finite value, such that the overall correction will scale as $\frac{1}{L}$ in the thermodynamic limit, once we consider $\lim_{L \rightarrow \infty} \langle \text{Tr}[iJ]^2 \rangle / L$.

For $0 < \gamma < 1$, we cannot do the sum analytically, but we can estimate the scaling of the correction. Clearly, replacing $\sin^2(\kappa L_A) \leq 1$ leads to an upper bound

$$z(\kappa) \leq z^+(\kappa) = \frac{\gamma^2}{2 + 2 \cos(\kappa) + (\gamma^2 - 1) \sin^2(\kappa) + \mathfrak{J}^2}, \quad (6.49)$$

that diverges at $\kappa = \pm\pi$. However, the function $z(\kappa)$ does not diverge, but it reaches its maximum

$$z(\pm\pi) = L_A^2, \quad (6.50)$$

where we used L'Hospital's rule twice. We can show that $\lim_{L \rightarrow \infty} Z(L_A, L)$ for fixed $r = L_A/L$ reaches a finite value. We can approximate $\sum_k \rightarrow \frac{L}{2\pi} \int_{-\pi}^{\pi} d\kappa$ and use the asymptotics

$$\frac{1}{L^2} \sum_{k=1-L}^{L-1} z(\pi k/L) \sim \frac{1}{\pi L} \underbrace{\int_{-\pi}^{\pi} d\kappa z(\kappa)}_{\sim \mathcal{O}(L_A)} \sim \mathcal{O}\left(\frac{L_A}{L}\right). \quad (6.51)$$

The function $z(\kappa)$ is shown in figure 6.2 and we can prove that the integral scales as L_A . The scaling can be studied analytically by bounding $z(\kappa)$ from below by the triangle function

$$z^-(\kappa) = \begin{cases} L_A^2 - 2L_A^3(1 - |\kappa|/\pi) & \pi\left(1 - \frac{1}{2L_A}\right) \leq |\kappa| \leq \pi \\ 0 & \text{else} \end{cases} \quad (6.52)$$

and from above either by either the maximum value L_A^2 or the asymptotic expansion $z^+(\kappa) = \frac{1}{(\pi - |\kappa|)^2}$ as $|\kappa| \rightarrow \pi$. Therefore, we were able to prove the overall scaling to be given by

$$\lim_{L \rightarrow \infty} \frac{Z(L_A, L)}{L} \sim \frac{1}{L} \mathcal{O}(L_A/L), \quad (6.53)$$

which means that the finite size correction is of order $1/L$.

- **Not critical at $\mathfrak{H} \neq \mathfrak{J}$**

In this case, we can bound the function $z(\kappa)$ by replacing $\sin^2(\kappa L_A) \leq 1$ leading to

$$z(\kappa) \leq z^+(\kappa) = \frac{\gamma^2 \mathfrak{J}^2}{\mathfrak{H}^2 + 2\mathfrak{H}\mathfrak{J} \cos(\kappa) + (\gamma^2 - 1) \mathfrak{J}^2 \sin^2(\kappa) + \mathfrak{J}^2}, \quad (6.54)$$

which would not be a meaningful bound for $\mathfrak{H} = \mathfrak{J}$ because $z^+(\kappa)$ would diverge for $\kappa \rightarrow \pm\pi$. If the system is not critical though, we find that $z^+(\kappa)$ takes its maximal values at $\kappa = \pm\pi$ given by

$$z^+(\pm\pi) = \frac{\gamma^2 \mathfrak{J}^2}{(\mathfrak{H} - \mathfrak{J})^2}. \quad (6.55)$$

Therefore, we can bound the sum by the integral leading to the inequality

$$Z(L_A, L) \leq \frac{1}{L} \int_{-\pi}^{\pi} z^+(\kappa) d\kappa \leq \frac{1}{L} \frac{2\pi \gamma^2 \mathfrak{J}^2}{(\mathfrak{H} - \mathfrak{J})^2} \quad (6.56)$$

After taking the thermodynamic limit $\lim_{L \rightarrow \infty} \langle \text{Tr}[iJ]^2 \rangle / L$, the overall scaling will be at most given by

$$\lim_{L \rightarrow \infty} \frac{Z(L_A, L)}{L} \sim \frac{1}{L^2} \mathcal{O}(L_A/L), \quad (6.57)$$

In summary, the first order bound approaches our universal first order bound for translationally invariant systems in the thermodynamic limit. Furthermore, we could show that the way this universal bounds is approached depends on the values \mathfrak{H} and \mathfrak{J} . At criticality, we find a $1/L$ -scaling, while for non-critical value the scaling is given at most by $1/L^2$.

6.2.2 Average entanglement entropy

We found that the first order bound approaches a universal function independent from the parameters of the XY model. Moreover, we saw that the finite size correction to this universal function depends on the parameters and in particular, the correction is of order $1/L$ if and only if $\mathfrak{H} = \mathfrak{J}$, while it is of order $1/L^2$ otherwise. The fact that the correction shows this singular behavior only for the critical regime $\mathfrak{H} = \mathfrak{J}$ indicates that we can learn about criticality of quadratic models in terms of entanglement properties of the full spectrum of eigenstates.

In order to understand this aspect better, we can study the entanglement entropy averaged over all eigenstates. Doing this analytically would require the calculations of all bounds up to arbitrary order which is not feasible. Instead, we approach this question numerically by computing the average over all eigenstates for finite system sizes. We are therefore limited to discrete parameter and subsystem choices. More concretely, we restrict ourselves to the transverse field Ising model (TFI) given by the subsector of XY with $\gamma = 1$. Furthermore, we only consider the subsystem fractions $r = L_A/L = 1/2$ and $r = L_A/L = 1/4$.

The numerical results are shown in figure 6.3. The data shows a behavior that is similar to what we saw analytically for the first order bound:

- **Critical at $\mathfrak{H} = \mathfrak{J}$ and $\gamma = 1$**

We find a leading order correction that scales as $1/L$ for $L \rightarrow \infty$. This reproduces exactly the behavior that we found for the first order bound. Moreover, we see that the finite size corrections in the even and odd sector are different, but both have the characteristic $1/L$ leading order scaling.

- **Critical at $\mathfrak{H} \neq \mathfrak{J}$ and $\gamma = 1$**

In contrast to the critical case, the finite size correction approaches zero much more rapidly with a leading order scaling of $1/L^2$. Again, this agrees with the behavior found for the first order bound. Furthermore, for $r = 1/4$ the even and odd sector show a very similar behavior which might indicate that the difference between even and odd sector vanishes quickly for $\mathfrak{H} \neq \mathfrak{J}$ and small r . This is a feature that we have not considered for the first order bound, because we found compact expressions directly for the full average.

In summary, we found numerical evidence that the average entanglement entropy of XY model shows the same features as the first order bound, at least within the sector of $\gamma = 1$. First, the average entanglement entropy appears to approach a universal function of the subsystem fraction r which is independent from the model parameters. Second, the scaling of the finite size correction to this universal value depends on whether we are at criticality with $\mathfrak{H} = \mathfrak{J}$ or now, namely we find an $1/L$ correction $\mathfrak{H} = \mathfrak{J}$ and $1/L^2$ otherwise.

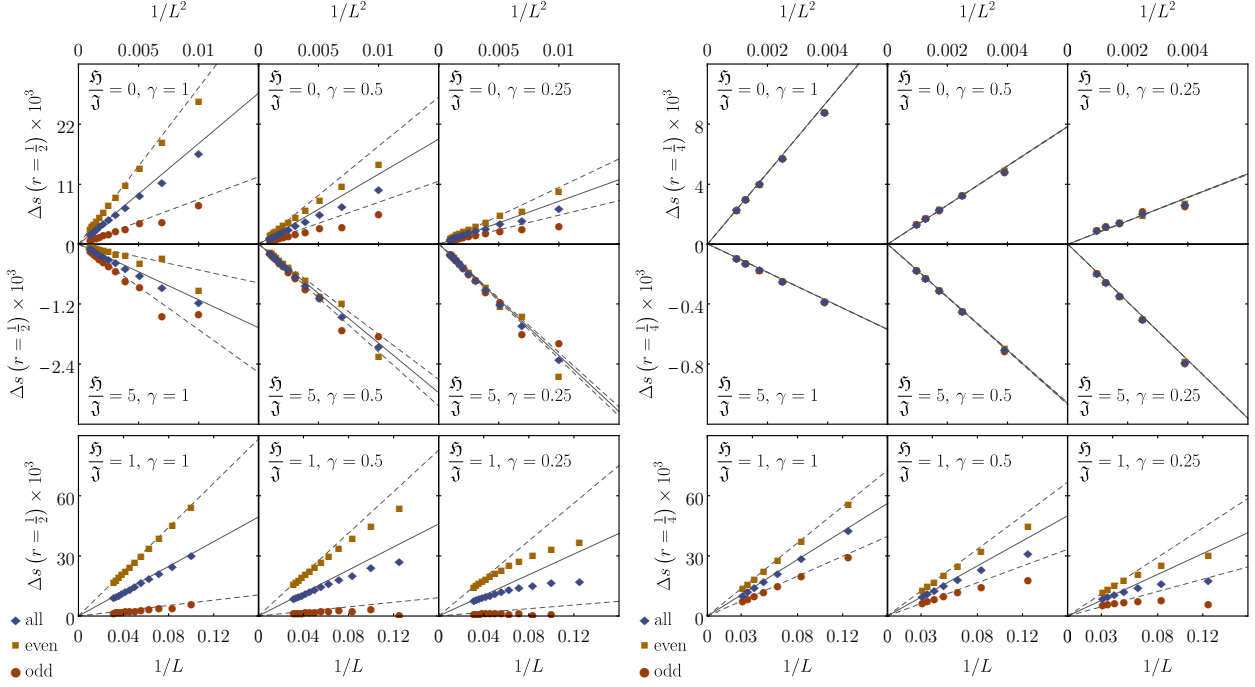


Figure 6.3: Average entanglement entropy for XY model. We compute the average entanglement entropy in the XY model for $\gamma \in \{0.25, .5, 1\}$ and $\frac{\mathfrak{H}}{\mathfrak{J}} \in \{0, 1, 5\}$. We show the difference $\Delta s(r) = \frac{2r}{\log 2} (\langle S_A \rangle / L - s(r))$ between the finite size average and the extrapolated limit $s(r)$ with $s(1/2) = 0.1863(9)$ and $s(1/4) = 0.1375(8)$ for free fermions (Hamiltonian with $\gamma = 0$). In each panel, we also show the average over the even and odd sectors separately (dashed lines) beside the full average (gray lines).

6.3 Conjecture about universality

In the previous section, we found a remarkable property of the XY model, namely that independent from its system parameters \mathfrak{H} , \mathfrak{J} and γ , the average entanglement entropy as a function of the subsystem size converged to the same value. We discussed some subtleties specific to the XY model and in particular, we found that the way this limit is approached differs depending on if we chose critical values for our system parameters. However, what we want to explore further is the class of systems, for which the average entanglement entropy approaches the same value in thermodynamic limit. Clearly, this class cannot be given by all quadratic systems, because we can always build ultra-local Hamiltonians of the form

$$\hat{H} = \frac{1}{2} \sum_{x=1}^L \epsilon(x) \hat{f}_x^\dagger \hat{f}_x + E_0 , \quad (6.58)$$

for which every single eigenstate has zero entanglement entropy. A natural class of systems consists of translationally invariant quadratic systems.

We consider the most general translationally invariant model on a one dimensional lattice with periodic boundary condition, which can be generalized to higher dimensions in a straight-forward way. In terms of creation and annihilation operators, the most general translationally invariant

quadratic model in one dimension is given by

$$\hat{H} = - \sum_{x=1}^L \sum_{y=1}^L \left(\mathfrak{d}_y \hat{f}_x^\dagger \hat{f}_{x+y}^\dagger + \mathfrak{d}_y^* \hat{f}_x \hat{f}_{x+y} + \mathfrak{t}_y \hat{f}_x^\dagger \hat{f}_{x+y} + \mathfrak{t}_y^* \hat{f}_{x+y}^\dagger \hat{f}_x \right), \quad (6.59)$$

where we assume that $x, y \in \mathbb{Z}_L$, *i.e.*, $x + L \equiv x$. The Hamiltonian can be diagonalized by first applying a Fourier transform and then performing a two mode squeezing. Explicitly, we define

$$\hat{c}_\kappa = \frac{1}{\sqrt{L}} \sum_{\kappa \in \mathcal{K}} e^{i\kappa x} \hat{f}_x \quad \text{and} \quad \hat{c}_\kappa^\dagger = \frac{1}{\sqrt{L}} \sum_{\kappa \in \mathcal{K}} e^{-i\kappa x} \hat{f}_x^\dagger, \quad (6.60)$$

with $\mathcal{K} = \left\{ \frac{2\pi k}{L} \mid k \in \mathbb{Z}, -\frac{L}{2} \leq k < \frac{L}{2} \right\}$ giving rise to the transformed Hamiltonian

$$\begin{aligned} \hat{H} &= - \sum_{\kappa \in \mathcal{K}} \left(\tilde{\Delta}_\kappa \hat{c}_\kappa^\dagger \hat{c}_{-\kappa}^\dagger + \tilde{\Delta}_\kappa^* \hat{c}_\kappa \hat{c}_{-\kappa} + (\tilde{t}_\kappa + \tilde{t}_\kappa^*) \hat{c}_\kappa^\dagger \hat{c}_\kappa \right) \\ \text{with } \tilde{\mathfrak{d}}_\kappa &= \sum_{\kappa \in \mathcal{K}} e^{i\kappa y} \mathfrak{d}_y \quad \text{and} \quad \tilde{\mathfrak{t}}_\kappa = \sum_{\kappa \in \mathcal{K}} e^{-i\kappa y} \mathfrak{t}_y. \end{aligned} \quad (6.61)$$

For the two mode squeezing we can determine the parameters u_κ and v_κ , such that using $\hat{\eta}_\kappa = u_\kappa \hat{c}_\kappa - v_\kappa^* \hat{c}_{-\kappa}^\dagger$ leads to the quadratic Hamiltonian

$$\hat{H} = \sum_{\kappa \in \mathcal{K}} \epsilon_\kappa \hat{\eta}_\kappa^\dagger \hat{\eta}_\kappa + E_0, \quad (6.62)$$

where E_0 is an overall constant. Note that u_κ and v_κ need to satisfy the conditions

$$u_\kappa = u_{-\kappa} \quad \text{and} \quad v_\kappa = -v_{-\kappa}, \quad (6.63)$$

which follows from the fact that we squeeze the mode pair $(\kappa, -\kappa)$. We always have $u_0 = 1$ and $v_0 = 0$, and for even L , we also have $u_\pi = 1$ and $v_\pi = 0$. In order to test if the average entanglement entropy approaches universal values in the thermodynamic limit, we can specify our model purely in terms of continuous functions u_κ and v_κ that we evaluate for increasing system size L . A natural choice of *regular* limit functions are continuous on the circle, *i.e.*, periodic such that $u_{-\pi} = u_\pi$ and $v_{-\pi} = v_\pi = 0$.

When computing the entanglement entropy for the eigenstates of \hat{H} , we need to find the linear complex structure iJ associated to the eigenstate labeled by the occupation numbers N_c associated to the number operators $\hat{N}_c \text{or} = 2\hat{\eta}_c \text{or}^\dagger \hat{\eta}_c \text{or} - 1$. The formula for iJ can be derived from (6.13) and is very similar to (6.36), namely

$$iJ = \frac{1}{L} \sum_{\kappa \in \mathcal{K}} N_\kappa \left(\frac{|u_\kappa|^2 e^{i\kappa(x-y)} - |v_\kappa|^2 e^{i\kappa(y-x)}}{u_\kappa v_\kappa (e^{i\kappa(y-x)} - e^{i\kappa(x-y)})} \middle| \frac{u_\kappa^* v_\kappa^* (e^{i\kappa(y-x)} - e^{i\kappa(x-y)})}{-|u_\kappa|^2 e^{i\kappa(y-x)} + |v_\kappa|^2 e^{i\kappa(x-y)}} \right). \quad (6.64)$$

We study the average entanglement entropy for general choices of u_κ and v_κ characterized by a well-defined limit that is a continuous function on the circle parametrized by $\kappa \in [-\pi, \pi]$. In figure 6.4, we provide the numerical results that supports and is consistent with the possibility of a universal limit for arbitrary choices of u_κ and v_κ . Note that the speed of convergence highly depends on the chosen model and due to numerical limitations, we were not able to probe every model choice with sufficient accuracy to show numerically that the limit is universal.

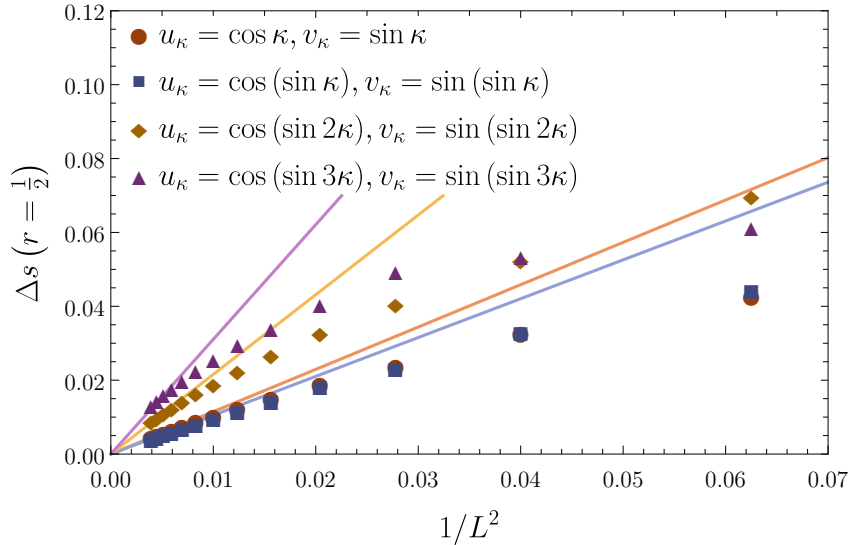


Figure 6.4: Average entanglement entropy for translationally invariant models. We study the average entanglement entropy for general translationally invariant models parametrized by u_κ and v_κ . Here, we restrict ourselves to a subsystem fraction of $r = \frac{V_A}{L}$. These model parameters can be complex and are subject to the constraints $u_\kappa = u_{-\kappa}$ and $v_\kappa = -v_{-\kappa}$ for $\kappa \in [-\pi, \pi]$. Furthermore, we assume that the model has a well-defined thermodynamic limit characterized by continuous functions u_κ and v_κ on the circle parametrized by $\kappa \in [-\pi, \pi]$. This implies $v_0 = v_\pi = v_{-\pi} = 0$. For finite L , we have $\kappa = \pi k/L$ with $k \in \{1, \dots, L\}$.

6.3.1 Typical entanglement

Based on the previous results, we formulate the following universality conjecture for translationally invariant quadratic systems.

Given a translationally invariant quadratic Hamiltonian describing spinless fermions in arbitrary dimension with V sites and a regular subsystem region consisting of V_A sites, the entanglement entropy per system site averaged over all energy eigenstates approaches a universal function $s(r)$ of the subsystem size $r = V_A/V$ that is independent from the detailed form of the Hamiltonian. The function $s(r)$ is given by the limit

$$s(r) = \lim_{V \rightarrow \infty} \frac{\langle S_A \rangle}{V} \quad \text{with} \quad r = \frac{V_A}{V}. \quad (6.65)$$

We should comment a little bit on our assumptions and the lines of evidence present.

Translational invariance refers to a discrete symmetry of a regular lattice with well-defined dimension D . For definiteness, we think of a cubic lattice with periodic boundary conditions and L sites along each dimension leading to a total number of sites given by $V = L^D$. This corresponds exactly to the setting we used to prove the universal first order bound in section 6.1.2 with a Hamiltonian that is invariant under discrete lattice translations. Furthermore, we think of subsystem regions consisting of V_A sites that have a well-defined geometry in the thermodynamic limit. Our proof in section 6.1.2 only considered subsystems defined cuboids of length L_d along the d -th dimension, but our intuition is that the results does not change if we deform these regions as long as they have a well-defined thermodynamic limit. This excludes fractal subsystems or other definitions that select subsystem sites based on some non-geometric criterion. The reason for this

condition lies in the fact that already on the level of the first order bound, we have the term

$$\langle \text{Tr}[\text{i}J]_A^2 \rangle = \frac{2V_A^2}{V} - \sum_{l=1}^V \sum_{i,j \in A} \frac{8|v_{\vec{k}_l}|^2 |u_{\vec{k}_l}|^2 \cos 2\vec{k}_l(\vec{x}_i - \vec{x}_j)}{V^2}, \quad (6.66)$$

where we could cherry pick the points \vec{x}_i in the subsystem as a function of the total system size to get specific contributions from the cosine function.

We have two lines of evidence, with the first coming from the numerical analysis of the XY model. This model is translationally invariant, but technically not quadratic due to the subtlety of the two Hilbert space sectors. However, the difference between the XY model and a general quadratic, translationally invariant model only consists of a boundary term which is expected to become irrelevant in the thermodynamic limit. Our conjecture is therefore supported by our numerical finding that the average entanglement entropy per degree of freedom as function of the subsystem size converges to a value independent of the model parameters. This result led us to the test the conjecture for a wider class of translationally invariant systems, where we just chose the free parameters u_κ and v_κ to be simple continuous and periodic functions on the interval $[0, \pi]$. It is conceivable that we may need to require certain regularity conditions from u_κ and v_κ that can be translated into additional conditions for the translationally invariant Hamiltonian, such as locality. However, it is difficult to check individual conditions, because for less regular functions u_κ and v_κ , it is very difficult to predict the limit numerically due to bad convergence properties.

Finally, we can meditate about what the reason for such a universal average (or possibly typical) entanglement entropy may be which might also suggest possible directions for a proof. We found strong deviation from Page's result which implies that the ensemble of energy eigenstates of quadratic Hamiltonians does not provide a representative sample for random states of the Hilbert space. We can extend this question and ask if our energy eigenstates form a representative sample of fermionic Gaussian state and the answer is again in the negative because we already know that the eigenstates of different quadratic Hamiltonians, such as the XY Hamiltonian and an ultra-local Hamiltonian without any entanglement, lead to different average entanglement entropies. Instead of giving up this line of thought, we can reformulate the question and ask: "Do the eigenstates of quadratic Hamiltonians provide a representative sample of a Gaussian subset encoded in the Hamiltonian?" For instance, all eigenstates of ultra-local Hamiltonians are tensor product states over lattice sites without any entanglement. Here, the set of eigenstates coincides with the set of tensor product Gaussian states, but in the case of translationally invariant systems, the situation is more complicated. The set of translationally invariant Gaussian states is larger than the various eigenstate ensembles that we considered for the XY model with different parameter choices. Following this line of argument, it might be true that the eigenstates of different translationally invariant Hamiltonians become representative ensembles with respect to the entanglement entropy when we take the thermodynamic limit. This idea shares some similarities to the well-known Gibbs ensemble where one predicts long time averages of local observables not using a the thermal state, but rather one that matches the preserved quantities of the initial state. In a similar way, the average or typical eigenstate entanglement entropy of quadratic Hamiltonians may not be correctly predicted by the set of *all* Gaussian states, but only by a subset that shares relevant symmetries with the Hamiltonian. In order to test this idea, we require efficient methods to average the entanglement entropy with respect to the Haar measure of the group $\text{SO}(2V)$ in the limit $V \rightarrow \infty$. In principal, the same techniques can be employed, including our perturbative expansion with upper and lower bounds, but we need to find an efficient parametrization of the Haar measure as a function of the linear complex structure. With this in hand, we could compute the average Gaussian entanglement entropy and the average, translationally invariant Gaussian entanglement entropy.

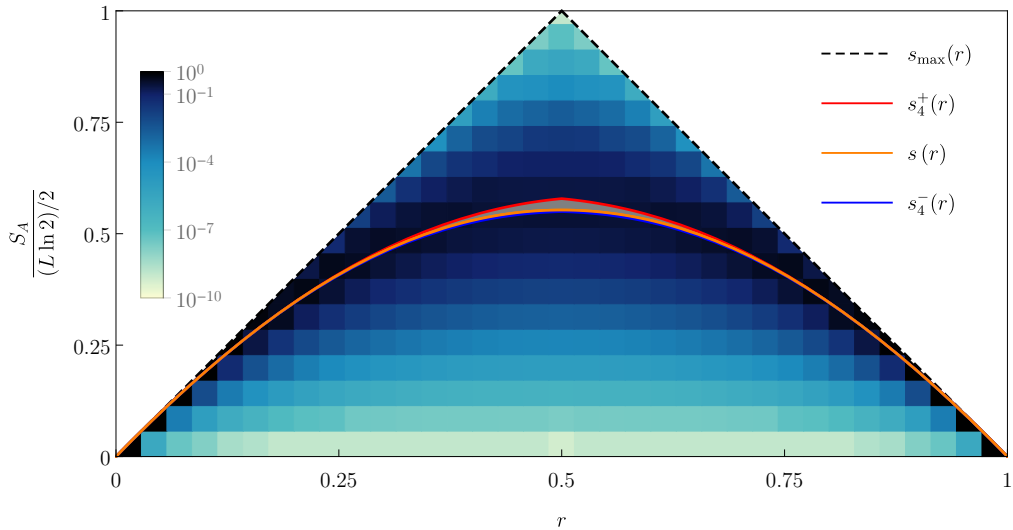


Figure 6.5: Density plot for XX model. For $L = 36$, we show the density of states for different values of the entanglement entropy. For vanishing subsystem fractions, *i.e.*, $r \rightarrow 0$, most states are maximally entangled but for finite subsystems, in particular $r = .5$, we find large deviation from the “typical” energy eigenstate entanglement entropy and the maximally possible entanglement entropy.

Note that these quantities are only well-defined for fermions, while for bosons one would encounter difficulties due to the non-compactness of symplectic groups leading to a non-compact manifold of bosonic Gaussian states.

6.4 XX model and free fermions

Computing higher order bounds for general translationally invariant systems is difficult due to the complicated dependence on u_κ and v_κ which can be arbitrary, as long as they satisfy $|u_\kappa|^2 + |v_\kappa|^2 = 1$. However, based on the numerical results of the previous section, we conjectured that the typical energy eigenstate entanglement entropy is universal for all translationally invariant systems, *i.e.*, there exists a universal curve

$$s(r) = \lim_{V \rightarrow \infty} \frac{\langle S_A \rangle}{V}, \quad (6.67)$$

where $r = V_A/V$ is called the subsystem fraction. If our conjecture is true, we do not need to compute the entanglement entropy of the most general translationally invariant quadratic system, but can focus on the simplest model that allows analytical treatment. We therefore consider the XX model arising from the XY model in the limit where we take $\gamma \rightarrow 0$ and $\hbar \rightarrow 0$. Again, we perform a Jordan-Wigner transformation to describe the system by a quadratic fermionic Hamiltonian.

For computational simplicity, we consider the system in one dimension corresponding to L lattice sites arranged in a circle. The resulting fermionic Hamiltonian is given by

$$\hat{H} = -\frac{\mathfrak{J}}{2} \sum_{x=1}^L \left(\hat{f}_x^\dagger \hat{f}_{x+1} + \hat{f}_{x+1}^\dagger \hat{f}_x \right), \quad (6.68)$$

Table 6.1: Expansion of even traces t_n . This table lists the expansion coefficients of $t_n(r) = \lim_{L \rightarrow \infty} \text{Tr}[\text{i}J_A^{2n}] / L$ in powers of $r = L_A / L$ for $n \leq 4$. Note that this corresponds to the asymptotic expansion in the limit $r \rightarrow 0$. For $t_4(r)$, the shown expansion is only correct for $r \in [0, 1/4]$, while we find a piecewise defined polynomial correction for $r > 1/4$.

$t_n = \lim_{L \rightarrow \infty} \frac{\langle [\text{i}J]_A^{2n} \rangle}{L}$	$\mathcal{O}(r^2)$	$\mathcal{O}(r^3)$	$\mathcal{O}(r^4)$	$\mathcal{O}(r^5)$	$\mathcal{O}(r^6)$	$\mathcal{O}(r^7)$	$\mathcal{O}(r^8)$
$n = 1$	2						
$n = 2$		$\frac{16}{3}$	-4				
$n = 3$			22	-48			
$n = 4$				$\frac{1816}{15}$	$-\frac{2592}{5}$	$\frac{54640}{63}$	-544

where $x + L \equiv x$. This Hamiltonian falls into the class of translational invariant Hamiltonian in (6.1), where the Bogoliubov coefficients have $u_k = 1$ and $v_k = 0$, so that the eigenstates are plane waves. This allows us to obtain closed form expressions for finite systems.

In the basis given by $\xi^a \equiv (f_1, \dots, f_L, f_1^\dagger, \dots, f_L^\dagger)$, the linear complex structure $\text{i}J$ is block diagonal and explicitly given by

$$\text{i}J \equiv \begin{pmatrix} \sum_{k=1}^L N_\kappa e^{i\frac{2\pi k}{L}(x-y)} & 0 \\ 0 & -\sum_{k=1}^L N_\kappa e^{i\frac{2\pi k}{L}(x-y)} \end{pmatrix}. \quad (6.69)$$

Using $\langle N_{k_1} N_{k_2} \rangle = \delta_{k_1 k_2}$, we can explicitly compute

$$\langle \text{Tr}[\text{i}J]_A^2 \rangle = \frac{2}{L^2} \sum_{x_1, x_2=1}^{L_A} \sum_{k_1, k_2=1}^L \langle N_{k_1} N_{k_2} \rangle e^{i\frac{2\pi}{L}(k_1 - k_2)(x_1 - x_2)} = \frac{2L_A^2}{L} \quad (6.70)$$

for finite systems. The first-order bounds for $\langle S \rangle$, for finite systems, are then given by (6.17) upon replacing $V \rightarrow L$ and $V_A \rightarrow L_A$. To simplify expressions, we are defining the normalized bounds

$$s_n^\pm(r) = \lim_{L \rightarrow \infty} \frac{S_n^\pm(L_A)}{L} \quad \text{with} \quad r = \frac{L_A}{L} \quad (6.71)$$

as function of the subsystem fraction r . The first order bounds for free fermions therefore take the form given by

$$s_1^+(r) = r \log 2 - \frac{1}{2} r^2, \quad (6.72)$$

$$s_1^-(r) = r (\log 2 - r). \quad (6.73)$$

We will see that the bound of order n describes the correct $r \rightarrow 0$ asymptotics at order $n+1$.

Computing higher order bounds requires more work and there are several subtleties to note. We will develop a general procedure to compute averages of traces of $[\text{i}J]_A^{2n}$ based on generalized Wick contractions. The main insight from our analysis is that the term $\langle \text{Tr}[\text{i}J]_A^{2n} \rangle / L$ is a polynomial that, when $L \rightarrow \infty$ and $r \rightarrow 0$, only contains powers from r^{n+1} to r^{2n} . Table 6.1 lists the relevant expansion coefficients up to fourth order. If we define

$$t_n(r) = \lim_{L \rightarrow \infty} \frac{\langle \text{Tr}[\text{i}J]_A^{2n} \rangle}{L}, \quad (6.74)$$

we can use this to express all higher order bounds $s_n^\pm(r)$ as

$$s_n^+(r) = r \log 2 - \sum_{m=1}^n \frac{t_m(r)}{4m(2m-1)}, \quad (6.75)$$

$$s_n^-(r) = s_{n-1}^+(r) - t_n(r) \left(\sum_{m=n}^{\infty} \frac{1}{4m(2m-1)} \right). \quad (6.76)$$

Putting all the results from table 6.1 together, we find the fourth order bounds to be given by

$$s_4^+(r) = r \log(2) - \frac{r^2}{2} - \frac{2r^3}{9} - \frac{r^4}{5} - \frac{59r^5}{210} + \frac{86r^6}{21} - \frac{3415r^7}{441} + \frac{34r^8}{7} - \frac{1}{28} t_4^{\text{cor}}(r), \quad (6.77)$$

$$\begin{aligned} s_4^-(r) = & r \log(2) - \frac{r^2}{2} - \frac{2r^3}{9} - \frac{r^4}{5} + r^5 \left(\frac{8579}{225} - \frac{908 \log(2)}{15} \right) + r^6 \left(\frac{1296 \log(2)}{5} - \frac{12028}{75} \right) \\ & + r^7 \left(\frac{50542}{189} - \frac{27320 \log(2)}{63} \right) + r^8 \left(272 \log(2) - \frac{2516}{15} \right) - t_4^{\text{cor}}(r) \sum_{m=4}^{\infty} \frac{1}{m(2m-1)}, \end{aligned} \quad (6.78)$$

where the function $t_4^{\text{cor}}(r)$ is piecewise defined correction that we carefully derive in 6.4.4. This correction is due to an important subtlety in the computation of the traces which only shows up starting at fourth order and for $r \in [0, 1/2]$, it is explicitly given by

$$t_4^{\text{cor}}(r) = \begin{cases} 0 & r \in [0, 1/4] \\ \frac{16384r^7}{315} - \frac{4096r^6}{45} + \frac{1024r^5}{15} - \frac{256r^4}{9} + \frac{64r^3}{9} - \frac{16r^2}{15} + \frac{4r}{45} - \frac{1}{315} & r \in [1/4, 1/3] \\ \frac{24272r^7}{63} - \frac{27424r^6}{45} + \frac{1112r^5}{3} - \frac{904r^4}{9} + \frac{64r^3}{9} + \frac{32r^2}{15} - \frac{4r}{9} + \frac{1}{45} & r \in [1/3, 1/2] \end{cases} \quad (6.79)$$

We plot all bounds from first to fourth order in figure 6.6.

In figure 6.7(a), we compare the first- and second-order bounds with the average $\langle S \rangle$ computed on a lattice with $L = 36$ sites. The bounds can be seen to be very close to the numerically computed average. At $L_A/L = 1/2$, where the relative deviation is largest, we get that $0.52 < \langle S \rangle / [(L/2) \log 2] < 0.59$. Finite-size effects are found to be exponentially small in L [189], and we obtain $\lim_{L \rightarrow \infty} \langle S \rangle / [(L/2) \log 2] = 0.5378(1)$.

In order to understand whether the average of the entanglement entropy over all eigenstates is representative of the entanglement entropy of typical eigenstates, we calculate the variance

$$\Sigma_s^2 = \frac{\langle S^2 \rangle - \langle S \rangle^2}{L^2} = \frac{1}{L^2} \sum_{m,n=1}^{\infty} F_{m,n}, \quad (6.80)$$

where

$$F_{m,n} = \frac{\langle \text{Tr}[iJ]_A^{2m} \text{Tr}[iJ]_A^{2n} \rangle - \langle \text{Tr}[iJ]_A^{2m} \rangle \langle \text{Tr}[iJ]_A^{2n} \rangle}{4m(2m-1) 4n(2n-1)}. \quad (6.81)$$

Technically, we compute the variance of the function $s(r)$, which continues to make sense in the thermodynamic limit. The computation of $F_{m,n}$ is, in general, a daunting task. However, by using a summation technique to compute higher-order traces explained in section 6.4.1, we are able to extract key properties of Σ_s . In particular, we are able to prove that Σ_s vanishes with increasing the system size as $\Sigma_s \sim 1/\sqrt{L}$ or faster 6.4.1. Furthermore, in the limit of vanishing subsystem fraction (fixed L_A for $L \rightarrow \infty$), we obtain the lowest order term in L to be

$$\Sigma_s^2(r) = \frac{1}{L} \left(\frac{r^3}{3} - \frac{r^2}{2L} + \frac{r}{6L^2} \right). \quad (6.82)$$

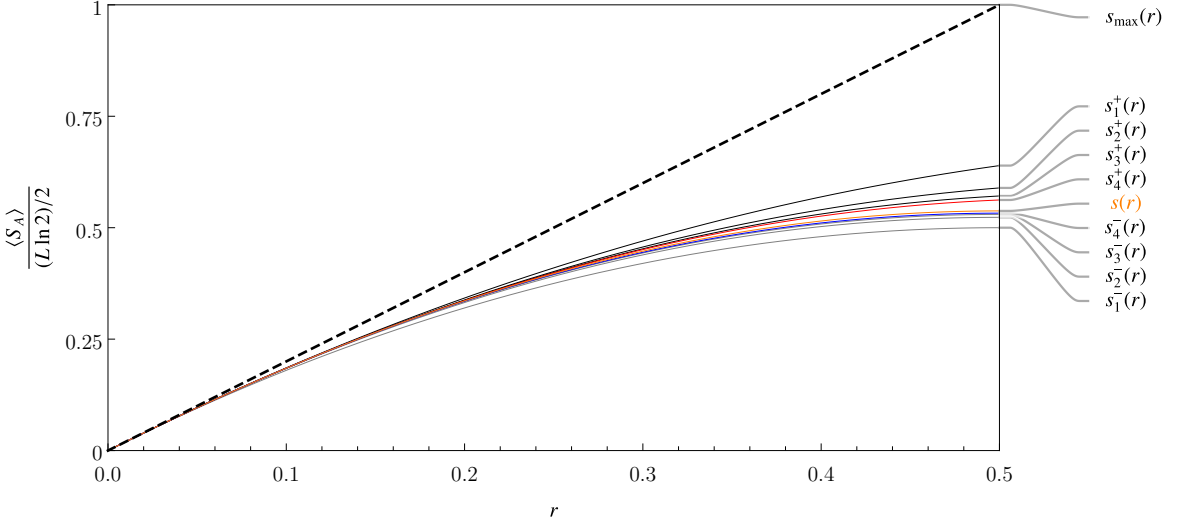


Figure 6.6: Upper and lower bounds from first to fourth order. This figure shows all upper and lower bounds s_n^\pm of the typical entanglement entropy $s(r) = \lim_{L \rightarrow \infty} \frac{\langle S(L_A) \rangle}{L}$ as function of the subsystem fraction $r = L_A/L$.

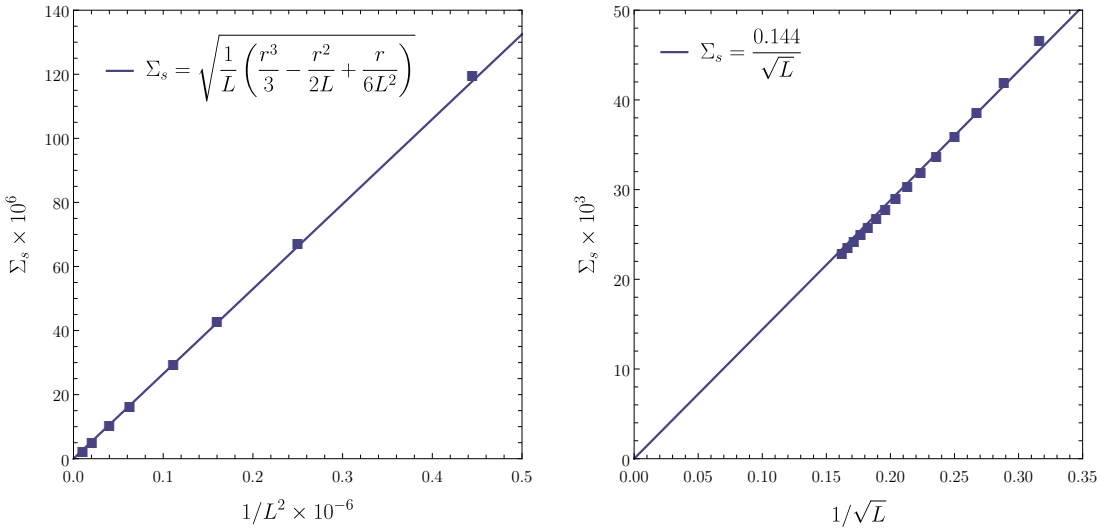


Figure 6.7: Variance of the entanglement entropy. We show numerical results to test our analytical predictions for the finite size scaling of variance Σ_s . In the left figure, we test formula (6.82) for fixed $L_A = 60$ and $L \rightarrow \infty$. In the right figure, we analyze the finite size scaling of the variance for fixed $r = L_A/L = 1/2$ as $L \rightarrow \infty$.

Numerical results for Σ_S in this limit, reported in Fig. 6.7(a), confirm the accuracy of this prediction. Numerical results for $L_A/L = 1/2$, reported in Fig. 6.7(b), confirm that $\Sigma_s \sim 1/\sqrt{L}$ for a nonvanishing subsystem fraction. The vanishing of the variance proves that the average and typical entanglement entropies are identical.

6.4.1 Generalized Wick contractions and second order terms

In order to compute the higher-order traces

$$\langle \text{Tr}[\text{i}J]_A^{2n} \rangle = 2 \sum_{x_1, \dots, x_{2n}=1}^{L_A} \langle j(x_1 - x_2) \cdots j(x_{2n} - x_1) \rangle, \quad (6.83)$$

with $j(d_i) = \frac{1}{L} \sum_{\kappa \in \mathcal{K}} e^{i\kappa d_i} N_\kappa$, we develop a systematic method of computing higher order correlation functions $\langle j(d_1) \cdots j(d_{2n}) \rangle$. Technically, these are Fourier transformed correlation functions of the binomial distribution. They can be computed by adopting a strategy analogous to the one used for computing correlation functions of Gaussian distributions:

1. The building blocks of correlation functions are the so-called $2n$ -contractions given by

$$\overbrace{j(d_1)j(d_2) \cdots j(d_{2n-1})}^{\square} j(d_{2n}) = \mathfrak{c}_n \frac{\bar{\delta}(\sum_{i=1}^{2n} d_i)}{L^{2n-1}}, \quad (6.84)$$

where $\bar{\delta}(D) = 1$ if $D = 0 \pmod{L}$ and zero otherwise, i.e., $D = \sum_{i=1}^{2n} d_i$ is restricted to be an integer multiple of L . The prefactors \mathfrak{c}_n can be computed systematically as $\mathfrak{c}_n = L^{2n-1} \langle j(1)^{2n-1} j(1-2n) \rangle$ by using the explicit form $j(d_i) = \frac{1}{L} \sum_{k=1}^L e^{i \frac{2\pi k d_i}{L}} N_\kappa$. From evaluating this formula for the first few cases, we can guess that they are given by the tangent numbers with alternating signs, namely

$$\mathfrak{c}_n = \frac{1}{L} \sum_{k_1=1, \dots, k_{2n}=1}^L \exp \frac{2\pi i}{L} \left(\sum_{i=1}^{2n} k_i - 2nk_{2n} \right) = \frac{2^{2n} (2^{2n}-1)}{2n} B_{2n}, \quad (6.85)$$

where B_{2n} refers to the $2n$ -th Bernoulli number. Up to fourth order, we only require

$$\mathfrak{c}_1 = 1, \quad \mathfrak{c}_2 = -2, \quad \mathfrak{c}_3 = 16, \quad \mathfrak{c}_4 = -272. \quad (6.86)$$

2. Once the $2n$ -contractions are known, one can compute a general correlation function as

$$\begin{aligned} \langle j(d_1) \cdots j(d_{2n}) \rangle &= \sum_{\text{all possible contractions}} \\ &= \overbrace{jj}^{\square} \cdots \overbrace{jj}^{\square} + \cdots + \overbrace{jj \cdots jj}^{\square}, \end{aligned} \quad (6.87)$$

where each contraction consists of a product of different pairings, quadruplings, etc., of the $2n$ j 's. This is a generalization of Wick's theorem because we have not only 2 -contractions, but also higher-order $2n$ -contractions.

To compute higher order traces up to order n , we need to determine all prefactors up to \mathfrak{c}_n . We can investigate the scaling in powers of $r = L_A/L$, which can appear in $\lim_{L \rightarrow \infty} \langle \text{Tr}[\text{i}J]_A^{2n} \rangle / L$. A general $2n$ correlation function is schematically given by

$$\begin{aligned} \langle j(d_1) \cdots j(d_{2n}) \rangle &= \overbrace{jj}^{\square} \cdots \overbrace{jj}^{\square} + \cdots + \overbrace{jj \cdots jj}^{\square} \\ &= \mathfrak{c}_1^n \frac{\bar{\delta}(d_1 + d_2) \cdots \bar{\delta}(d_{2n_1} + d_{2n})}{L^n} + \cdots + \mathfrak{c}_n \frac{\bar{\delta}(\sum_{i=1}^{2n} d_i)}{L^{2n-1}}. \end{aligned} \quad (6.88)$$

To compute $\langle \text{Tr}[\text{i}J]_A^{2n} \rangle / L$, we sum over x_i with $1 \leq i \leq 2n$, with $\sum_{i=1}^{2n} d_i$ automatically ensured to vanish, which implies that there is one redundant delta in each addend of (6.88).

The $2n$ -correlation functions consists of various products of contractions. We will refer to such a type of product of contractions as $(2n_1, \dots, 2n_l)$ -contraction if it consists l contractions of types determined by $2n_i$. Moreover, we refer to the full set or sum of $(2n_1, \dots, 2n_l)$ -contractions as $\mathcal{C}_{(2n_1, \dots, 2n_l)}$. A specific contraction $\mathfrak{C} \in \mathcal{C}_{(2n_1, \dots, 2n_l)}$ will give l delta functions $\bar{\delta}(D_i)$ with D_i being specific sums of the d_i s according to the chosen contraction, namely

$$\mathfrak{C} = \prod_{i=1}^l \mathfrak{c}_{n_i} \frac{\bar{\delta}(D_i)}{L^{2n_i-1}}. \quad (6.89)$$

Provided that $D_i \leq L$, we can ignore the $(\text{mod } L)$ condition in $\bar{\delta}$ and replace it with regular δ . This product of deltas appearing in the sum (6.83) then gives

$$\sum_{x_1, \dots, x_{2n}=1}^{L_A} \delta(D_1) \cdots \delta(D_l) = \mathcal{O}(L_A^{2n-l+1}), \quad (6.90)$$

where we use the fact that each of the l deltas reduces the dimension of the sum by one, except one because one of them is redundant one due to $\sum_{i=1}^l D_i = \sum 2n_i d_i = 0$. Therefore, the sum gives a polynomial of degree $2n - l + 1$. Applying this result to all contractions, we find

$$\sum_{x_1, \dots, x_{2n}}^{L_A} \langle j(d_1) \cdots j(d_{2n}) \rangle \sim \frac{\mathcal{O}(L_A^{n+1})}{L^n} + \cdots + \frac{\mathcal{O}(L_A^{2n})}{L^{2n-1}} \quad \text{as } L_A/L \rightarrow 0, \quad (6.91)$$

where $\mathcal{O}(L_A^{n+1})$ refers to a polynomial of degree $n+1$. Note that we included the requirement that all $D_i < L$ by considering this expression in the limit $L_A/L \rightarrow 0$. Therefore, we conclude that

$$\lim_{L \rightarrow \infty} \frac{\langle \text{Tr}[iJ]_A^{2n} \rangle}{L} \sim \mathcal{O}(r^{n+1}) + \cdots + \mathcal{O}(r^{2n}) \quad \text{as } r \rightarrow 0, \quad (6.92)$$

i.e., it is a polynomial function containing only powers from $r^{n+1} = (L_A/L)^{n+1}$ up to $r^{2n} = (L_A/L)^{2n}$. This result is instrumental in the analysis of the behavior of the entropy for vanishing subsystem fraction $L_A/L \rightarrow 0$. It implies that it is sufficient to compute the entropy function up to order n to get the dominating terms up to order r^{n+1} . Note however that in general for $r > 1/n$, we expect additional corrections due to the $(\text{mod } L)$ condition in $\bar{\delta}$. Interestingly, these corrections are absent in the relevant interval $r \in [0, 1/2]$ for $n \leq 3$, but for $n = 4$ we will see that additional terms show up for $r > 1/4$.

Second order trace. To illustrate this method, let us apply it to the second order correction containing $\langle \text{Tr}[iJ]_A^4 \rangle$. We compute the 4-point correlation function $\langle j(d_1)j(d_2)j(d_3)j(d_4) \rangle$. We find three 2-contractions and one 4-contraction given by

$$\begin{aligned} \langle j(d_1)j(d_2)j(d_3)j(d_4) \rangle &= \mathcal{C}_{(2,2)} + \mathcal{C}_{(4)} \\ &= \left(\overline{\square \square} \overline{\square \square} + \overline{\square \square} \overline{\square \square} + \overline{\square \square} \overline{\square \square} \right) + \overline{\square \square \square \square} \\ &= \mathfrak{c}_1^2 \left(\frac{\bar{\delta}(d_1+d_2)\bar{\delta}(d_3+d_4)}{L^2} + \frac{\bar{\delta}(d_1+d_4)\bar{\delta}(d_2+d_3)}{L^2} + \frac{\bar{\delta}(d_1+d_3)\bar{\delta}(d_2+d_4)}{L^2} \right) \\ &\quad + \mathfrak{c}_2 \frac{\bar{\delta}(\sum_{i=1}^4 d_i)}{L^3}. \end{aligned} \quad (6.93)$$

Plugging this expression into our sum (6.83) for the trace gives

$$\langle \text{Tr}[\text{i}J]_A^4 \rangle = \frac{16L_A^3 + 2L_A}{3L^2} - \frac{4L_A^4}{L^3} \quad \Rightarrow \quad t_2(r) = \lim_{L \rightarrow \infty} \frac{\langle \text{Tr}[\text{i}J]_A^4 \rangle}{L} = \frac{16}{3}r^3 - 4r^4, \quad (6.94)$$

where the first term comes from the sum over the 2-contractions, while the second term comes from the 4-contraction for which $\bar{\delta}(\sum_{i=1}^4 d_i) = 1$ due to $\sum_{i=1}^4 d_i = (x_1 - x_2) + \dots + (x_4 - x_1) = 0$. Note that, in (6.94), we assume $L_A \leq L/2$ to avoid the complication that $\bar{\delta}(d_{i_1} + d_{i_2})$ is also nonzero for $d_{i_1} + d_{i_2} = 0 \pmod{L}$.

6.4.2 Scaling of the entanglement entropy variance

We introduced the entanglement entropy variance $\Sigma_s(r)$ in (6.80), which contains the term

$$F_{m,n} = \frac{\langle \text{Tr}[\text{i}J]_A^{2m} \text{Tr}[\text{i}J]_A^{2n} \rangle - \langle \text{Tr}[\text{i}J]_A^{2m} \rangle \langle \text{Tr}[\text{i}J]_A^{2n} \rangle}{4m(2m-1)4n(2n-1)}. \quad (6.95)$$

Both terms in the numerator of $F_{m,n}$ can be computed as sums over contractions as discussed in Sec. 6.4.1. While general contractions appear in the first term, the second term contains no contractions between $\text{Tr}[\text{i}J]_A^{2m}$ and $\text{Tr}[\text{i}J]_A^{2n}$. We can evaluate the difference by computing all contractions of the first term that contain at least one contraction crossing from the first to the second trace, as all contractions without such a crossing will be canceled by the second term. Let us define the symbol $\langle j(d_1) \cdots j(d_{2m}) | j(d_{2m+1}) \cdots j(d_{2(m+n)}) \rangle$ as the sum over all contractions, for which at least one contraction crosses the separator indicated by the symbol $|$.

The contractions are schematically given by

$$\begin{aligned} \langle j \cdots j | j \cdots jjj \cdots jj \rangle &= \overbrace{j \cdots j}^1 | \overbrace{j \cdots jjj \cdots jj}^2 + \cdots + \overbrace{j \cdots j}^1 | \overbrace{j \cdots jjj \cdots jj}^2 \\ &= \frac{\bar{\delta}(D_1) \cdots \bar{\delta}(D_{n+m})}{L^{m+n}} + \cdots + \frac{\bar{\delta}(\sum_{i=1}^{n+m} d_i)}{L^{2(n+m)-1}}. \end{aligned} \quad (6.96)$$

In order to find the scaling in L , we need to sum over x_i coming from the trace expressions, and determine how many deltas are redundant. We find

$$\sum_{x_1, \dots, x_{2(n+m)}=1}^{L_A} \langle j(d_1) \cdots j(d_{2m}) | j(d_{2m+1}) \cdots j(d_{2(m+n)}) \rangle = \frac{\mathcal{O}(L_A^{m+n+1})}{L^{m+n}} + \cdots + \frac{\mathcal{O}(L_A^{2(m+n)})}{L^{2(m+n)-1}}, \quad (6.97)$$

where we only have a single redundant delta per term as in the previous case. Even though the two traces imply $\sum_{i=1}^{2m} d_i = 0$ as well as $\sum_{i=2m+1}^{2(m+n)} d_i = 0$, which should lead to some contractions with two redundant deltas, these terms are specifically excluded from the sum because they do not contain any crossing contractions. We therefore find that

$$f_{m,n}(r) = \lim_{L \rightarrow \infty} \frac{\langle \text{Tr}[\text{i}J]_A^{2m} | \text{Tr}[\text{i}J]_A^{2n} \rangle}{L} \quad (6.98)$$

is a polynomial function containing only powers r^{m+n+1} up to $r^{2(m+n)}$. Moreover, in the limit $L \rightarrow \infty$, we have

$$\Sigma_s^2 = \frac{1}{L} \sum_{m,n=1}^{\infty} \frac{f_{m,n}(L_A/L)}{4m(2m-1)4n(2n-1)}, \quad (6.99)$$

which scales as $1/L$. Finding the coefficient analytically requires the summation of the full series. The coefficient can be computed numerically from a finite-size scaling analysis.

In order to compute the variance scaling for a vanishing fraction $r \rightarrow 0$, it is sufficient to compute the first term in (6.99). In fact, our analysis ensures that higher-order terms appear as higher powers in r . Truncating the series in (6.99) at $m = n = 1$ provides an expansion that is correct up to order $m + n = 2$ in r . At this order, we find

$$\Sigma_s^2(r) = \frac{1}{L} \left(\frac{r^3}{3} - \frac{r^2}{2L} + \frac{r}{6L^2} \right), \quad (6.100)$$

as already presented in (6.82).

6.4.3 Wick diagrams and third order terms

When computing higher order correlation functions, we will need to sum a large number of possible contractions and it is important to keep track of all cases. An efficient way to organize contractions is to take symmetry into account. The evaluation of a contraction where we shift all d_i by an overall constant will not change. It is important to emphasize that the d_i should be thought of as arranged in a circle, so representing the equivalence class of contractions under translations is best done on a circle. We refer to such a pictorial representation as Wick diagram



where we connect the $2n$ dots associated to the d_i accordingly to get a specific Wick diagram. Each diagram $\mathfrak{C} \in \mathcal{C}_{(n_1, \dots, n_l)}$ comes with some multiplicity $\#\mathfrak{C}$ associated to translations that do not lead to the same diagram. We refer to the underlying product of Kronecker deltas in a given diagram \mathfrak{C} as

$$\delta_{\mathfrak{C}} = \delta(D_1) \cdots \delta(D_l), \quad (6.102)$$

where we ignore any contributions from $(\text{mod } L)$ in $\bar{\delta}(D_i)$. In the thermodynamics limit, we can evaluate the sum over $\delta_{\mathfrak{C}}$ as

$$\lim_{L \rightarrow \infty} \sum_{x_1=1}^{L_A} \cdots \sum_{x_{2n}=1}^{L_A} \delta_{\mathfrak{C}} = \int_0^{L_A} d^{2n}x \delta(D_1) \cdots \delta(D_{l-1}) \quad (6.103)$$

$$= L_A^{2n+1-l} \underbrace{\int_0^1 d^{2n}x \delta(D_1) \cdots \delta(D_{l-1})}_{=\int \mathfrak{C}}, \quad (6.104)$$

where we could replace the summation by an integration with formally changing from Kronecker deltas to delta distribution that we do not distinguish in our notation. Note, however, that we had

to remove one of the Kronecker deltas due to the redundancy mentioned earlier to avoid having an ill defined $\delta(0)$. Moreover, we defined the dimensionless quantity

$$\int \mathfrak{C} = \int_0^1 d^{2n}x \delta_{\mathfrak{C}} \quad (6.105)$$

where we removed the dependence on L_A by making the replacement $x_i \rightarrow x_i L_A$. As long as we can ignore the $(\text{mod } L)$ condition in $\bar{\delta}$, *i.e.*, for $r \in [0, 1/n]$, we have

$$\lim_{L \rightarrow \infty} \frac{1}{L} \sum_{x_1=1}^{L_A} \cdots \sum_{x_{2n}=1}^{L_A} \mathfrak{C} = \mathfrak{c}_{2n_1} \cdots \mathfrak{c}_{2n_l} r^{2n+1-l} \int \mathfrak{C}. \quad (6.106)$$

Finally, the summation over all diagrams within a class $\mathcal{C}_{(n_1, \dots, n_l)}$ is given by

$$\int \mathcal{C}_{(n_1, \dots, n_l)} = \sum_{\mathfrak{C} \in \mathcal{C}_{(n_1, \dots, n_l)}} \lim_{L \rightarrow \infty} \frac{1}{L} \sum_{x_1=1}^{L_A} \cdots \sum_{x_{2n}=1}^{L_A} \mathfrak{C} = \sum_{\mathfrak{C} \in \mathcal{C}_{(n_1, \dots, n_l)}} \mathfrak{c}_{2n_1} \cdots \mathfrak{c}_{2n_l} r^{2n+1-l} \#\mathfrak{C} \int \mathfrak{C}. \quad (6.107)$$

Representing contractions by Wick diagrams and replacing summation by integration will prove to be very efficient to evaluate the third order trace in the thermodynamic limit. Before going there, let us quickly reconsider the simpler example of second order trace.

Second order trace. When we computed the terms of order 2, we had four generalized Wick contractions. These correspond to only three Wick diagrams, namely

$$\text{Diagram 1} , \quad \text{Diagram 2} , \quad \text{Diagram 3} , \quad (6.108)$$

because the second diagram has multiplicity 2. We can compute their prefactors quickly as

$$\int \text{Diagram 1} = \int_0^1 d^4x \delta(x_1 - x_3) = 1, \quad \int \text{Diagram 2} = \int_0^1 d^4x \delta(x_1 - x_2 + x_3 - x_4) = \int \text{Diagram 3} = \int_0^1 d^4x = 1, \quad (6.109)$$

of which only the second diagram requires some work. An efficient way of evaluating such integrals is to introduce dummy a variable y leading to

$$\int \text{Diagram 2} = \int_0^2 dy (I_2(y))^2 \quad \text{with} \quad I_2(y) \int_0^1 d^2x \delta(x_1 + x_2 - y), \quad (6.110)$$

where we defined the piecewise polynomial function $I_2(y)$ over the intervals $[0, 1]$ and $[1, 2]$. Distinguishing between the two cases where y is in either of the two intervals gives

$$I_2(y) = \begin{cases} I_2^{(1)}(y) & y \in [0, 1] \\ I_2^{(1)}(2-y) & y \in [1, 2] \end{cases} \quad \text{with} \quad I_2^{(1)}(y) = \frac{y}{2}. \quad (6.111)$$

With this result, it is easy to compute $2/3$ as prefactor. When adding up the contributions of the three diagrams taking their multiplicity $\#\mathfrak{C}$ into account, we find again

$$t_2(r) = \lim_{L \rightarrow \infty} \frac{\langle \text{Tr}[iJ_A^4] \rangle}{L} = \frac{16}{3}r^3 - 4r^4, \quad (6.112)$$

Table 6.2: List of all $(2, 2, 2)$ -contractions. This table lists all $(2, 2, 2)$ -contractions \mathfrak{C} , their multiplicity $\#\mathfrak{C}$ under translational symmetry, their delta constraint $\delta_{\mathfrak{C}}$ and integrated prefactor $\int \delta_{\mathfrak{C}}$. Summing all terms weighted with their multiplicity gives $\int \mathcal{C}_{(2,2,2,2)} = 11$.

\mathfrak{C}	$\#\mathfrak{C}$	$\delta_{\mathfrak{C}}$	$\int \mathfrak{C}$
	2	$\delta(x_1 - x_3)\delta(x_3 - x_5)\delta(x_5 - x_1)$	1
	3	$\delta(x_1 - x_3)\delta(x_3 - x_4 + x_6 - x_1)\delta(x_4 - x_6)$	1
	6	$\delta(x_1 - x_3)\delta(x_3 - x_4 + x_5 - x_6)\delta(x_4 - x_5 + x_6 - x_1)$	2/3
	3	$\delta(x_1 - x_2 + x_3 - x_4)\delta(x_2 - x_3 + x_5 - x_6)\delta(x_4 - x_5 + x_6 - x_1)$	1/2
	1	$\delta(x_1 - x_2 + x_4 - x_5)\delta(x_2 - x_3 + x_5 - x_6)\delta(x_3 - x_4 + x_6 - x_1)$	1/2

which reproduces the earlier result from (6.94).

Third order trace. We can apply the representation of contractions as Wick diagrams to compute the third order terms. The main ingredients is the trace

$$\langle \text{Tr}[iJ]_A^6 \rangle = 2 \sum_{x_1=1, \dots, x_6=1}^{L_A} \langle j(d_1) \cdots j(d_6) \rangle \quad (6.113)$$

$$= 2 \sum_{x_1=1, \dots, x_6=1}^{L_A} (\mathcal{C}_{(2,2,2)} + \mathcal{C}_{(2,4)} + \mathcal{C}_{(6)}) . \quad (6.114)$$

- **(2, 2, 2)-contraction:** $\int \mathcal{C}_{(2,2,2)} = 11 \mathfrak{c}_1^3 = 11$

The 15 distinct contractions fall into 5 different symmetry classes with multiplicities ranging from one to six. We list a representative \mathfrak{C} of each class in table 6.2 and note its multiplicity $\#\mathfrak{C}$, the relevant deltas $\delta_{\mathfrak{C}}$ and the prefactor $\int \mathfrak{C}$ resulting from the integration over the subsystem.

- **(2, 4)-contraction:** $\int \mathcal{C}_{(2,4)} = 12 \mathfrak{c}_1 \mathfrak{c}_2 = -24$

Due to the redundancy in Kronecker deltas, we can ignore the delta from the 4-contraction and only focus onto the 2-contraction. Clearly, there are 15 distinct 2-contractions, of which 6 contract adjacent points, while the remaining 9 do not. The prefactor is 1 for the adjacent ones and 2/3 for the remaining ones. Overall, we thus find $\int \mathcal{C}_{(2,4)} = 6 \cdot 1 + 9 \cdot 2/3 = 12$.

- **(6)-contraction:** $\int \mathcal{C}_{(6)} = \mathfrak{c}_3 = 16$

This integration is trivial because the only contraction leads to a redundant delta leading to the prefactor 1.

Combining all terms, we therefore find

$$t_3 = \lim_{L \rightarrow \infty} \frac{\langle \text{Tr}[iJ]_A \rangle}{L} = 22r^4 - 48r^5 + 32r^6, \quad (6.115)$$

where $r = L_A/L$.

6.4.4 Delta subtlety and fourth order terms

Starting with the fourth order bound an important subtlety arises, because it matters that our generalized Kronecker deltas are defined $(\text{mod } L)$. This means that we have $\delta(D) = 1$ not only for $D = 0$, but also any multiples of the full system size L . We will see that this leads to surprising effects and will turn the bounds into piecewise defined polynomials rather than a single analytical polynomial for $r \in [0, \frac{1}{2}]$. Such a correction is expected to appear for $r > 1/n$ for traces t_n of order n . This subtlety comes from the fact that our generalized Kronecker deltas are defined as

$$\bar{\delta}(D) = \begin{cases} 1 & D = 0 \pmod{L} \\ 0 & \text{else} \end{cases}, \quad (6.116)$$

where $D = \sum_{i=1}^{2j} d_i$ with $d_l = x_l - x_{l+1}$ and $x_{L+1} = x_1$. Until third order, we never needed to worry about the $(\text{mod } L)$ condition. The explanation for this consists of two parts:

1. For a 2-contraction $j(d_l)j(d_m) = \frac{c_1}{L}\delta(x_l - x_{l+1} + x_m - x_{m+1})$, the largest possible value of $D = d_l + d_m$ is given by $D_{\max} = 2(L_A - 1)$, namely for $x_l = x_m = L_A$ and $x_{l+1} = x_{m+1} = 1$. However, we only compute the trace for $L_A \leq L/2$ leading to $D_{\max} \leq L - 2 < L$. Thus for any 2-contraction, we can just ignore the $(\text{mod } L)$ condition all together.
2. Based on the first statement, we only need to take the $(\text{mod } L)$ condition into account for $\delta(\sum_{i=1}^{2j} d_i)$ for $j > 2$. Such generalized Kronecker deltas only appear for 4-contractions and higher orders. Moreover, we should recall that at bound order n , we always have $\sum_{i=1}^n d_i = 0$, which implies that we can always choose one generalized Kronecker delta to be redundant. In the second and third order bounds, we do have terms that contain 4-contractions and 6-contractions, but they always appear alone or in a product with only 2-contractions. Thus in these cases, we can always choose the 4- or 6-contraction to be the redundant one and are left with 2-contractions, for which we do not need to worry about the $(\text{mod } L)$ condition.

To understand how we can take this subtlety into account and its effects are, let us consider the fourth order trace.

Fourth order trace. The fourth order bound is computed from

$$\langle \text{Tr}[iJ]_A^8 \rangle = 2 \sum_{x_1=1, \dots, x_8=1}^{L_A} \langle j(d_1) \cdots j(d_8) \rangle \quad (6.117)$$

Using again the generalized Wick's theorem, the structure of the 8-point correlation function is given by

$$\langle j(d_1) \cdots j(d_8) \rangle = \mathcal{C}_{(2,2,2,2)} + \mathcal{C}_{(2,2,4)} + (\mathcal{C}_{(4,4)} + \mathcal{C}_{(2,6)}) + \mathcal{C}_{(8)}, \quad (6.118)$$

where we grouped the $(4,4)$ -contractions together with the $(2,6)$ -contractions, because both of them will contribute a power L_A^7 . Using simple combinatorics, we can count how many contractions there are per type,

$$\#\mathcal{C}_{(2,2,2,2)} = 105, \quad \#\mathcal{C}_{(2,2,4)} = 210, \quad \#\mathcal{C}_{(4,4)} = 70, \quad \#\mathcal{C}_{(2,6)} = 28, \quad \#\mathcal{C}_{(8)} = 1, \quad (6.119)$$

leading to a total of 414 distinct contractions. As before, many contraction are related by translational symmetry, so that it is sufficient to compute one representative per symmetry class.

Table 6.3: List of all $(2, 2, 2, 2)$ -contractions. This table lists all $(2, 2, 2, 2)$ -contractions \mathfrak{C} , their multiplicity $\#$ under translational symmetry and their integration $\int \mathfrak{C}$ over the subsystem per L_A^5/L^4 . Summing all terms weighted with their multiplicity gives $\mathcal{C}_{(2,2,2,2)} = \frac{908}{15}$.

\mathfrak{C}	#	$\int \mathfrak{C}$	\mathfrak{C}	#	$\int \mathfrak{C}$	\mathfrak{C}	#	$\int \mathfrak{C}$
	8	1		4	1		2	1
	8	$\frac{2}{3}$		8	$\frac{2}{3}$		8	$\frac{2}{3}$
	4	$\frac{2}{3}$		8	$\frac{11}{30}$		8	$\frac{11}{30}$
	4	$\frac{11}{30}$		2	$\frac{11}{30}$		8	$\frac{1}{2}$
	8	$\frac{1}{2}$		8	$\frac{1}{2}$		8	$\frac{1}{2}$
	4	$\frac{9}{20}$		4	$\frac{2}{5}$		1	$\frac{2}{5}$

- **(2, 2, 2, 2)-contractions:** $\int \mathcal{C}_{(2,2,2,2)} = \frac{908}{15} \mathfrak{c}_1^4 = \frac{908}{15}$

The 105 distinct contractions fall into 18 different symmetry classes with multiplicities ranging from one to eight. We list a representative \mathfrak{C} of each class in table 6.3 and note both, its multiplicity $\#\mathfrak{C}$ and the prefactor $\int \mathfrak{C}$ under integration over the subsystem.

- **(2, 2, 4)-contractions:** $\int \mathcal{C}_{(2,2,4)} = \frac{648}{5} \mathfrak{c}_1^2 \mathfrak{c}_2 = -\frac{1296}{5}$

The 210 distinct contractions fall into 29 different symmetry classes with multiplicities ranging from one to eight. We list a representative \mathfrak{C} of each class in table 6.4 and note both, its multiplicity $\#\mathfrak{C}$ and the prefactor $\int \mathfrak{C}$ under integration over the subsystem.

- **(4, 4)-contractions:** $\int \mathcal{C}_{(4,4)} = \frac{1454}{63} \mathfrak{c}_2^2 = \frac{5816}{63}$

The 70 distinct contractions fall into 7 different symmetry classes with multiplicities ranging from one to eight. We list a representative \mathfrak{C} of each class in table 6.4 and note both, its multiplicity $\#\mathfrak{C}$ and the prefactor $\int \mathfrak{C}$ under integration over the subsystem.

- **(2, 6)-contractions:** $\int \mathcal{C}_{(2,6)} = \frac{64}{3} \mathfrak{c}_1 \mathfrak{c}_3 = -\frac{1024}{3}$

Similar to $\mathcal{C}_{(2,4)}$, we can ignore the delta from the 6-contraction and only focus onto the 2-contraction. Clearly, there are $8 \cdot 7/2 = 28$ distinct 2-contractions, of which 8 contract adjacent points, while the remaining 20 do not. As before, the prefactor for adjacent contractions is 1 and $2/3$ for the remaining ones. Overall, we thus find $\int \mathcal{C}_{(2,4)} = 8 \cdot 1 + 20 \cdot 2/3 = \frac{64}{3}$.

- **(8)-contractions:** $\mathfrak{c}_4 = \int \mathcal{C}_{(8)} = \mathfrak{c}_4 = -272$

This integration is trivial because the only contraction leads to a redundant delta leading to the prefactor 1.

Putting all terms together, gives us the fourth order trace given by

$$t_4(r) = \lim_{L \rightarrow \infty} \frac{\langle \text{Tr}[iJ]_A^8 \rangle}{L} = \frac{1816}{15} r^5 - \frac{2592}{5} r^6 + \frac{54640}{63} r^7 - 544 r^8. \quad (6.120)$$

However, this expression of $t_4(r)$ will only hold for $r \leq 1/4$. The reason for this is exactly the subtlety mentioned before, namely that we will now find diagrams, for which $\bar{\delta}(D_i)$ actually gives contributions due to the $\mod L$ condition. Clearly, only (4, 4)-contractions can give such a contribution,

Table 6.4: List of all $(2, 2, 4)$ - and $(4, 4)$ -contractions. This table lists all $(2, 2, 4)$ -contractions and $(4, 4)$ -contractions, their multiplicity $\#\mathfrak{C}$ under translational symmetry and prefactor $\int \mathfrak{C}$ under integration. Summing all terms weighted with their multiplicity gives $\mathcal{C}_{(2,2,4)} = \frac{648}{5}$ and $\mathcal{C}_{(4,4)} = \frac{1454}{63}$.

\mathfrak{C}	$\#\mathfrak{C}$	$\int \mathfrak{C}$	\mathfrak{C}	$\#\mathfrak{C}$	$\int \mathfrak{C}$
	8	1		4	1
	4	1		8	$\frac{2}{3}$
	8	$\frac{2}{3}$		8	$\frac{2}{3}$
	8	$\frac{2}{3}$		2	$\frac{2}{3}$
	8	$\frac{1}{2}$		8	$\frac{11}{20}$
	4	$\frac{1}{2}$		4	$\frac{11}{20}$
	8	$\frac{9}{20}$		1	$\frac{151}{315}$
	4	$\frac{4}{9}$			
	2	$\frac{4}{9}$			

because all other contractions only consist of 2-contractions plus 4- or 6-contractions that we can choose to be the redundant ones. Going through the list of $(4, 4)$ -contractions in table 6.4, we find the following contractions that lead to $\bar{\delta}(D_i)$ with $D_i = \pm L$ for $L_A/L < 1/2$, namely

$$\text{Diagram} = \frac{\bar{\delta}(x_1 - x_2 + x_3 - x_4 + x_5 - x_6 + x_7 - x_8)}{L^6}, \quad (6.121)$$

$$\text{Diagram} = \frac{\bar{\delta}(x_1 - x_2 + x_3 - x_4 + x_5 - x_7)}{L^6}, \quad \text{Diagram} = \frac{\bar{\delta}(x_1 - x_2 + x_3 - x_5 + x_6 - x_7)}{L^6}. \quad (6.122)$$

With our previous treatment of computing $\int \mathfrak{C}$ as listed in table 6.4, we already covered the case where $D_i = 0$, but for the Wick diagrams in (6.121), we also need to compute the contributions from

$$\int_0^{L_A} d^8x \delta(x_1 - x_2 + x_3 - x_4 + x_5 - x_6 + x_7 - x_8 \pm L) = \int_0^4 dy I_4(y) I_4(y \pm r^{-1}), \quad (6.123)$$

where $I_4(y) = \int_0^1 d^4x \delta(x_1 + x_2 + x_3 + x_4 - y)$. Here, we used again a trick of introducing a dummy variable y and we rescaled by L_A such that the mod L condition becomes mod $L/L_A = \text{mod } r^{-1}$. Computing the function $I_4(r)$ explicitly requires some work because we need to do several cases differentiations, but eventually we find a piecewise defined polynomial with compact support on the interval $[0, 4]$ given by

$$I_4(y) = \begin{cases} I_4^{(1)}(y) & y \in [0, 1] \\ I_4^{(2)}(y) & y \in [1, 2] \\ I_4^{(2)}(4-y) & y \in [2, 3] \\ I_4^{(1)}(4-y) & y \in [3, 4] \end{cases} \quad \text{with} \quad \begin{aligned} I_4^{(1)}(y) &= \frac{y^3}{6} \\ I^{(2)}(y) &= \frac{1}{6} (-3y^3 + 12y^2 - 12y + 4) \end{aligned}. \quad (6.124)$$

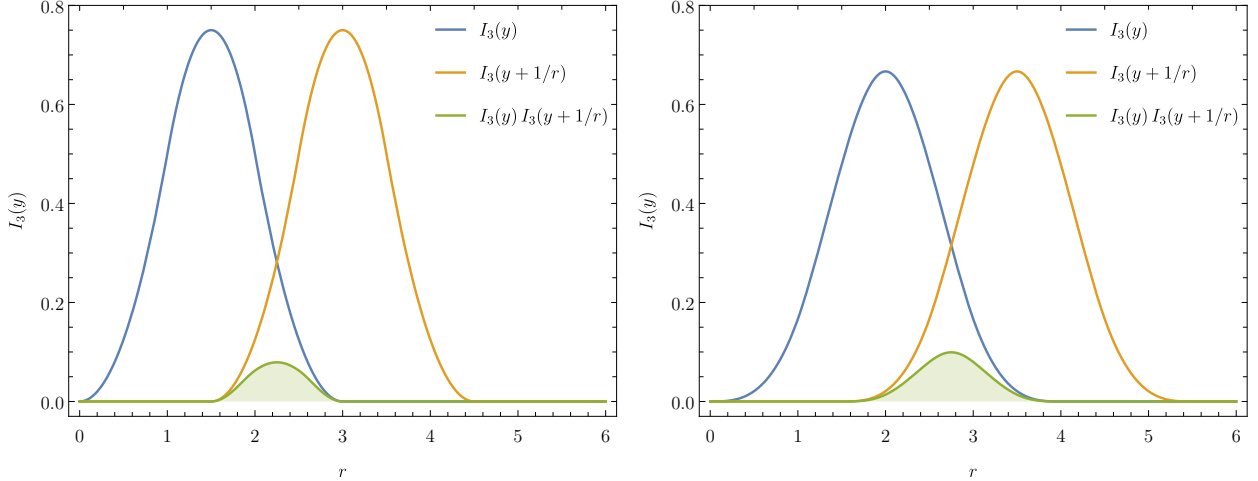


Figure 6.8: Integrand $I_3(y)$ and $I_4(y)$. This figure shows the integrands $I_3(y)$ and $I_4(y)$. When integrating their product $I_n(y)I_n(y - 1/r)$ with a relative shift $1/r$, we compute the shaded area indicated.

Analogously, we can treat the other Wick diagrams in (6.122), for which we find

$$\int_0^{L_A} d^8x \delta(x_1 - x_2 + x_3 - x_4 + x_5 - x_6 + x_7 - x_8 \pm L) = \int_0^3 dy I_3(y) I_3(y \pm r^{-1}), \quad (6.125)$$

where the integral of both diagrams can be identified by renaming the variables x_i . We also defined $I_3(y) = \int_0^1 d^4x \delta(x_1 + x_2 + x_3 - y)$ which can be computed to be given by

$$I_3(y) = \begin{cases} I_3^{(1)}(y) & y \in [0, 1] \\ I_3^{(2)}(y) & y \in [1, 2] \\ I_3^{(1)}(3 - y) & y \in [2, 3] \end{cases} \quad \text{with} \quad \begin{aligned} I_3^{(1)}(y) &= \frac{y^2}{2} \\ I_3^{(2)}(y) &= -y^2 + 3y - \frac{3}{2} \end{aligned}. \quad (6.126)$$

In order to compute the two integrals, we need to do again several case differentiations associated to the different piecewise defined regions in $I_n(y)$, but eventually one finds the following terms

$$\int_0^3 dy I_3(y) I_3(y \pm r^{-1}) = \begin{cases} -\frac{1}{120r^5} + \frac{1}{8r^4} - \frac{3}{4r^3} + \frac{9}{4r^2} - \frac{27}{8r} + \frac{81}{40} & r \in [1/3, 1/2] \\ 0 & \text{else} \end{cases}, \quad (6.127)$$

$$\int_0^4 dy I_4(y) I_4(y \pm r^{-1}) = \begin{cases} -\frac{1}{5040r^7} + \frac{1}{180r^6} - \frac{1}{15r^5} + \frac{4}{9r^4} - \frac{16}{9r^3} + \frac{64}{15r^2} - \frac{256}{45r} + \frac{1024}{315} & r \in [1/4, 1/3] \\ \frac{1}{720r^7} - \frac{1}{36r^6} + \frac{7}{30r^5} - \frac{19}{18r^4} + \frac{49}{18r^3} - \frac{23}{6r^2} + \frac{217}{90r} - \frac{139}{630} & r \in [1/3, 1/2] \\ 0 & \text{else} \end{cases}. \quad (6.128)$$

In general, the relevant function $I_n(y)$ will be compactly supported in the region $[0, n]$ and the shift $r^{-1} \geq 2$ for $r \in [0, 1/2]$. Only for $r^{-1} > n$, there will be non-zero overlap and thus, we only expect non-analytical deviations starting at order n for $r > 1/n$. To compute the correction for $t_4(r)$, let recall that each of these terms comes with an additional multiplicity of 2 due to the two different choices $\pm L$ in the $(\text{mod } L)$ condition that can be translated into two distinct choices of $\pm r^{-1}$ in our rescaled variables. Furthermore, we need to take the prefactors $\epsilon^2 = 4$ and the diagram

multiplicities

$$\# \text{ } \text{ } \text{ } = 1, \quad \# \text{ } \text{ } \text{ } = 8, \quad \# \text{ } \text{ } \text{ } = 4 \quad (6.129)$$

into account. With this in hand, we find the correction term

$$t_4^{\text{cor}}(r) = \lim_{L \rightarrow \infty} \frac{\langle \text{Tr}[iJ_A]^8 \rangle}{L} - t_4(r) \quad (6.130)$$

$$= \begin{cases} 0 & r \in [0, 1/4] \\ \frac{16384r^7}{315} - \frac{4096r^6}{45} + \frac{1024r^5}{15} - \frac{256r^4}{9} + \frac{64r^3}{9} - \frac{16r^2}{15} + \frac{4r}{45} - \frac{1}{315} & r \in [1/4, 1/3] \\ \frac{24272r^7}{63} - \frac{27424r^6}{45} + \frac{1112r^5}{3} - \frac{904r^4}{9} + \frac{64r^3}{9} + \frac{32r^2}{15} - \frac{4r}{9} + \frac{1}{45} & r \in [1/2, 1/3] \end{cases} \quad (6.131)$$

Note that the trace formula (6.83) contains an additional factor of 2 and we need to include the power r^7 again that we separated from the integral by rescaling $x_i \rightarrow x_i L_A$.

Chapter 7

Circuit complexity of Gaussian states

In this chapter, we explore the geometry of bosonic and fermionic Gaussian states to show that different approaches of defining Gaussian circuit complexity in field theories agree. This chapter is largely based on [LH13] with some results already discussed in [LH10, LH12].

Holographic complexity has been suggested as a new tool with which to gain insight in the role of entanglement in the emergence of spacetime geometry in quantum gravity [79, 190–194]. In particular, it has drawn attention to new gravitational observables to probe the bulk spacetime in the holographic theories. The complexity=volume (CV) conjecture suggests that complexity is dual to the volume of an extremal (codimension-one) bulk surface anchored to a certain time slice in the boundary [190, 192]. Alternatively, the complexity=action (CA) conjecture identifies the complexity with the gravitational action evaluated on a particular bulk region, known as the Wheeler-DeWitt (WDW) patch, which is again anchored on a boundary time slice [193, 194].¹

Both of the holographic complexity conjectures point out new classes of interesting gravitational observables and there has been a growing interest in studying these new observables and the corresponding conjectures [195–207]. At present, both conjectures appear to provide viable candidates for holographic complexity, but this research program is still at a preliminary stage. While understanding the properties of the new gravitational observables certainly deserves further study, providing concrete, even qualitative, tests of the two conjectures is hampered because we lack a good understanding of what complexity actually means in the boundary CFT, or in quantum field theory, more generally. Certainly, this lack of understanding stands as an obstacle to constructing a precise translation between the new bulk observables and specific quantities in the boundary theory, for example in an analogous way that the translation of the replica construction in the boundary yielded a derivation of holographic entanglement entropy [208–210]. Beyond gaining new insights into holographic complexity, developing an understanding of complexity in quantum field theory is an interesting research program in its own right. For example, it may lead to progress in quantum simulations of field theories [211–214] or in our understanding of Hamiltonian complexity [215, 216] and the description of many-body wave functions [217, 218].

Recently, some preliminary steps were taken to provide a precise definition of circuit complexity in quantum field theories [80, 81, 219–224]. Our current investigation is closely related to the discussions in [80, 81], which studied the ground state complexity of a free scalar field theory. In particular, [80] adapted a geometric approach, which was developed by Nielsen and collaborators [225–227], to evaluate circuit complexity in a scalar field theory, and here we apply Nielsen’s approach to defining the complexity of states in a fermionic field theory. We might note that a

¹One can think of the WDW patch as the causal development of the spacelike extremal surface picked out in the CV construction.

possible connection between Nielsen's approach and holographic complexity had been advocated by Susskind [191, 228, 229], but further, the complexity for the free scalar [80] was found to show some surprising similarities to holographic complexity, despite the enormous differences between the quantum field theories appearing in these two settings. We should also point out that [81] developed an alternative approach of defining complexity for the free scalar field theory using the Fubini-Study metric, which matched many results found using Nielsen's approach.

7.1 Approaches to define circuit complexity

The concept of complexity stems from the notion of computational complexity in computer science [230, 231]. The question of interest is to ask how much of certain computational resources are required to solve a given task. For a digital computer, we can ask what is minimal number of computational gates required to implement a specific algorithm, *i.e.*, a specific map between a certain sets of input bits and output bits. This question readily extends to quantum information science where the question becomes what is the minimal number of gates chosen from some set of elementary unitaries $\{V_I\}$ to implement a unitary transformation U , which produces a desired map from some n -qubit inputs to the corresponding n -qubit outputs [232, 233]. An implementation of U becomes a string of elementary unitaries, *i.e.*, $U = \prod_{k=1}^D V_{I_k}$ where D defines the circuit depth of this particular implementation. The circuit complexity then corresponds to the depth of the optimal construction, *i.e.*, the minimal number of gates needed to build U . To be even more precise, it is rarely possible to write a given U *exactly* as a finite string of discrete gates V_I , but rather only up an error ϵ . Hence the circuit complexity of a unitary transformation U is usually defined with respect to some gate set $\{V_I\}$ and a given tolerance ϵ as the minimal number of V_I required to implement U , up to an error of ϵ .

In the context of holography, or in applying these concepts to quantum field theory, we are interested in quantifying the effort required to prepare a certain target state $|\psi_T\rangle$ from a specific reference state $|\psi_R\rangle$ by applying a sequence of unitary gates. Here, $|\psi_R\rangle$ will be chosen with some notion of simplicity in mind, for example the degrees of freedom are completely unentangled. Hence the complexity of a family of target states is defined with respect to the reference state $|\psi_R\rangle$, as well as the gate set $\{V_I\}$ and the tolerance ϵ .² Again, we wish to construct the optimal unitary or shortest circuit which implements

$$|\psi_T\rangle = U |\psi_R\rangle , \quad (7.1)$$

and the complexity of the state $|\psi_T\rangle$ is simply defined as the number of elementary gates comprising this optimal U . Of course, generally there will exist infinitely many different sequences of gates which produce the same target state from a given reference state. Hence, our challenge is to identify the optimal circuit from amongst the infinite number of possibilities.

7.1.1 Approach A (Nielsen): minimal geodesics on transformation group

Nielsen and collaborators [225–227], introduced a geometric approach to identify the optimal circuit, which was adapted in [80] to evaluate the complexity of the ground state of a free scalar field. In contrast to the previous discussion, where U is constructed as a string of discrete gates, this new

²Hence the concept of state complexity differs slightly from the computational complexity introduced above. The later requires constructing the optimal U which implements a particular map for many different inputs. With a state complexity, we consider a single fixed input (*i.e.*, the reference state) and construct a new (optimal) circuit for each output (*i.e.*, the target states). This differences introduces an ambiguity in the boundary conditions.

approach begins with a continuous description of the unitary

$$U = \tilde{\mathcal{P}} \exp \left[-i \int_0^1 ds H(s) \right] \quad \text{where } H(s) = \sum_I Y^I(s) \mathcal{O}_I , \quad (7.2)$$

where the ‘time-dependent Hamiltonian’ $H(s)$ is expanded in terms of a basis of Hermitian operators \mathcal{O}_I , and the $\tilde{\mathcal{P}}$ indicates a ‘time’ ordering such that the circuit is built from right to left as s increases.³ Here one might think of the elementary gates taking the form $V_I = \exp[-i\varepsilon \mathcal{O}_I]$ where ε is some small parameter, and then the control functions $Y^I(s)$ indicate which gates are being applied at a given time s in the circuit represented by (7.2). Further, rather than only considering the complete circuit (7.2), Nielsen extends this construction to consider trajectories in the space of unitaries,

$$U(s) = \tilde{\mathcal{P}} \exp \left[-i \int_0^s d\tilde{s} H(\tilde{s}) \right] . \quad (7.3)$$

In this space, the circuits of interest are the trajectories satisfying the boundary conditions $U(s=0) = \mathbb{1}$ and $U(s=1) = U$.⁴ In this framework, $\vec{Y}(s) = (Y^1(s), Y^2(s), \dots)$ can also be interpreted as the tangent vector of the corresponding trajectory,

$$Y^I(s) \mathcal{O}_I = \partial_s U(s) U^{-1}(s) . \quad (7.4)$$

Let us also note that there is no need to consider a tolerance ϵ with this continuous description, since the $\vec{Y}(s)$ can always be adjusted to produce exactly the desired transformation (7.1).

Now Nielsen’s approach is to optimize the circuit (7.2) by minimizing a particular *cost* defined by

$$\mathcal{D}(U(t)) = \int_0^1 ds F(U(s), \vec{Y}(s)) , \quad (7.5)$$

where the cost function $F(U, \vec{Y})$ is a local functional along the trajectory of the position $U(s)$ and the tangent vector $\vec{Y}(s)$. Some simple examples would include:

$$\begin{aligned} F_1(U, \vec{Y}) &= \sum_I |Y^I| , & F_{1p}(U, \vec{Y}) &= \sum_I p_I |Y^I| , \\ F_2(U, \vec{Y}) &= \sqrt{\sum_I (Y^I)^2} , & F_\kappa(U, \vec{Y}) &= \sum_I |Y^I|^\kappa . \end{aligned} \quad (7.6)$$

Given the interpretation of the Y^I as indicating when certain gates appear in the circuit, the F_1 measure is the closest to the original definition of simply counting the number of gates in the circuit. In F_{1p} , penalty factors p_I are introduced to favour certain directions in the circuit space over others, *i.e.*, to give a higher cost to certain classes of gates. Of course, the F_2 measure can be recognized as the proper distance in a Riemannian geometry on the space of unitaries. This choice will be the focus of much of our discussion in the following. The κ measures F_κ were introduced in [80] because the resulting complexity compared well with results for holographic complexity. Of course, with $\kappa = 2$, the F_κ measure yields the same optimal trajectories as F_2 with a test particle action in the corresponding geometry, while with $\kappa = 1$, this reverts back to the F_1 measure.

³Note that our notation here differs slightly from that in [80] where the overall factor of $-i$ was absorbed in the \mathcal{O}_I , which were then anti-Hermitian operators.

⁴We define the boundary conditions more precisely below in the discussion around (7.11).

In applying the above approach to a free scalar field theory in [80], a group theoretic structure was found to naturally appear. To produce a tractable problem, only a limited basis of operators \mathcal{O}_I were used in constructing the unitary circuit (7.2) and these operators naturally formed a closed algebra, *i.e.*, a Lie algebra \mathfrak{g} with $[\mathcal{O}_I, \mathcal{O}_J] = i f_{IJ}{}^K \mathcal{O}_K$. In [80], a $GL(N, \mathbb{R})$ algebra appeared in the construction of the free scalar ground state using a lattice of N bosonic degrees of freedom. We will be making use of the analogous group structure for fermions, which turns out to be $O(2N)$. One advantage of this group theoretic perspective is that the physical details of the operators \mathcal{O}_I become less important. Rather, we can simply think of the generators in (7.2) as the elements of the Lie algebra \mathfrak{g} and the circuits are then trajectories in the corresponding group manifold \mathcal{G} , without making reference to a specific representation, or rather we can choose whichever representation is most convenient for our calculations.

Let us phrase the preceding description of Nielsen's approach in the corresponding group theoretic language. In particular, the circuits (7.2) of interest become continuous trajectories $\gamma : [0, 1] \rightarrow \mathcal{G}$ which connect the identity $\mathbb{1}$ with the desired unitary transformation U . In identifying the elementary generators with a basis of the Lie algebra \mathfrak{g} , we are presented a natural cost function which is inherited from the geometry of the underlying group structure. That is, we restrict ourselves to a cost function

$$\|A\| = \sqrt{\langle A, A \rangle_{\mathbb{1}}} \quad (7.7)$$

that is induced by a positive definite metric $\langle \cdot, \cdot \rangle_{\mathbb{1}} : \mathfrak{g} \times \mathfrak{g} \rightarrow \mathbb{R}$ on the Lie algebra.⁵ If we extend a circuit $U \rightarrow e^{-\varepsilon A} U$ by applying the gate $\exp[-\varepsilon A]$ from the right, then $\delta U \approx -i\varepsilon A U$ and we expect that the length of the circuit should increase by a step $\varepsilon \|A\|$, irrespective of the precise form of U , or equivalently that the tangent vector $A U \in T_U \mathcal{G}$ has the same length as $A \in T_{\mathbb{1}} \mathcal{G}$. We can therefore extend the metric $\langle \cdot, \cdot \rangle_{\mathbb{1}}$ to arbitrary tangent spaces via right-translation, leading to the right-invariant metric

$$\langle X, Y \rangle_U = \langle X U^{-1}, Y U^{-1} \rangle_{\mathbb{1}}. \quad (7.8)$$

Using the F_2 cost function, the circuit complexity of a given $U \in \mathcal{G}$ is then defined as the minimal path length

$$\mathcal{C}_2(U) = \min_{\gamma} \int_0^1 dt \|\dot{\gamma}(t)\|, \quad (7.9)$$

which is nothing else than the *geodesic distance* between $\mathbb{1}$ and U on \mathcal{G} , which was turned into a Riemannian manifold by the metric $\langle \cdot, \cdot \rangle_U$. If instead, we wished to consider the $F_{\kappa=2}$ measure, the circuit complexity becomes

$$\mathcal{C}_{\kappa=2}(U) = \min_{\gamma} \int_0^1 dt \|\dot{\gamma}(t)\|^2, \quad (7.10)$$

Recall that evaluating the complexity of a given target state amounts to finding the optimal circuit U which produces the desired transformation in (7.1). However, this prescription typically does not actually fix the boundary condition $U(s = 1)$. That is, one will find that there are simple transformations u which leave the reference state invariant, *i.e.*, $|\psi_R\rangle = u|\psi_R\rangle$ and then given any unitary U_0 satisfying (7.1), $U = U_0 u$ will produce the desired transformation as well.

⁵Here, we use the standard identification of the Lie algebra \mathfrak{g} with the tangent space $T_{\mathbb{1}} \mathcal{G}$ at the identity.

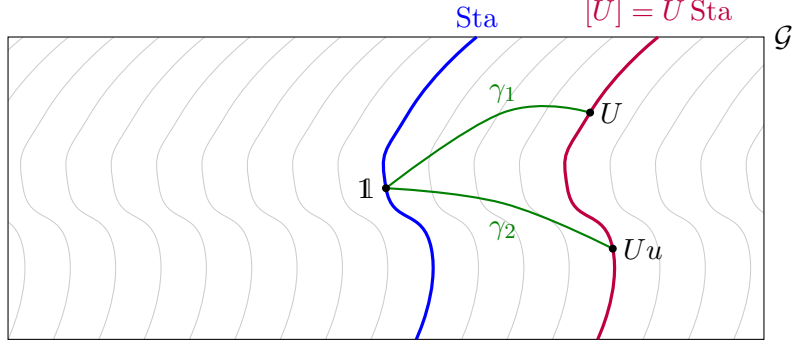


Figure 7.1: *Group foliation through stabilizer subgroup.* This figure illustrates the geometry of the Lie group \mathcal{G} with stabilizer subgroup Sta , whose elements u satisfy $u|\psi_R\rangle = |\psi_R\rangle$. This subgroup induces a fibration of \mathcal{G} into equivalence classes given by displaced stabilizers $[U] = U\text{Sta}$. The complexity of a target state $|\psi_T\rangle = U|\psi_R\rangle$ is then given by the minimal path γ to a point on $[U]$, of which we illustrate two examples. γ_1 goes from 1 to U and γ_2 from 1 to Uu where $u \in \text{Sta}$.

This ambiguity is elegantly characterized in our group theoretic approach if we define the stabilizer subgroup

$$\text{Sta} = \{u \in \mathcal{G} \text{ s.t. } u|\psi_R\rangle = |\psi_R\rangle\}, \quad (7.11)$$

that preserves $|\psi_R\rangle$. We can then define the equivalence relation $U \sim V$ iff $U = Vu$ with $u \in \text{Sta}$, *i.e.*, iff $U|\psi_R\rangle = V|\psi_R\rangle$. Hence the problem of finding the minimal circuit now involves a double extremization. First, we must find the family of geodesics running from 1 to all unitaries in the equivalence class $[U] \in \mathcal{G}/\text{Sta}$. Secondly, we must find the shortest geodesic amongst this family. Note that the equivalence class $[U]$ is just given by $U\text{Sta}$, where we displace the stabilizer by multiplying with an arbitrary representative U from the left. We illustrate the involved geometry in figure 7.1.

We consider the transformation group \mathcal{G} of bosonic or fermionic Gaussian states given by $\text{Sp}(2N, \mathbb{R})$ or $\text{SO}(2N)$ respectively. Given a reference state $|J_R\rangle$ and a target state $|J_T\rangle$, we define circuit complexity to be given by the length of the minimal geodesic

$$\gamma(t) : [0, 1] \rightarrow \mathcal{G} : t \mapsto M(t), \quad (7.12)$$

such that $U(M(1))|J_R\rangle = |J_T\rangle$. This can be compactly captured by requiring

$$J_T = M(1)J_R M(1)^{-1}. \quad (7.13)$$

In order to compute the length of a path γ , we need to introduce a measure of length on the tangent bundle of the Lie group $T\mathcal{G}$. We do this by defining such a notion at the tangent bundle at the identity $T_1\mathcal{G}$ and then extending this notion to other tangent spaces by requiring right invariance.

7.1.2 Approach B (Fubini-Study): minimal geodesics on state manifold

An alternative approach to circuit complexity was pioneered in [81] for bosons and further explored in [223]. The idea is to use the natural geometry of the state manifold \mathcal{M} consisting of the set of all pure states ρ , *i.e.*, the complex phase in its representation as normalized state vector $|\psi\rangle$ does not change the associated pure state $\rho = |\psi\rangle\langle\psi|$. The natural geometry on this manifold is induced by

the inner product on the Hilbert space. Put simply, we take the unit sphere $S(\mathcal{H}) = \{|\psi\rangle \mid \langle\psi|\psi\rangle = 1\}$ as Riemannian submanifold of the Hilbert space \mathcal{H} , that is itself a (flat) Riemannian manifold as vector space equipped with an inner product. On this set, we have the equivalence relation $|\psi\rangle \sim |\tilde{\psi}\rangle$ if and only if $|\tilde{\psi}\rangle = e^{i\varphi}|\psi\rangle$ for some $\varphi \in \mathbb{R}$. We can then define the state manifold as the quotient space

$$\mathcal{M} = S(\mathcal{H}) / \sim, \quad (7.14)$$

where we have a natural and state-independent Riemannian metric on the tangent space orthogonal to the equivalence classes.

This manifold is naturally equipped with a positive definite metric induced from the Hilbert space inner product. It is commonly referred to as the Fubini-Study metric [234]. Due to removing the complex phase, we need to remove any dependence on the complex phase. Given two one parameter families of normalized states $|\psi_A(t)\rangle$ and $|\psi_B(s)\rangle$ with $|\psi_A(t)\rangle = |\psi_B(s)\rangle$, their tangent vectors are given by

$$\partial_t|\psi_A(t)\rangle|_{t=0} \quad \text{and} \quad \partial_s|\psi_B(s)\rangle|_{s=0}. \quad (7.15)$$

We could evaluate their inner product directly as $\partial_t\partial_s\langle\psi_A(t)|\psi(s)\rangle|_{t=s=0}$, but this way a family $e^{i\varphi(t)}|\psi_A(0)\rangle$ would have a non-zero tangent vector. We therefore need to remove the contributions due to a phase shift, which is commonly done by defining the Fubini-Study metric [234] as

$$\left\langle \partial_t|\psi_A(t)\rangle|_{t=0}, \partial_s|\psi_B(s)\rangle|_{s=0} \right\rangle = \partial_t\partial_s(\langle\psi_A(t)|\psi_B(s)\rangle - \langle\psi_A(0)|\psi_B(s)\rangle\langle\psi_A(t)|\psi_B(0)\rangle)|_{t=s=0}. \quad (7.16)$$

For our purpose, it is even more useful to express the Fubini-Study metric in terms of the absolute value of the inner product, namely

$$\left\langle \partial_t|\psi_A(t)\rangle|_{t=0}, \partial_s|\psi_B(s)\rangle|_{s=0} \right\rangle = \partial_t\partial_s|\langle\psi_A(t)|\psi_B(s)\rangle|. \quad (7.17)$$

The key advantage of this expression is that we can directly apply our formula for the absolute value of the inner product of two Gaussian states in terms of the relative covariance matrix Δ , namely

$$|\langle J_A | J_B \rangle|^2 = \det \frac{\sqrt{2}\Delta^{1/4}}{\sqrt{1 + \Delta}} \quad \text{with} \quad \Delta = -J_A J_B. \quad (7.18)$$

Given two normalized states $|\psi_A\rangle$ and $|\psi_B\rangle$, it is well-known [234, 235] that the shortest path on \mathcal{M} connecting the two states is just given by the great circle in the plane spanned by the two states. We can define the orthogonal normalized state

$$|\psi'_B\rangle = \frac{|\psi_B\rangle - \langle\psi_A|\psi_B\rangle|\psi_A\rangle}{\||\psi_B\rangle - \langle\psi_A|\psi_B\rangle|\psi_A\rangle\|} \quad (7.19)$$

satisfying $\langle\psi_A|\psi'_B\rangle = 0$. If we define $\varphi = \cos^{-1}|\langle\psi_A|\psi_B\rangle| \leq \pi/2$, the path

$$|\psi(t)\rangle = \cos(t)|\psi_A\rangle + \sin(t)|\psi'_B\rangle \quad (7.20)$$

will connect $|\psi(0)\rangle = |\psi_A\rangle$ with $|\psi(\varphi)\rangle \sim |\psi_B\rangle$, where we do not care about phase differences. The geodesic length with respect to the Fubini-Study metric of this path is given by $0 \leq \varphi \leq \pi/2$.

At this point, it does not seem very interesting to define circuit complexity using the Fubini-Study metric, because the distance between two states is fully determined by their inner product. However, instead of modifying the metric, we can restrict to sub manifolds of $S(\mathcal{H})$, for which the minimal geodesic will be longer than the one just found. This is equivalent to restricting the set of physical gates that we allow to act on a reference state. For our purpose, we will restrict to the manifold of bosonic and fermionic Gaussian states, on which the geometry of minimal geodesics is less trivial than on the full manifold $S(\mathcal{H})$, but we will see that we can still find all minimal geodesics analytically.

7.2 Minimal geodesics in approach A (Nielsen)

We will give a general proof on which geodesics are the minimal ones connecting the identity with an equivalent class of unitaries that prepare the same state. In particular, we show that any such geodesic is nothing else than a collection of fermionic two-mode squeezing operations in fermionic normal modes. The geometry involved is illustrated in figure 7.2.

7.2.1 Lie group metric

In the Nielsen approach to complexity, we equip the Lie group \mathcal{G} with the right invariant and positive metric. Such a metric is completely characterized by its value at the identity where we identify the tangent space $T_1\mathcal{G}$ with its Lie algebra \mathfrak{g} . We represent a generator $A \in \mathfrak{g}$ as matrices, namely linear maps $A^a{}_b$.

A natural choice for the invariant metric on \mathfrak{g} is given by

$$\langle A, B \rangle_1 = A^a{}_b G_R^{bc} (B^\top)_c{}^d (g_R)_{da} = \text{Tr}(A g_R B^\top g_R), \quad (7.21)$$

where we use $G_R^{ab} = \langle J_R | \hat{\xi}^a \hat{\xi}^b + \hat{\xi}^b \hat{\xi}^a | J_R \rangle$. This metric is the Hilbert-Schmidt inner product induced by the metric G_R^{ab} on dual phase space. Technically, it only depends on the state $|J_R\rangle$ for bosonic systems, while $G_R^{ab} = G^{ab}$ is completely fixed through the canonical anti-commutation relations for fermionic systems. We can extend this metric to the full tangent bundle in the following way: Given two tangent vectors $X, Y \in T_M\mathcal{G}$ represented as matrices at point $M \in \mathcal{G}$, we can compute their inner product by multiplying with M^{-1} from the right, leading to

$$\langle X, Y \rangle_M = \langle XM^{-1}, YM^{-1} \rangle_1 = \text{Tr}(XM^{-1} g_R YM^{-1} g_R). \quad (7.22)$$

7.2.2 Fiber bundle structure

The choice of the reference state $|J_R\rangle$ equips the Lie group \mathcal{G} with a fiber bundle structure. There exist group elements M that leave the reference state invariant, such that $J_R = MJ_RM^{-1}$. Such group elements are both orthogonal (with respect to G_R) and symplectic (with respect to Ω_R), so that they form the subgroup

$$U(N) = SO(2N) \cap Sp(2N, \mathbb{R}). \quad (7.23)$$

The different choices of subgroups are in one-to-one correspondence to the different choices of reference states J_R .

We define the equivalence relation $M \sim \tilde{M}$ if and only if $MJ_RM^{-1} = \tilde{M}J_R\tilde{M}^{-1}$. This means acting with M and \tilde{M} on J_R will give the same target state. In particular, the subgroup $U(N)$ is equal to the equivalence class $[1]$ of the identity. Moreover, for every pair $M \sim \tilde{M}$, there exists a

$u \in \mathrm{U}(N)$, such that $Mu = \tilde{M}$. Therefore, \mathcal{G} becomes a fiber bundle where the fibers correspond to the different equivalence classes diffeomorphic to $\mathrm{U}(N)$ and the base manifold is given by the quotient

$$\mathcal{M} = \mathcal{G}/\sim = \mathcal{G}/\mathrm{U}(N). \quad (7.24)$$

For general N , this space has some non-trivial topology and is generally referred to as symmetric space of type CI for bosonic systems ($\mathcal{G} = \mathrm{Sp}(2N, \mathbb{R})$) and DIII for fermionic systems ($\mathcal{G} = \mathrm{SO}(2N)$). We will refer to it as \mathcal{M} , the space of pure Gaussian states, and identify a point $[M] \in \mathcal{M}$ with the Gaussian state $|MJ_R M\rangle$ up to an overall complex phase.

7.2.3 Cartan decomposition

Identifying the Lie algebra \mathfrak{g} with the tangent space at the identity, we have a natural “vertical” subalgebra $\mathfrak{u}(N) \subset \mathfrak{g}$ that is tangential to the fiber $[1] = \mathrm{U}(N)$. A priori, there is no natural “horizontal” complement to write the Lie algebra as a direct sum of a vertical and a horizontal part. However, by equipping the Lie algebra with the inner product $\langle \cdot, \cdot \rangle_{\mathbb{1}}$, we can choose the orthogonal complement

$$\mathfrak{u}_{\perp}(N) := \{A \in \mathfrak{g} | \langle A, B \rangle_{\mathbb{1}} = 0 \forall B \in \mathfrak{u}(N)\} \quad (7.25)$$

In contrast to $\mathfrak{u}(N)$, $\mathfrak{u}_{\perp}(N)$ is not a subalgebra. We can describe elements of $\mathfrak{u}(N)$ and $\mathfrak{u}_{\perp}(N)$ in a natural way using the linear complex structure J_R of the reference state:

- **Vertical subspace $\mathfrak{u}(N)$**

A generator B in the subspace $\mathfrak{u}(N)$ must generate transformations that preserve the reference state $|J_R\rangle$. It therefore needs to satisfy $e^B J_R e^{-B} = J_R$ leading to the infinitesimal condition

$$BJ_R - J_R B = [B, J_R] = 0. \quad (7.26)$$

This means elements in $\mathfrak{u}(N)$ commute with J_R .

- **Horizontal subspace $\mathfrak{u}_{\perp}(N)$**

A generator A that is orthogonal to all elements $B \in \mathfrak{u}(N)$ satisfies

$$0 = \langle A, B \rangle_{\mathbb{1}} = \mathrm{Tr}(AG_R B^\dagger g_R), \quad (7.27)$$

where we could drop the index R in the fermionic case, because the metric G and its inverse g are governing the anti-commutation relations and are universal for all states. We will now show that an element $A \in \mathfrak{u}_{\perp}(N)$ is characterized by the condition that it anti-commutes with J_R , namely

$$AJ_R + J_R A = \{A, J_R\} = 0. \quad (7.28)$$

Let us show that any $A \in \mathfrak{g}$ satisfying above condition is orthogonal to any element $B \in \mathfrak{u}(N)$. We can use $\mathbb{1} = -J_R^2$ and $AJ_R = \frac{1}{2}(AJ_R - J_R A)$ to compute

$$\langle A, B \rangle_{\mathbb{1}} = \mathrm{Tr}(AG_R B^\dagger g_R) \quad (7.29)$$

$$= \mathrm{Tr}(A(-J_R^2)G_R B^\dagger g_R) \quad (7.30)$$

$$= \mathrm{Tr}((J_R A - AJ_R)J_R G_R B^\dagger g_R) \quad (7.31)$$

$$= \mathrm{Tr}(J_R AG_R \underbrace{(J_R B - BJ_R)^\dagger g_R}_{=[J_R,B]=0}) \quad (7.32)$$

$$= 0. \quad (7.33)$$

In this computation, we also made use of the cyclicity of the trace and the relation $J_R G_R = G_R J_R^\top$. In order to show that above condition is sufficient to characterize all elements in $\mathfrak{u}_\perp(N)$, we can use the fact that every algebra element $K \in \mathfrak{g}$ can be uniquely decomposed into the parts

$$K_\parallel = \frac{1}{2} (K + J_R K J_R) \quad \text{and} \quad B_\perp = \frac{1}{2} (K - J_R K J_R), \quad (7.34)$$

such that $K = K_\parallel + K_\perp$ and $\{K_\parallel, J_R\} = [K_\perp, J_R] = 0$ are satisfied.⁶ This ensures that all elements in $A \in \mathfrak{u}_\perp(N)$ satisfy $\{A, J_R\} = 0$. We can use G_R and g_R to compute

$$(G_R A^\top g_R)^a{}_b = (G_R)^{ac} (A^\top)_c{}^d (g_R)_{db} = \pm A^a{}_b, \quad (7.35)$$

with (+) for bosons and (-) for fermions, respectively. For bosons, this only holds for $A \in \mathfrak{u}_\perp(N)$ and follows from the condition that A is orthogonal to all $B \in \mathfrak{u}(N)$ with $e^B G_R e^{B^\top} = G_R$. For fermions, this statement holds for all generators, because it is direct consequence of $e^A G e^{A^\top} = G$.

Exponentiating $\mathfrak{u}_\perp(N)$ defines the submanifold

$$\exp(\mathfrak{u}_\perp(N)) = \{e^A \mid A \in \mathfrak{u}_\perp(N)\}. \quad (7.36)$$

Clearly, all group elements $M \in \exp(\mathfrak{u}_\perp(N))$ satisfy the condition

$$M J_R = J_R M^{-1}. \quad (7.37)$$

The Cartan decomposition of a general group element M is given by

$$M = Tu \quad \text{with} \quad T = \sqrt{M J_R M^{-1} J_R} \in \exp(\mathfrak{u}_\perp(N)) \quad \text{and} \quad u = T^{-1} M \in U(N). \quad (7.38)$$

It is unique⁷ and provides *locally* (around the identity) a diffeomorphism between the group \mathcal{G} and the Cartesian product $\exp(\mathfrak{u}_\perp(N)) \times U(N)$. In particular, it provides a *local* trivialization of the group \mathcal{G} interpreted as fiber bundle. The base manifold is identified with the surface $\exp(\mathfrak{u}_\perp(N))$ from which we can move up and down along the fiber by multiplying with group elements $u \in U(N)$. Due to the fact that $\exp(\mathfrak{u}_\perp(N))$ is *locally* diffeomorphic to $\text{asym}(N)$, we can use the pair (A, u) as generalized coordinates for group elements $M(T, u)$ in a neighborhood around the identity:

$$M(A, u) = e^A u \quad \text{with} \quad A \in \mathfrak{u}_\perp(N) \quad \text{and} \quad u \in U(N). \quad (7.39)$$

7.2.4 Cylindrical foliation

We can foliate the symplectic group by generalized cylinders defined as

$$C_\sigma = \{e^A u \mid A \in \text{asym}(N), \|A\| = \sigma, u \in U(N)\} \quad (7.40)$$

⁶Note that the only non-trivial aspect of this decomposition is the question if $J_R K J_R$ is still in the Lie algebra \mathfrak{g} , which can be easily confirmed for both, the symplectic and the orthogonal algebra.

⁷One can show that the group element $M J_R M^{-1} J_R$ is diagonalizable with eigenvalue pairs $e^{\pm 2r}$ with $r \in \mathbb{R}_{\geq 0}$ for bosons and $e^{\pm i 2\varphi}$ with $\varphi \in [0, \pi/2]$ for fermions. We can use this to define the square root as $e^{\pm r}$ for bosons and $e^{\pm i \varphi}$ for fermions. This is unique except for $\varphi = \pi/2$, in which case one has the eigenvalues pair $e^{\pm i 2\varphi} = -1$. Its square roots are then given by the pair $e^{\pm i \pi/2}$ with an ambiguity whose square root is which. This very special case does not cause any problems and either choice can be used.

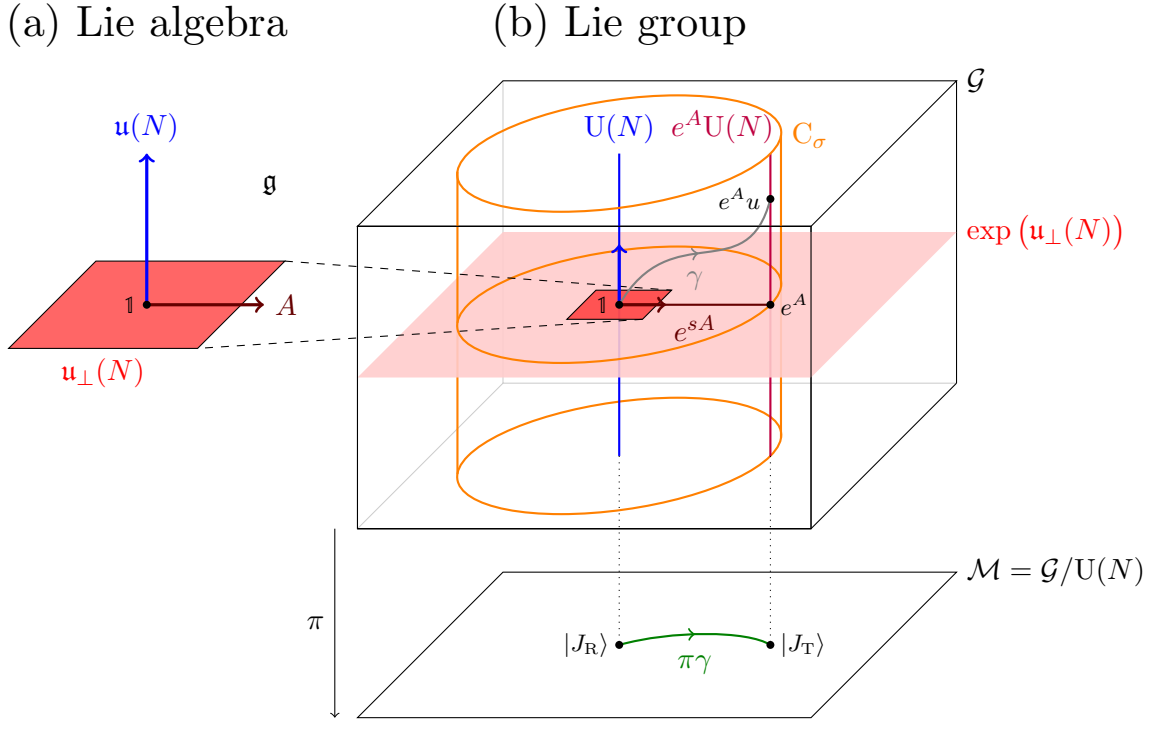


Figure 7.2: *Geometry of Gaussian circuits.* This sketch illustrates the geometry of the Lie algebra \mathfrak{g} and the Lie group \mathcal{G} . (a) The Lie algebra can be decomposed as $\mathfrak{g} = \mathfrak{u}(N) \oplus \mathfrak{u}_\perp$. In particular, we can choose a vector $A \in \mathfrak{u}_\perp$ to find the path e^{sA} that connects $\mathbb{1}$ with $e^A \in \exp(\mathfrak{u}_\perp(N)) \subset \mathcal{G}$. (b) The Lie group can be represented as fiber bundle over its quotient given by the symmetric space $\mathcal{G}/U(N)$. This base manifold can be interpreted as the space of Gaussian quantum states. The fiber over the reference state $|G_R\rangle$ is given by the subgroup $U(N) \subset \mathcal{G}$, while the fiber $e^A U(N)$ over any target state $|G_T\rangle$ is not a subgroup. We consider a path γ in the group that connects $\mathbb{1}$ to some other group element $M = e^A u$. Such a point lies on the cylinder C_σ for $\sigma = \|A\|$. Every curve γ in the group can be projected down to a curve $\pi\gamma$ in the manifold of Gaussian states. The vertical submanifold $\exp(\mathfrak{u}_\perp(N))$ is generated by exponentiating $\mathfrak{u}_\perp(N)$ and it plays an important role because it contains the minimal geodesics. Note that the $\exp(\mathfrak{u}_\perp(N))$ is homeomorphic to $\mathbb{R}^{N(N+1)}$ for bosonic systems, while it has a complicated topology and intersects the fibers several times for fermions. The straight line e^{sA} connecting $\mathbb{1}$ with e^A will turn out to be the minimal geodesic between $\mathbb{1}$ and the fiber $e^A U(N)$. Note that we do not show the vector field R consisting of radially outwards pointing unit vectors on the cylindric surfaces C_σ , such that the curves $e^{sA} u$ are its integral curves.

with the topology $S^{N(N\pm 1)-1} \times \mathrm{U}(N)$ for bosons (+) and fermions (-) respectively. Moreover, we will define the radial vector field R at point $M(A, u) \in \mathcal{G}$ given by

$$\mathcal{R}_{M(A, u)} = \frac{e^A A u}{\|A\|}. \quad (7.41)$$

We will prove that this vector fields points radially outwards and is everywhere orthogonal to the cylindrical surfaces C_σ . Therefore, we need to show that R is indeed orthogonal to the surfaces C_σ . We will prove this individually for different directions. Note that the normalization $1/\|A\|$ is irrelevant here.

- **Orthogonality to the $\mathrm{U}(N)$ fiber:**

We show that R is orthogonal to any vector pointing along the $\mathrm{U}(N)$ fiber. Let $X \in \mathfrak{u}(N)$, so that $e^A u X$ points in the direction of the $\mathrm{U}(N)$ fiber at point $M(A, u)$. We can compute the inner product

$$\langle \mathcal{R}_{M(A, u)}, e^A u X \rangle = \frac{1}{\|A\|} \langle e^A A u, e^A u X \rangle_{e^A u} \quad (7.42)$$

We define $Y = u X u^{-1}$ which lies in $\mathfrak{u}(N)$ because $\mathfrak{u}(N)$ is a sub algebra. This implies $u X = Y u$. We can therefore compute

$$\langle e^A u X, e^A A u \rangle_{e^A u} = \langle e^A Y u, e^A A u \rangle_{e^A u} = \langle e^A Y, e^A A \rangle_{e^A} = \langle e^A Y e^{-A}, A \rangle_1. \quad (7.43)$$

At this point, we can use the explicit form of the metric at the identity given by

$$\langle e^A Y e^{-A}, A \rangle_1 = \mathrm{Tr}(e^A Y e^{-A} G_R A^\dagger g_R) = \pm \mathrm{Tr}(e^A Y e^{-A} A) = \pm \mathrm{Tr}(YA) = 0, \quad (7.44)$$

where we used $G_R A^\dagger g_R = \pm A$ for bosons (+) and fermions (-) respectively.

- **Orthogonality to a generator $A \in \mathfrak{u}_\perp(N)$ preserving C_σ :**

This second computation is slightly more involved. Let us look at a point $M = e^A u$ and ask what are the directions in \mathcal{G} that are tangential to the surface C_σ , but also to the surface $\exp(\mathfrak{u}_\perp(N))u$. We can describe such elements by choosing a second generator $B \in \mathfrak{u}_\perp(N)$ that is orthogonal to A with $\|A\| = \|B\|$. The circle

$$\gamma(t) = e^{(\cos(t)A + \sin(t)B)}u \quad (7.45)$$

lies in $\exp(\mathfrak{u}_\perp(N))u$ and on C_σ with $\sigma = \|A\| = \|B\|$. This gives rise to the tangent vector

$$\dot{\gamma}(0) = \frac{d}{dt} e^{(A+tB)}|_{t=0}. \quad (7.46)$$

We can compute the inner product with $\mathcal{R}_{M(A, u)}$ using $G_R A^\dagger g_R = \pm A$ for bosons (+) and fermions (-) respectively, namely

$$\langle \mathcal{R}_{M(A, u)}, \dot{\gamma}(0) \rangle_{e^A u} = \frac{1}{\|A\|} \langle \dot{\gamma}(0) u^{-1} e^{-A}, A \rangle_1 = \frac{1}{\|A\|} \mathrm{Tr} \left(A e^{A+tB} e^{-A} \underbrace{G_R A^\dagger g_R}_{=\pm A} \right). \quad (7.47)$$

At this point, we can write out the full exponential as

$$\sum_{n,m=0}^{\infty} \frac{d}{dt} \frac{\mathrm{Tr}[(A+tB)^n(-A)^m(\pm A)]|_{t=0}}{n!m!} = \mathrm{Tr} \left[B \sum_{n=1,m=0}^{\infty} \frac{(A)^{n-1}(-A)^m}{(n-1)!m!} (\pm A) \right] \quad (7.48)$$

$$= \pm \mathrm{Tr}(BA) = 0, \quad (7.49)$$

where we used the fact that trace is cyclic and that B was chosen orthogonal to A , such that $\mathrm{Tr}(BA) = 0$. Note that the sum just gives the identity.

This proves that we have indeed a vector field R that is everywhere orthogonal to the cylindrical surfaces C_σ . Furthermore, we can quickly confirm that this vector field has indeed constant length equal to 1, by computing

$$\langle \mathcal{R}_{M(A,u)}, \mathcal{R}_{M(A,u)} \rangle_{M(A,u)} = \frac{\langle e^A A u, e^A A u \rangle_{e^A u}}{\|A\|^2} = \frac{\langle A, A \rangle_1}{\|A\|^2} = 1. \quad (7.50)$$

Given a trajectory $\gamma : [0, 1] \rightarrow \mathcal{G} : t \mapsto \gamma(t)$, we can compute how the coordinate $\sigma(\gamma)$ changes. Due to the fact that the vector field R is orthogonal to the surface C_σ of constant σ and correctly normalized, we have

$$\frac{d\sigma}{dt} = \langle \mathcal{R}_{\gamma(t)}, \dot{\gamma}(t) \rangle_{\gamma(t)}. \quad (7.51)$$

7.2.5 Inequality for the geodesic length

We will now use the cylindrical structure to bound the geodesic length from below. Given an arbitrary point $M(A, u) = e^A u$ on the cylinder C_σ , let us assume that we have already found the shortest path connecting the identity 1 with $M(A, u)$. This path may be given by $\gamma(s)$ with $\gamma(0) = 1$ and $\gamma(1) = M(A, u)$. We can compute the change $d\sigma$ as the inner product

$$d\sigma(s) = ds \langle \dot{\gamma}(s), \mathcal{R}_{\gamma(s)} \rangle_{\gamma(s)}. \quad (7.52)$$

Clearly, if we integrate this inner product we find how far we move in the σ -direction. This follows directly from the fact that moving in the direction of R increases σ with a constant rate, while moving along any orthogonal direction does not change σ . Therefore, we have

$$\sigma = \int_0^1 d\sigma(s) = \int_0^1 ds \langle \dot{\gamma}(s), \mathcal{R}_{\gamma(s)} \rangle_{\gamma(s)}. \quad (7.53)$$

We can compare this with the actual length of the geodesic given by

$$\|\gamma\| := \int_0^1 ds \|\dot{\gamma}(s)\|. \quad (7.54)$$

At this point, we should note that $\langle \dot{\gamma}(s), \mathcal{R}_{\gamma(s)} \rangle_{\gamma(s)} \leq \|\dot{\gamma}(s)\|$ for all s . This follows from the fact that we are projecting onto the unit vector R , so this projection is at most the length of $\dot{\gamma}(s)$. We can combine these two equations to find the important inequality

$$\sigma \leq \|\gamma\|, \quad (7.55)$$

stating compactly that any path connecting 1 with $M \in C_\sigma$ must have a length of σ or more.

At this point, we have not proven that for every $M \in C_\sigma \subset \mathcal{G}$ there exists a path with length σ connecting 1 with M and there certainly are points M where we cannot find such a shortest path. However, we are interested in the minimal geodesic that connects the identity 1 with an arbitrary point in the fiber $[M]$. This means if we find a single path that does this with length σ , we have proven that this is indeed the optimal path and there is no shorter one.

7.2.6 Shortest path to a fiber $e^A U(N)$

We will now show explicitly that for every fiber $e^A U(N)$ with $\sigma = \|A\|$ and $A \in \mathfrak{u}_\perp(N)$, there exists a path of length σ that connects the identity with the point e^A on this fiber. This path is given by

$$\gamma(s) = e^{sA} \quad (7.56)$$

and reaches the representative e^A at $s = 1$. This path has length $\|\gamma\| = \|A\| = \sigma$. At this point, we have proven that for our chosen inner product $\langle A, B \rangle_{\mathbb{1}}$, the shortest path is indeed always given by e^{sA} with $A \in \text{asym}(N)$.

We can now ask how A is related to the target state $|J_T\rangle$. We must have

$$J_T = e^A J_R e^{-A}. \quad (7.57)$$

Now requiring that $A \in \mathfrak{u}_\perp(N)$ implies that $e^A J_R = J_R e^{-A}$. With this in hand, we can claim that the linear map

$$M = \sqrt{-J_T J_R} \quad (7.58)$$

will do the job. We can check explicitly

$$\sqrt{-J_T J_R} J_R \sqrt{-J_T J_R}^{-1} = \sqrt{-J_T J_R}^2 J_R = -J_T J_R^2 = J_T. \quad (7.59)$$

The algebra element that generates M is given by $A = \log M = \frac{1}{2} \log(-J_T J_R)$. We have $\sigma = \|A\| = \|\log(-J_T J_R)\|/2$. Note that one can show that the square root is well-defined and it is useful to define the relative covariance matrix

$$\Delta^a{}_b = -(J_T)_c^a (J_T)^c_b. \quad (7.60)$$

The eigenvalues of Δ come in conjugate pairs, either as (e^{r_i}, e^{-r_i}) for bosonic systems or as (e^{ir_i}, e^{-ir_i}) for fermionic systems. In both cases, we find that the norm is given by

$$\|A\| = \frac{1}{2} \sqrt{\sum_{i=1}^N r_i^2} = \frac{\sqrt{\text{Tr} |\log \Delta|^2}}{2}. \quad (7.61)$$

7.3 Minimal geodesics in approach B (Fubini-Study)

Let us recall that the choice of a reference state $|J_R\rangle$ allows us to interpret the group \mathcal{G} as fiber bundle over the state Gaussian state manifold \mathcal{M}_N . If we use the fundamental representation to identify group elements with linear maps $M : V \rightarrow V$ and Kähler methods to identify Gaussian states $\rho_J = |J\rangle\langle J|$ with their linear complex structure $J : V \rightarrow V$, the projection map of this $U(N)$ fiber bundle is given by

$$\pi : \mathcal{G} \rightarrow \mathcal{M}_N : M \mapsto M J_R M^{-1}. \quad (7.62)$$

Given the positive definite⁸ Fubini-Study metric, we can use the projection map π to pull back it back onto the group. This pull back $\langle \cdot, \cdot \rangle_M^{(\text{FS})} : T_M \mathcal{G} \times T_M \mathcal{G} \rightarrow \mathbb{R}$ can be completely understood by following steps:

1. Left-invariance

We first show that $\langle \cdot, \cdot \rangle^{(\text{FS})}$ is left-invariant, namely that the inner product of two tangent vectors $X, Y \in T_M \mathcal{G}$ at M can be computed as

$$\langle X, Y \rangle_M^{(\text{FS})} = \langle M^{-1} X, M^{-1} Y \rangle_{\mathbb{1}}^{(\text{FS})}, \quad (7.63)$$

which allows us to evaluate all inner products on the tangent space at the identity, *i.e.*, the Lie algebra \mathfrak{g} .

⁸Its pull back will turn out to be only non-negative, due to fact that the pull back will vanish for tangent vectors along the $U(N)$ fibers.

2. Inner product at identity

We then find an explicit representation of the inner product at the identity, *i.e.*, of two Lie algebra elements $A, B \in \mathfrak{g}$, which turns out to be given by

$$\langle A, B \rangle_{\mathbb{1}}^{(\text{FS})} = \frac{1}{16} \text{Tr} \left([A, J_R] G_R [B, J_R]^T g_R \right). \quad (7.64)$$

Therefore, the metric vanishes for Lie generators that commute with J_R and coincides with our Nielsen metric $\langle A, B \rangle_{\mathbb{1}}^{(\text{FS})}$ for generators that anti-commute with J_R , *i.e.*, if they satisfy $[A, J_R] = 2AJ_R = -2J_RA$. This is exactly the sub space $\mathfrak{u}_\perp(N)$.

3. Geodesics

Using left-invariance, we can show that the sub manifold $\exp(\mathfrak{u}_\perp(N))$ with the metric $\langle A, B \rangle^{(\text{FS})}$ restricted to it has a very similar geometry as the state manifold \mathcal{M} equipped with the Fubini-Study metric. Using the relation to the Nielsen metric, we can prove that the geodesics actually agree and their length only differ by an overall normalization constant.

In the following sections, we will apply each step in detail.

7.3.1 Left-invariance

In order to prove that the pull back $\langle \cdot, \cdot \rangle^{(\text{FS})}$ is indeed left-invariant, we need to use an explicit representation. Let us assume we are at the point M in the group \mathcal{G} which is mapped to the state $|MJ_RM^{-1} \in \mathcal{M}\rangle$ on the state manifold. Given two Lie algebra generators $A, B \in \mathfrak{g}$, we can move from $M \in \mathcal{G}$ into the tangent directions $MA, MB \in T_M\mathcal{G}$ leading to the following projected trajectories on the state manifold:

$$J_A(t) = M e^{tA} J_R e^{-tA} M^{-1}, \quad (7.65)$$

$$J_B(s) = M e^{sB} J_R e^{-sB} M^{-1}. \quad (7.66)$$

The tangent vectors at M along those trajectories in the Lie group are given by AM and BM respectively. If we take their inner product with respect to the Fubini-Study metric, we need to compute

$$\langle MA, MB \rangle_M^{(\text{FS})} = \partial_t \partial_s \langle J_A(t) | J_B(s) \rangle|_{t=s=0}. \quad (7.67)$$

We can plug-in the identity $\mathbb{1} = \hat{U}(M)\hat{U}^\dagger(M)$ to find

$$\langle MA, MB \rangle_M^{(\text{FS})} = \partial_t \partial_s |\langle J_A(t) | J_B(s) \rangle| \quad (7.68)$$

$$= \partial_t \partial_s |\langle J_A(t) | \hat{U}(M)\hat{U}^\dagger(M) | J_B(s) \rangle|_{t=s=0} \quad (7.69)$$

$$= \partial_t \partial_s |\langle e^{tA} J_R e^{-tA} | e^{sB} J_R e^{-sB} \rangle|_{t=s=0} \quad (7.70)$$

$$= \langle A, B \rangle_{\mathbb{1}}^{(\text{FS})}. \quad (7.71)$$

From this, we see that the Fubini-Study metric is indeed left-invariant when pulled back to the Lie group \mathcal{G} . Obviously, $\langle \cdot, \cdot \rangle^{(\text{FS})}$ is not positive definite because all Lie algebra generators in $\mathfrak{u}(N) \subset \mathfrak{g}$ will have zero length as they do not change the state and thus above derivatives will vanish.

7.3.2 Inner product at identity

Given two one parameter families of normalized quantum states $|\psi_A(t)\rangle$ and $|\psi_B(s)\rangle$, such that $|\psi_A(0)\rangle = |\psi_B(0)\rangle$, the Fubini-Study metric determines the inner product between the two tangent vectors $\partial_t|\psi_A(t)\rangle|_{t=0}$ and $\partial_s|\psi_B(s)\rangle|_{s=0}$ via the equation

$$\left\langle \partial_t|\psi_A(t)\rangle|_{t=0}, \partial_s|\psi_B(s)\rangle|_{s=0} \right\rangle = \partial_t \partial_s |\langle \psi_A(t)|\psi_B(s)\rangle|_{t=s=0}, \quad (7.72)$$

where the absolute value on the RHS ensures that a change of phase, *i.e.*, $|\psi_A(t)\rangle = e^{it}|\psi\rangle$, will have a tangent vector $\partial_t|\psi_A(t)\rangle|_{t=0}$ of zero length.

In order to compute the pull back of the Fubini-Study metric explicitly, we need to compute the change of the inner product

$$|\langle J|\tilde{J}\rangle| = (\det F(\Delta))^{\pm 1/2} \quad \text{with} \quad F(\Delta) = \frac{\sqrt{2}\Delta^{1/4}}{\sqrt{1+\Delta}} \quad \text{and} \quad \Delta = -J\tilde{J}, \quad (7.73)$$

where we have (+) for bosonic and (-) for fermionic systems respectively. Let us consider changes of state generated by A and B , such that

$$J_A(t) = e^{tA}J_R e^{-tA}, \quad J_B(s) = e^{sB}J_R e^{-sB} \quad \text{with} \quad \Delta = -J_A(t)J_B(s). \quad (7.74)$$

We can compute the linear variation to be given by

$$\partial |\langle J_A(t)|J_B(s)\rangle|_{\Delta=1} = \pm \frac{1}{2} (\det F(\Delta))^{\pm 1/2-1} \text{Tr}(F(\Delta)^{-1}\partial F(\Delta)) \Big|_{\Delta=1} \quad (7.75)$$

where $\partial F(\Delta)$ is explicitly given by

$$\partial F(\Delta)|_{\Delta=1} = F(\Delta) \frac{1-\Delta}{4\Delta(1+\Delta)} \partial \Delta \Big|_{\Delta=1} = 0, \quad (7.76)$$

which will vanish at $\Delta = 1$, around which we perform our perturbation. This is not surprising because we have a local maximum of the inner product at $\Delta = 1$. We therefore, consider the full perturbation

$$\partial_t \partial_s |\langle J_A(t)|J_B(s)\rangle|_{\Delta=1} = \pm \frac{1}{2} (\det F(\Delta))^{\pm 1/2-1} \text{Tr}(F(\Delta)^{-1}\partial_s \partial_t F(\Delta)) \Big|_{\Delta=1}, \quad (7.77)$$

where the only non-zero term appears in $\partial_t \partial_s F(\Delta)|_{\Delta=1}$. We can compute explicitly the contribution

$$\partial_t \partial_s F(\Delta)|_{\Delta=1} = F(\Delta) \frac{5\Delta^2 - 10\Delta - 3\mathbb{1}}{16\Delta^2(\Delta+1)^2} \partial_t \Delta \partial_s \Delta \Big|_{\Delta=1}. \quad (7.78)$$

Using $F(\Delta)|_{\Delta=1} = 1$, we find overall

$$\partial_t \partial_s |\langle J_A(t)|J_B(s)\rangle|_{\Delta=1} = \mp \frac{1}{16} \text{Tr}(\delta_t \Delta \delta_s \Delta) \Big|_{\Delta=1} \quad (7.79)$$

where the variations of Δ are explicitly given by

$$\partial_t \Delta|_{\Delta=1} = \partial_t (-e^{tA}J_R e^{-tA}e^{sB}J_R e^{-sB})|_{\Delta=1} = [A, J_R] J_R, \quad (7.80)$$

$$\partial_s \Delta|_{\Delta=1} = \partial_s (-e^{tA}J_R e^{-tA}e^{sB}J_R e^{-sB})|_{\Delta=1} = J_R [B, J_R], \quad (7.81)$$

from which we can conclude $\partial_s \Delta \partial_t \Delta|_{\Delta=1} = -[A, J_R] [B, J_R]$ leading to

$$\partial_t \partial_s \langle J_A(t) | J_B(s) \rangle_{\Delta=1} = \pm \frac{1}{16} \text{Tr} \left([A, J_R] [B, J_R] \right) \quad (7.82)$$

$$= \pm \frac{1}{16} \text{Tr} \left([A, J_R] (-J_R^2) [B, J_R] \right) \quad (7.83)$$

$$= \pm \frac{1}{4} \text{Tr} \left(\frac{A - J_R A J_R}{2} \frac{B - J_R B J_R}{2} \right) \quad (7.84)$$

$$= \frac{1}{4} \text{Tr} (A_\perp G_R B_\perp^\top g_R) , \quad (7.85)$$

where we used $A_\perp = \frac{1}{2}(A - J_R A J_R)$ and $G_R A_\perp^\top g_R = \pm A_\perp$. This implies that the pullback of the Fubini-Study metric to the tangent bundle at the identity is given by

$$\langle A, B \rangle_{\mathbb{1}}^{(\text{FS})} = \frac{1}{4} \text{Tr} (A_\perp G_R B_\perp^\top g_R) , \quad (7.86)$$

where we used the previously introduced notion of a generator K being decomposed as $K = K_{\parallel} + K_{\perp}$ with $K_{\parallel} \in \mathfrak{u}(N)$ and $K_{\perp} \in \mathfrak{u}_{\perp}(N)$. It ensures $\langle K_{\parallel}, A \rangle_{\mathbb{1}}^{(\text{FS})} = 0$, *i.e.*, the pullback of the Fubini-Study metric is degenerate with $\mathfrak{u}(N)$ being its kernel. This is not surprising because any element $J_{\parallel} \in \mathfrak{u}(N)$ does not change the reference state $|e^{tA_{\parallel}} J_R e^{-tA_{\parallel}}\rangle = |J_R\rangle$ and thus is projected onto the zero vector in the state manifold.

Our choice of Nielsen metric restricted to $\mathfrak{u}_{\perp}(N)$ is given by $\langle A_{\perp}, B_{\perp} \rangle_{\mathbb{1}}^{(N)} = \text{Tr}(A_{\perp} G_R B_{\perp}^\top g_R)$ for bosons (+) and fermions (-) respectively. It implies that on $\mathfrak{u}_{\perp}(N)$ the pullback of the Fubini Study metric coincides with our Nielsen metric up to an overall constant $1/4$, *i.e.*,

$$\langle \cdot, \cdot \rangle_{\mathbb{1}}^{\text{FS}} \Big|_{\mathfrak{u}_{\perp}(N)} = \frac{1}{4} \langle \cdot, \cdot \rangle_{\mathbb{1}}^{(N)} \Big|_{\mathfrak{u}_{\perp}(N)} . \quad (7.87)$$

7.3.3 Geodesics

For bosonic systems, the metric restricted to $\exp(\mathfrak{u}_{\perp}(N))$ disagree, because the Fubini-Study metric is left-invariant, while the Nielsen metric is right-invariant. We could in principal redo the whole Nielsen construction for a left-invariant metric and the two geometries would agree, but this would violate the original idea that applying additional gates from the left should always add the same amount of ‘‘cost’’, *i.e.*, their generators should be assigned the same geometric length regardless of the operations already applied to the right. However, for the computation of complexity with respect to a specific reference state $|J_R\rangle$, it does not matter which of the approaches we use. This is due to the fact that the complexity as minimal geodesic length from the identity to an arbitrary $U(N)$ fiber will be the same in both approaches. For fermionic systems, the situation is even simpler, because for fermions the Nielsen geometry is actually bi-invariant. This is due to the fact that our choice of metric coincides with the negative Killing form on the Lie algebra, which is known to give rise to a positive definite bi-invariant metric for compact Lie groups, such as $SO(2N)$.⁹

The best way to see that the pull-back of geodesics agrees with the ones found with approach A is based on the local identification of the state manifold \mathcal{M} with $\exp(\mathfrak{u}_{\perp}(N))$. For bosons, this identification provides a global diffeomorphism, while for fermions this identification only applies to a local patch around the identity, but this patch is sufficient to find the minimal geodesics. The

⁹For non-compact Lie groups, such as $Sp(2N, \mathbb{R})$, the Killing form would still give rise to a bi-invariant symmetric linear form, but it would not be positive definite. Such a bilinear form might be useful for various applications, but it wouldn't be useful to define circuit complexity if we could find non-trivial paths with zero or even negative length.

shortest path to a point e^A was given by $\gamma(t) = e^{tA}$, where $A \in \mathfrak{u}_\perp(N)$ with respect to both metrics. If we now want to compute the length of the tangent vector, we find

$$\|\dot{\gamma}(t)\|_{\gamma(t)}^{(\text{FS})} = \sqrt{\langle e^{tA} A, e^{tA} A \rangle_{\gamma(t)}^{(\text{FS})}} = \sqrt{\langle A, A \rangle_1^{(\text{FS})}} = \|A\|^{(\text{FS})}, \quad (7.88)$$

$$\|\dot{\gamma}(t)\|_{\gamma(t)}^{(\text{N})} = \sqrt{\langle Ae^{tA}, Ae^{tA} \rangle_{\gamma(t)}^{(\text{N})}} = \sqrt{\langle A, A \rangle_1^{(\text{N})}} = \|A\|^{(\text{N})}, \quad (7.89)$$

from which we observe that both trajectories will give the same length. The fact that there is no shorter geodesic than these straight lines, we already proved for the Nielsen method. For the Fubini-Study metric, we can run the same argument as for the Nielsen metric, because the same cylindrical foliation C_σ of \mathcal{G} will be projected to a spherical foliation of \mathcal{M} , *i.e.*, to reach any Gaussian state on $\pi(C_\sigma) \subset \mathcal{M}$, we need to have at least path of length σ .

7.4 Relation between the two approaches

We introduced two different approaches towards defining circuit complexity in free quantum field theories, *i.e.*, for the set of Gaussian states. In approach A, we made a natural choice for a right-invariant metric on the Lie group \mathcal{G} , while approach B was based on the canonical Fubini-Study metric on the state manifold of Gaussian states that was inherited from the Hilbert space inner product.

Our main finding is the proof of equivalence up to an overall normalization constant when one uses these approaches to compute the circuit complexity as minimal geodesic distance, either between the identity and a group element preparing the target from the reference state (approach A) or between the reference and target state directly on the Gaussian state manifold.

A natural question is what the precise relation between the two geometries is. In particular, we may wonder if we can isometrically embed the Gaussian state manifold equipped with the Fubini-Study metric (approach B) in the larger group manifold equipped with our choice of right-invariant metric. Interestingly, the answer of this question differs for bosons and fermions. While it is in the negative for the former, we can isometrically embed the fermionic state manifold in $\text{SO}(2N)$. Let us present the precise arguments for each case.

- **Bosonic systems:**

Due to the non-compactness of $\mathcal{G} = \text{Sp}(2N, \mathbb{R})$, the Killing form is not negative-definite implying that we cannot choose a bi-invariant positive-definite metric on the group manifold, *i.e.*, a metric that is both left- and right-invariant. Instead we used the phase space inner product G_R determined by the reference state to define the Hilbert-Schmidt inner product between Lie algebra elements given by

$$\langle A, B \rangle_1^{(N)} = \text{Tr}(AG_RB^\top g_R). \quad (7.90)$$

This inner product was extended to a positive definite Riemannian metric on the full group manifold by requiring right-invariance. In contrast, we could show that the pull of the Fubini-Study metric, namely $\langle \cdot, \cdot \rangle^{(\text{FS})}$, is left-invariant on the group manifold. We could show that the two inner products coincide (up to a constant) on the subspace $u_\perp(N) \subset \mathfrak{sp}(2N, \mathbb{R})$. If we want to embed the Gaussian state manifold \mathcal{M} into $\text{Sp}(2N, \mathbb{R})$ via an embedding map $\varphi : \mathcal{M} \rightarrow \text{Sp}(2N, \mathbb{R})$, it is natural to require compatibility with the projection $\pi : \text{Sp}(2N, \mathbb{R}) \rightarrow \mathcal{M} : M \mapsto |MJ_R M^{-1}\rangle$, *i.e.*, we require $\pi \circ \varphi = \text{id}_{\mathcal{M}}$. The natural candidate for such an

embedding map is

$$\varphi : \mathcal{M} \rightarrow \exp(\mathfrak{u}_\perp(N)) : |J\rangle \mapsto \sqrt{-JJ_R}, \quad (7.91)$$

that maps each state to the squareroot of the relative covariance matrix $\Delta = -JJ_R$ that would prepare J from J_R via $J = \sqrt{-JJ_R}J_R\sqrt{-JJ_R}^{-1}$. For tangent vectors $X, Y \in T_M\varphi(\mathcal{M}) = T_M\exp(\mathfrak{u}_\perp(N))$, the two inner products are related by

$$\langle X, Y \rangle_M^{\text{FS}} = \frac{1}{4}\langle M^{-1}XM, M^{-1}YM \rangle_M^N, \quad (7.92)$$

where we used the fact that the tangent vectors of $(\mathfrak{u}_\perp(N))$ are mapped to $\mathfrak{u}_\perp(N)$ for both left and right translations. In particular, for tangent vectors along the curve $\gamma(t) = e^{tA}$, we have

$$\langle \dot{\gamma}(t), \dot{\gamma}(t) \rangle_{\gamma(t)}^{\text{FS}} = \frac{1}{4}\langle \dot{\gamma}(t), \dot{\gamma}(t) \rangle_{\gamma(t)}^N, \quad (7.93)$$

due to $\gamma(t)^{-1}\dot{\gamma}(t)\gamma(t) = \dot{\gamma}(t)$. This is the reason why the minimal geodesic lengths agree up to a normalization constant, but it also explains why the geometries are different. In particular, computing the minimal geodesics between two group elements $M, \tilde{M} \in \exp(\mathfrak{u}_\perp(N))$ would lead to different curves, unless one of the group elements is equal to the identity. There also cannot be any better embedding because any deformation would mean that the projection will matter and the tangent vectors as measured by the Nielsen metric would be longer than the ones measured by the Fubini-Study metric.

- **Fermionic systems:** The situation changes dramatically for fermionic systems. In this case, our Nielsen metric

$$\langle A, B \rangle_1^{(N)} = \text{Tr}(AGB^\top g) = -\text{Tr}(AB) \quad (7.94)$$

is independent from the reference state and just given by the negative Killing form on the Lie group. This immediately implies that the Nielsen metric is bi-invariant, in particular also left-invariant. Knowing that Nielsen metric and the pullback of the Fubini-Study metric agree on the subspace $\mathfrak{u}_\perp(N)$ at the identity thus implies that they agree everywhere on the subspace that resulting from left-translating $\mathfrak{u}_\perp(N)$. For the sub manifold $\varphi(\mathcal{M}) = \exp(\mathfrak{u}_\perp(N))$ as defined before, it is clear that each tangent space is the result of left- or right-translation of $(\mathfrak{u}_\perp(N))$ which implies that we have for all $X, Y \in T_M\exp(\mathfrak{u}_\perp(N))$

$$\langle X, Y \rangle_M^{\text{FS}} = \frac{1}{4}\langle X, Y \rangle_M^N, \quad (7.95)$$

which means we found an isometric embedding of \mathcal{M} into $\text{SO}(2N, \mathbb{R})$.¹⁰

¹⁰Note that there is another subtlety due to the fact that fiber bundle $\text{SO}(2N, \mathbb{R})$ over \mathcal{M} is not trivial. Therefore, our isometric embedding is only uniquely defined in a local patch around J_R , but can be extended to all of \mathcal{M} by ripping it apart at the “opposite pole” of J_R . However, the length of minimal geodesics from reference to target state is unaffected.

Summary and Outlook

Chapter 8

Overview of results

In this chapter, we summarize the results of part one and two. We would like to emphasize that the contributions to the mathematical framework presented in the first part mostly focuses on developing a convenient formalism for computations. Computing entanglement entropy of Gaussian states or their time evolution through quadratic Hamiltonians is usually done using their covariance matrices. Our approach unifies the formulation of bosonic and fermionic systems and provides some new geometric insights that are useful for practical applications, such as studying the production of entanglement entropy based on the phase space geometry involved. In the following, we will review our formalism for both bosons and fermions in parallel and then summarize our results for the three applications presented in this dissertation.

8.1 Mathematics of Gaussian states

In the first part, we developed a unifying mathematical framework for the treatment of bosonic and fermionic Gaussian states based on the triangle of Kähler structures, consisting of a symplectic form, positive definite metric and a linear complex structure. The key advantage lies in simple matrix formulas for time evolution, entanglement entropies, the inner product and various other relevant quantities that can be computed for Gaussian states. The underlying computational techniques are not new and even linear complex structures have been used before, but our framework provides a convenient and elegant formalism that can be applied to bosonic and fermionic Gaussian states with applications ranging from quantum information and condensed matter systems to cosmology and quantum field theory.

Our mathematical formalism is based on identifying the triangle of Kähler structures, consisting of a symplectic form Ω (with inverse ω), a positive definite metric G (with inverse g) and a linear complex structure J , as natural framework for the treatment of Gaussian states. For a system with N degrees of freedom, the classical phase space V is a $2N$ -dimensional vector space with vectors $\xi^a \in V$. For every Gaussian state ρ , we can uniquely decompose the expectation values

$$\langle \hat{\xi}^a \hat{\xi}^b \rangle - \langle \hat{\xi}^a \rangle \langle \hat{\xi}^b \rangle = \frac{1}{2}(G^{ab} + i\Omega^{ab}), \quad (8.1)$$

into a symmetric part G^{ab} (positive definite metric) and an antisymmetric part Ω^{ab} (symplectic form) where $\langle \hat{O} \rangle = \text{Tr}(\hat{O}\rho)$. For pure Gaussian states, Ω and G are compatible and give rise to a well-defined linear complex structure $J = G\omega$, while for mixed states the object $G\omega$ is *not* a linear complex structure, but a *restricted* linear complex structure $[J] = G\omega$. This is equivalent

to having a pure Gaussian state¹ $|J\rangle$ in the full system V and then restricting it to a subsystem $A \subset V$ where it gives rise to a mixed state ρ_A . The restrictions $[G]_A$ and $[\Omega]_A$ will in general not compatible anymore and their failure of being compatible is measured by the failure of the restriction $[J]_A = [G\omega]_A$ being a linear complex structure. In particular, the entanglement entropy $S_A(|J\rangle)$ with respect to the system decomposition $V = A \oplus B$ can be compactly computed as

$$S_A(|J\rangle) = \text{Tr} \left| \left(\frac{\mathbb{1}_A + i[J]_A}{2} \right) \log \left| \frac{\mathbb{1}_A + i[J]_A}{2} \right| \right|, \quad (8.2)$$

which unifies the respective expressions for bosonic and fermionic systems. Similar formulas can be found for all Renyi entropies and even the full entanglement spectrum, *i.e.*, the eigenvalues of the restricted density operators ρ_A .

When considering two Gaussian states $|J\rangle$ and $|\tilde{J}\rangle$, their relative properties are fully encoded in their relative covariance matrix $\Delta = -J\tilde{J}$. In particular, their inner product is given by

$$|\langle J|\tilde{J}\rangle| = \exp \left(-\frac{1}{2} \left| \log \det \frac{\sqrt{2}\Delta^{1/4}}{\sqrt{1+\Delta}} \right| \right). \quad (8.3)$$

Again, this expression unifies the respective formulas for bosonic and fermionic Gaussian states.²

For Gaussian states it is natural to consider their time evolution with respect to quadratic Hamiltonians, because this ensures that Gaussian states evolve into Gaussian states. Given a general quadratic Hamiltonian $\hat{H}(t) = \frac{1}{2}h_{ab}(t)\hat{\xi}^a\hat{\xi}^b$, we can phrase everything in terms of Lie group and Lie algebra elements represented as linear maps on the classical phase space. The Lie algebra generator $K(t)$ is given by

$$K^a{}_b(t) = \begin{cases} \Omega^{ac}h_{cb}(t) \in \mathfrak{sp}(2N, \mathbb{R}) & \text{bosons} \\ G^{ac}h_{cb}(t) \in \mathfrak{so}(2N) & \text{fermions} \end{cases}. \quad (8.4)$$

The classical time evolution is then determined by the classical Hamiltonian flow

$$\frac{d}{dt} M(t) = K(t)M(t) \quad \text{solved by} \quad M(t) = \mathcal{T} e^{\int_0^t dt' K(t')}, \quad (8.5)$$

where we used the time ordered exponential and $M(0) = \mathbb{1}$ as initial condition. The quantum evolution of the Gaussian states $|J(t)\rangle$ is governed by the Schrödinger's equation written in terms of $J(t)$, namely

$$\frac{d}{dt} J(t) = [K(t), J(t)] \quad \text{solved by} \quad J(t) = M(t)J(0)M^{-1}(t). \quad (8.6)$$

Again, bosonic and fermionic Gaussian states can be treated in the same way. A very detailed comparison table summarizing the key aspects of our formalism can be found in table 4.1.

8.2 Applications

The second part of this dissertation was devoted to applications of the previously introduced methods. Thereby, we would like to emphasize the breadth of possible applications ranging from entanglement production in bosonic systems to typical entanglement entropies in fermionic systems and circuit complexity in field theory. Our results are widely applicable in research fields ranging from fundamental theory, cosmology and quantum field theory in curved spacetime to condensed matter physics and quantum information theory.

¹For bosonic Gaussian states, we also allow $z^a = \langle \hat{\xi}^a \rangle$ to be non-zero, so that we would refer to pure states as $|J, z\rangle$ labeled by both J and z .

²For this formula, we assume $\langle \hat{\xi}^a \rangle = 0$ for both states.

8.2.1 Entanglement production at instabilities

We studied the relationship between entropy production in classical dynamical systems and the growth of the entanglement entropy in their quantum analogue in the semiclassical regime. Most importantly, we found that in both cases the production rates are given by a sum over Lyapunov exponents λ_i characterizing stable and unstable phase space directions. For classical systems, there is a standard notion of rate, the Kolmogorov-Sinai entropy rate

$$h_{\text{KS}} = \sum_{\lambda_i > 0} \lambda_i \quad (8.7)$$

given by the sum over all positive Lyapunov exponents. For the associated quantum system and a subsystem A , we find that the production rate of the entanglement entropy $S_A(t) \sim \Lambda_A t$ is given by a subsystem exponent Λ_A . We have shown that $\Lambda_A \leq h_{\text{KS}}$ and found that this inequality is saturated for sufficiently large subsystems. Moreover, the rate Λ_A is independent of the initial state of the system and—except for a set of measure zero of subsystems—it depends on the choice of subsystem A only via its classical dimension N_A , i.e.

$$\Lambda_{A \text{ generic}} = \sum_{i=1}^{2N_A} \lambda_i, \quad (8.8)$$

where λ_i are the $2N_A$ largest Lyapunov exponents of the system. Our rigorous derivation of this result is based on the assumption of unstable quadratic Hamiltonian and Gaussian initial state. The derivation takes into account the case of time-dependent Hamiltonians with Floquet instabilities.

The derivation of the main theorem proving $S_A(t) \sim \Lambda_A t$ consists of three parts. First, the subsystem exponent Λ_A is introduced at the classical level as a generalization of Lyapunov exponents and defined to encode the exponential rate of growth of the volume of a symplectic cube in a subsystem under Hamiltonian evolution. Second, the time evolution of a Gaussian initial state through an unstable quadratic Hamiltonian is conveniently encoded in terms of complex structures or equivalently phase space metrics and their classical Hamiltonian flow. Third, the evolution of entanglement entropy is shown to be asymptotically the same as the one of the Renyi entropy which can then be shown to grow with the rate of the subsystem exponent Λ_A . We interpret the exponent Λ_A as a quantum analogue of the Kolmogorov-Sinai entropy rate of a given subsystem A .

The predicted linear growth of the entanglement entropy shows up in a wide range of physical systems such as unstable quadratic potentials, periodic quantum quenches in many-body quantum systems and instabilities in quantum field theory models. We presented three examples of the latter where entanglement is produced through different mechanisms, namely unstable modes due to a symmetry-breaking instability, parametric resonance in models of post-inflationary reheating, and cosmological perturbations in an inflationary spacetime.

For time-independent Hamiltonians, we can use Jordan normal form of the symplectic generator to distinguish three different types of contributions to the time evolution of the entanglement entropy: (a) an unstable part leading to linear growth associated to Lyapunov exponents, (b) a stable part leading to bounded oscillations of the entropy and (c) a metastable part contributing a logarithmic behavior of the entanglement entropy. Unstable Hamiltonians are not bounded from below and therefore are not physical as a complete description of a system. Rather they can appear as quadratic a expansion of an interacting Hamiltonian that is bounded from below or as Floquet Hamiltonian describing the characteristic features of a periodically driven system with explicit time-dependence.

An important question is how much of our results are still applicable to systems with non-quadratic Hamiltonians and non-Gaussian initial states. Due to the fact that there are very limited analytical tools available, we investigated this question numerically and could show that for quadratic Hamiltonians, but non-Gaussian initial states our results appear to hold without adjustment. For non-quadratic Hamiltonians, the situation is more difficult and in general we expect deviations. However, our numerical results suggest that for non-quadratic Hamiltonians with a leading quadratic part, we still see a phase of linear entropy growth predicted by the theorem. This phase stops at a scale when the higher order terms become relevant and the entanglement entropy saturates. This also implies that this linear phase is only seen for low entangled initial states and only if the scale of linear production is sufficiently separated from the scale of saturation.

We believe that our results are also relevant in the context of thermalization of isolated quantum systems. A subsystem of a chaotic quantum system is expected to thermalize with equilibrium entropy $S_{\text{eq}}(E)$ determined by the average energy E of the initial state. In the semiclassical regime we conjecture that the time-scale of this equilibration process is $\tau_{\text{eq}} \sim S_{\text{eq}}(E)/\Lambda_A(E)$ where $\Lambda_A(E)$ is the subsystem exponent of the energy-shell E .

8.2.2 Typical energy eigenstate entanglement

We studied the entanglement entropy averaged over all eigenstates of quadratic fermionic Hamiltonians. We could apply our methods because for every quadratic fermionic Hamiltonian, there exists a complete basis of energy eigenstates that are Gaussian. We derived a series of upper and lower bounds that converge to the average entanglement entropy as function of the subsystem fraction, *i.e.*, the number of sites V_A in the subsystem A divided by the total number of sites V . For translationally invariant Hamiltonians, we prove that the first order upper and lower bound is universal and explicitly given by

$$S^+(V_A) = V_A \ln 2 - \frac{1}{2} \frac{V_A^2}{V} \quad \text{and} \quad S^-(V_A) = V_A \ln 2 \left(1 - \frac{V_A^2}{V} \right). \quad (8.9)$$

An important implication of these bounds is that the average entanglement entropy for finite V_A/V is not maximally entangled, *i.e.*, given by $V_A \ln 2$. This implies that the ensemble of translationally invariant Gaussian energy eigenstates is not representative for the full ensemble of pure states in the full system, for which Don Page [162] proved that their average entanglement entropy with respect to the Haar measure becomes maximal in the thermodynamic limit.

As a concrete example, we analyzed the average bipartite entanglement entropy for the XY spin model by considering its Jordan-Wigner transform describing fermionic degrees of freedom. We consider a system in one dimension with L lattice sites and periodic boundary conditions, but our work can be generalized to higher dimensional models. The model requires careful treatment of the subtlety that the system Hamiltonian is only *almost* quadratic, *i.e.*, it is the sum of two quadratic Hamiltonian projected onto the even and odd Hilbert space sectors. We show that our methods apply and confirm analytically the previously established universal first order bound for the entanglement entropy as function of the subsystem size L_A . Moreover, we analyze how this bound is approached in the thermodynamic limit and find that the leading order correction is of order $\mathcal{O}(1/L^2)$, except when the model is critical and the leading order correction is given by $\mathcal{O}(1/L)$. A numerical study of this model shows the same behavior of the entanglement entropy, *i.e.*, not just the first order bound, but also the full von Neumann entropy approaches a universal value that only depends on the subsystem fraction $r = L_A/L$. Moreover, the numerics suggests that the finite size correction shows the same behavior as the analytical first order bound, namely that the finite size correction is of order $\mathcal{O}(1/L^2)$ except at criticality when we find $\mathcal{O}(1/L)$. This provides a

new perspective on criticality based on the average entanglement entropy rather than correlations in the ground state.

Based on the numerical results for XY model, we raised the question of whether the average entanglement entropy as function of the subsystem fraction $r = V_A/V$ approaches a universal value in the thermodynamic limit for translationally invariant systems. We investigate this question numerically for a specific subsystem sizes and different choices of translationally invariant quadratic models. Our numerical results strongly suggests that the answer is in the affirmative, which leads us to the formulation of a concrete and testable conjecture about the universal behavior of the entanglement entropy.

Based on this conjecture, we focus in our detailed analysis on the simplest translationally invariant model given by free fermions or, equivalently, by the Jordan-Wigner transform of the XX spin model. For this model, we developed a systematic method to compute the average trace of even powers of the linear complex structure based on generalized Wick contractions. We considered a system with L lattice sites arranged in a circle, but the results generalize to arbitrary dimensions. We could prove that the variance of the entanglement entropy per fermionic degree of freedom in a subsystem approaches zero as $1/\sqrt{L}$ in the thermodynamic limit $L \rightarrow \infty$. Applying our methods allowed us to compute the analytical bounds up to fourth order in the thermodynamic. At third order, we explain an efficient way of taking the thermodynamic limit to get a continuous function of the subsystem fraction $r = L_A/L$. At fourth order, we notice an important subtlety in computing higher order bounds due to additional non-analytical contributions for finite subsystem fraction. At this point, one can improve our bounds systematically in a straight forward way to any order that one wishes to compute.

8.2.3 Circuit complexity of Gaussian states

Our main result on circuit complexity of Gaussian states is our proof showing that the two different approaches of defining circuit complexity in field theories agree up to an overall normalization constant. This explains why different research groups using either of the two approaches have found very similar results when computing the circuit complexity of Gaussian states.

Approach A is based on work of Nielsen and collaborators [226] and defines circuit complexity as geodesic distance between group elements in the Gaussian Lie, *i.e.*, the symplectic group for bosons and the orthogonal group for fermions, where one needs to choose a right-invariant metric. Approach B defines circuit complexity directly on the manifold of Gaussian states, namely as the geodesic distance between two states with respect to the canonical Fubini-Study metric induced by the Hilbert space inner product. Even though both approaches define circuit complexity as the geodesic distance, there are important differences. Approach A requires a choice of metric and is based on the higher dimensional group manifold, while approach B uses a canonical metric and is thus completely fixed once one decides to compute it on the manifold of Gaussian states, *i.e.*, a sub manifold of the space of all pure states where geodesics are trivially given by generalized great circles.

For approach A, we choose a canonical right-invariant metric that is induced by a positive definite metric G_R^{ab} on dual phase space, namely the symmetric covariance matrix of the reference state $|J_R\rangle$. For this choice, we prove that the minimal geodesic that connects the identity to a group element preparing a specified target state $|J_T\rangle$ is generated by a Lie algebra element in $\mathfrak{u}_\perp(N)$, namely the orthogonal complement of sub Lie algebra $\mathfrak{u}(N)$ of generators that leave the reference state invariant. This leads to the simple formula

$$\mathcal{C}_2^{(N)}(|J_R\rangle \rightarrow |J_T\rangle) = \frac{1}{2} \sqrt{\text{Tr}|\log \Delta|^2} \quad \text{with} \quad \Delta = -J_T J_R, \quad (8.10)$$

that expresses the circuit complexity in approach A (Nielsen) in terms of a trace over the relative covariance matrix Δ .

For approach B, we compute the pullback of the Fubini-Study metric to the Lie group considered in approach A. We show that the pullback is a left-invariant metric on the group manifold and the inner product on the Lie algebra, *i.e.*, the tangent space at the identity, agrees up to a constant when restricted to the subspace $\mathfrak{u}_\perp(N)$. This allows us to identify geodesics on the state manifold in approach B with the minimal geodesics found in approach A on the sub manifold generated by $\mathfrak{u}_\perp(N)$. In particular, we prove that the geodesic length agrees in both approaches up to the overall normalization constant.

Chapter 9

Beyond Gaussian states

We conclude by discussing directions to generalize some of the presented methods beyond Gaussian states. In the language of quantum field theory or condensed matter physics, Gaussian states correspond to ground states of free theories and as soon as we are interested in interacting theories, the true eigenstates are not Gaussian anymore. In particular, when studying time-evolution of non-quadratic systems, an initially Gaussian state will not stay Gaussian. For general non-Gaussian states, we do not have analytical expressions of the entanglement entropy and the general eigenvalues of the reduced density operators (entanglement spectrum). We cannot hope to generalize our tools to any state in the Hilbert space, but it might be possible to extend the manifold of Gaussian states meaningfully. The challenge is to find a compromise between giving up enough structure to increase the set of states sufficiently to capture new interesting physical properties, while retaining the ability to perform efficient analytical computations.

In this dissertation, we saw that we can use Gaussian states for a wide range of applications and are even able to probe some aspects of the non-Gaussian regime. In the context of entanglement production, we saw that we can use the covariance matrix of non-Gaussian states to bound their entanglement entropy from above by using the inequality presented in section 5.1.3 for bosons. We can run the same argument also for fermionic systems, which means that we can use Gaussian methods to compute an upper bound for the entanglement entropy of any state with a well-defined covariance matrix.¹ Time evolution and ground states of interacting Hamiltonians can also be approximated by Gaussian states using variational methods, where we restrict the Hamiltonian flow to the manifold of Gaussian states and look for the Gaussian state with the lowest energy expectation value. However, there are certain shortcomings of Gaussian states that cannot be overcome in principle. A very important limitation lies in the fact that Gaussian states cannot admit quantum correlations between bosonic and fermionic degrees of freedom in mixed systems, because Gaussian states are necessarily product states. Another limitation concerns the type of superpositions that they can describe. Bosonic Gaussian states naturally describe semi-classical configurations associated to the phase space point where the Gaussian is peaked. The covariance matrix encodes the quantum fluctuations around such a classical configuration. However, when one is interested in describing the superposition of two or more classical configurations, Gaussian states cannot capture enough features of the original states. This can be directly understood from the fact that Gaussian states will always be peaked at a single phase space point and even for a double peak distribution, a Gaussian approximation would not be very suitable.

Gaussian states are widely used due to their desirable properties for analytic calculations. We found rich structures that allowed compact expressions and elegant formulas that capture relevant

¹For instance, there are mixed bosonic states where the covariance matrix diverges and is thus ill defined.

features. Our intuition was often guided by finding standard forms of finite dimensional objects, such as the covariance matrix, which encoded the correlations between bosonic or fermionic degrees of freedom. Let us list the most important features that were crucial for understanding of Gaussian states.

1. Wick's theorem

Being able to compute all higher order n -point functions from the two point function (covariance matrix) is not only useful for practical calculations, but provides the conceptual justification why we can label states in large or infinite dimensional Hilbert spaces by finite dimensional objects, namely the covariance matrix or linear complex structures. Expanding states in a Hilbert space basis would not be feasible for many analytical computations and any numerical approach would be restricted to Hilbert space truncations or systems with only a few degrees of freedom. Moreover, the interplay between parametrization and the natural group actions enables us to consider dynamical situations where Gaussian states evolve into other Gaussian states.

2. Natural group action

Bosonic and fermionic Gaussian states come naturally with a group action that is closed on the set of Gaussian states. For bosons, this group is either the symplectic group, when considering homogeneous Gaussian states, or the inhomogeneous symplectic group, when considering inhomogeneous Gaussian states. For fermions, the group is given by the orthogonal or special orthogonal group. By using some natural parametrization of Gaussian states, for instance the covariance matrix or the linear complex structure, we can discuss time evolution and perturbations of Gaussian states purely in terms of finite dimensional group representations, without any requirement to deal with the high dimensional Hilbert space.

When moving beyond Gaussian states, we need to give up some structure and in particular, we will not be able to extend the natural group action. The Lie algebra of the symplectic or orthogonal group was generated by quadratic operators

$$\hat{H} = \frac{1}{2} h_{ab} \hat{\xi}^a \hat{\xi}^b, \quad (9.1)$$

such that it might seem natural to extend the set of Gaussian states by allowing for higher order generators. Unfortunately, the bosonic commutation relations and the fermionic anti commutation relations imply that the Lie algebra of generators up to order n is not closed, *i.e.*, commutators of these generators give rise to new generators of order higher than n . From a group theoretic perspective, we are asking if there is a Lie group that is larger than the symplectic or orthogonal group, but smaller than the full unitary group $U(\mathcal{H})$ of the Hilbert space \mathcal{H} . Unfortunately, the answer is in the negative, so that we cannot expect to construct a class of generalized Gaussian states directly from some group action.²

Instead of demanding that there is a natural group action on the extended manifold of generalized Gaussian states (GGS) \mathcal{M}_{GGS} , we can at least require that the Gaussian group \mathcal{G} , *i.e.*, the symplectic group for bosons and the orthogonal group for fermions, preserves the manifold. Given a group element M , we can refer to the associated unitary map as $U(M)$. Given two generalized Gaussian states $|\psi\rangle$ and $|\tilde{\psi}\rangle$, we can define the equivalence relation $|\psi\rangle \sim |\tilde{\psi}\rangle$ if and only if there exists a group element $M \in \mathcal{G}$, such that $|\tilde{\psi}\rangle = U(M)|\psi\rangle$. One of the resulting equivalence classes is

²We should emphasize that there are of course other subgroups of $U(\mathcal{H})$, for instance for $\mathcal{H} = \mathcal{H}_A \otimes \mathcal{H}_B$, we have the subgroups $U(\mathcal{H}_A) \otimes \mathbb{1}, \mathbb{1} \otimes U(\mathcal{H}_B) \subset U(\mathcal{H})$. However, these subgroups are restricted to subsystems and do not provide the desired properties of parameterizing low dimension sub manifold of states.

given by the manifold of Gaussian states $\mathcal{M}_G \subset \mathcal{M}_{GS}$ isomorphic to $\mathcal{G}/U(N)$. For a non-Gaussian states, we do not expect to find a non-trivial stabilizer subgroup

$$\text{Sta}_{|\psi\rangle} = \{M \in \mathcal{G} \mid U(M)|\psi\rangle = |\psi\rangle\}. \quad (9.2)$$

Therefore, we do expect the equivalence class $[\!| \psi \rangle]$ to be generically diffeomorphic to \mathcal{G} , but exploring the details of the resulting geometry depends highly on the particular choice of extending the manifold \mathcal{M}_{GS} of Gaussian states.

For Gaussian states, we could use the linear complex structure J as an invariant way to describe the space of annihilation operators associated to the Gaussian state $|J\rangle$. This worked well because this space could always be identified with a subspace $V^+ \subset V_{\mathbb{C}}$ of complexified phase space. For generalized Gaussian states, we may still be able to define a space of annihilation operators, but this space will in general be a linear sub space of complexified algebra of observables, *i.e.*, the complex vector space spanned by arbitrary powers of $\hat{\xi}^a$. Given a non-Gaussian state $|\psi\rangle$, we can always find unitaries U , such that $U|J\rangle = |\psi\rangle$ for some Gaussian state $|J\rangle$. Any annihilation operator a_i with $a_i|J\rangle = 0$ will be mapped to an operator $b_i = Ua_iU^\dagger$ that annihilates $|\psi\rangle$. The non-Gaussian annihilation operators b_i will not be linear in ξ^a , but can be encoded through a non-linear Bogoliubov transformation that captures the relevant information contained in U to define $|\psi\rangle$. However, we will need to face the challenge that U is not unique and different choices will give rise to different spaces of annihilation operators. In order to generalize our methods based on linear complex structures, we will most likely need to find a way to get rid of this redundancy—for example by restricting to certain classes of sub spaces of the algebra of observables. Again, these ideas are best tested with a concrete proposal for the manifold \mathcal{M}_{GGS} in mind.

A set of promising ideas to define generalized Gaussian states was proposed by Tao Shi and collaborators in [35]. Here, the idea is to start with a Gaussian state $|J\rangle$ and then act with an operator of the form $e^{i\gamma_{ij}\hat{n}^i\hat{n}^j}$ on it, where \hat{n}^i refer to some set of number operators (not the ones associated $|J\rangle$). This was proposed for bosonic and fermionic systems, but a similar operator $e^{i\gamma_{ia}\hat{n}^i\hat{\xi}^a}$ can also be applied to mixtures where \hat{n}^i is a fermionic number operator, while $\hat{\xi}^a$ refers to the bosonic degrees of freedom. The focus of [35] was mostly to define extended variational manifolds to approximate ground states and low excited states, but we can also ask about the information theoretic properties of these states, in particular about their entanglement entropy. Even though, these states do not satisfy Wick's theorem directly, the computations of higher order correlation functions can be reduced to expectation values of Gaussian states where Wick can be applied. However, to use such extended classes of states it is important to understand any redundancies in their parametrization and develop a solid intuition for the resulting geometry of the state manifold \mathcal{M}_{GGS} .

A consistent framework for the treatment and parametrization of generalized Gaussian states will have a wide range of applications, but it is not clear yet which tools and methods from Gaussian states can be generalized in a meaningful way. We believe that a geometric approach combined with Lie group theoretic methods appears to be promising.

Appendices

Appendix A

Standard form of restricted linear complex structures

When we use linear complex structures to parametrize Gaussian states, we are particularly interested properties of pure states restricted to subsystems. Restricted states are in general mixed and their properties are fully encoded in the restriction of the linear complex structure to the sub phase space associated to the subsystem. Most properties of the restricted state, such as the von Neumann entropy and the full entanglement spectrum, are independent from any choice of basis that we use to represent the linear complex structure as matrix. They are encoded in the eigenvalues of the restricted complex structure and we will derive their properties due to compatibility conditions with the symplectic form for bosonic systems or positive-definite metric for fermionic systems. This appendix is based on the respective appendix in [LH15].

Definition 1

Given a finite-dimensional real vector space V , we refer to a linear map $J : V \rightarrow V$ as complex structure if it satisfies $J^2 = -\mathbb{1}$.

The spectrum of a linear complex structure takes the following simple form.

Proposition 1

A complex structure is diagonalizable with eigenvalues that come in conjugate pairs as $\pm i$ with equal multiplicity. This also implies that V must be even dimensional.

Proof: As a linear map, J can be decomposed in a sum of a diagonalizable (over \mathbb{R}) map D and a nilpotent map N , such that $J = D + N$ and $DN = ND$. We can therefore read

$$J^2 = D^2 + (2D + N)N = -\mathbb{1}. \quad (\text{A.1})$$

At this point, we must have $(2D + N)N = 0$ which implies $N = 0$ because the linear map $(2D + N) = J + D$ has full rank (due to the fact that J^2 has full rank).

We have $J^2 = D^2$ which implies that every eigenvalue squares to -1 . Moreover, J is a real map which means that all eigenvalues come in complex conjugate pairs of equal multiplicity. Thus, the spectrum of J is given by $\pm i$ with equal multiplicity equal to half of the dimension of V .

The last part implies that such a linear map J can only exist in an even dimensional real vector space V . \square

We will be particularly interested in the restriction of linear complex structures.

Proposition 2

Given a complex structure J over V , every direct sum decomposition of $V = A \oplus B$ with

$A, B \subset V$ gives rise to unique decomposition of J as

$$J = \left(\begin{array}{c|c} J_A & J_{AB} \\ \hline J_{BA} & J_B \end{array} \right) \quad \text{with} \quad \begin{array}{lll} J_A : A \rightarrow A & : a \mapsto p_A(Ja), \\ J_B : B \rightarrow B & : b \mapsto p_B(Jb), \\ J_{AB} : B \rightarrow A & : b \mapsto p_A(Jb), \\ J_{BA} : A \rightarrow B & : a \mapsto p_B(Ja), \end{array} \quad (\text{A.2})$$

where the projection maps $p_A : V \rightarrow A$ and $p_B : V \rightarrow B$ with $p_A + p_B = \mathbb{1}$ provide the unique decomposition of a vector $v = a + b$ into its part in $a = p_A(v) \in A$ and $b = p_B(v) \in B$.

Given such a decomposition, the spectrum of J_A^2 and J_B^2 is the same except for the number of -1 as eigenvalues. Put differently, given an eigenvalue λ of J_A^2 , we have $\lambda = -1$ or J_B^2 also must have λ as an eigenvalue.

Proof: We can write down $J^2 = -\mathbb{1}$ in blocks to find

$$J^2 = \left(\begin{array}{c|c} J_A^2 + J_{AB}J_{BA} & J_AJ_{AB} + J_{AB}J_B \\ \hline J_BJ_{BA} + J_{BA}J_A & J_B^2 + J_{BA}J_{AB} \end{array} \right) = \left(\begin{array}{c|c} -\mathbb{1}_A & 0 \\ \hline 0 & -\mathbb{1}_B \end{array} \right) = -\mathbb{1}, \quad (\text{A.3})$$

Let us consider the eigenvector $a \in A$ with $J_A^2 a = \alpha a$. From the first diagonal block equation, we find that a must also be eigenvector of $J_{AB}J_{BA}$ with $J_{AB}J_{BA} a = -(1 + \alpha)a$. Let us define $b := J_{BA} a$. Now there are two possibilities: Either $b = 0$ which implies $\alpha = -1$ or $b \neq 0$, in which case we must have $J_{BA}J_{AB} b = -(1 + \alpha)J_{BA} a = -(1 + \alpha)b$. The second diagonal block equation then implies $J_B^2 b = \alpha b$. \square

A.1 Compatible symplectic form (bosons)

For bosonic systems, we are interested in linear complex structures that are compatible with the underlying symplectic form or vice versa.

Definition 2

An antisymmetric, non-degenerate bilinear form $\omega : V \times V \rightarrow \mathbb{R}$ is called compatible to a complex structure $J : V \rightarrow V$ if and only if it satisfies the following conditions:

- (I) Skew-symmetry: The symplectic form satisfies $\omega(Jv, w) = -\omega(v, Jw)$.
- (II) Taming: The bilinear form $g(v, w) := \omega(v, Jw)$ is positive definite.

We will just refer to ω as a J -compatible symplectic form and to J as a ω -compatible complex structure.

The compatibility conditions implies the following invariance property.

Proposition 3

A J -compatible symplectic form ω is invariant under J meaning $\omega(Jv, Jw) = \omega(v, w)$ for all $v, w \in V$ which implies $J \in \text{Sp}(V, \omega)$. The bilinear form $g(v, w) := \omega(v, Jw)$ is symmetric and positive definite and thus a proper metric.

Proof: The computation is straightforward and we find

$$\omega(Jv, Jw) = -\omega(v, J^2w) = -\omega(v, -\mathbb{1}w) = \omega(v, w). \quad (\text{A.4})$$

Every linear map $M : V \rightarrow V$ that preserves the symplectic form ω in the sense of $\omega(Mv, Mw) = \omega(v, w)$ is part of the symplectic group $\text{Sp}(V, \omega)$. We can now define the positive bilinear form

$g(v, w) = \omega(v, Jw)$ which is also symmetric due to

$$g(v, w) = \omega(v, Jw) = -\omega(Jw, v) = \omega(w, Jv) = g(w, v). \quad (\text{A.5})$$

Moreover, the property (II) Taming of a ω -compatible complex structure ensures that g is also positive definite and thus a proper positive definite metric. \square

The compatibility condition alone determines the possible spectra of the linear complex structure restricted to symplectic subspaces.

Proposition 4

Given a compatible pair of a complex structure J and a symplectic form ω , we can decompose the vector space V into a direct sum of even dimensional symplectic complements $V = A \oplus B$. In this case, the restricted complex structure J_A is diagonalizable and its spectrum consists of complex conjugate pairs $\pm ic$ with $c \in [1, \infty)$. We can always bring J_A and ω_A simultaneously in the following block diagonal form:

$$J_A \equiv \bigoplus_{i=1}^{N_A} \begin{pmatrix} 0 & -c_i \\ c_i & 0 \end{pmatrix} \quad \text{and} \quad g_A \equiv \bigoplus_{i=1}^{N_A} \begin{pmatrix} 0 & -1 \\ 1 & 0 \end{pmatrix}. \quad (\text{A.6})$$

Here, we have $c_i \in [1, \infty)$.

Proof: The restricted complex structure J_A is itself anti-hermitian with respect to the metric g_A because we have for $a_1, a_2 \in A$

$$g_A(J_A a_1, a_2) = g(J_A a_1, a_2) = \omega(J_A a_1, J_A a_2) = -\omega(a_1, J^2 a_2) = -g_A(a_1, J_A a_2). \quad (\text{A.7})$$

Therefore, J_A is normal¹ with respect to g_A . This ensures that J_A is diagonalizable (with a complete set of eigenvectors) and so is J_A^2 .

Given a non-zero eigenvector $a \in A$ with $J_A^2 a = \alpha a$, we have $\alpha \in (-\infty, -1]$ due to the following argument. Let us compute

$$\underbrace{\alpha g(a, a)}_{>0} = g(a, J_A^2 a) = -\underbrace{g(J_A a, J_A a)}_{\geq 0}. \quad (\text{A.8})$$

This already implies that $\alpha \leq 0$. Moreover, we can also compute

$$g(J_A a, J_A a) = g(Ja - J_B a, Ja - J_B a) \quad (\text{A.9})$$

$$= \underbrace{g(Ja, Ja)}_{=g(a,a)\geq 0} + \underbrace{g(J_B a, J_B a)}_{\geq 0} - 2 \underbrace{g(Ja, J_B a)}_{=0}, \quad (\text{A.10})$$

where we used in the last step that A and B are symplectic complements with $g(Ja, J_B a) = \omega(Ja, JJ_B a) = -\omega(J^2 a, J_B a) = \omega(a, J_B a) = 0$. We thus find the inequality $g(J_A a, J_A a) \geq g(a, a)$ leading to $\alpha \in (-\infty, -1]$.

From here, we find that J_A must have eigenvalues appearing in complex conjugate pairs $\pm ic$ with $c = \sqrt{-\alpha}$ meaning that also every eigenvalue α of J_A^2 appears with even multiplicity unless $\alpha = 0$. In particular, for odd dimensional subspaces A and B , there must be at least one zero eigenvalue of both J_A^2 and J_A .

Every linear real map with complex conjugated eigenvalues $\pm ic_i$ can be brought into block diagonal form with antisymmetric blocks proportional to c_i . Due to the fact that J is symplectic, we can always choose a symplectic Darboux basis in which J_A and ω take the described form. \square

¹Recall that a linear map is called normal if it commutes with its adjoint. Finding that J_A is anti-hermitian with respect to the metric g_A implies that the adjoint is given by $J_A^* = -J_A$ which obviously commutes with J_A .

This result is central for computing the entanglement spectrum of bosonic systems. In particular, the fact that the magnitude of possible eigenvalues lies in the interval $[1, \infty)$ implies that the entanglement entropy of bosonic systems can be arbitrarily large. This can also be related to the non-compactness of symplectic group whose group elements relate different linear complex structures.

A.2 Compatible positive definite metric (fermions)

We can repeat a very similar analysis for fermionic systems, where we study the properties of a linear complex structure compatible to a positive definite metric.

Definition 3

A positive definite symmetric bilinear form $g : V \times V \rightarrow \mathbb{R}$ is called compatible to a complex structure $J : V \rightarrow V$ if and only if it satisfies

$$g(Jv, w) = -g(v, Jw) \quad \text{for all } v, w \in V. \quad (\text{A.11})$$

We will just refer to g as a J -compatible metric and to J as a g -compatible complex structure.

The compatibility conditions implies the following invariance property.

Proposition 5

A J -compatible metric g is invariant under J meaning $g(Jv, Jw) = g(v, w)$ for all $v, w \in V$ which implies $J \in O(V, g)$. Moreover, we can define the antisymmetric bilinear form $\omega(v, w) = g(Jv, w)$ which is a well-defined symplectic form on V .

Proof: The computation is straightforward and we find

$$g(Jv, Jw) = -g(v, J^2w) = -g(v, -\mathbb{1}w) = g(v, w). \quad (\text{A.12})$$

Every linear map $M : V \rightarrow V$ that preserves metric g in the sense of $g(Mv, Mw) = g(v, w)$ is part of the orthogonal group $O(V, g)$. A symplectic form on a vector space V is required to be (a) antisymmetric and (b) non-degenerate:

- (a) Antisymmetry: We compute $\omega(v, w) = g(Jv, w) = g(w, Jv) = -g(Jw, v) = -\omega(w, v)$.
- (b) Non-Degeneracy: We need to show that for every non-zero vector v , there is at least one vector w , such that $\omega(v, w) \neq 0$. This can easily be done by choosing $w = Jv$, where we find $\omega(v, w) = g(Jv, Jv) > 0$.

This proves that every compatible pair of a complex structure J and a metric g defines a symplectic form ω . \square

Again, the compatibility condition alone determines the possible spectra of the linear complex structure restricted to even dimensional subspaces.

Proposition 6

Given a compatible pair of a complex structure J and a metric g , we can decompose the vector space V into a direct sum of orthogonal sum of orthogonal complements $V = A \oplus B$. In this case, the restricted complex structure J_A is diagonalizable and its spectrum consists of complex conjugate pairs $\pm ic$ with $c \in [0, 1]$. If A is odd-dimensional, J_A also has the eigenvalue 0. Provided that we choose a decomposition into even-dimensional orthogonal complements with dimensions $2N_A$ and $2N_B$, we can always bring J_A and g_A simultaneously in the following block

diagonal form:

$$J_A \equiv \bigoplus_{i=1}^{N_A} \begin{pmatrix} 0 & -c_i \\ c_i & 0 \end{pmatrix} \quad \text{and} \quad g_A \equiv \bigoplus_{i=1}^{N_A} \begin{pmatrix} 1 & 0 \\ 0 & 1 \end{pmatrix}. \quad (\text{A.13})$$

Here, we have $c_i \in [0, 1]$.

Proof: The restricted complex structure J_A is itself anti-hermitian with respect to the metric g_A because we have for $a_1, a_2 \in A$

$$g_A(J_A a_1, a_2) = g(J a_1, a_2) = -g(a_1, J a_2) = -g_A(a_1, J_A a_2). \quad (\text{A.14})$$

Therefore, J_A is normal with respect to g_A . This ensures that J_A is diagonalizable (with a complete set of eigenvectors) and so is J_A^2 .

Given a non-zero eigenvector $a \in A$ with $J_A^2 a = \alpha a$, we have $\alpha \in [-1, 0]$ due to the following argument. Let us compute

$$\underbrace{\alpha g(a, a)}_{>0} = g(a, J_A^2 a) = -\underbrace{g(J_A a, J_A a)}_{\geq 0}. \quad (\text{A.15})$$

This already implies that $\alpha \leq 0$. Moreover, we can also compute

$$g(a, a) = g(J a, J a) = g(J_A a + J_{BA} a, J_A a + J_{BA} a) = g(J_A a, J_A a) + g(J_{BA} a, J_{BA} a), \quad (\text{A.16})$$

where we used in the last step that A and B are orthogonal which eliminates crossing terms. This equation implies the inequality $g(a, a) \geq g(J_A a, J_A a)$ leading to $\alpha \in [-1, 0]$.

From here, we find that J_A must have eigenvalues appearing in complex conjugate pairs $\pm i c$ with $c = \sqrt{-\alpha}$ meaning that also every eigenvalue α of J_A^2 appears with even multiplicity unless $\alpha = 0$. In particular, for odd dimensional subspaces A and B , there must be at least one zero eigenvalue of both J_A^2 and J_A .

Every linear real map with complex conjugated eigenvalues $\pm i c_i$ can be brought into block diagonal form with antisymmetric blocks proportional to c_i . Due to the fact that J is orthogonal, we can always choose an orthonormal basis in which J_A takes the described form. \square

This result is central for computing the entanglement spectrum of fermionic systems. In particular, the fact that the magnitude of possible eigenvalues lies in the interval $[0, 1]$ implies that the entanglement entropy of fermionic systems is bounded by $\log 2$ per fermionic degree of freedom.

Appendix B

Dynamical systems and Lyapunov exponents

We summarize relevant properties of Lyapunov exponents in the context of Hamiltonian systems. In particular, we make precise the notion of *regular Lyapunov system*. This appendix is based on the respective appendix in [LH08].

B.1 Linear Hamiltonian systems

We consider a $2N$ -dimensional linear phase space V with symplectic form ω . A time-dependent Hamiltonian H is a smooth map

$$H : V \times \mathbb{R} \rightarrow \mathbb{R} : (\xi, t) \rightarrow H(\xi, t). \quad (\text{B.1})$$

The equations of motion are given by

$$\dot{\xi}^a(t) = \Omega^{ab}(dH)_b(t), \quad (\text{B.2})$$

where Ω^{ab} satisfies $\omega_{ac}\Omega^{bc} = \delta_a^b$ and $(dH)_b(t)$ is the gradient of H at time t . The solution of these equations can be conveniently described by a flow

$$\Phi_t : V \rightarrow V : \xi \rightarrow \Phi_t \xi. \quad (\text{B.3})$$

This map is a diffeomorphism that preserves the symplectic form ω , namely the push-forward satisfies $(\Phi_t)_*\omega = \omega$. For a given point $\xi_0 \in V$, the push-forward $(\Phi_t)_*$ maps a tangent vector $\delta\xi \in T_{\xi_0}V$ to the tangent vector $(\Phi_t)_*\delta\xi \in T_{\Phi_t(\xi_0)}V$. Due to the linearity of V , we can identify the tangent spaces at all points with V itself. Formally, we have an isomorphism $\phi_\xi : V \rightarrow T_\xi V$ that maps $v \in V$ to the tangent vector $\phi_\xi v \in T_\xi V$ that acts on a function $f : V \rightarrow \mathbb{R}$ as $\phi_\xi v(f) = \frac{d}{dt}f(\xi + tv)$. Using ϕ_ξ , we can define the linear map $M_{\xi_0}(t) : V \rightarrow V$

$$M_{\xi_0}(t) = \phi_{\Phi_t(\xi_0)}^{-1} \circ (\Phi_t)_* \circ \phi_{\xi_0}, \quad (\text{B.4})$$

that corresponds to the above push-forward after we identify $T_{\xi_0}V$ and $T_{(\Phi_t)\xi_0}V$ with V .

In the special case, where the Hamiltonian H is given by a linear quadratic function

$$H(\xi, t) = f_a(t)\xi^a + \frac{1}{2}h_{ab}(t)\xi^a\xi^b \quad (\text{B.5})$$

for every t , the Hamiltonian flow is given by an inhomogeneous symplectic transformation $(M(t), \eta(t))$ via

$$\Phi_t \xi_0 = M(t) \xi_0 + \eta(t), \quad (\text{B.6})$$

whose differential is given by $M_{\xi_0}(t) = M(t)$, independent of ξ_0 . This follows from the fact that a quadratic Hamiltonian gives rise to linear and homogeneous equations of motion. The symplectic group element $M(t)$ is formally given by the time-ordered exponential

$$M(t)^a{}_b = \mathcal{T} \exp \left(\int_0^t dt' K(t')^a{}_b \right) \quad \text{with} \quad K(t)^a{}_b = \Omega^{ac} h(t)_{cb}, \quad (\text{B.7})$$

where the generator $K(t)$ is an element of the symplectic Lie algebra $\text{sp}(2N)$.

In the general case, where H is not quadratic, we can still find the time-dependent generator $K_{\xi_0}(t)^a{}_b = \Omega^{ac} h_{\xi_0}(t)_{cb}$. In this case, however, the generator also depends on the initial ξ_0 . To find $h_{\xi_0}(t)_{cb}$, we just need to Taylor expand the Hamiltonian $H(t)$ along the trajectory $\xi(t) = \Phi_t \xi_0$ which amounts to finding its Hessian

$$h_{\xi_0}(t)_{ab} = \partial_a \partial_b H(t)|_{\Phi_t \xi_0}. \quad (\text{B.8})$$

At this point, we understand that the difference between the special (quadratic) and general case (arbitrary Hamiltonian) in regards of the linear map $M_{\xi_0}(t)$ are the following:

- If the Hamiltonian is quadratic or affine quadratic, the linear map $M(t)$ describing the push-forward of the Hamiltonian flow Φ_t is independent of the starting point ξ_0 and completely characterized by the quadratic part $h(t)_{ab}$ of $H(t)$.
- For a more general Hamiltonian, we can still compute its quadratic part $h_{\xi_0}(t)_{ab}$ as Hessian of $H(t)$ along the trajectory $\xi(t)$. This means $h_{\xi_0}(t)_{ab}$ depends on the initial condition ξ_0 and the corresponding solution $\xi(t)$ with $\xi(t) = \xi_0$. In particular, the quadratic map $M_{\xi_0}(t)$ will differ for different initial conditions ξ_0 .

The linear symplectic map $M_{\xi_0}(t)$ contains all the information about how two sufficiently close trajectories converge or diverge. This behavior will be captured in the so called Lyapunov exponents.

In order to define Lyapunov exponents, we need to equip phase space V with a positive definite metric g_{ab} that gives rise to a norm $\|\delta\xi\| = \sqrt{g_{ab}\delta\xi^a\delta\xi^b}$. Equivalently, we can use the inverse metric G^{ab} to define the norm $\|\ell\| = \sqrt{G^{ab}\ell_a\ell_b}$ on the dual phase space V^* . We will show that Lyapunov exponents are actually independent of the specific choice of a positive metric. In order to show this, it is useful to have the following theorem at hand.

Proposition 7

Given a finite dimensional, real vector space V and two distinct positive metrics g and \tilde{g} , we can compute the following two values

$$a := \min_{\|v\|_g=1} \|v\|_{\tilde{g}} > 0, \quad b := \max_{\|v\|_g=1} \|v\|_{\tilde{g}} > 0, \quad (\text{B.9})$$

which allow us to relate norms and angles measured by the different metrics:

• Norm inequality

Given a vector $v \in V$, its norm $\|v\|_{\tilde{g}}$ with respect to \tilde{g} is related to $\|v\|_g$ via:

$$a\|v\|_g \leq \|v\|_{\tilde{g}} \leq b\|v\|_g. \quad (\text{B.10})$$

- **Angle inequality**

Given an angle $\tilde{\psi}$ between two vectors measured with respect to \tilde{g} , it is related to the angle ψ measured with respect to g via the following inequality:

$$\frac{1 - (b/a)^2 \tan^2(\psi/2)}{1 + (b/a)^2 \tan^2(\psi/2)} \leq \cos \tilde{\psi} \leq \frac{1 - (a/b)^2 \tan^2(\psi/2)}{1 + (a/b)^2 \tan^2(\psi/2)}. \quad (\text{B.11})$$

This inequality can be simplified to the slightly weaker version given by:

$$\frac{a\psi}{b} \leq \tilde{\psi} \leq \frac{b\psi}{a}. \quad (\text{B.12})$$

- **Volume inequality**

Given the d -volume $\text{Vol}_{\tilde{g}}(\mathcal{V}_A)$ of some region \mathcal{V}_A in an arbitrary d -dimensional subspace $A \subset V$ measured by the metric \tilde{g} , it is related to the d -volume $\text{Vol}_g(\mathcal{V}_A)$ measured by g via the following inequality:

$$a^d \text{Vol}_{\tilde{g}}(\mathcal{V}_A) \leq \text{Vol}_{\tilde{g}}(\mathcal{V}_A) \leq b^d \text{Vol}_g(\mathcal{V}_A). \quad (\text{B.13})$$

If consider the same equations for the dual phase space V^* with the replacements $g \rightarrow G$ and $\tilde{g} \rightarrow \tilde{G}$, all inequalities hold if we replace $a \rightarrow 1/b$ and $b \rightarrow 1/b$.

Proof: Let us prove the different inequalities:

- Norm inequality

Let us take two different norms induced by the two positive metrics g and \tilde{g} . Over a finite dimensional vector space V the set $S = \{v \in V \mid \|v\|_g = 1\}$ is compact. This means that the continuous function $\|v\|_{\tilde{g}}$ will take a minimal and maximum value on S :

$$a := \min_{v \in S} \|v\|_{\tilde{g}} > 0, \quad b := \max_{v \in S} \|v\|_{\tilde{g}} > 0. \quad (\text{B.14})$$

Linearity of the induced norm implies than the inequality that we wanted to prove:

$$a\|v\|_g \leq \|v\|_{\tilde{g}} \leq b\|v\|_g \quad \text{for all } v \in V. \quad (\text{B.15})$$

- Angle inequality

Let us choose a two-dimensional plane $P \subset V$. On this plane, we have the restricted metrics $g|_P$ and $\tilde{g}|_P$. The two are related by a linear map $D : P \rightarrow P$ with

$$(\tilde{g}|_P)_{ab} = D^c{}_a D^d{}_b (g|_P)_{cd}, \quad (\text{B.16})$$

where D is not unique. We can always choose it to be diagonalizable with ordered eigenvalues d_i and eigenvectors e_i . At this point, we can identify the inner product with respect to \tilde{g} as the one with respect to g after having acted with D on the vectors. This implies $a \leq d_i \leq b$ to not violate the norm inequality. Let us choose two unit vectors $v, w \in P$ that form an angle ψ with respect to g and whose angle bisector lies at an angle of ϕ to e_1 :

$$v = \cos(\phi + \psi/2)e_1 + \sin(\phi + \psi/2)e_2 \quad (\text{B.17})$$

$$w = \cos(\phi - \psi/2)e_1 + \sin(\phi - \psi/2)e_2 \quad (\text{B.18})$$

We can compute the deformed angle $\tilde{\psi}(\psi, \phi)$ from the deformed vectors

$$Dv = d_1 \cos(\phi + \psi/2)e_1 + d_2 \sin(\phi + \psi/2)e_2 \quad (\text{B.19})$$

$$Dw = d_1 \cos(\phi - \psi/2)e_1 + d_2 \sin(\phi - \psi/2)e_2, \quad (\text{B.20})$$

by using the arctangent rules with respect to g based on $\langle v, w \rangle_{\tilde{g}} = \langle Dv, Dw \rangle_g$:

$$\tilde{\psi}(\psi, \phi) = \arctan(d_2/d_1 \tan(\phi + \psi/2)) - \arctan(d_2/d_1 \tan(\phi - \psi/2)). \quad (\text{B.21})$$

By taking the derivative with respect to ϕ , we can find the minimum and maximum of this function for fixed ψ . The minimum is at $\phi = 0$ and the maximum at $\phi = \pi/2$ (recall that we chose $d_2 > d_1$). Evaluating $\tilde{\psi}(\psi, \phi)$ at these values leads to the inequality

$$\frac{1 - (d_2/d_1)^2 \tan^2(\psi/2)}{1 + (d_2/d_1)^2 \tan^2(\psi/2)} \leq \cos \tilde{\psi} \leq \frac{1 - (d_1/d_2)^2 \tan^2(\psi/2)}{1 + (d_1/d_2)^2 \tan^2(\psi/2)}. \quad (\text{B.22})$$

This interval becomes maximal when d_1/d_2 is as small as possible, but for a given metric \tilde{g} , we have $d_1/d_2 \in [a/b, 1]$ for any plane $P \in V$. Thus, we find the following bound

$$\frac{1 - (b/a)^2 \tan^2(\psi/2)}{1 + (b/a)^2 \tan^2(\psi/2)} \leq \cos \tilde{\psi} \leq \frac{1 - (a/b)^2 \tan^2(\psi/2)}{1 + (a/b)^2 \tan^2(\psi/2)}, \quad (\text{B.23})$$

which holds in general. For small angles, we can Taylor expand this and find

$$\frac{a\psi}{b} \leq \tilde{\psi} \leq \frac{b\psi}{a}. \quad (\text{B.24})$$

- Volume inequality:

If we use a metric to measure the volume of some region $\mathcal{V}_A \subset A$, we use the Lebesgue measure in \mathbb{R}^d by identifying with A with \mathbb{R}^d by choosing an orthonormal basis in A . For two metrics g and \tilde{g} , linearity implies that there exists a unique number c , such that $\text{Vol}_{\tilde{g}}(\mathcal{V}_A) = c \text{Vol}_g(\mathcal{V}_A)$ holds for any region $\mathcal{V}_A \subset A$. In order to bound this constant, we can use the norm inequality to show that the d -dimensional unit ball $B_{\tilde{g}}^d = \{v \in A \text{ with } \|v\|_{\tilde{g}} \leq 1\}$ contains the ball $B_g^d(a) = \{v \in A \text{ with } \|v\|_{\tilde{g}} \leq a\}$ and is contained in the ball $B_g^d(b) = \{v \in A \text{ with } \|v\|_{\tilde{g}} \leq b\}$. This implies $a^d \leq c \leq b^d$ which leads to the volume inequality

$$a^d \text{Vol}_g(\mathcal{V}_A) \leq \text{Vol}_{\tilde{g}}(\mathcal{V}_A) \leq b^d \text{Vol}_g(\mathcal{V}_A), \quad (\text{B.25})$$

we wanted to prove.

If we replace $V \rightarrow V^*$ and accordingly $g \rightarrow G$ and $\tilde{g} \rightarrow \tilde{G}$, we can run exactly the same arguments, but we need to compute

$$1/b = \min_{\|v\|_G=1} \|v\|_{\tilde{G}}, \quad 1/a = \max_{\|v\|_G=1} \|v\|_{\tilde{G}} > 0. \quad (\text{B.26})$$

This follows from the fact that a and b are the smallest and largest eigenvalue of the linear map $(G\tilde{g})^a_b = G^{ac}\tilde{g}_{cb}$. Under above replacement, we need to consider its inverse map $(g\tilde{G})_a^b = g_{ac}\tilde{G}^{cb}$ whose smallest and largest eigenvalues are therefore $1/b$ and $1/a$, respectively. \square

B.2 Lyapunov exponents

In what follows, we restrict ourselves to quadratic systems where $M(t)$ is independent of the initial value ξ_0 . This generalizes to non-quadratic systems by replacing $M(t)$ by $M_{\xi_0}(t)$. In this case, Lyapunov exponents and vectors depend on the specific trajectory $\xi(t) = \Phi_t(\xi_0)$.

Definition 4 (Lyapunov exponent)

Given a linear Hamiltonian flow $M(t) : V \rightarrow V$ and a vector $\delta\xi \in V$, we define the Lyapunov exponent $\lambda_{\delta\xi}$ as the limit

$$\lambda_{\delta\xi} = \lim_{t \rightarrow \infty} \frac{1}{t} \log \frac{\|M(t)\delta\xi\|_g}{\|\delta\xi\|_g}, \quad (\text{B.27})$$

provided it exists. This definition is independent of the positive definite metric g that induces the norm $\|\cdot\|$. Analogously, we define the Lyapunov exponent of a dual vector $\ell \in V^*$ as the limit

$$\lambda_\ell = \lim_{t \rightarrow \infty} \frac{1}{t} \log \frac{\|M^\top(t) \ell\|_G}{\|\ell\|_G}, \quad (\text{B.28})$$

provided it exists. Here, the definition is independent of the inverse metric G .

Proof: We need to prove the independence of this definition from the chosen norm $\|\cdot\|_g$ induced by some metric g . We can use the norm inequality (B.10) to show $\|M(t) \delta\xi\|_{\tilde{g}} = c_t \|M(t) \delta\xi\|_g$ with factor $c_t \in [a, b]$. Let λ_p be the Lyapunov exponent of $\delta\xi \in V$ with respect to the norm $\|\cdot\|_g$. We can now compute

$$\tilde{\lambda}_{\delta\xi} = \lim_{t \rightarrow \infty} \frac{1}{t} \log \frac{\|M(t) \delta\xi\|_{\tilde{g}}}{\|\delta\xi\|_{\tilde{g}}} = \lim_{t \rightarrow \infty} \frac{1}{t} \log \frac{\|M(t) \delta\xi\|_g}{\|\delta\xi\|_g} + \underbrace{\lim_{t \rightarrow \infty} \frac{c_t}{t} \frac{\|\delta\xi\|_g}{\|\delta\xi\|_{\tilde{g}}}}_{=0} = \lambda_{\delta\xi}, \quad (\text{B.29})$$

where the second term vanishes because c_t is a bounded function. For dual Lyapunov vectors $\ell \in V^*$, we can use the same arguments where only our bounds for c_t change to $c_t \in [1/b, 1/a]$. \square

To characterize the Lyapunov exponents of all vectors in a $2N$ -dimensional vector space, it is sufficient to select a representative sample of $2N$ vectors. Such a basis is called Lyapunov basis and is defined as follows.

Definition 5 (*Lyapunov basis and spectrum*)

Given the linear flow $M(t)$, we define the limit matrix

$$L_a{}^b \equiv \lim_{t \rightarrow \infty} \frac{1}{2t} \log \left(g_{ac} M^c{}_d G^{de} M^b{}_e \right), \quad (\text{B.30})$$

provided it exists. We then define a complete set of eigenvectors as Lyapunov basis $\mathcal{D}_L = (\ell^1, \dots, \ell^{2N})$ if it is chosen as Darboux basis, such that $\{\ell^i, \ell^{2N-i+1}\} = 1$ for $i = 1, \dots, N$ are the only non-trivial Poisson brackets and such that the associated Lyapunov exponents $\lambda_i := \lambda_{\ell_i}$ are ordered with $\lambda_i \geq \lambda_{i+1}$. The set $(\lambda_1, \dots, \lambda_{2N})$ is called Lyapunov spectrum.

Proof: The construction of a Lyapunov basis as eigenvectors of the limiting matrix L is an important part of Oseledets multiplicative ergodic theorem. A comprehensible proof with further details can be found [94]. The fact that the eigenvectors can always be chosen to form a Darboux basis follows from the fact that $L_a{}^b$ is an element of the symplectic algebra $\mathrm{sp}(2N, \mathbb{R})$. \square

When restricting to a subsystem $A \subset V$, it is natural to ask what is the Lyapunov spectrum of the subsystem.

Definition 6 (*Subsystem Lyapunov basis and spectrum*)

Given the linear flow $M(t)$ and a symplectic subspace $A \subset V$, we define the subsystem Lyapunov basis of A as the $2N_A$ vectors $(\ell_A^1, \dots, \ell_A^{2N_A})$ with associated subsystem Lyapunov spectrum

$$\lambda_1^A \geq \dots \geq \lambda_{2N_A}^A, \quad (\text{B.31})$$

such that a linear observable $\theta \in A^*$ with $\theta = \sum_{i=1}^{2N_A} c_i \ell_A^i$ has Lyapunov exponent λ_j^A where $j \geq$ is the smallest number, such that $T_j \neq 0$.

The subsystem Lyapunov spectrum does in general not consist of conjugated pairs $(\lambda, -\lambda)$. Moreover, it is important to emphasize that the Lyapunov spectrum of A is defined as those Lyapunov

exponents of linear observables $\theta \in A^*$, rather than of perturbations $\delta\xi \in A$, because the two are not the same.

The following proposition explains in detail how one can compute the subsystem Lyapunov basis and spectrum when the Lyapunov basis and spectrum of the full system is known.

Proposition 8

Given a the linear flow $M(t)$ with Lyapunov basis \mathcal{D}_L and Lyapunov spectrum $(\lambda_1, \dots, \lambda_{2N})$, we can compute the subsystem Lyapunov basis and spectrum of a subsystem $A \subset V$ using the following three steps:

1. Choose a Darboux basis $\mathcal{D}_A = (\theta^1, \dots, \theta^{2N_A})$ of the symplectic subspace $A^* \subset V^*$.
2. Compute the unique transformation matrix T that expresses \mathcal{D}_A in terms of the Lyapunov basis $\mathcal{D}_L = (\ell^1, \dots, \ell^{2N})$:

$$\begin{pmatrix} \theta^1 \\ \vdots \\ \theta^{2N_A} \end{pmatrix} = \begin{pmatrix} T_1^1 & \cdots & T_{2N}^1 \\ \vdots & \ddots & \vdots \\ T_1^{2N_A} & \cdots & T_{2N}^{2N_A} \end{pmatrix} \begin{pmatrix} \ell^1 \\ \vdots \\ \ell^{2N} \end{pmatrix} \quad (\text{B.32})$$

$\underbrace{\hspace{1cm}}_{\vec{t}_1} \qquad \qquad \qquad \underbrace{\hspace{1cm}}_{\vec{t}_{2N}}$

We refer to the $2N$ columns of T as \vec{t}_i .

3. Find the first $2N_A$ linearly independent ¹ columns \vec{t}_i of T which we can label by \vec{t}_{i_k} with k ranging from 1 to $2N_A$. The result is a map $k \mapsto i_k \in (1, \dots, 2N)$ with $i_{k+1} > i_k$.

The subsystem Lyapunov spectrum is given by $(\lambda_1^A, \dots, \lambda_{2N_A}^A)$ with $\lambda_k^A = \lambda_{i_k}$ and the subsystem Lyapunov basis is given by $(\ell_A^1, \dots, \ell_A^{2N_A})$ with

$$\ell_A^k = (U^{-1}\theta)^k, \quad (\text{B.33})$$

where $U = (\vec{t}_{i_1}, \dots, \vec{t}_{i_{2N_A}})$ is the invertible $2N_A \times 2N_A$ matrix consisting of the columns \vec{t}_{i_k} .

Proof: The rectangular matrix T in (B.32) allows us to express the elements of the Darboux basis \mathcal{D}_A of the subsystem in terms of the Lyapunov basis, $\theta^r = \sum^{2N} T_i^r \ell^i$. Denoting the columns of T by \vec{t}_i we can select the first $2N_A$ linearly independent columns in the ordered set $(\vec{t}_1, \dots, \vec{t}_{2N})$. We label them \vec{t}_{i_k} and organize them in the $2N_A \times 2N_A$ square matrix U ,

$$U = (\vec{t}_{i_1} \mid \dots \mid \vec{t}_{i_{2N_A}}). \quad (\text{B.34})$$

Due to their linear independence, the inverse U^{-1} exists and turns T into an upper triangular matrix \tilde{T} of the form

$$\tilde{T} = U^{-1}T = \begin{pmatrix} 0 & \dots & 0 & 1 & * & * & \dots & \dots & * \\ 0 & \dots & \dots & 0 & 1 & * & * & \dots & * \\ \vdots & & & \vdots & & \vdots & & \vdots & \\ 0 & \dots & \dots & \dots & 0 & 1 & * & * & \dots & * \end{pmatrix}, \quad (\text{B.35})$$

where the $*$ represents an unspecified value. Acting with U^{-1} on the left and the right-hand side of (B.32) and acting on θ^k , we find

$$\ell_A^k := (U\theta)^k = \ell^{i_k} + \sum_{j>i_k}^{2N} \tilde{T}_j^k \ell^j, \quad (\text{B.36})$$

where $\ell_A^k = (U^{-1}\theta)^k = \sum_{j=1}^{2N_A} U_j^k \theta^j$. Clearly, the vectors ℓ_A^k satisfy

$$\lim_{t \rightarrow \infty} \frac{1}{t} \log \|M^\tau(t)\ell_A^k\| / \|\ell_A^k\| = \lambda_{i_k}. \quad (\text{B.37})$$

Given an arbitrary vector $\theta = \sum_{i=1}^{2N_A} c_i \ell_A^i$, its Lyapunov exponent is clearly given by the $\lambda_k^A = \lambda_{i_k}$ where k is the smalles $i \geq 1$, for which c_i is non-zero. \square

In our geometric representations of the Rényi entropy, we are interested in how the volume of some initial region changes under the Hamiltonian flow $M^\tau(t)$. Due to the linearity of $M^\tau(t)$, we can restrict ourselves to studying the time-dependent volume of parallelepipeds laying in some subspace $A \subset V$. The evolution will in general evolve this parallelepiped out of A .

Definition 7 (*Subsystem exponent*)

Given the linear flow $M(t)$ and a symplectic subspace $A \subset V$ of dimension $2N_A$, we can define the Subsystem exponent as the limit

$$\Lambda_A = \lim_{t \rightarrow \infty} \frac{1}{t} \log \frac{\text{Vol}_G(M^\tau(t)\mathcal{V}_A)}{\text{Vol}_G(\mathcal{V}_A)}, \quad (\text{B.38})$$

provided it exists. The set $\mathcal{V}_A \subset A$ is an arbitrary parallelepiped spanning all dimensions of A . This definition is independent of the metric that one uses to measure the volume and independent of the choice of parallelepiped \mathcal{V}_A .

Proof: We need to prove the independence of this definition from the choice of positive definite metric G . We can use the volume inequality (B.13) which ensures that for a different metric \tilde{G} , we have $\text{Vol}_{\tilde{G}}(M^\tau(t)\mathcal{V}_A) = c_t \text{Vol}_G(M^\tau(t)\mathcal{V}_A)$ with $c_t \in [(1/b)^{2N_A}, (1/a)^{2N_A}]$. We compute

$$\tilde{\Lambda}_A = \lim_{t \rightarrow \infty} \frac{1}{t} \log \frac{\text{Vol}_{\tilde{G}}(M^\tau(t)\mathcal{V}_A)}{\text{Vol}_{\tilde{G}}(\mathcal{V}_A)} = \lim_{t \rightarrow \infty} \frac{1}{t} \log \frac{\text{Vol}_G(M^\tau(t)\mathcal{V}_A)}{\text{Vol}_G(\mathcal{V}_A)} + \underbrace{\lim_{t \rightarrow \infty} \frac{c_t}{t} \log \frac{\text{Vol}_G(\mathcal{V}_A)}{\text{Vol}_{\tilde{G}}(\mathcal{V}_A)}}_{=0} = \Lambda_A, \quad (\text{B.39})$$

where the second term vanishes because c_t is a bounded function. \square

B.3 Regular Hamiltonian systems

The central theorem of this paper connects quantum mechanical entanglement with the classical notion of Lyapunov exponents. In order to avoid technical complications, we introduce the class of *regular Hamiltonian Lyapunov systems*. Most standard Hamiltonian systems that one studies in classical or quantum physics with a finite number of bosonic degrees of freedom fall into this class.

Definition 8

A regular Hamiltonian Lyapunov system consists of a finite dimensional phase space and a (possibly time-dependent) Hamiltonian $H(t) : V \rightarrow \mathbb{R}$ with linerized flow $M_{\xi_0}(t)$, such that the following two conditions are satisfied:

- (i) All Lyapunov exponents are well defined. This means that for an arbitrary initial condition ξ_0 as well as for every initial separation $\delta\xi \in T_{\xi_0}V$, the corresponding limit

$$\lambda_{\delta\xi} = \lim_{t \rightarrow \infty} \frac{1}{t} \log \frac{\|M(t)\delta\xi\|_G}{\|\delta\xi(0)\|_G} \quad (\text{B.40})$$

exists.

- (ii) All Lyapunov exponents appear in conjugate pairs $(\lambda, -\lambda)$, such that the geometric multiplicity of the two conjugate exponents agrees.

In short, condition (i) excludes systems with above-exponential or below-exponential growth, while condition (ii) excludes systems where two or more vectors become exponentially fast collinear under evolution by $M_{\xi_0}(t)$. Let us give an example for each condition that is not a regular Hamiltonian Lyapunov system. For both examples, we consider a single degree of freedom, such that we can express everything with respect to the Darboux basis $\mathcal{D}_V = (q, p)$.

- (i) Above-exponential growth and decay

The time-dependent quadratic Hamiltonian $H(t) = e^t qp$ leads to the Hamiltonian flow

$$M(t) = \begin{pmatrix} e^{e^t} & 0 \\ 0 & e^{-e^t} \end{pmatrix}, \quad (\text{B.41})$$

for which the Lyapunov exponents are ill defined because the defining limits do not exist. Thus, this system violates the first condition of regular Hamiltonian Lyapunov systems.

- (ii) Exponential collinearity

The time dependent quadratic Hamiltonian $H(t) = \frac{1}{2}e^t p^2$ leads to the Hamiltonian flow

$$M(t) = \begin{pmatrix} 1 & 0 \\ e^t & 1 \end{pmatrix}, \quad (\text{B.42})$$

which has Lyapunov exponents given by $\lambda_1 = 1$ and $\lambda_2 = 0$. The symplectic volume is still preserved under time evolution because arbitrary initial vectors become exponentially fast collinear, for instance

$$M^\top(t)q = q, \quad M(t)p = p + e^t q, \quad (\text{B.43})$$

where the angle between the two vectors behaves as

$$\theta(t) = \cos^{-1} \left(\frac{\langle M^\top(t)q, M^\top(t)p \rangle_G}{\|M^\top(t)q\|_G \|M^\top(t)p\|_G} \right) \sim e^{-t} \quad \text{as } t \rightarrow \infty, \quad (\text{B.44})$$

regardless of which positive definite metric we use. Clearly, this system does not have two conjugate Lyapunov exponents and does not fall into the class of regular Hamiltonian Lyapunov systems.

The following notion of Lyapunov defect is important to show that for regular Hamiltonian systems the subsystem exponent can be simply computed using theorem 3.

Definition 9 (*Subsystem defect*)

Given the inverse linear flow $M(t)$ and a subsystem $A \subset V$ with Lyapunov associated subsystem Lyapunov spectrum $(\lambda_1^A, \dots, \lambda_{2N_A}^A)$, we define the Lyapunov defect

$$\Lambda_A^* = \sum_{i=1}^{2N_A} \lambda_i^A - \Lambda_A, \quad (\text{B.45})$$

where $\mathcal{V}_A \subset A^*$ is an arbitrary $2N_A$ -dimensional parallelepiped in A . If this limit exists, it is independent of the metric G with which we measure the volume and we have $\Lambda_A^* \geq 0$.

Proof: The volume of a parallelepiped can be computed from the length of its $2N_A$ sides $M^\top(t)\ell^i$ and the $(2N_A - 1)$ angles $\psi_i(t)$, which is the angle between $M^\top(t)\ell^i$ and the hyperplane spanned by the vectors $M^\top(t)\ell^j$ with $j = 1, \dots, i-1$. The time dependent volume is then given by

$$\text{Vol}_G(M^\top(t)\mathcal{V}_A) = \prod_{i=1}^{2N_A} \|M^\top(t)\ell^i\| \sin \psi_i(t). \quad (\text{B.46})$$

Given two distinct metrics G and \tilde{G} , we can use the angle and length inequalities from above, to find the volume inequality

$$(1/b)^{2N_A} \text{Vol}_G(M^\top(t)\mathcal{V}_A) \leq \text{Vol}_{\tilde{G}}(M^\top(t)\mathcal{V}_A) \leq (1/a)^{2N_A} \text{Vol}_G(M^\top(t)\mathcal{V}_A). \quad (\text{B.47})$$

This inequality already insures that the above limit is independent of the chosen metric. Moreover, the explicit expression in (B.46) shows also that the volume is bounded from above by

$$\text{Vol}_G(M^\top(t)\mathcal{V}_A) \leq \prod_{i=1}^{2N_A} \|M^\top(t)\ell^i\| \propto \exp \sum_{i=1}^{2N_A} \lambda_i^A t. \quad (\text{B.48})$$

This implies $\Lambda_A \leq \sum^{2N_A}$ and thus, $\Lambda_A^* \geq 0$. \square

For regular Hamiltonian systems, we can prove the following statements that we will need in the proof of our central theorem of this paper.

Proposition 9

In a regular Hamiltonian system, the Lyapunov defect Λ_A^* of any subspace $A \subset V$ vanishes. This implies that the asymptotic behavior of any volume $\mathcal{V}_A \subset A \subset V$ is given by

$$\Lambda_A = \sum_{i=1}^{2N_A} \lambda_i^A \quad (\text{B.49})$$

where λ_i^A refers to subsystem Lyapunov spectrum of A .

Proof: Let us recall that there is a special class of metrics on V , for which every symplectic transformation $M(t)$ and thus also $M^\top(t)$ preserves the $2N$ -dimensional volume. These are all the metrics that give rise to the same volume form as the one induced by the symplectic form. This implies that the asymptotic behavior of every $2N$ -dimensional region $\mathcal{V} \subset V$ shows the following asymptotic behavior

$$\Lambda_V = \lim_{t \rightarrow \infty} \frac{1}{t} \log \frac{\text{Vol}_G(M^\top(t)\mathcal{V})}{\text{Vol}_G(\mathcal{V})} = 0, \quad (\text{B.50})$$

which holds with respect to all metrics G .

From our previous discussion, we also recall that we must have

$$\Lambda_V = \sum_{i=1}^{2N} \lambda_i - \Lambda_V^*. \quad (\text{B.51})$$

If all Lyapunov exponents λ_i come in conjugate pairs with equal multiplicities the sum in this expression vanishes. Thus, we have $\Lambda_V = -\Lambda_V^*$ which implies $\Lambda_V^* = 0$ due to $\Lambda_V = 0$. At this point, we only need to show that $\Lambda_V^* = 0$ for the full system implies that we also have $\Lambda_A^* = 0$ for all subsystems $A \subset V$. This follows from the fact that we can choose an initial parallelepiped $\mathcal{V} = \mathcal{V}_A \times \mathcal{V}_B$ with well known inequality

$$\text{Vol}_G(M^\top(t)\mathcal{V}) \leq \text{Vol}_G(M^\top(t)\mathcal{V}_A) \text{Vol}_G(M^\top(t)\mathcal{V}_B). \quad (\text{B.52})$$

This inequality implies $-\Lambda_V^* \leq -\Lambda_A^* - \Lambda_B^*$ where we recall $\lambda_A^* > 0$ and $\lambda_B^* > 0$. Thus, $\Lambda_V^* = 0$ implies that $\Lambda_A^* = 0$ for all subspaces $A \subset V$ leading to $\Lambda_A = \sum_{i=1}^{2N_A} \lambda_i^A$. \square

Let us emphasize that proposition 8 and 9 together provide an alternative full proof of theorem 3, the main result of this paper. Put simply, the subsystem exponent Λ_A for regular Hamiltonian systems is just given by the sum over the subsystem spectrum λ_i^A which can be computed using the procedure explained in theorem 3 or equivalently in proposition 8.

Appendix C

Decomposition of symplectic generators

When studying the time evolution of the entanglement entropy under quadratic time-independent Hamiltonians, we are interested in understanding how the associated classical Hamiltonian flow acts on phase space. This can be understood by decomposing the relevant symplectic generator into its real, imaginary and nilpotent part. We will review the Jordan-Chevalley decomposition and Jordan normal form for symplectic generators and the resulting properties of the Hamiltonian flow they generate. This appendix is based on the respective appendix in [LH09].

C.1 Jordan normal form of real matrices

Most square matrices are diagonalizable. By “most”, we mean all but a subset of measure zero. However, there exists a subset of matrices that cannot be brought into diagonal form by an equivalence transformation and so they are non-diagonalizable. We consider the most general decomposition that can be applied to all real square matrices, even if they are not diagonalizable. The Jordan normal form is standard material in linear algebra [236]. However, it is useful to review the construction procedure using a convention that illuminates its application in this paper.

Theorem 8 (Jordan normal form)

Given a real linear map $K^\dagger : V^* \rightarrow V^*$ on a finite dimensional real vector space V^* with n distinct eigenvalues $\kappa_1, \dots, \kappa_n$ satisfying $\text{Im}(\kappa_i) \geq 0$ (meaning, for complex eigenvalues we only take the one with positive imaginary part), there always exists a basis, such that the matrix representation of K is block-diagonal as

$$K^\dagger \equiv \begin{pmatrix} \boxed{\mathcal{J}(\kappa_1)} & & & \\ & \boxed{\mathcal{J}(\kappa_2)} & & \\ & & \ddots & \\ & & & \boxed{\mathcal{J}(\kappa_n)} \end{pmatrix} \quad \text{with} \quad \mathcal{J}(\kappa) \equiv \begin{pmatrix} \boxed{\mathcal{J}_1(\kappa)} & & & \\ & \ddots & & \\ & & \ddots & \\ & & & \boxed{\mathcal{J}_{j_\kappa}(\kappa)} \end{pmatrix} \quad (\text{C.1})$$

where the Jordan blocks $\mathcal{J}_k(\kappa)$ are real square matrices of the following form:

- **Real eigenvalue** $\kappa = \lambda \in \mathbb{R}$

For real eigenvalues κ , the Jordan block $\mathcal{J}_k(\kappa)$ can have an arbitrary dimension $j_i(\kappa)$ and

takes the following form

$$\mathcal{J}_k(\kappa) = \underbrace{\begin{pmatrix} \lambda & & & \\ & \lambda & & \\ & & \ddots & \\ & & & \lambda \end{pmatrix}}_{A_k(\kappa)} + \underbrace{\begin{pmatrix} 0 & 1 & & \\ & 0 & \ddots & \\ & & \ddots & 1 \\ & & & 0 \end{pmatrix}}_{C_k(\kappa)}. \quad (\text{C.2})$$

- **Complex eigenvalue** $\kappa = \lambda + i\omega \in \mathbb{C}$

For a complex eigenvalue κ , the Jordan block $\mathcal{J}_k(\kappa)$ must have an even dimension $\dim \mathcal{J}_k(\kappa)$ and takes the following form

$$\mathcal{J}_k(\kappa) = \underbrace{\begin{pmatrix} \lambda \mathbb{1}_2 & & & \\ & \lambda \mathbb{1}_2 & & \\ & & \ddots & \\ & & & \lambda \mathbb{1}_2 \end{pmatrix}}_{A_k(\kappa)} + \underbrace{\begin{pmatrix} \omega \mathbb{B}_2 & & & \\ & \omega \mathbb{B}_2 & & \\ & & \ddots & \\ & & & \omega \mathbb{B}_2 \end{pmatrix}}_{B_k(\kappa)} + \underbrace{\begin{pmatrix} 0 & \mathbb{1}_2 & & \\ & 0 & \ddots & \\ & & \ddots & \mathbb{1}_2 \\ & & & 0 \end{pmatrix}}_{C_k(\kappa)}, \quad (\text{C.3})$$

where each entry represents a 2-by-2 matrix block that is either proportional to the identity $\mathbb{1}_2$ or to the antisymmetric matrix

$$\mathbb{B}_2 = \begin{pmatrix} 0 & 1 \\ -1 & 0 \end{pmatrix}. \quad (\text{C.4})$$

Note that we did all considerations for K^\top the transpose of K to match the notation in the main text where K^\top plays an important role. Due to the fact that the eigenvalues of K and K^\top are the same, the full analysis could be equivalently carried out for K .

Proof: We construct explicitly a basis in which K takes the Jordan normal form as described above. The construction only involves computing eigenvalues and solving linear equations to find the kernel of a matrix.

Step 1. Compute the n distinct eigenvalues $\kappa_1, \dots, \kappa_n$ with $\text{Im}(\kappa_i) \geq 0$ by finding the roots of the characteristic polynomial

$$\chi(\kappa) = \det(K^\top - \kappa \mathbb{1}). \quad (\text{C.5})$$

Complex eigenvalues always appear in conjugate pairs and we only include the one with positive imaginary part in our list.

Step 2. For every eigenvalue κ , we construct the corresponding block $J(\kappa)$ and its Jordan blocks $\mathcal{J}_k(\kappa)$. For this, we need to study generalized eigenspaces. The generalized eigenspace of order m is defined as

$$E^{(m)}(\kappa) = \ker(K^\top - \kappa \mathbb{1})^m. \quad (\text{C.6})$$

The first order eigenspace $E^{(1)}(\kappa)$ is just the regular eigenspace, but higher order eigenspaces are larger. The number j_κ of distinct Jordan blocks $\mathcal{J}_k(\kappa)$ is given by $j_\kappa = \dim E^{(1)}(\kappa)$. The number of Jordan blocks of dimension m is given by

$$t_m = 2 \dim E^{(m)}(\kappa) - \dim E^{(m-1)}(\kappa) - \dim E^{(m+1)}(\kappa), \quad (\text{C.7})$$

and each Jordan block is generated by a highest weight vector $\mathcal{E}_k(\kappa)$. A highest weight vector generates a sequence of $m_k(\kappa)$ vectors

$$\mathcal{E}_k^1(\kappa), \dots, \mathcal{E}_k^{m_k(\kappa)}(\kappa). \quad (\text{C.8})$$

by repeatedly applying $(K^\top - \kappa \mathbb{1})$ to it: $\mathcal{E}_k^l(\kappa) = (K^\top - \kappa \mathbb{1})^{m_k(\kappa)-l} \mathcal{E}_k^1(\kappa)$. One can apply the following induction to find all highest weight vectors:

1. We start with the largest m , for which $t_m \neq 0$ and select t_m linearly independent vectors in $\mathcal{E}_k(\kappa) \in E^{(m)}(\kappa) \setminus E^{(m-1)}(\kappa)$. After this, we construct for each vector $\mathcal{E}_k(\kappa)$ the corresponding sequence

$$\mathcal{E}_k^1(\kappa), \dots, \mathcal{E}_k^{m_k(\kappa)}(\kappa), \quad (\text{C.9})$$

by repeatedly applying $(K^\top - \kappa \mathbb{1})$ to it.

2. Next, we can go to $m-1$ and select t_{m-1} additional vectors $\mathcal{E}_k(\kappa)$ out of $E^{(m-1)}(\kappa) \setminus E^{(m-2)}(\kappa)$, which must not just be linearly independent among themselves, but also linearly independent from the vectors $\mathcal{E}_k^l(\kappa)$ in the sequences generated so far. We can continue this process until we reach $m=1$ and need to select t_1 vectors in $E^{(1)}(\kappa)$ that must be linearly independent from all the vectors $\mathcal{E}_k^l(\kappa)$ generated so far. This leaves us with j_κ distinct sequences of the form

$$\mathcal{E}_k^1(\kappa), \dots, \mathcal{E}_k^{m_k(\kappa)}(\kappa), \quad (\text{C.10})$$

which span the space for the Jordan block $\mathcal{J}_k(\kappa)$.

Note that, for complex eigenvalues, the corresponding vectors $\mathcal{E}_k^l(\kappa)$ are complex. Later, we construct real vectors out of them.

Step 3: Having constructed the sequences of generalized eigenvectors, we are ready to construct the different Jordan blocks explicitly. We need to distinguish two cases:

- **Real eigenvalue** $\kappa = \lambda \in \mathbb{R}$

Let us look at the sequence of $v_k^1(\kappa), \dots, v_k^{m_k}(\kappa)$ of generalized eigenvectors. We can write down the action of K^\top on each element and find

$$K^\top \mathcal{E}_k^l(\kappa) = \lambda \mathcal{E}_k^l(\kappa) + \mathcal{E}_k^{l-1}(\kappa), \quad (\text{C.11})$$

$$K^\top \mathcal{E}_k^1(\kappa) = \lambda \mathcal{E}_k^1(\kappa), \quad (\text{C.12})$$

where we have $m_k \geq l > 1$ in the first equation. This means that the action of K^\top with respect to the generalized eigenvectors of the sequence $\mathcal{E}_k^1(\kappa), \dots, \mathcal{E}_k^{m_k}(\kappa)$ is completely described by the matrix

$$\mathcal{J}_k(\kappa) = \begin{pmatrix} \lambda & 1 & & \\ & \lambda & \ddots & \\ & & \ddots & 1 \\ & & & \lambda \end{pmatrix}. \quad (\text{C.13})$$

- **Complex eigenvalues** $\kappa = \lambda + i\omega \in \mathbb{C}$

For complex eigenvalues κ , K^\top is only diagonalizable over the complex numbers, but not over the reals. However, due to the fact that K^\top is a real matrix, we know that all sequences of generalized eigenvectors $\mathcal{E}_k^l(\kappa)$, which we constructed in the previous step, are actually complex. Their complex conjugated counterparts $\mathcal{E}_k^l(\kappa)^*$ are themselves generalized eigenvectors associated with the eigenvalue $\kappa^* = \lambda - i\omega$:

$$K^\top \mathcal{E}_k^l(\kappa)^* = (\lambda - i\omega) \mathcal{E}_k^l(\kappa)^* + \mathcal{E}_k^{l-1}(\kappa)^*, \quad (\text{C.14})$$

$$K^\top \mathcal{E}_k^1(\kappa)^* = (\lambda - i\omega) \mathcal{E}_k^1(\kappa)^*, \quad (\text{C.15})$$

where we have $m_k \geq l > 1$ in the first equation. We can take linear combinations of generalized eigenvectors and their complex conjugates to find the real vectors

$$\mathcal{E}_k^{l+}(\kappa) = \frac{1}{\sqrt{2}} [\mathcal{E}_k^l(\kappa) + \mathcal{E}_k^l(\kappa)^*], \quad (\text{C.16})$$

$$\mathcal{E}_k^{l-}(\kappa) = \frac{i}{\sqrt{2}} [\mathcal{E}_k^l(\kappa) - \mathcal{E}_k^l(\kappa)^*]. \quad (\text{C.17})$$

The action of K on these real vectors is then given by

$$K^\top \mathcal{E}_k^{l+}(\kappa) = \lambda \mathcal{E}_k^{l+}(\kappa) + \omega \mathcal{E}_k^{l-}(\kappa) + \mathcal{E}_k^{(l-1)+}(\kappa), \quad (\text{C.18})$$

$$K^\top \mathcal{E}_k^{l-}(\kappa) = \lambda \mathcal{E}_k^{l-}(\kappa) - \omega \mathcal{E}_k^{l+}(\kappa) + \mathcal{E}_k^{(l-1)-}(\kappa). \quad (\text{C.19})$$

This means that the action of K^\top on the generalized eigenvectors of the sequence

$$\mathcal{E}_k^{1+}(\kappa), \mathcal{E}_k^{1-}(\kappa), \dots, \mathcal{E}_k^{m_k+}(\kappa), \mathcal{E}_k^{m_k-}(\kappa) \quad (\text{C.20})$$

is completely described by the matrix

$$\mathcal{J}_k(\kappa) = \begin{pmatrix} a & b & 1 & & & \\ -b & a & & 1 & & \\ & & a & b & \ddots & \\ & & -b & a & & \ddots \\ & & & & \ddots & & 1 \\ & & & & & \ddots & \\ & & & & & & a & b \\ & & & & & & -b & a \end{pmatrix} = \begin{pmatrix} a\mathbb{1}_2 + b\mathbb{B}_2 & & & & & \\ & a\mathbb{1}_2 + b\mathbb{B}_2 & & & & \\ & & \ddots & & & \\ & & & \ddots & & \\ & & & & \mathbb{1}_2 & \\ & & & & & a\mathbb{1}_2 + b\mathbb{B}_2 \end{pmatrix}.$$

This is our original claim. \square

Bringing a linear map K^\top into its Jordan normal form is a generalized diagonalization that can be applied even if K^\top is non-diagonalizable. If K^\top is diagonalizable over the real numbers, all Jordan blocks are 1×1 and the Jordan normal form is just the traditional diagonalization. We can use the construction presented here to decompose every linear map into three parts, which we call the Jordan-Chevalley decomposition.¹

Corollary 2 (Jordan-Chevalley decomposition)

The decomposition of each block $\mathcal{J}_k(\kappa)$ into the three parts $A_k(\kappa)$, $B_k(\kappa)$, and $C_k(\kappa)$, where the block $B_k(\kappa)$ vanishes for real κ , induces an overall decomposition of the matrix representation of K^\top with respect to our generalized eigenvectors into

$$K^\top = A^\top + B^\top + C^\top. \quad (\text{C.21})$$

Knowing this decomposition in a specific basis allows us to compute the decomposition of K^\top , or, equivalently, of K into three parts

$$K = K_{\text{real}} + K_{\text{imaginary}} + K_{\text{nilpotent}}, \quad (\text{C.22})$$

which can be expressed in an arbitrary basis. Here, K_{real} is diagonalizable with purely real eigenvalues, $K_{\text{imaginary}}$ is diagonalizable with purely imaginary eigenvalues, and $K_{\text{nilpotent}}$ is not diagonalizable, but a nilpotent linear map. All three maps commute with each other.

¹Usually, the Jordan-Chevalley decomposition just refers to the decomposition of K^\top into a diagonalizable part $K_{\text{diagonalizable}}^\top$ and a nilpotent part $K_{\text{nilpotent}}^\top$. However, for our purposes, it is important to split $K_{\text{diagonalizable}}^\top$ into its real and imaginary parts as well. This is a straightforward generalization of the Jordan-Chevalley decomposition.

C.2 Hamiltonian flow of time-independent quadratic systems

Given a quadratic time-independent Hamiltonian $H = \frac{1}{2}h_{ab}\xi^a\xi^b$, the classical equations of motion are given by the Hamilton equations²

$$\dot{\xi}^a(t) = \Omega^{ab}h_{bc}\xi^c(t). \quad (\text{C.23})$$

This is a linear ordinary differential equation whose solution can be completely characterized by the Hamiltonian flow $M(t) : V \rightarrow V$ with $\xi^a(t) = M(t)^a{}_b\xi^b(0)$. This implies the equation

$$\frac{d}{dt}M(t)^a{}_b = \Omega^{ac}h_{cb}. \quad (\text{C.24})$$

If we define $K^a{}_b = \Omega^{ac}h_{cb}$, the solution $M(t)^a{}_b$ can be written as a matrix exponential:

$$M(t)^a{}_b = \exp(tK)^a{}_b. \quad (\text{C.25})$$

The matrix K is the infinitesimal generator of the canonical transformation $M(t)$ and satisfies³

$$K^a{}_c\Omega^{cb} + \Omega^{ac}(K^\top)_c{}^b = 0, \quad (\text{C.26})$$

where K^\top is the transpose of K . Therefore, the exponential $M(t)$ preserves Ω through

$$M(t)^a{}_c\Omega^{cd}M^\top(t)_d{}^b = \Omega^{ab}, \quad (\text{C.27})$$

which ensures that $M(t)$ is a proper canonical transformation preserving the Poisson bracket.

Studying the time evolution of the entanglement entropy of Gaussian states is equivalent to asking how the classical time evolution $M(t)$ stretches regions of subspaces in classical phase space. For time-independent Hamiltonians, the time evolution $M(t)$ is completely characterized by the Jordan normal form of the symplectic generator K . We can use the Jordan-Chevalley decomposition $K = K_{\text{real}} + K_{\text{imaginary}} + K_{\text{nilpotent}}$ to decompose

$$M(t) = e^{Kt} = e^{K_{\text{real}}t}e^{K_{\text{imaginary}}t}e^{K_{\text{nilpotent}}t}, \quad (\text{C.28})$$

where we use the fact that the three parts commute with each other. Let us analyze the action of the three parts on an arbitrary generalized eigenvector $\mathcal{E}_k^{l\pm}(\kappa)$ for some complex eigenvalue pair $\kappa = \lambda \pm i\omega$.

(a) **Real part: Exponential stretching** $S(t) \sim \Lambda_A t$

The real part K_{real} has the simplest effect. We find immediately

$$e^{K_{\text{real}}t}\mathcal{E}_k^{l\pm}(\kappa) = e^{\lambda t}\mathcal{E}_k^{l\pm}(\kappa), \quad (\text{C.29})$$

which means the generalized eigenvector is stretched (or squeezed if $\lambda < 0$) exponentially with a factor $e^{\lambda t}$. For a generic $2N_A$ dimensional region, only the $2N_A$ directions that are stretched the fastest will contribute. In summary, the real part contributes an exponential part $e^{\Lambda_A t}$ to the time dependence of a volume, where Λ_A is a sum over the largest real parts λ_i of the eigenvalues κ_i . This leads to a linear contribution $\Lambda_A t$ to the entanglement entropy.

²We use the symplectic form Ω whose matrix representation in a canonical basis is $\Omega \equiv \begin{pmatrix} 0 & 1 \\ -1 & 0 \end{pmatrix}$.

³In matrix notation, this is the well-known condition $K\Omega + \Omega K^\top = 0$ for K to be an element of the symplectic algebra $\text{sp}(2N)$. It is equivalent to requiring $K^a{}_b = \Omega^{ac}h_{cb}$ with symmetric $h_{ab} = h_{ba}$.

(b) **Imaginary part: Rotations** $\Rightarrow S_A \sim X_A(t)$

Let us recall that the imaginary eigenvalues of $K_{\text{imaginary}}$ always come in conjugate pairs. If we only consider the action of generalized eigenvectors, we find

$$K_{\text{imaginary}} \mathcal{E}_k^{l+}(\kappa) = \omega \mathcal{E}_k^{l-}(\kappa), \quad (\text{C.30})$$

$$K_{\text{imaginary}} \mathcal{E}_k^{l-}(\kappa) = -\omega \mathcal{E}_k^{l+}(\kappa). \quad (\text{C.31})$$

This implies that the exponentiated action is given by

$$e^{K_{\text{imaginary}} t} \begin{pmatrix} \mathcal{E}_k^{l+}(\kappa) \\ \mathcal{E}_k^{l-}(\kappa) \end{pmatrix} = \begin{pmatrix} \cos \omega t & \sin \omega t \\ -\sin \omega t & \cos \omega t \end{pmatrix} \begin{pmatrix} \mathcal{E}_k^{l+}(\kappa) \\ \mathcal{E}_k^{l-}(\kappa) \end{pmatrix}, \quad (\text{C.32})$$

which corresponds to a rotation in the plane spanned by $\mathcal{E}_k^{l\pm}(\kappa)$. Note that we cannot distinguish a rotation on a circle from an elliptical orbit unless we choose a metric to compute the length of vectors. However, the orbit is always bounded, which means that the imaginary part of K can only change the volume of a region by a constant. A vector that is a general linear combination of many different generalized eigenvectors will follow a complicated, but bounded, trajectory resulting from a superposition of the rotations in different planes with different frequencies $\omega_i = \text{Im}(\kappa_i)$. The imaginary part is responsible for the bounded and oscillating contribution $X_A(t)$ to the entanglement entropy.

(c) **Nilpotent part: Shearing** $\Rightarrow S_A(t) \sim C_A \ln(t)$

The nilpotent part $K_{\text{nilpotent}}$ corresponds to a shearing in the plane spanned by all the vectors of a specific Jordan block $\mathcal{J}_k(\kappa)$. The action of the generator

$$K_{\text{nilpotent}} \mathcal{E}_k^{l\pm}(\kappa) = \mathcal{E}_k^{(l-1)\pm}(\kappa), \quad \mathcal{E}_k^0(\kappa) = 0, \quad (\text{C.33})$$

exponentiates to the action

$$e^{K_{\text{nilpotent}} t} \mathcal{E}_k^{l\pm}(\kappa) = \sum_{l'=1}^l \frac{t^{l-l'}}{(l-l')!} \mathcal{E}_k^{l'\pm}(\kappa). \quad (\text{C.34})$$

The volume of a region spanned by *all* vector $\mathcal{E}_k^{l'\pm}(\kappa)$ with $1 \leq l' \leq l$ does not change under this time evolution, but for a generic region that is only stretched along some directions of this subspace, there will be a polynomial stretching. The largest exponent of a single direction is clearly given by $\dim \mathcal{J}_k(\kappa) - 1$. If we need to choose $n_k(\kappa)$ vectors in the Jordan block $\mathcal{J}_k(\kappa)$, the maximal exponent is given by

$$[\dim \mathcal{J}_k(\kappa) - n_k(\kappa)] n_k(\kappa). \quad (\text{C.35})$$

In summary, the nilpotent part only contributes a polynomial growth with integer exponents C_A to the time dependence of a volume. After taking the logarithm, we have a contribution $C_A \ln(t)$ to the entanglement entropy.

Publications

- [LH01] Simon Badger, Benedikt Biedermann, Lucas Hackl, Jan Plefka, Theodor Schuster, Peter Uwer, “*Comparing efficient computation methods for massless QCD tree amplitudes: Closed Analytic Formulae versus Berends-Giele Recursion,*” Physical Review D 87 (3), 034011 [[arXiv:1206.2381](#)].
- [LH02] Lucas Hackl, Yasha Neiman “*Horizon complementarity in elliptic de Sitter space,*” Physical Review D 91 (4), 044016 [[arXiv:1409.6753](#)].
- [LH03] Eugenio Bianchi, Lucas Hackl, Nelson Yokomizo “*Entanglement entropy of squeezed vacua on a lattice,*” Physical Review D 92 (8), 085045 [[arXiv:1507.01567](#)].
- [LH04] Eugenio Bianchi, Lucas Hackl, Nelson Yokomizo “*Entanglement time in the primordial universe,*” International Journal of Modern Physics D 24 (12), 1544006 [[arXiv:1512.08959](#)].
- [LH05] Eugenio Bianchi, Jonathan Guglielmon, Lucas Hackl, Nelson Yokomizo “*Squeezed vacua in loop quantum gravity,*” submitted to Classical and Quantum Gravity [[arXiv:1605.05356](#)].
- [LH06] Eugenio Bianchi, Jonathan Guglielmon, Lucas Hackl, Nelson Yokomizo “*Loop expansion and the bosonic representation of loop quantum gravity,*” Physical Review D 94 (8), 086009 [[arXiv:1609.02219](#)].
- [LH07] Lev Vidmar, Lucas Hackl, Eugenio Bianchi, Marcos Rigol “*Entanglement Entropy of Typical Eigenstates of Translationally Invariant Quadratic Hamiltonians,*” Physical Review Letters 119, 020601 [[arXiv:1703.02979](#)].
- [LH08] Eugenio Bianchi, Lucas Hackl, Nelson Yokomizo “*Linear growth of the entanglement entropy and the Kolmogorov-Sinai rate,*” Journal for High Energy Physics (2018) 2018: 25 [[arXiv:1709.00427](#)].
- [LH09] Lucas Hackl, Eugenio Bianchi, Ranjan Modak, Marcos Rigol “*Entanglement production in bosonic systems: Linear and logarithmic growth,*” Physical Review A 97, 032321 [[arXiv:1710.04279](#)].
- [LH10] Lucas Hackl, Robert C. Myers “*Circuit complexity of free fermions,*” Journal for High Energy Physics (2018) 2018: 139 [[arXiv:1803.10638](#)].
- [LH11] Lev Vidmar, Lucas Hackl, Eugenio Bianchi, Marcos Rigol “*Volume Law and Quantum Criticality in the Entanglement Entropy of Excited Eigenstates of the Quantum Ising Model,*” Physical Review Letters 121, 220602 [[arXiv:1808.08963](#)].
- [LH12] Shira Chapman, Lucas Hackl, Michal P. Heller, Robert A. Jefferson, Hugo Marrochio, Robert C. Myers “*Complexity and entanglement for thermofield double states,*” submitted to SciPost [[arXiv:1810.05151](#)].

- [LH13] Lucas Hackl, Robert C. Myers “*Circuit complexity of bosonic and fermionic Gaussian states,*” in preparation.
- [LH14] Lucas Hackl, Lev Vidmar, Marcos Rigol, Eugenio Bianchi “*Average eigenstate entanglement in the XY model and its universality for translationally invariant models,*” in preparation.
- [LH15] Eugenio Bianchi, Lucas Hackl “*Bosonic and fermionic Gaussian states from Kähler structures,*” in preparation.
- [LH16] Eugenio Bianchi, Miguel Fernandez, Lucas Hackl, Monica Rincon-Ramirez, Alejandro Satz “*Adiabatic vacua in cosmology,*” in preparation.

Bibliography

- [1] L. Isserlis, *On a formula for the product-moment coefficient of any order of a normal frequency distribution in any number of variables*, *Biometrika* **12** (1918) 134.
- [2] G.-C. Wick, *The evaluation of the collision matrix*, *Physical Review* **80** (1950) 268.
- [3] M. E. Peskin and D. V. Schroeder, *An introduction to quantum field theory*. Addison-Wesley Publishing Company, 1995, [10.1063/1.2807734](https://doi.org/10.1063/1.2807734).
- [4] R. P. Feynman, *The theory of positrons*, *Physical Review* **76** (1949) 749.
- [5] A. Ashtekar and A. Magnon, *Quantum fields in curved space-times*, in *Proceedings of the Royal Society of London A: Mathematical, Physical and Engineering Sciences*, vol. 346, pp. 375–394, The Royal Society, 1975, DOI.
- [6] R. M. Wald, *Quantum field theory in curved spacetime and black hole thermodynamics*. University of Chicago Press, 1994.
- [7] S. Hawking, *Particle Creation by Black Holes*, *Communications in Mathematical Physics* **43** (1975) 199.
- [8] S. A. Fulling, *Nonuniqueness of canonical field quantization in riemannian space-time*, *Physical Review D* **7** (1973) 2850.
- [9] P. C. Davies, *Scalar production in schwarzschild and rindler metrics*, *Journal of Physics A* **8** (1975) 609.
- [10] W. G. Unruh, *Notes on black-hole evaporation*, *Physical Review D* **14** (1976) 870.
- [11] PLANCK collaboration, P. A. R. Ade et al., *Planck 2015 results. XVII. Constraints on primordial non-Gaussianity*, *Astron. Astrophys.* **594** (2016) A17 [[1502.01592](https://arxiv.org/abs/1502.01592)].
- [12] A. Ashtekar and P. Singh, *Loop Quantum Cosmology: A Status Report*, *Class. Quant. Grav.* **28** (2011) 213001 [[1108.0893](https://arxiv.org/abs/1108.0893)].
- [13] N. Bartolo, E. Komatsu, S. Matarrese and A. Riotto, *Non-Gaussianity from inflation: Theory and observations*, *Phys. Rept.* **402** (2004) 103 [[astro-ph/0406398](https://arxiv.org/abs/astro-ph/0406398)].
- [14] A. D. Linde and V. Mukhanov, *The curvaton web*, *JCAP* **0604** (2006) 009 [[astro-ph/0511736](https://arxiv.org/abs/astro-ph/0511736)].
- [15] E. Nelson and S. Shandera, *Statistical Naturalness and non-Gaussianity in a Finite Universe*, *Phys. Rev. Lett.* **110** (2013) 131301 [[1212.4550](https://arxiv.org/abs/1212.4550)].

- [16] M. A. Nielsen and I. L. Chuang, *Quantum computation and quantum information*. Cambridge University Press, Cambridge, 2000.
- [17] C. Weedbrook, S. Pirandola, R. García-Patrón, N. J. Cerf, T. C. Ralph, J. H. Shapiro et al., *Gaussian quantum information*, *Reviews of Modern Physics* **84** (2012) 621 [[1110.3234](#)].
- [18] G. Adesso, S. Ragy and A. R. Lee, *Continuous variable quantum information: Gaussian states and beyond*, *Open Systems & Information Dynamics* **21** (2014) 1440001.
- [19] G. Adesso, *Entanglement of gaussian states*, arXiv preprint (2007) [[quant-ph/0702069](#)].
- [20] J. Eisert and M. M. Wolf, *Gaussian quantum channels*, in *Quantum information with continuous variables of atoms and light*, pp. 23–42. World Scientific, 2007.
- [21] A. Peres and D. R. Terno, *Quantum information and relativity theory*, *Rev. Mod. Phys.* **76** (2004) 93 [[quant-ph/0212023](#)].
- [22] D. R. Terno, *Introduction to relativistic quantum information*, in *NATO ASI on Quantum Computation and Quantum Information Chania, Crete, Greece, May 2-13, 2005*, 2005, [[quant-ph/0508049](#)].
- [23] B. S. DeWitt, *Quantum gravity: the new synthesis*, in *General relativity*. 1979.
- [24] E. Martin-Martinez, *Relativistic Quantum Information: developments in Quantum Information in general relativistic scenarios*, Ph.D. thesis, Waterloo U., 2011. [1106.0280](#).
- [25] E. Martn-Martnez, D. Aasen and A. Kempf, *Processing quantum information with relativistic motion of atoms*, *Phys. Rev. Lett.* **110** (2013) 160501 [[1209.4948](#)].
- [26] N. W. Ashcroft, N. D. Mermin and S. Rodriguez, *Solid state physics*. AAPT, 1978.
- [27] E. P. Gross, *Structure of a quantized vortex in boson systems*, *Il Nuovo Cimento (1955-1965)* **20** (1961) 454.
- [28] L. Pitaevskii, *Vortex lines in an imperfect bose gas*, *Sov. Phys. JETP* **13** (1961) 451.
- [29] F. Dalfovo, S. Giorgini, L. P. Pitaevskii and S. Stringari, *Theory of bose-einstein condensation in trapped gases*, *Reviews of Modern Physics* **71** (1999) 463.
- [30] J. Hubbard, *Electron correlations in narrow energy bands*, *Proc. R. Soc. Lond. A* **276** (1963) 238.
- [31] J. Haegeman, J. I. Cirac, T. J. Osborne, I. Pižorn, H. Verschelde and F. Verstraete, *Time-dependent variational principle for quantum lattices*, *Physical review letters* **107** (2011) 070601.
- [32] R. Barankov, L. Levitov and B. Spivak, *Collective rabi oscillations and solitons in a time-dependent bcs pairing problem*, *Physical review letters* **93** (2004) 160401.
- [33] R. A. Barankov and L. S. Levitov, *Synchronization in the bcs pairing dynamics as a critical phenomenon*, *Physical review letters* **96** (2006) 230403.
- [34] A. L. Fetter and J. D. Walecka, *Theoretical mechanics of particles and continua*. Courier Corporation, 2003.

- [35] T. Shi, E. Demler and J. I. Cirac, *Variational study of fermionic and bosonic systems with non-gaussian states: Theory and applications*, *Annals of Physics* (2017) .
- [36] J. Bardeen, *J. bardeen, ln cooper, and jr schrieffer, phys. rev. 108, 1175 (1957)*, *Physical Review* **108** (1957) 1175.
- [37] W. Nie, H. Katsura and M. Oshikawa, *Ground-state energies of spinless free fermions and hard-core bosons*, *Physical review letters* **111** (2013) 100402.
- [38] P. Pfeuty, *The one-dimensional ising model with a transverse field*, *ANNALS of Physics* **57** (1970) 79.
- [39] E. Lieb, T. Schultz and D. Mattis, *Two soluble models of an antiferromagnetic chain*, *Annals of Physics* **16** (1961) 407.
- [40] P. Woit, *Quantum theory, groups and representations: An introduction*. Springer, 2017.
- [41] A. S. Holevo, *Quantum systems, channels, information: a mathematical introduction*, vol. 16. Walter de Gruyter, 2012, [10.1515/9783110273403](https://doi.org/10.1515/9783110273403).
- [42] M. Mimura and H. Toda, *Topology of Lie groups, I and II*, vol. 91. American Mathematical Soc., 1991, [10.1090/mmono/091](https://doi.org/10.1090/mmono/091).
- [43] D. Bump, *Lie groups*. Springer, 2004, [10.1007/978-1-4614-8024-2](https://doi.org/10.1007/978-1-4614-8024-2).
- [44] B. Dutta, N. Mukunda, R. Simon et al., *The real symplectic groups in quantum mechanics and optics*, *Pramana* **45** (1995) 471 [[quant-ph/9509002v3](https://arxiv.org/abs/quant-ph/9509002v3)].
- [45] F. Berezin, *The method of second quantization*, Pure and applied physics. Academic Press, 1966.
- [46] D. F. Walls and G. J. Milburn, *Quantum optics*. Springer, 2007, [10.1007/978-0-387-30420-5](https://doi.org/10.1007/978-0-387-30420-5).
- [47] G. B. Folland, *Harmonic Analysis in Phase Space. (AM-122)*. Princeton University Press, f first edition ed., 3, 1989, [10.1515/9781400882427](https://doi.org/10.1515/9781400882427).
- [48] M. A. de Gosson, *Symplectic geometry and quantum mechanics*, vol. 166. Springer, 2006, [10.1007/3-7643-7575-2](https://doi.org/10.1007/3-7643-7575-2).
- [49] J. v. Neumann, *Die eindeutigkeit der schrödingerschen operatoren*, *Mathematische Annalen* **104** (1931) 570.
- [50] H. J. Groenewold, *On the principles of elementary quantum mechanics*, *Physica* **12** (1946) 405.
- [51] E. Bianchi, L. Hackl and N. Yokomizo, *Entanglement entropy of squeezed vacua on a lattice*, *Physical Review D* **92** (2015) 085045 [[1507.01567](https://arxiv.org/abs/1507.01567)].
- [52] S. L. Braunstein and P. Van Loock, *Quantum information with continuous variables*, *Reviews of Modern Physics* **77** (2005) 513 [[quant-ph/0410100](https://arxiv.org/abs/quant-ph/0410100)].
- [53] A. Ferraro, S. Olivares and M. G. Paris, *Gaussian states in continuous variable quantum information*, *Bibliopolis, Napoli, 2005*. (2005) [[quant-ph/0503237](https://arxiv.org/abs/quant-ph/0503237)].

- [54] G. Adesso, S. Ragy and A. R. Lee, *Continuous variable quantum information: Gaussian states and beyond*, *Open Systems & Information Dynamics* **21** (2014) 1440001 [[1401.4679](#)].
- [55] J. Rosenberg, *A selective history of the stone-von neumann theorem*, *Contemporary Mathematics* **365** (2004) 331.
- [56] A. Polkovnikov, K. Sengupta, A. Silva and M. Vengalattore, *Colloquium: Nonequilibrium dynamics of closed interacting quantum systems*, *Reviews of Modern Physics* **83** (2011) 863 [[1007.5331](#)].
- [57] C. Gogolin and J. Eisert, *Equilibration, thermalisation, and the emergence of statistical mechanics in closed quantum systems*, *Reports on Progress in Physics* **79** (2016) 056001 [[1503.07538](#)].
- [58] L. D'Alessio, Y. Kafri, A. Polkovnikov and M. Rigol, *From quantum chaos and eigenstate thermalization to statistical mechanics and thermodynamics*, *Advances in Physics* **65** (2016) 239 [[1509.06411](#)].
- [59] W. H. Zurek and J. P. Paz, *Decoherence, chaos, and the second law*, *Physical Review Letters* **72** (1994) 2508 [[gr-qc/9402006](#)].
- [60] P. A. Miller and S. Sarkar, *Signatures of chaos in the entanglement of two coupled quantum kicked tops*, *Physical Review E* **60** (1999) 1542.
- [61] A. K. Pattanayak, *Lyapunov exponents, entropy production, and decoherence*, *Physical Review Letters* **83** (1999) 4526 [[chao-dyn/9911017](#)].
- [62] D. Monteoliva and J. P. Paz, *Decoherence and the rate of entropy production in chaotic quantum systems*, *Physical Review Letters* **85** (2000) 3373 [[quant-ph/0007052](#)].
- [63] A. Tanaka, H. Fujisaki and T. Miyadera, *Saturation of the production of quantum entanglement between weakly coupled mapping systems in a strongly chaotic region*, *Physical Review E* **66** (2002) 045201 [[quant-ph/0209086](#)].
- [64] H. Kim and D. A. Huse, *Ballistic spreading of entanglement in a diffusive nonintegrable system*, *Physical Review Letters* **111** (2013) 127205 [[1306.4306](#)].
- [65] P. Calabrese and J. L. Cardy, *Evolution of entanglement entropy in one-dimensional systems*, *Journal of Statistical Mechanics* **0504** (2005) P04010 [[cond-mat/0503393](#)].
- [66] P. Calabrese and J. L. Cardy, *Entanglement entropy and quantum field theory*, *Journal of Statistical Mechanics* **0406** (2004) P06002 [[hep-th/0405152](#)].
- [67] J. S. Cotler, M. P. Hertzberg, M. Mezei and M. T. Mueller, *Entanglement growth after a global quench in free scalar field theory*, *Journal of High Energy Physics* **2016** (2016) 166 [[1609.00872](#)].
- [68] V. Balasubramanian, A. Bernamonti, J. de Boer, N. Copland, B. Craps, E. Keski-Vakkuri et al., *Thermalization of strongly coupled field theories*, *Physical Review Letters* **106** (2011) 191601 [[1012.4753](#)].
- [69] V. Balasubramanian, A. Bernamonti, J. de Boer, N. Copland, B. Craps, E. Keski-Vakkuri et al., *Holographic thermalization*, *Physical Review D* **84** (2011) 026010 [[1103.2683](#)].

- [70] T. Hartman and J. Maldacena, *Time Evolution of Entanglement Entropy from Black Hole Interiors*, *Journal of High Energy Physics* **1305** (2013) 014 [[1303.1080](#)].
- [71] H. Liu and S. J. Suh, *Entanglement Tsunami: Universal Scaling in Holographic Thermalization*, *Physical Review Letters* **112** (2014) 011601 [[1305.7244](#)].
- [72] H. Liu and S. J. Suh, *Entanglement growth during thermalization in holographic systems*, *Physical Review D* **89** (2014) 066012 [[1311.1200](#)].
- [73] B. Müller and A. Schäfer, *Entropy creation in relativistic heavy ion collisions*, *International Journal of Modern Physics E* **20** (2011) 2235 [[1110.2378](#)].
- [74] T. Kunihiro, B. Müller, A. Ohnishi, A. Schäfer, T. T. Takahashi and A. Yamamoto, *Chaotic behavior in classical yang-mills dynamics*, *Physical Review D* **82** (2010) 114015 [[1008.1156](#)].
- [75] K. Hashimoto, K. Murata and K. Yoshida, *Chaos in chiral condensates in gauge theories*, *Physical Review Letters* **117** (2016) 231602 [[1605.08124](#)].
- [76] Y. Sekino and L. Susskind, *Fast scramblers*, *Journal of High Energy Physics* **2008** (2008) 065 [[0808.2096](#)].
- [77] M. Van Raamsdonk, *Building up spacetime with quantum entanglement*, *General Relativity and Gravitation* **42** (2010) 2323 [[1005.3035](#)].
- [78] E. Bianchi and R. C. Myers, *On the Architecture of Spacetime Geometry*, *Classical and Quantum Gravity* **31** (2014) 214002 [[1212.5183](#)].
- [79] L. Susskind, *Entanglement is not enough*, *Fortschritte der Physik* **64** (2016) 49 [[1411.0690](#)].
- [80] R. A. Jefferson and R. C. Myers, *Circuit complexity in quantum field theory*, *Journal of High Energy Physics* **10** (2017) 107 [[1707.08570](#)].
- [81] S. Chapman, M. P. Heller, H. Marrochio and F. Pastawski, *Towards Complexity for Quantum Field Theory States*, *Physical Review Letters* **120** (2017) 121602 [[1707.08582](#)].
- [82] V. Latora and M. Baranger, *Kolmogorov-sinai entropy rate versus physical entropy*, *Physical Review Letters* **82** (1999) 520 [[chao-dyn/9806006](#)].
- [83] M. Falcioni, L. Palatella and A. Vulpiani, *Production rate of the coarse-grained gibbs entropy and the kolmogorov-sinai entropy: A real connection?*, *Physical Review E* **71** (2005) 016118 [[nlin/0407056](#)].
- [84] A. N. Kolmogorov, *A new metric invariant of transient dynamical systems and automorphisms in lebesgue spaces*, in *Dokl.Akad.Nauk SSSR (NS)*, vol. 119, pp. 861–864, 1958.
- [85] Y. Sinai, *Kolmogorov-Sinai entropy*, *Scholarpedia* **4** (2009) 2034.
- [86] G. M. Zaslavsky, *Hamiltonian chaos and fractional dynamics*. Oxford University Press, 2008.
- [87] M. Cencini, F. Cecconi and A. Vulpiani, *Chaos: from simple models to complex systems*, vol. 17. World Scientific, 2010.
- [88] T. Kunihiro, B. Müller, A. Ohnishi and A. Schäfer, *Towards a theory of entropy production in the little and big bang*, *Progress of Theoretical Physics* **121** (2009) 555 [[0809.4831](#)].

- [89] C. T. Asplund and D. Berenstein, *Entanglement entropy converges to classical entropy around periodic orbits*, *Annals of Physics* **366** (2016) 113 [[1503.04857](#)].
- [90] A. S. Holevo, *Probabilistic and statistical aspects of quantum theory*, vol. 1. Springer, 2011, [10.1007/978-88-7642-378-9](#).
- [91] V. Vedral, *The role of relative entropy in quantum information theory*, *Reviews of Modern Physics* **74** (2002) 197 [[quant-ph/0102094v1](#)].
- [92] M. Ohya and D. Petz, *Quantum entropy and its use*. Springer Science & Business Media, 2004.
- [93] V. I. Arnold, *Mathematical methods of classical mechanics*, vol. 60. Springer, 2013.
- [94] J.-P. Eckmann and D. Ruelle, *Ergodic theory of chaos and strange attractors*, *Reviews of Modern Physics* **57** (1985) 617.
- [95] F. Ginelli, P. Poggi, A. Turchi, H. Chaté, R. Livi and A. Politi, *Characterizing dynamics with covariant lyapunov vectors*, *Physical Review Letters* **99** (2007) 130601 [[0706.0510](#)].
- [96] Y. B. Pesin, *Characteristic lyapunov exponents and smooth ergodic theory*, *Russian Mathematical Surveys* **32** (1977) 55.
- [97] G. Bennetin, L. Galgani, A. Giorgilli and J. Strelcyn, *Lyapunov characteristic exponents for smooth dynamical systems and for hamiltonian systems: A method for computing all of them*, *Meccanica* **15** (1980) .
- [98] G. Floquet, *Sur les équations différentielles linéaires*, *Annales scientifiques de l'cole normale suprieure* **12** (1883) 47.
- [99] C. Chicone, *Ordinary Differential Equations with Applications*. Springer, 1999.
- [100] A. Ashtekar and A. Magnon-Ashtekar, *A geometrical approach to external potential problems in quantum field theory*, *General Relativity and Gravitation* **12** (1980) 205.
- [101] R. Haag, *Local quantum physics: Fields, particles, algebras*. Springer, 2012.
- [102] D. Shale, *Linear symmetries of free boson fields*, *Transactions of the American Mathematical Society* (1962) 149.
- [103] D. Shale and W. F. Stinespring, *States of the clifford algebra*, *Annals of Mathematics* (1964) 365.
- [104] J. T. Ottesen, *Infinite dimensional groups and algebras in quantum physics*, vol. 27. Springer, 2008.
- [105] N. D. Birrell and P. C. W. Davies, *Quantum Fields in Curved Space*, Cambridge Monographs on Mathematical Physics. Cambridge Univ. Press, Cambridge, UK, 1984, [10.1017/CBO9780511622632](#).
- [106] L. Parker and D. Toms, *Quantum field theory in curved spacetime: quantized fields and gravity*. Cambridge University Press, 2009, [10.1017/cbo9780511813924](#).
- [107] J. Schwinger, *On gauge invariance and vacuum polarization*, *Physical Review* **82** (1951) 664.

- [108] W. Greiner, B. Muller and J. Rafelski, *Quantum electrodynamics of strong fields*. Springer, 1985, [10.1007/978-3-642-82272-8](https://doi.org/10.1007/978-3-642-82272-8).
- [109] H. B. Casimir, *On the attraction between two perfectly conducting plates*, in *Proceedings of the Koninklijke Nederlandse Akademie Van Wetenschappen*, vol. 51, pp. 793–795, 1948.
- [110] G. T. Moore, *Quantum theory of the electromagnetic field in a variable-length one-dimensional cavity*, *Journal of Mathematical Physics* **11** (1970) 2679.
- [111] C. G. Torre and M. Varadarajan, *Functional evolution of free quantum fields*, *Classical and Quantum Gravity* **16** (1999) 2651 [[hep-th/9811222](#)].
- [112] I. Agullo and A. Ashtekar, *Unitarity and ultraviolet regularity in cosmology*, *Physical Review D* **91** (2015) 124010 [[1503.03407](#)].
- [113] R. D. Sorkin, *On the entropy of the vacuum outside a horizon*, in *Tenth International Conference on General Relativity and Gravitation (held in Padova, 4-9 July, 1983), Contributed Papers*, vol. 2, pp. 734–736, 1983, [1402.3589](#).
- [114] M. Srednicki, *Entropy and area*, *Physical Review Letters* **71** (1993) 666 [[hep-th/9303048](#)].
- [115] J. Eisert, M. Cramer and M. B. Plenio, *Colloquium: Area laws for the entanglement entropy*, *Reviews of Modern Physics* **82** (2010) 277 [[0808.3773](#)].
- [116] S. Hollands and K. Sanders, *Entanglement measures and their properties in quantum field theory*, [1702.04924](#).
- [117] L. Bombelli, R. K. Koul, J. Lee and R. D. Sorkin, *Quantum source of entropy for black holes*, *Physical Review D* **34** (1986) 373.
- [118] H. Casini and M. Huerta, *Remarks on the entanglement entropy for disconnected regions*, *Journal of High Energy Physics* **03** (2009) 048 [[0812.1773](#)].
- [119] E. Bianchi, T. De Lorenzo and M. Smerlak, *Entanglement entropy production in gravitational collapse*, *Journal of High Energy Physics* **06** (2015) 180 [[1409.0144](#)].
- [120] C. Holzhey, F. Larsen and F. Wilczek, *Geometric and renormalized entropy in conformal field theory*, *Nuclear Physics B* **B424** (1994) 443 [[hep-th/9403108](#)].
- [121] E. Bianchi and A. Satz, “Entropy of a subalgebra of observables and the geometric entanglement entropy.” 2018.
- [122] S. Weinberg, *The quantum theory of fields*, vol. 2. Cambridge University press, 1995, [10.1017/cbo9781139644198](https://doi.org/10.1017/cbo9781139644198).
- [123] F. Strocchi, *Symmetry breaking*, vol. 643. Springer, 2005, [10.1007/978-3-540-73593-9](https://doi.org/10.1007/978-3-540-73593-9).
- [124] E. Calzetta and B.-L. Hu, *Nonequilibrium quantum fields: Closed-time-path effective action, wigner function, and boltzmann equation*, *Physical Review D* **37** (1988) 2878.
- [125] J. Berges, *Nonequilibrium Quantum Fields: From Cold Atoms to Cosmology*, *Lecture Notes of the Les Houches Summer School* (2015) [[1503.02907](#)].
- [126] J. Berges and J. Serreau, *Parametric resonance in quantum field theory*, *Physical Review Letters* **91** (2003) 111601 [[hep-ph/0208070](#)].

- [127] J. H. Traschen and R. H. Brandenberger, *Particle production during out-of-equilibrium phase transitions*, *Physical Review D* **42** (1990) 2491.
- [128] L. Kofman, A. Linde and A. A. Starobinsky, *Reheating after inflation*, *Physical Review Letters* **73** (1994) 3195 [[hep-th/9405187](#)].
- [129] R. Allahverdi, R. Brandenberger, F.-Y. Cyr-Racine and A. Mazumdar, *Reheating in inflationary cosmology: theory and applications*, *Annual Review of Nuclear and Particle Science* **60** (2010) 27 [[1001.2600](#)].
- [130] M. A. Amin, M. P. Hertzberg, D. I. Kaiser and J. Karouby, *Nonperturbative dynamics of reheating after inflation: a review*, *International Journal of Modern Physics D* **24** (2015) 1530003 [[1410.3808](#)].
- [131] S. Mrówczyński and B. Müller, *Reheating after supercooling in the chiral phase transition*, *Physics Letters B* **363** (1995) 1 [[nucl-th/9507033](#)].
- [132] X. Busch, R. Parentani and S. Robertson, *Quantum entanglement due to a modulated dynamical casimir effect*, *Physical Review A* **89** (2014) 063606 [[1404.5754](#)].
- [133] P. O. Fedichev and U. R. Fischer, *Cosmological quasiparticle production in harmonically trapped superfluid gases*, *Physical Review A* **69** (2004) 033602 [[cond-mat/0303063](#)].
- [134] I. Carusotto, R. Balbinot, A. Fabbri and A. Recati, *Density correlations and analog dynamical casimir emission of bogoliubov phonons in modulated atomic bose-einstein condensates*, *European Physical Journal D* **56** (2010) 391 [[0907.2314](#)].
- [135] J.-C. Jaskula, G. B. Partridge, M. Bonneau, R. Lopes, J. Ruaudel, D. Boiron et al., *Acoustic analog to the dynamical casimir effect in a bose-einstein condensate*, *Physical Review Letters* **109** (2012) 220401 [[1207.1338](#)].
- [136] J. Steinhauer, *Observation of quantum Hawking radiation and its entanglement in an analogue black hole*, *Nature Physics* **12** (2016) 959 [[1510.00621](#)].
- [137] D. Campo and R. Parentani, *Inflationary spectra and partially decohered distributions*, *Physical Review D* **72** (2005) 045015 [[astro-ph/0505379](#)].
- [138] D. Polarski and A. A. Starobinsky, *Semiclassicality and decoherence of cosmological perturbations*, *Classical and Quantum Gravity* **13** (1996) 377 [[gr-qc/9504030](#)].
- [139] C. Kiefer, D. Polarski and A. A. Starobinsky, *Entropy of gravitons produced in the early universe*, *Physical Review D* **62** (2000) 043518 [[gr-qc/9910065](#)].
- [140] J. Martin and V. Vennin, *Quantum Discord of Cosmic Inflation: Can we Show that CMB Anisotropies are of Quantum-Mechanical Origin?*, *Physical Review D* **93** (2016) 023505 [[1510.04038](#)].
- [141] V. Arnold and A. Givental, *Symplectic geometry*, *encyclopedia of mathematical science vol. 4*, 1990.
- [142] P. Calabrese and J. Cardy, *Quantum quenches in extended systems*, *Journal of Statistical Mechanics* **2007** (2007) P06008.

- [143] G. De Chiara, S. Montangero, P. Calabrese and R. Fazio, *Entanglement entropy dynamics of Heisenberg chains*, *Journal of Statistical Mechanics* **2006** (2006) P03001.
- [144] M. Fagotti and P. Calabrese, *Evolution of entanglement entropy following a quantum quench: Analytic results for the x y chain in a transverse magnetic field*, *Physical Review A* **78** (2008) 010306 [0804.3559v1].
- [145] V. Eisler and I. Peschel, *Entanglement in a periodic quench*, *Annalen der Physik* **17** (2008) 410 [0803.2655v2].
- [146] A. M. Läuchli and C. Kollath, *Spreading of correlations and entanglement after a quench in the one-dimensional bose–hubbard model*, *Journal of Statistical Mechanics* **2008** (2008) P05018.
- [147] V. Alba and P. Calabrese, *Entanglement and thermodynamics after a quantum quench in integrable systems*, *Proceedings of the National Academy of Sciences* (2017) 201703516 [1608.00614v2].
- [148] J. M. Deutsch, *Quantum statistical mechanics in a closed system*, *Physical Review A* **43** (1991) 2046.
- [149] M. Srednicki, *Chaos and quantum thermalization*, *Physical Review E* **50** (1994) 888 [cond-mat/9403051v2].
- [150] M. Rigol, V. Dunjko and M. Olshanii, *Thermalization and its mechanism for generic isolated quantum systems*, *Nature* **452** (2008) 854 [0708.1324v2].
- [151] M. C. Gutzwiller, *Chaos in classical and quantum mechanics*, vol. 1. Springer, 2013.
- [152] F. Haake, *Quantum signatures of chaos*, vol. 54. Springer, 2013.
- [153] L. Reichl, *The transition to chaos: conservative classical systems and quantum manifestations*. Springer, 2013.
- [154] T. Biro, S. G. Matinyan and B. Muller, *Chaos and gauge field theory*, *World Sci. Lect. Notes Phys.* **56** (1994) 1.
- [155] C. C. Martens, R. L. Waterland and W. P. Reinhardt, *Classical, semiclassical, and quantum mechanics of a globally chaotic system: Integrability in the adiabatic approximation*, *The Journal of Chemical Physics* **90** (1989) 2328.
- [156] J. Maldacena, S. H. Shenker and D. Stanford, *A bound on chaos*, *Journal of High Energy Physics* **08** (2016) 106 [1503.01409].
- [157] D. Berenstein and A. M. Garcia-Garcia, *Universal quantum constraints on the butterfly effect*, 1510.08870.
- [158] J. Eisert, M. Cramer and M. B. Plenio, *Colloquium: Area laws for the entanglement entropy*, *Reviews of Modern Physics* **82** (2010) 277.
- [159] R. Islam, R. Ma, P. M. Preiss, M. E. Tai, A. Lukin, M. Rispoli et al., *Measuring entanglement entropy in a quantum many-body system*, *Nature* **528** (2015) 77.

- [160] A. M. Kaufman, M. E. Tai, A. Lukin, M. Rispoli, R. Schittko, P. M. Preiss et al., *Quantum thermalization through entanglement in an isolated many-body system*, *Science* **353** (2016) 794 [[1603.04409v3](#)].
- [161] D. N. Page, *Information in black hole radiation*, *Physical Review Letters* **71** (1993) 3743 [[hep-th/9306083v2](#)].
- [162] D. N. Page, *Average entropy of a subsystem*, *Physical Review Letters* **71** (1993) 1291 [[gr-qc/9305007v2](#)].
- [163] E. Lubkin, *Entropy of an n -system from its correlation with a k -reservoir*, *Journal of Mathematical Physics* **19** (1978) 1028.
- [164] S. Lloyd and H. Pagels, *Complexity as thermodynamic depth*, *Annals of Physics* **188** (1988) 186.
- [165] S. K. Foong and S. Kanno, *Proof of Page's conjecture on the average entropy of a subsystem*, *Physical Review Letters* **72** (1994) 1148.
- [166] J. Sánchez-Ruiz, *Simple proof of Page's conjecture on the average entropy of a subsystem*, *Physical Review E* **52** (1995) 5653.
- [167] S. Sen, *Average entropy of a quantum subsystem*, *Physical Review Letters* **77** (1996) 1.
- [168] S. Goldstein, J. L. Lebowitz, R. Tumulka and N. Zanghì, *Canonical typicality*, *Physical Review Letters* **96** (2006) 050403 [[cond-mat/0511091v2](#)].
- [169] S. Popescu, A. J. Short and A. Winter, *Entanglement and the foundations of statistical mechanics*, *Nature Physics* **2** (2006) 754.
- [170] H. Tasaki, *From quantum dynamics to the canonical distribution: General picture and a rigorous example*, *Physical Review Letters* **80** (1998) 1373 [[cond-mat/9707253v3](#)].
- [171] R. Nandkishore and D. A. Huse, *Many-body localization and thermalization in quantum statistical mechanics*, *Annual Review of Condensed Matter Physics* **6** (2015) 15.
- [172] E. Altman and R. Vosk, *Universal dynamics and renormalization in many-body-localized systems*, *Annual Review of Condensed Matter Physics* **6** (2015) 383.
- [173] L. F. Santos, A. Polkovnikov and M. Rigol, *Weak and strong typicality in quantum systems*, *Physical Review E* **86** (2012) 010102 [[1202.4764v2](#)].
- [174] J. M. Deutsch, H. Li and A. Sharma, *Microscopic origin of thermodynamic entropy in isolated systems*, *Physical Review E* **87** (2013) 042135 [[1202.2403v1](#)].
- [175] J. R. Garrison and T. Grover, “Does a single eigenstate encode the full Hamiltonian?.” arXiv:1503.00729. 10.1103/physrevx.8.021026.
- [176] W. Beugeling, A. Andreeanov and M. Haque, *Global characteristics of all eigenstates of local many-body Hamiltonians: participation ratio and entanglement entropy*, *Journal of Statistical Mechanics* (2015) (2015) P02002.
- [177] A. Osterloh, L. Amico, G. Falci and R. Fazio, *Scaling of entanglement close to a quantum phase transition*, *Nature* **416** (2002) 608 [[quant-ph/0202029v2](#)].

- [178] T. J. Osborne and M. A. Nielsen, *Entanglement in a simple quantum phase transition*, *Physical Review A* **66** (2002) 032110 [[quant-ph/0202162v1](#)].
- [179] G. Vidal, J. I. Latorre, E. Rico and A. Kitaev, *Entanglement in quantum critical phenomena*, *Physical Review Letters* **90** (2003) 227902 [[quant-ph/0211074v1](#)].
- [180] M. B. Hastings, *An area law for one-dimensional quantum systems*, *Journal of Statistical Mechanics* (2007) (2007) P08024.
- [181] M. Storms and R. R. P. Singh, *Entanglement in ground and excited states of gapped free-fermion systems and their relationship with Fermi surface and thermodynamic equilibrium properties*, *Physical Review E* **89** (2014) 012125.
- [182] H.-H. Lai and K. Yang, *Entanglement entropy scaling laws and eigenstate typicality in free fermion systems*, *Physical Review B* **91** (2015) 081110 [[1409.1224v2](#)].
- [183] S. Nandy, A. Sen, A. Das and A. Dhar, *Eigenstate Gibbs ensemble in integrable quantum systems*, *Physical Review B* **94** (2016) 245131 [[1605.09225v1](#)].
- [184] V. Alba, *Eigenstate thermalization hypothesis and integrability in quantum spin chains*, *Physical Review B* **91** (2015) 155123.
- [185] I. Peschel, *Calculation of reduced density matrices from correlation functions*, *Journal of Physics A* **36** (2003) L205.
- [186] I. Peschel and V. Eisler, *Reduced density matrices and entanglement entropy in free lattice models*, *Journal of Physics A* **42** (2009) 504003.
- [187] B. Dierckx, M. Fannes and M. Pogorzelska, *Fermionic quasifree states and maps in information theory*, *Journal of Mathematical Physics* **49** (2008) 032109 [[0709.1061v1](#)].
- [188] L. Vidmar and M. Rigol, *Generalized Gibbs ensemble in integrable lattice models*, *Journal of Statistical Mechanics* (2016) (2016) 064007.
- [189] D. Iyer, M. Srednicki and M. Rigol, *Optimization of finite-size errors in finite-temperature calculations of unordered phases*, *Physical Review E* **91** (2015) 062142 [[1505.03620v3](#)].
- [190] L. Susskind, *Computational Complexity and Black Hole Horizons*, *Fortschritte der Physik* **64** (2016) 24 [[1403.5695](#)].
- [191] L. Susskind and Y. Zhao, *Switchbacks and the Bridge to Nowhere*, [1408.2823](#).
- [192] D. Stanford and L. Susskind, *Complexity and Shock Wave Geometries*, *Physical Review D* **90** (2014) 126007 [[1406.2678](#)].
- [193] A. R. Brown, D. A. Roberts, L. Susskind, B. Swingle and Y. Zhao, *Holographic Complexity Equals Bulk Action?*, *Physical Review Letters* **116** (2016) 191301 [[1509.07876](#)].
- [194] A. R. Brown, D. A. Roberts, L. Susskind, B. Swingle and Y. Zhao, *Complexity, action, and black holes*, *Physical Review D* **93** (2016) 086006 [[1512.04993](#)].
- [195] M. Alishahiha, *Holographic Complexity*, *Physical Review D* **92** (2015) 126009 [[1509.06614](#)].
- [196] R.-G. Cai, S.-M. Ruan, S.-J. Wang, R.-Q. Yang and R.-H. Peng, *Action growth for AdS black holes*, *Journal of High Energy Physics* **09** (2016) 161 [[1606.08307](#)].

- [197] L. Lehner, R. C. Myers, E. Poisson and R. D. Sorkin, *Gravitational action with null boundaries*, *Physical Review D* **94** (2016) 084046 [[1609.00207](#)].
- [198] R.-Q. Yang, *Strong energy condition and complexity growth bound in holography*, *Physical Review D* **95** (2017) 086017 [[1610.05090](#)].
- [199] S. Chapman, H. Marrochio and R. C. Myers, *Complexity of Formation in Holography*, *Journal of High Energy Physics* **01** (2017) 062 [[1610.08063](#)].
- [200] D. Carmi, R. C. Myers and P. Rath, *Comments on Holographic Complexity*, *Journal of High Energy Physics* **03** (2017) 118 [[1612.00433](#)].
- [201] D. Carmi, S. Chapman, H. Marrochio, R. C. Myers and S. Sugishita, *On the Time Dependence of Holographic Complexity*, *Journal of High Energy Physics* **11** (2017) 188 [[1709.10184](#)].
- [202] A. Reynolds and S. F. Ross, *Divergences in Holographic Complexity*, *Classical and Quantum Gravity* **34** (2017) 105004 [[1612.05439](#)].
- [203] Y. Zhao, *Complexity, boost symmetry, and firewalls*, [1702.03957](#).
- [204] A. Reynolds and S. F. Ross, *Complexity in de Sitter Space*, *Classical and Quantum Gravity* **34** (2017) 175013 [[1706.03788](#)].
- [205] J. Couch, S. Eccles, W. Fischler and M.-L. Xiao, *Holographic complexity and non-commutative gauge theory*, [1710.07833](#).
- [206] B. Swingle and Y. Wang, *Holographic Complexity of Einstein-Maxwell-Dilaton Gravity*, [1712.09826](#).
- [207] Z. Fu, A. Maloney, D. Marolf, H. Maxfield and Z. Wang, *Holographic complexity is nonlocal*, *Journal of High Energy Physics* **02** (2018) 072 [[1801.01137](#)].
- [208] H. Casini, M. Huerta and R. C. Myers, *Towards a derivation of holographic entanglement entropy*, *Journal of High Energy Physics* **05** (2011) 036 [[1102.0440](#)].
- [209] A. Lewkowycz and J. Maldacena, *Generalized gravitational entropy*, *Journal of High Energy Physics* **08** (2013) 090 [[1304.4926](#)].
- [210] X. Dong, A. Lewkowycz and M. Rangamani, *Deriving covariant holographic entanglement*, *Journal of High Energy Physics* **11** (2016) 028 [[1607.07506](#)].
- [211] S. P. Jordan, K. S. M. Lee and J. Preskill, *Quantum Algorithms for Quantum Field Theories*, *Science* **336** (2012) 1130 [[1111.3633](#)].
- [212] S. P. Jordan, K. S. M. Lee and J. Preskill, *Quantum Computation of Scattering in Scalar Quantum Field Theories*, [1112.4833](#).
- [213] S. P. Jordan, K. S. M. Lee and J. Preskill, *Quantum Algorithms for Fermionic Quantum Field Theories*, [1404.7115](#).
- [214] S. P. Jordan, H. Krovi, K. S. M. Lee and J. Preskill, *BQP-completeness of Scattering in Scalar Quantum Field Theory*, [1703.00454](#).

- [215] T. J. Osborne, *Hamiltonian complexity*, *Reports on Progress in Physics* **75** (2012) 022001.
- [216] S. Gharibian, Y. Huang, Z. Landau, S. W. Shin et al., *Quantum hamiltonian complexity*, *Foundations and Trends® in Theoretical Computer Science* **10** (2015) 159 [[1401.3916v4](#)].
- [217] R. Orus, *A Practical Introduction to Tensor Networks: Matrix Product States and Projected Entangled Pair States*, *Annals of Physics* **349** (2014) 117 [[1306.2164](#)].
- [218] G. Vidal, *Entanglement Renormalization: an introduction*, in *Understanding Quantum Phase Transitions* (L. D. Carr, ed.). CRC press, 2010. [0912.1651](#). DOI.
- [219] K. Hashimoto, N. Iizuka and S. Sugishita, *Time Evolution of Complexity in Abelian Gauge Theories - And Playing Quantum Othello Game -*, [1707.03840](#).
- [220] R.-Q. Yang, *A Complexity for Quantum Field Theory States and Application in Thermofield Double States*, *Physical Review D* (2017) [[1709.00921](#)].
- [221] R.-Q. Yang, C. Niu, C.-Y. Zhang and K.-Y. Kim, *Comparison of holographic and field theoretic complexities for time dependent thermofield double states*, *Journal of High Energy Physics* **02** (2018) 082 [[1710.00600](#)].
- [222] A. P. Reynolds and S. F. Ross, *Complexity of the AdS Soliton*, [1712.03732](#).
- [223] R. Khan, C. Krishnan and S. Sharma, *Circuit Complexity in Fermionic Field Theory*, [1801.07620](#).
- [224] R.-Q. Yang, Y.-S. An, C. Niu, C.-Y. Zhang and K.-Y. Kim, *Axiomatic complexity in quantum field theory and its applications*, [1803.01797](#).
- [225] M. A. Nielsen, *A geometric approach to quantum circuit lower bounds*, [quant-ph/0502070](#).
- [226] M. A. Nielsen, M. R. Dowling, M. Gu and A. M. Doherty, *Quantum Computation as Geometry*, *Science* **311** (2006) 1133 [[quant-ph/0603161](#)].
- [227] M. A. Nielsen and M. R. Dowling, *The geometry of quantum computation*, *Quantum Information & Computation* **8** (2008) 861 [[quant-ph/0701004](#)].
- [228] A. R. Brown, L. Susskind and Y. Zhao, *Quantum Complexity and Negative Curvature*, *Physical Review D* **95** (2017) 045010 [[1608.02612](#)].
- [229] A. R. Brown and L. Susskind, *The Second Law of Quantum Complexity*, *Physical Review D* **97** (2018) 086015 [[1701.01107](#)].
- [230] S. Arora and B. Barak, *Computational Complexity: A Modern Approach*. Cambridge University Press, 2009, [10.1017/cbo9780511804090](#).
- [231] C. Moore and S. Mertens, *The Nature of Computation*. Oxford University Press, 2011, [10.1093/acprof:oso/9780199233212.001.0001](#).
- [232] S. Aaronson, *The Complexity of Quantum States and Transformations: From Quantum Money to Black Holes*, 2016, [1607.05256](#), <https://inspirehep.net/record/1476631/files/arXiv:1607.05256.pdf>.
- [233] J. Watrous, *Quantum computational complexity*, in *Encyclopedia of complexity and systems science*, pp. 7174–7201. Springer, 2009. DOI.

- [234] I. Bengtsson and K. Życzkowski, *Geometry of quantum states: an introduction to quantum entanglement*. Cambridge University Press, 2017, [10.1017/9781139207010](https://doi.org/10.1017/9781139207010).
- [235] A. Ashtekar and T. A. Schilling, *Geometrical formulation of quantum mechanics*, [gr-qc/9706069](https://arxiv.org/abs/gr-qc/9706069).
- [236] S. H. Weintraub, *Jordan canonical form: theory and practice*, *Synthesis Lectures on Mathematics and Statistics* **2** (2009) 1.

Vita

Lucas Hackl completed his undergraduate studies at the Humboldt-Universität zu Berlin in August 2011. He then did his Master's at the University of Waterloo as a part of the Perimeter Scholars International program in conjunction with the Perimeter Institute for Theoretical Physics. Before beginning his graduate studies in August 2013, he spent six months as teaching assistant at the African Institute for Mathematical Sciences in Senegal and subsequently interned with Global Public Policy Institute in Berlin. In August 2013, he joined the Institute for Gravitation and the Cosmos for his graduate studies, where he worked under the supervision of professor Eugenio Bianchi on quantum gravity and quantum field theory in curved spacetime at the intersection between fundamental theory and quantum information. In July 2018 he successfully defended his PhD before starting his postdoctoral fellowship in the Theory Division of Max-Planck-Institut für Quantenoptik at the Max Planck Harvard Research Center for Quantum Optics.